

Lecture Notes in Chemistry 81

Konstantin N. Mikhelson

Ion-Selective Electrodes

 Springer

Lecture Notes in Chemistry

Volume 81

Series Editors

- B. Carpenter, Cardiff, UK
- P. Ceroni, Bologna, Italy
- B. Kirchner, Leipzig, Germany
- A. Koskinen, Helsinki, Finland
- K. Landfester, Mainz, Germany
- J. Leszczynski, Jackson, MS, USA
- T.-Y. Luh, Taipei, Taiwan
- C. Mahlke, Erlangen, Germany
- N. C. Polfer, Gainesville, FL, USA
- R. Salzer, Dresden, Germany

For further volumes:
<http://www.springer.com/series/632>

The Lecture Notes in Chemistry

The series Lecture Notes in Chemistry (LNC) reports new developments in chemistry and molecular science—quickly and informally, but with a high quality and the explicit aim to summarize and communicate current knowledge for teaching and training purposes. Books published in this series are conceived as bridging material between advanced graduate textbooks and the forefront of research. They will serve the following purposes:

- provide an accessible introduction to the field to postgraduate students and nonspecialist researchers from related areas,
- provide a source of advanced teaching material for specialized seminars, courses and schools, and
- be readily accessible in print and online.

The series covers all established fields of chemistry such as analytical chemistry, organic chemistry, inorganic chemistry, physical chemistry including electrochemistry, theoretical and computational chemistry, industrial chemistry, and catalysis. It is also a particularly suitable forum for volumes addressing the interfaces of chemistry with other disciplines, such as biology, medicine, physics, engineering, materials science including polymer and nanoscience, or earth and environmental science.

Both authored and edited volumes will be considered for publication. Edited volumes should however consist of a very limited number of contributions only. Proceedings will not be considered for LNC.

The year 2010 marks the relaunch of LNC.

Konstantin N. Mikhelson

Ion-Selective Electrodes

 Springer

Konstantin N. Mikhelson
Ion-Selective Electrode Laboratory
St. Petersburg State University
St. Petersburg
Russia

ISSN 0342-4901 ISSN 2192-6603 (electronic)
ISBN 978-3-642-36885-1 ISBN 978-3-642-36886-8 (eBook)
DOI 10.1007/978-3-642-36886-8
Springer Heidelberg New York Dordrecht London

Library of Congress Control Number: 2013933589

© Springer-Verlag Berlin Heidelberg 2013

This work is subject to copyright. All rights are reserved by the Publisher, whether the whole or part of the material is concerned, specifically the rights of translation, reprinting, reuse of illustrations, recitation, broadcasting, reproduction on microfilms or in any other physical way, and transmission or information storage and retrieval, electronic adaptation, computer software, or by similar or dissimilar methodology now known or hereafter developed. Exempted from this legal reservation are brief excerpts in connection with reviews or scholarly analysis or material supplied specifically for the purpose of being entered and executed on a computer system, for exclusive use by the purchaser of the work. Duplication of this publication or parts thereof is permitted only under the provisions of the Copyright Law of the Publisher's location, in its current version, and permission for use must always be obtained from Springer. Permissions for use may be obtained through RightsLink at the Copyright Clearance Center. Violations are liable to prosecution under the respective Copyright Law. The use of general descriptive names, registered names, trademarks, service marks, etc. in this publication does not imply, even in the absence of a specific statement, that such names are exempt from the relevant protective laws and regulations and therefore free for general use.

While the advice and information in this book are believed to be true and accurate at the date of publication, neither the authors nor the editors nor the publisher can accept any legal responsibility for any errors or omissions that may be made. The publisher makes no warranty, express or implied, with respect to the material contained herein.

Printed on acid-free paper

Springer is part of Springer Science+Business Media (www.springer.com)

Preface

This book is devoted to ion-selective electrodes (ISEs)—potentiometric chemical sensors comprising widely used tools for sensing ions in various real samples of clinical, environmental, industrial, and laboratory research relevance. ISEs on the one hand belong to well-established and thoroughly studied analytical devices, and on the other hand still experience significant progress in understanding the basics of the sensor response and in the development of more efficient application techniques.

For decades I was involved in research and development works in the area of ISEs, and started giving courses in ISEs to students in St. Petersburg State University in 2005. These courses differ in their depth, dependent on the audience, on what exactly these particular students need to know for their projects, and for their future scientific and technical career (although it is not possible to foresee ones future needs for sure).

In spite of this experience, when Prof. Yury Zolotov proposed me to contact Prof. Rainer Salzer and Dr. Steffen Pauly, and discuss a possibility of preparing this book for Springer, I rather squirmed at first. Indeed, so many excellent books (I try to refer to these books in [Chap. 1](#)) have already been published by world-class specialists. However, after some hesitation I realized that most of these monographs do not cover the latest achievements in ISEs research and application. Therefore, it is time to try to describe the current state of the art in ISEs in a systematic, and, in the same time—in a comprehensible way, addressing the basics, the commonly recognized concepts, and also the most recent, sometimes questionable issues. The author hopes that this book to some extent meets this challenging task, and will be of interest to students, academic scholars, and practical people who decide to work on ISEs or to use these kinds of chemical sensors.

I am grateful to my wife Tamara for her understanding and patience and to my colleagues in my lab for their kind advices.

My special thanks go to my young American friends Kristin Maria Alexy and Robin Michelle Winz for their priceless help in improving my English.

Financial support from St. Petersburg State University, grants 12.0.16.2010 and 12.38.17.2011, is greatly acknowledged.

Contents

1	Introductory Issues	1
1.1	Ion-Selective Electrodes: What are These?	1
1.2	Brief Survey of the ISE Applications	5
1.3	ISEs Classification by the Membrane Type: Glass, Crystalline, Polymeric Membrane ISEs	6
1.4	Brief History of ISEs	7
	References	9
2	The Basics of the ISEs	11
2.1	The Membrane Model	11
2.2	Boundary (Interfacial) Potential, the Nernst Equation	12
2.2.1	The Physical Nature of the Boundary Potential	12
2.2.2	Formal Thermodynamical Description of Boundary Potential	15
2.3	Diffusion Potential	17
2.3.1	The Physical Nature of the Diffusion Potential	17
2.3.2	The Mathematical Description of the Diffusion Potential	19
2.3.3	The Segmented Model of the Overall Membrane Potential	21
2.4	Galvanic Cells without Liquid Junction and with Liquid Junction, Advantages and Disadvantages Thereof	22
2.4.1	Cells without Liquid Junction	22
2.4.2	Cells with Liquid Junction	25
2.5	The Mean Electrolyte Activity and the Single-Ion Activity. The Elements of the Debye–Hückel Theory	29
	References	31
3	Ion-Selective Electrode Characteristics	33
3.1	Ion-Selective Electrode Working Range and Response Slope	33
3.2	Potentiometric Selectivity Coefficient	35

3.3	Measurements of the Selectivity Coefficients	38
3.3.1	Separate Solutions Method	38
3.3.2	Fixed Interference Method	39
3.3.3	Matched Potentials Method	42
3.3.4	Unbiased Selectivity and the Bakker Protocol	42
3.4	Response Time	45
3.5	Stability and Piece-to-Piece Reproducibility of the ISE Response	46
	References	48
4	Ionophore-Based ISEs	51
4.1	Ion Exchangers and Charged Ionophores	51
4.2	Neutral Ionophores	55
4.3	Polymers and Plasticizers in ISE Membranes	58
4.3.1	Poly(vinylchloride) Plasticized Membranes	58
4.3.2	Non-PVC Polymeric Membranes, ISEs with Ion-Exchanger Sites and Ionophores Covalently Bound to Polymer Backbone	63
4.4	The Theory of the Ionophore-Based Membranes Response and Selectivity	65
4.4.1	Response and Selectivity of ISEs with Membranes Containing Ion Exchangers and Charged Ionophores	65
4.4.2	The Hofmeister Series	69
4.4.3	Selectivity of the ISEs Based on Neutral Ionophores	71
4.4.4	Co-Ion Interference with the Response of ISEs Based on Neutral Ionophores	73
4.5	Generalized Theories of Ionophore-Based ISE Membranes	75
4.5.1	The Sandblom–Eisenman–Walker Theory	75
4.5.2	Phase-Boundary Potential Approaches, Ionic Additives, Selectivity Optimization	77
4.5.3	Multispecies Approximation	78
4.6	Studies of the Species Interactions in Ionophore-Based Membranes	82
4.6.1	Complexation of Ions by Neutral Ionophores	82
4.6.2	Quantification of Ion-Site Association in Membranes	85
4.7	Potentiometric Sensing of Nonionic Species	87
4.8	Studies of the Interfacial Kinetics at the Membrane/Solution Boundary	89
	References	91
5	Glass Electrodes	97
5.1	Materials of the Glass Electrode Membranes	97
5.2	The Theories of the pH and Metal Ion Glass Electrode Response and Selectivity	101

5.2.1	The Nikolsky “Simple” Theory	101
5.2.2	The Eisenman Theory	104
5.2.3	The Nikolsky–Shultz Generalized Theory	105
5.2.4	The Baucke Theory, Comparison with the Nikolsky Theory	106
5.3	Glass Electrodes for RedOx Sensing	110
	References	111
6	Ion-Selective Electrodes with Crystalline Membranes	113
6.1	Materials of Crystalline Electrode Membranes	113
6.2	Fluoride Electrode Based on Lanthanum Fluoride Monocrystal	115
6.3	Analytical Characteristics of ISEs with Polycrystalline Membranes	116
6.3.1	Electrode Response and Detection Limit	116
6.3.2	Crystalline Electrodes Responding to Heavy Metal Cations	119
6.3.3	Selectivity of ISEs with Crystalline Membranes	120
6.3.4	Diffusion Layer Model by Lewenstam and Hulanicki	121
6.4	Chalcogenide Glass ISEs	122
	References	123
7	Modern Trends in the ISEs Theory and Applications	125
7.1	Real Time and Space Modeling of ISEs	125
7.2	ISEs in Trace Analysis	126
7.3	Use of ISEs Under Nonzero Current Conditions	129
7.4	Multisensor Arrays, Electronic Tongue	131
	References	132
8	ISE Constructions	135
8.1	Conventional ISEs with Internal Filling Solution	135
8.2	Solid-Contact ISEs	138
8.2.1	Why Solid Contact?	138
8.2.2	Solid-Contact ISEs with Glass and Crystalline Membranes	139
8.2.3	Ionophore-Based Solid-Contact ISEs Without Transducer Layer	140
8.2.4	Solid-Contact ISEs with Electron–Ion-Exchanger Resins in the Transducer Layer	141
8.2.5	Solid-Contact ISEs with Conducting Polymers in the Transducer Layer	142
8.2.6	Influence of Water Uptake on the Stability of Solid-Contact ISEs	143

8.3	Combination Electrodes	145
8.4	Micro-ISEs for Cellular Studies.	145
8.5	Flow-Through ISE Cells.	146
	References	147
9	The Basics of the Routine Analysis with ISEs	149
9.1	Reference Electrodes	149
9.2	Instrumentation for the Measurements with ISEs.	150
9.3	Direct Potentiometry with ISEs, Calibrators, and Buffer Solutions	152
9.4	Standard Addition Methods, Potentiometric Titration with ISEs	154
	References	157
	Index	159

Chapter 1

Introductory Issues

1.1 Ion-Selective Electrodes: What are These?

When I give a course in ion-selective electrodes, I normally ask my students in the very beginning of the first lecture: did you ever measure pH? Almost always, even if these are young first-year students, their answer is “yes.” Indeed, the most common and most frequently used ISE, the glass pH electrode, is familiar to nearly everybody who is doing chemistry, biology, in many branches of technology in industry, in agriculture, in environmental monitoring, and in various other activities. Thus, most of us know at least a little bit about ISEs and, more generally, about chemical and also physical sensors.

In this book, we will try to look at ISEs and related devices in a systematic way.

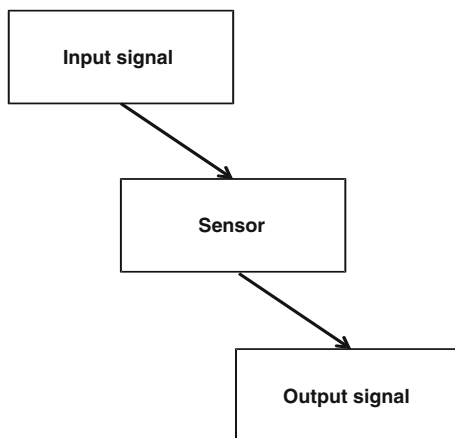
Ion-selective electrodes became routinely used analytical tool, and sometimes we even miss to realize the relation between ISEs and other kind of sensors. It may be therefore useful to outline briefly what is sensor and what kinds of sensors we currently know.

Normally, we call such measuring devices which transform the measured property into another kind of signal, mostly, an electrical signal which can be transmitted and registered by some instrument, as sensors. From this point of view, a traditional thermometer is not a sensor because we check the temperature by our own eyes, looking at the height of the mercury bar. However, a thermometer based on a thermocouple can be considered sensor. Sensor is a device which somehow gives a signal of the current state of the ambient, and if this state changes, the signal also changes. This happens due to some changes in the sensor caused by the changes in the environment. This we call “sensor response.”

Thus, for a sensor, we always have an input signal, a property which we wish to quantify, and an output signal which we can somehow register, see Fig. 1.1.

The input signal can be, for example, mass, pressure, temperature, humidity. The respective sensors are called “physical sensors.” Relatively modern kind of physical sensors comprise accelerometers used in automotive industry. For chemical sensors, the input signal is the chemical composition of the media with which the sensor is in contact. These can be liquid or gaseous samples, and also some semi-solid samples like soils. The output signal can be of the electrical nature:

Fig. 1.1 Basic principle of sensing: sensor accepts an input signal and transforms it into an output signal



voltage, current, capacitance—and then, we denote the respective devices as electrochemical sensors. The output signal can be also the optical density, in optical sensors (optodes), or oscillation frequency, in sensors based on quartz crystal microbalances, or in acoustic sensors (surface wave or bulk wave acoustic sensors).

In this book, we will deal with ion-selective electrodes which comprise an important class of electrochemical sensors, giving potentiometric signal. Ideally, the potential of an electrode obeys equation below, known as the Nernst equation:

$$\varphi = \varphi^0 + \frac{RT}{z_I F} \ln a_I \quad (1.1)$$

In the Nernst equation, φ is the electrode potential, φ^0 is the so-called standard value of the potential, a_I is the activity and z_I is the charge number of the target analyte, R is the gas constant, T is the absolute temperature, and F is the Faraday constant. The electrode gains its standard potential value when $a_I = 1$.

One cannot measure a potential of an individual electrode, the measurable quantity is always the electromotive force (EMF), the difference between the potentials of two electrodes immersed into a solution, see Fig. 1.2, left side. A pair of electrodes immersed into a solution makes the so-called galvanic cell (galvanic element).

If one of the electrodes (the so-called indicator electrode) in the galvanic cell obeys the Nernst equation, while the potential of the other electrode (reference electrode) is constant (see Sect. 2.4), the EMF follows the equation below:

$$E = E^0 + S \log a_I. \quad (1.2)$$

Here, E is the measured EMF, E^0 is the standard EMF value at $a_I = 1$, and S is the response slope. Ideally, the slope is $S = dE/d \log a_I = 2.3026 RT/F$.¹ At 25 °C, the ideal value of the slope is $S_{25} = 59.18/z_I$ mV. Equation (1.2) represents

¹ Coefficient 2.3026 appears because in practical use of ISEs we always plot EMF against decimal logs instead of natural logs, and $\ln 10 = 2.3026$.

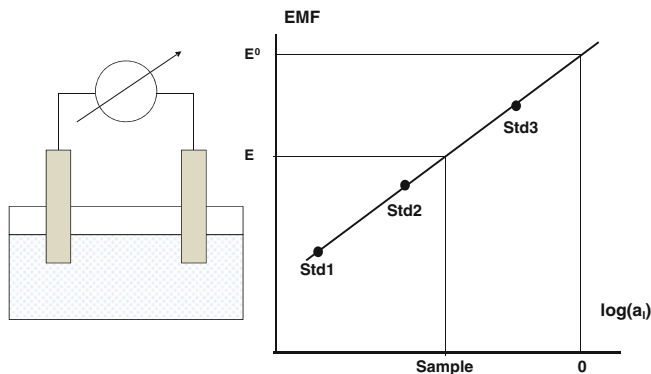


Fig. 1.2 Galvanic cell with two electrodes immersed into solution (*left*) and electrode calibration (*right*)

the practical form of the Nernst equation providing for some possible non-ideality of the response of the indicator electrode as well as that of the reference electrode. This is why instead of the ideal value $RT/z_I F$, the practical experimental slope $S = dE/d \log a_I$ appears in Eq. (1.2).

The values of E^0 the standard potential and S the slope are not *a priori* known. Therefore, one has to relate the measured signal (EMF) to the concentration (strictly activity) of the target analyte. This is made by performing calibration of the electrode, in fact, of the whole galvanic cell, using a series of standard solutions with known composition. Figure 1.2 (right side) illustrates a 3-point calibration procedure followed by the measurement of the activity of the analyte in the sample. First, the electrodes are immersed in several standard solutions (three in this example). The EMF values are measured, and in the respective 2D plot a line is obtained by linear regression. Ideally, it should be a straight line; therefore, it is recommended to use at least 3 standards to see whether it is true. The slope must be close to $RT/z_I F$ although it often deviates from this number in about 0.2–2 mV.

Once the calibration curve is obtained, and the calibration parameters: E^0 the standard EMF value and S the slope are known, one can use the electrode as measuring tool. The electrodes are now immersed into sample solution, and the measured EMF value delivers the value of the activity of the target analyte:

$$a_I = 10^{\frac{E-E^0}{S}}. \quad (1.3)$$

One can see that the values of interest: the activity and therefore also the concentration of the analyte are exponentially dependent on E the EMF measured in the sample, E^0 the standard EMF value and S the slope. Thus, the stability of the calibration curve of the electrode is of crucial importance. Normally, the slope is much better stable and reproducible than the individual EMF value. Bearing this in mind, we obtain from Eq. (1.2) the relative error of the analyte activity value:

$$\frac{da_I}{a_I} \approx SdE. \quad (1.4)$$

The commonly used unit for the EMF measurements with ISEs is mV. An error of 1 mV in the EMF measurement translates into 4 % relative error in the concentration of a univalent analyte and into 8 % relative error for a divalent analyte. Normally, EMF values are registered with error significantly lower than 1 mV. Anyhow, the accuracy of the direct measurements with ISEs is relatively low. For better accuracy of analysis, the EMF values must be registered with precision of 0.1 and even 0.01 mV. On the other hand, Eq. (1.4) shows that the relative error of the analysis with ISEs remains constant within the whole linear range of the response, covering also diluted samples. This is a big and nearly unique advantage of the potentiometric analysis because in most of other analytical techniques, the relative error gets significantly increased along dilution of the sample.

The term “Ion-selective electrodes” reflects the capability of ISEs to discriminate between ions. Ideally, an ISE responds to only one kind of species in a mixed sample. Of course, the real-world electrodes show only limited selectivity. For decades, the glass pH electrode appeared the most selective. Some of glass electrodes work at pH 12 or even 14, that is, sustain huge excess of sodium and other electrolytes: up to 10^{12} or 10^{14} times. More recently, it was shown that some ionophore-based and solid state ISEs show even higher selectivity if the measurements are performed under certain protocols (see [Chap. 3](#) for details). The selectivity of an ISE to, for example, I^+ ions in the presence of J^+ ions is quantified with the so-called selectivity coefficient: the parameter K_{IJ} in the Nikolsky equation [1]:

$$E = E^0 + S \log(a_I + K_{IJ}a_J). \quad (1.5)$$

Here, I^+ ions are the target analyte, the so-called “primary” or “main” ions, while J^+ ions are normally called “interfering” ions. Obviously, the smaller K_{IJ} value the smaller is the whole interference effect caused by J^+ ions, and the ISE is closer to the ideal case: primary ions only give impact on the electrode response. The term “selectivity coefficient” is therefore a bit confusing: high selectivity of the response requires low selectivity coefficient. However, everybody who works with ISEs are used with this terminology and suggestions to rename the selectivity coefficient into “interference coefficient” did not get support.

The physical nature of the selectivity coefficient, how exactly it depends on the ISE membrane composition and the nature of the competing ions, is very different for different kinds of membranes. More sophisticated equations have been suggested for more accurate description of the ISE response in mixed solutions. However, Eq. (1.5) remains the most widely used, partly due to its simplicity.

1.2 Brief Survey of the ISE Applications

Normally, analysis with ISEs does not require pretreatment of the sample, more of this, in line and in vivo measurements are possible offering great opportunities for continuous monitoring in clinical, industrial, and environmental applications. Unlike other analytical techniques, measurements with ISEs provide with data on the activity of the analyte. In many cases, this is a critical advantage because the Gibbs free energy (and other thermodynamic potentials) is characterized by activity rather than by concentration. Therefore, the activity of the analyte provides with the data whether the respective chemical process will or will not occur spontaneously. This knowledge is especially useful in industry. Both ISEs themselves and the instrumentation for measuring the potentiometric signal are inexpensive and easy in use, not requiring high-skilled operator. The power consumption for the measurements is low. This is why ISEs became so widely used in practice. Table 1.1 presents some examples of the applications of ISEs.

Examples presented in Table 1.1 illustrate the variety of the ISEs applications. Clinical analysis with ISEs appears the most important. A number of companies produce automatic clinical analyzers which measure dozens of parameters, blood electrolytes among them. Human homeostasis requires a very narrow window for the pH: approx. 7.44 ± 0.05 . The normal level of the potassium ions concentration is 4.5 mM, it may be about 1 mM higher or lower, and these deviations indicate several various disorders including those related to cardiovascular system. Sodium

Table 1.1 Some applications of ion-selective electrodes

Branch of activity	Typical samples	Typical analytes
Clinical analysis	Blood serum, plasma, whole blood, saliva, urine, lymph	pH, K^+ , Na^+ , Ca^{2+} , Li^+ , Cl^- , Mg^{2+} , HCO_3^-
Agricultural industry	Soil, vegetables, fruits, milk, meat	pH, NO_3^- , K^+ , NH_4^+ , Ca^{2+} , Cl^- , Na^+
Industrial manufacturing	Metal plating solutions, paper bleaching solutions, fertilizers	pH, Cu^{2+} , Ag, Au, NO_3^- , Ca^{2+} , K^+ , Na^+ , NH_4^+
Environmental monitoring	Natural, industrial, waste waters, soil, plants, human and animal tissues	pH, Pb^{2+} , Hg^{2+} , Cu^{2+} , NO_3^- , ionic and nonionic surfactants
Pharmaceutical industry	Medical drugs, liniments, mixtures	Biologically active amines, alkaloids, acids
Food industry	Juices, beverages, dough, pastry, wine	pH, Ca^{2+} , NO_3^- , CH_3COO^-
Power stations	Cooling water	pH, Na^+
Control of gases in air	Air in chemical factories	NH_3 , NO_2 , "acidic" gases
Control of enzymatic activity	Medical and biological liquids and tissues, pesticide polluted soils and plants	Enzymes, substrates, enzyme inhibitors

comprises the main cationic electrolyte in blood; its normal concentration value is about 140 mM/l. The control of lithium is especially important for patients suffering from manic-depressive psychosis. In the cases of calcium and magnesium, ISEs provide unique information because the clinically-relevant information can be extracted from the concentration of the free (not complexed) Ca^{2+} and Mg^{2+} ions. Other techniques like atomic absorption show only total content of these ions which is about 2 times higher than the free ion concentration. Less frequently performed but also important is analysis of electrolytes in saliva, urine, and lymph.

Acidity and salinity of soils, suitable concentrations of nitric, amino, and potassium fertilizers are quantified with the respective ISEs. These electrolytes often have to be controlled also in various agricultural products. Many ions must be monitored in industrial manufacturing. Among these are gold and silver which are present in industrial solutions mostly as anionic complexes, and therefore present in Table 1.1 without charge. Toxic heavy metals, pH, nitrate, surfactants are of interest for the environmental control. Dozens of ionic drugs of pharmaceutical relevance are measured with the respective ISEs. Food industry also needs tools for ions control, while pipelines in cooling systems of power stations are sensitive to the pH and to minute quantities of salt. One can see that the pH is always present among other electrolytes to measure, and therefore, the glass pH electrode, the oldest among all chemical sensors, remains, probably, the most important and most demanded.

Although ISEs are, rigorously speaking, ion sensors, one can use them in special devices: gas and biosensors. Earlier, these devices constituted a large branch of the ISE application. Currently, ammonia gas sensors based on the Severinghaus principle² and enzyme-based urea ISEs are still in use. However, other analytes used to be measured by gas and biosensors based on ISEs are measured by sensors with other work principles. Therefore, this application of ISEs is not discussed in this book.

1.3 ISEs Classification by the Membrane Type: Glass, Crystalline, Polymeric Membrane ISEs

ISEs are normally classified by the membrane material, although one can group them according to construction or other feature. The oldest group of ISEs is those with glass membranes. These are mostly silicate glasses and electrodes for the pH measurements. However, sometimes also boric and phosphorous glasses also are in use. On the other hand, there are glass membranes for Na^+ , K^+ , Li^+ , and Ag^+ assay. Among these, only Na^+ glass electrodes are really practical. Glass electrodes are described in Chap. 5.

² Change of the analyte gas concentration causes change of pH in a thin aqueous film on a surface of a glass pH electrode, and in this way the analyte concentration is measured.

Crystalline electrodes can be subdivided into those with polycrystalline and with monocrystalline membranes. The latter kind is represented by F^- -selective electrode with membrane made of LaF_3 monocrystal doped with EuF_2 . Other crystalline electrodes have polycrystalline membranes containing mixtures of low-soluble silver salts like $Ag_2S + AgX$ ($X^- = Cl^-, Br^-, I^-, SCN^-, CN^-$). These ISEs are suitable for assay of the respective X^- ions and also S^{2-} . Other group of polycrystalline membranes contains mixtures of Ag_2S with low-soluble metal sulfides: $Ag_2S + MeS$ ($Me^{2+} = Pb^{2+}, Cd^{2+}, Cu^{2+}$, and Hg^{2+}). Similar compositions doped with B, Al, Ga, Ge, Sn, As, Sb, Bi compounds allow obtaining amorphous chalcogenide glass membranes. Crystalline and chalcogenide glass ISEs are described in [Chap. 6](#).

ISEs with polymeric membranes containing ionophores comprise the most numerous group of electrodes. Ionophores are neutral or charged species selectively binding ions. This selectivity of association or complexation makes the basis for the potentiometric selectivity of the respective ISEs. The large variety of selective ionophores makes the main basis for the variety of selectively assayed analytes. Among these are various inorganic and organic cations and anions, ionic surfactants, it is possible to make ionophore-based ISEs sensitive to nonionic species like nonionic surfactants and some phenols.

Among the polymers used in ionophore-based membranes, polyvinylchloride is the most widely used although some other polymers became more and more popular. ISEs with polymeric membranes containing ionophores are described in [Chap. 4](#).

The materials for the ISE membranes change over time. For years heterogeneous membranes were in use, containing low-soluble salts dispersed in polyethylene or other inert polymers, or membranes made of ion-exchange resins. Now these ISEs belong to the past. On the other hand, it was very recently suggested to modify gold nano-filters with adsorbed ionophores and make ISEs in this very novel way [2].

1.4 Brief History of ISEs

The history of ISEs started in the beginning of the XX century (1906) when Cremer [3] noticed that the potential of a glass membrane depends on the pH of the solution. On the basis of this observation, Haber and Klemensiewicz invented glass pH electrode in 1909 [4]. However, these electrodes only got wide use much later when Beckman in 1936 started commercial production of glass pH electrodes and pH meters. At about the same time, Nikolsky published his article devoted to the theory of the glass electrode response [1] with the derivation of the Nikolsky equation and coined the term “selectivity constant.” Nikolsky considered the ion exchange between the glass phase and the aqueous phase, this was his crucial idea. Later on, this particular version of the Nikolsky theory was called “the simple theory of the glass electrode.” This simple theory considered all ion-exchange

sites in glass equal to one another with respect of the ability to dissociate and neglected the diffusion potential within the glass membrane phase. In 1950s, Nikolsky and Shultz published a series of papers inventing what they called “the generalized theory of the glass electrode” [5, 6]. The generalization was done in two distinctively different respects. One was rather formal introducing “partial” activity coefficients for species in the membrane. The other one accounted for different dissociation degree for different ionogenic groups in glass. In early 1960s, Shultz and Stefanova for the first time considered the glass electrode potential as “membrane potential,” that is, containing not only boundary potential drops but also the diffusion potential within the membrane [7]. Eisenman (who himself made enormous contribution to the theory and practice of ISEs) edited an excellent book devoted to the then state of the art in glass electrodes for the pH and alkali metal sensing [8].

By early 1960s, the progress in ISEs was almost exclusively connected to glass electrodes. In 1961, Pungor invented ISEs with heterogeneous membranes: low-soluble salts dispersed in a polymer (polyethylene) matrix [9]. The second half of the 1960s was the time of several breakthrough inventions. Frant and Ross in 1966 proposed fluoride electrode with membrane of monocrystalline LaF_3 doped with EuF_2 [10]. In the same year, Simon invented first ISE with liquid membrane containing a neutral ionophore (at that time called carrier or ligand) [11]. This was potassium-selective electrode with nonactin as the ionophore. Later on, it turned out that nactins are more selective to ammonium cations, while valinomycin is much more suitable for K^+ -ISEs. Eisenman published a book devoted to various aspects of natural cell membranes and their artificial models [12]. In 1967, Ross proposed first Ca^{2+} -ISE with liquid membrane containing organophosphorous charged ionophore [13]. Also in 1967, Bloch, Shatkey and Saroff published their pioneering work devoted to ISEs with plasticized polyvinylchloride membranes [14]. The plasticizer imparts to the elasticity of the membrane and, in the same time, acts as solvent for ionophores. Moody and Thomas [15] also contributed very much to this basic principle of the ionophore-based ISEs, which until now remains highly relevant. Durst published a book summarizing the achievements in the theory and practice of ISEs made by the early 1970s [16]. The book consists of chapters written by the world-leading scientists in the field.

Bergveld in 1970 invented ion-selective field effect transistors [17]. These devices effectively combine ion-selective membrane with semiconductor unit enhancing the signal. Rapid evolution in the field of ISEs lasted until the late 1970s. At that time, a number of excellent books [18–22] have been published devoted to the theory, development and applications of ISEs. By early 1980s, ISEs became mature. At that time, Morf published his fundamental book on the principles of the ISEs [23] which for years became a kind of handbook for those who were involved in this branch of science and technology.

New impetus for the ISEs studies, in particular for those based on ionophores, was given by Bakker in mid-1990s when apparently well-established concepts were re-examined, and many turned out being inaccurate or even incorrect. The results of this re-addressing were summarized in two excellent reviews published

by Pretsch, Bakker and Bühlmann in late 1990s [24, 25]. Review [24] is primarily devoted to the theory of ionophore-based sensors: ISEs and optodes, and review [25] summarizes known ionophores in the course of their selectivity to a given analyte. In analogy with the so-called electronic nose based on array of gas sensors, Vlasov invented “electronic tongue”: an array of ISEs with limited selectivity in combination with sophisticated software [26]. This system is capable of providing with qualitative and quantitative information of the composition of various kinds of rather complicated real samples.

Another breakthrough achieved in the late 1990s was made by Sokalski and referred to the sensitivity of ISEs in strongly diluted solutions [27]. Efforts aimed at measurements with electrodes in nano- and sub-nanomolar concentration range became the mainstream in the ISE research and application in the beginning of the XXI century. At that time, it also became clear that ISEs are not necessarily pure potentiometric sensors, that is, applied only under zero current conditions. More of this, polarized electrodes showed certain advantages over classical ISEs for a number of practical tasks [28–30]. A large success in theoretical description of ISE potential in real time and space was achieved in early 2000s [31–34] in Lewenstam group. Recently, the fundamentals of ISEs, together with that of other kind of sensors, were described by Janata [35].

In this book, I tried to describe the basics of the measuring with ISEs, the state of the art in ISEs with different types of membranes (with special emphasis on the ionophore-based ISEs), and some modern trends in the ISE research and application. Ion-selective field effect transistors (ISFETs) are not discussed here.

References

1. B.P. Nikolsky, *Acta Physicochim. URSS*, 1937, 7, 597.
2. G. Jagerszki, A. Takacs, I. Bitter, R.E. Gyurcsanyi, *Angew. Chem. Int. Ed.* 2011, 50, 1656.
3. M. Cremer, *Z. Biol.* 1906, 47, 562.
4. F. Haber, Z. Klemensiewicz, *Z. Phys. Chem.*, 1909, 65, 385.
5. B.P. Nikolsky, M.M. Shultz, *Russ. J. Phys. Chem.*, 1953, 27, 724 (Russ.).
6. B.P. Nikolsky, M.M. Shultz, *Russ. J. Phys. Chem.*, 1962, 36, 1327 (Russ.).
7. O.K. Stefanova, M.M. Shultz, E.A. Materova, B.P. Nikolsky, *Herald of St.Peterburg Univ.*, 1963, 4, 93 (Russ.).
8. G. Eisenman (ed), *Glass electrodes for hydrogen and other cations. Principles and practice.* M. Dekker, New York., 1967.
9. E. Pungor, E. Hollos-Rokosinyi, *Acta Chem. Hung.*, 1961, 27, 63.
10. M.S. Frant, J.W. Ross, *Science*, 1066, 154, 1553.
11. Z. Stefanac, W. Simon, *Chimia*, 1966, 20, 436.
12. G. Eisenman (ed) *Membranes*, 1-2, M. Dekker, N.Y., 1972/1973.
13. J.W. Ross, *Science*, 1967, 156, 1378.
14. R. Bloch, A. Shatkey, H.A. Saroff, *Biophys. J.*, 1967, 7, 865.
15. G.J. Moody, R.B. Oke, J.D.R. Thomas, *Analyst*, 1970, 95, 910.
16. R. Durst (editor) *Ion-selective electrodes*, NBS special publication 314, 1969.
17. P. Bergveld, *IEEE Trans. Biomed. Eng.*, 1970, 17, 70.

18. N. Lakshminarayanaiah, *Membrane electrodes*, Academic Press, NY, San Francisco, London, 1976.
19. H. Freiser (ed), *Ion-selective Electrodes in Analytical Chemistry*, Plenum Press, N.Y., 1978.
20. B.P. Nikolsky, E.A. Materova, *Ion-selective Electrodes*, Khimia, 1980, 239 p. (Russ.).
21. K. Cammann, *Das Arbeiten mit ionenselektiven Electroden*, Springer, Berlin, 1973.
22. J. Koryta, K. Stulik, *Iontove-selectivni electrody*, Acadeia, Praha (1984).
23. W.E. Morf, *The principles of Ion-selective Electrodes and of Membrane Transport*, Akademiai Kiado, Budapest, 1981.
24. E. Bakker, P. Bühlmann, E. Pretsch, *Chem. Rev.*, 1997, 97, 3083.
25. P. Bühlmann, E. Pretsch, E. Bakker, *Chem. Rev.*, 1998, 98, 1593.
26. A.V. Legin, A.M. Rudnitskaya, Yu.G. Vlasov, C. Di Natale, F. Davide, A. D'Amico, *Sens. Act. B*, 1997, 44, 291.
27. T. Sokalski, A. Ceresa, T. Zwickl, E. Pretsch, *J. Am. Chem. Soc.*, 1997, 119, 11347.
28. E. Lindner, R.E. Gyurcsanyi, R.P. Buck, *Electroanalysis*, 1999, 695.
29. A. Shvarev, E. Bakker, *Anal. Chem.*, 2003, 75, 4541.
30. M.A. Peshkova, T. Sokalski, K.N. Mikhelson, A. Lewenstam, *Anal. Chem.*, 2008, 80, 9181.
31. T. Sokalski, A. Lewenstam, *Electrochem. Commun.*, 2001, 3, 107.
32. T. Sokalski, P. Lingenfelter, A. Lewenstam, *J. Phys. Chem.*, 2003, 107, 2443.
33. J. Bobacka, A. Ivaska, A. Lewenstam, *Chem. Rev.*, 2008, 108, 329.
34. T. Sokalski, W. Kucza, M. Danielewski, A. Lewenstam, *Anal. Chem.*, 2009, 81, 5016.
35. J. Janata, *Principles of Chemical Sensors*, Springer, 2009, 395 p.

Chapter 2

The Basics of the ISEs

In this chapter, we will discuss the formalism of the practically relevant representation of the signals obtained from an “ideal” electrode. We will do this using a macroscopic, thermodynamic approach. We will not go into the microscopic details on why and when the electrodes respond in this particular way, leaving this discussion, and also the discussion of the “real-world electrodes”, which are not that ideal, for subsequent chapters.

The consideration of the mechanism of ISE response relies on two types of electric potentials: boundary potential and diffusion potential. We will start the discussion of these two potentials with the description of their physical origin and then turn to the respective thermodynamical formalism.

2.1 The Membrane Model

Basically, a membrane is a phase which separates two other phases. In this way, ion-selective electrode membranes are true membranes. These separate the sample (or the calibrator) solution from either the internal solution of the electrode, or the internal solid contact. The model to be considered is based on several assumptions:

1. The membrane comprises a flat parallel ionically conducting piece of matter placed in between two aqueous electrolyte solutions. Although the system is three-dimensional, any changes may happen only along one axis: the x -axis which is perpendicular to the membrane plane. Therefore, the system is effectively one-dimensional.
2. There are no gradients of temperature and pressure within the system.
3. The interfaces between the membrane and solutions are at electrochemical equilibrium, while the system as a whole is in a steady state.

2.2 Boundary (Interfacial) Potential, the Nernst Equation

2.2.1 *The Physical Nature of the Boundary Potential*

Electric potentials at the interface between two phases may arise due to (1) partitioning of electrolytes, or due to (2) adsorption of charged species, or (3) even in the total absence of individual charged species (ions)—just due to some regular orientation of dipole molecules at the interface. Potentials caused by effects (2) and (3) are only stable in electrolyte-free systems. Otherwise, only in the case (1) are the potentials stable and reproducible. Therefore, since in this book we discuss practically relevant issues, we will focus on the interfacial potential formed due to partitioning of electrolytes between the phases in contact. As example, we consider here two liquid phases.

First, we will consider a very simple and highly idealized situation: how an electric potential arises at the interface between two initially neutral (non-charged) phases. We will start with a single phase comprising, for example, an aqueous electrolyte solution with uniform distribution of ions within the whole volume of the phase (no concentration gradient). Ions bear electric charge, and therefore, there is some microscopic electric field within the vicinity of any ion in the solution. However, the microscopic fields produced by individual ions compensate each other, and the resulting macroscopic field over the whole phase is zero.

Let us see what will happen if we join this aqueous electrolyte solution with, for example, an organic phase consisting of a pure organic solvent immiscible with water. When the phases are in contact, the electrolyte distributes between the aqueous phase and the organic phase. Basically, cations and anions of the electrolyte distribute between the two phases in equivalent quantities. However, this equivalence is not exact, especially in the beginning of the distribution process, producing small deviations from the electroneutrality of the two phases. Generally speaking, the main role in the preferential uptake of ions with a particular charge sign is played by $\Delta G_{I_{\text{aq}}}^{\text{org}}$: the Gibbs free energy of the ion transfers from one phase to another. This value depends on the Gibbs free energy of the ion hydration in the aqueous phase ΔG_I^{hydr} and that of the ion solvation in the organic phase ΔG_I^{solv} as follows: $\Delta G_{I_{\text{aq}}}^{\text{org}} = \Delta G_I^{\text{solv}} - \Delta G_I^{\text{hydr}}$. If the hydration of cations and anions is about the same, while, for whatever reason, the affinity of cations to the organic phase is higher than that of anions, the number of cations crossing the interface and getting into the organic phase will slightly exceed the number of anions. This may happen if the organic solvent is a Lewis base, and therefore, cations (which, obviously, are Lewis acids) are more strongly solvated in this solvent than anions. On the contrary, if the solvent comprises a Lewis acid, its affinity to anions is stronger than its affinity to cations. It may also happen that the inequality of the ion distribution is mainly due to difference in hydration. A preferential distribution of the cation of an electrolyte to the organic phase is due to, respectively, strong hydration of the anion, or vice versa. Thus, the difference in

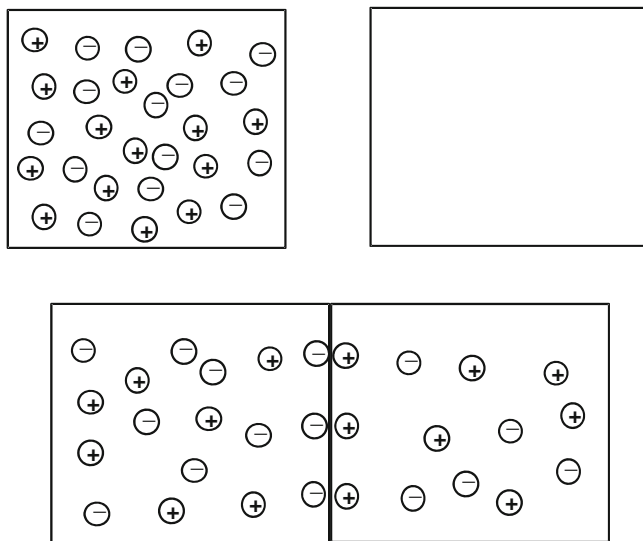


Fig. 2.1 Schematic representation of the formation of the electrical double layer. *Top*: two phases separately, left phase with randomly distributed ions, right phase—without ions. *Bottom*: two phases joined, electrolyte partitioned between the phases, most ions distribute randomly, but some—regularly at the interface

the affinities of ions to water and to the organic solvent is the driving force of the initial slightly unequal ion distribution.

Thus, after a very short time of the contact, the organic solvent contains some small excess of cations over anions, while the aqueous phase contains an equal excess of anions, so both phases acquire some electric charge, as shown in Fig. 2.1. It is very important that the number of these non-compensated charges is much smaller than the total number of ions in any of the phases. It is also important that the non-compensated (excessive) ions are localized in the immediate vicinity of the interface, forming the so-called electrical double layer. In the bulk of any phase, the electric fields produced by individual randomly distributed and chaotically moving ions compensate each other.¹ Unlike this situation, ions within the double layer are arranged relatively regularly, and the superposition of the respective fields is not zero. Therefore, as soon as this double layer is formed, the respective Coulombic forces between the ions result in attraction of anions to positively charged organic phase, and rejection of cations. Thus, “chemical” driving force (the non-equal affinity of ions to the solvent) which causes the non-equal ion distribution gets counterbalanced with the electric driving force: the electric field created by ions regularly arranged within the double layer. Once both driving forces become equal, a stable electric potential is established at the

¹ Except of a phase with a gradient of an electrolyte, see Sect. 2.3.

interface between the two phases. As soon as this happens, the ions of the electrolyte distribute between the two phases in exactly equal quantities, so that the phases will not take more and more charge. The potential in question is called interfacial or boundary potential, and the condition of the two-phase system under consideration is called “electrochemical equilibrium.” The most crucial difference between this two-phase system and the single phase we considered before is a regular charge separation established at the interface. Without regular charge separation, no electric field exists. The model discussed is, obviously, oversimplified and relates to the so-called dense part of the electrical double layer. The diffuse parts of the double layers may penetrate deep into the phases, up to hundreds of nm (in the case of solvent-polymeric membranes [1]).

Boundary potentials cannot be measured experimentally, because one cannot separate the “pure chemical” and “pure electrical” contributions to the whole free energy of the interfacial ion transfer from one another. However, boundary potentials can be estimated theoretically using some model calculations. According to the theoretical estimations, these potentials can reach up to several hundred mVs [2–7].

In reality, the mechanism of the boundary potential formation is more complicated. In the first place, no real-world objects are ideally neutral: they always bear some small electric charge. For instance, even if you have an ideally neutral solution in an ideally neutral bottle, and you pour this solution into an ideally neutral beaker, all these phases will acquire some electric charge. This happens due to the wall friction of solution in the bottle and in the beaker while pouring. Thus, the aqueous phase and the organic phase in our aforementioned example must bear some accidental, fortuitous charges already before contact. Furthermore, both phases (not only the aqueous solution) may contain electrolytes before fusion. However, this does not change the final result. The only difference is that if the organic phase is initially charged, for example, more positively than the aqueous phase, the number of the excessive cations in the organic phase will be smaller than in the “ideal” case, and the “gap” will be filled with the accidental charges acquired due to friction or to some other force. The distribution of the electrolytes between the two phases will not be affected by the accidental charges, because the number of the latter is negligible when compared with the total number of partitioning ions. As for the interfacial potential, its value is the same as in the “ideal” case, although some of the ions forming the electrical double layer belong to the partitioning electrolyte while the rest are of “accidental” origin. In the opposite case, when the organic phase is initially negatively charged, it will gain a few more excessive cations than in the “ideal” case. The only issue of importance is the equality of the two driving forces: chemical and electric.

Although we have discussed the origin of the boundary potentials considering the interface between aqueous and organic phases, the same physics underlies boundary potentials between various materials. This includes interfaces between aqueous solutions and ionically conducting inorganic phases like crystals and glasses, which are used as ion-selective membrane materials, along with organic liquids and polymers. The processes underlying potentials between an ionically conducting phase and an electronic conductor (metal) are slightly different, see [Sect. 8.2](#).

2.2.2 Formal Thermodynamical Description of Boundary Potential

Now, having the physical idea about the origin of boundary potentials between aqueous solution and some other phase (which we will call “electrode”), we will discuss this kind of potentials using a strict thermodynamic approach.

If an electrode is immersed into a solution, and the interface between the solution and the electrode is at electrochemical equilibrium in relation to species I^z (z_I stands for the *charge number*² of the species), the value of the *electrochemical potential* $\tilde{\mu}$ of this species is the same in the solution phase and in the electrode phase:

$$\tilde{\mu}_I^{\text{solution}} = \tilde{\mu}_I^{\text{electrode}} \quad (2.1)$$

In turn, the electrochemical potential of a species located in a certain part within the phase relates to μ_I the *chemical potential* of this species and ϕ the *electrical potential* in this part of the phase:

$$\tilde{\mu}_I = \mu_I + z_I F \phi \quad (2.2)$$

Here, F is the Faraday constant. The sensitivity of a species to the electric potential is proportional to the species charge, and this is why z_I appears in Eq. (2.2).

Note, in contrast with the chemical potential μ_I and the charge z_I , the electric potential term ϕ does not contain index I . This is because the former parameters refer to the particular species I^z and their values are different for different species, while the electric field—and therefore also the electric potential—is the same in the particular part of the space, resulting from all the species involved, and also affecting all the species involved.

Combining Eqs. (2.1) and (2.2), we obtain for boundary potential at equilibrium:

$$\varphi_b = \phi^{\text{electrode}} - \phi^{\text{solution}} = -\frac{\mu_I^{\text{electrode}} - \mu_I^{\text{solution}}}{z_I F} \quad (2.3)$$

Equation (2.3) represents the intuitive physical description of the electrochemical equilibrium in strict terms. Indeed, at equilibrium, the electric potential difference compensates for the difference between the chemical potentials of the

² Charge number (valency) is an integer indicating the number of elementary charges carried by the species. One elementary charge equals 1.60×10^{-19} C. For instance, an electron carries an electric charge of -1.60×10^{-19} C, and a calcium cation carries an electric charge of $+3.20 \times 10^{-19}$ C, so the respective charge numbers are -1 and $+2$. Rigorously speaking, we must use term “charge number” to characterize the electric charge of the species. In practice, however, we never do so, and instead of “charge number”, we just say “charge,” like charge of electron is -1 and charge of calcium cation is $+2$. Therefore, throughout the text, the term “charge” will be used for “charge number.”

species in the two phases, which refer to the affinity of the species to the respective phases.

The chemical potential of the species within a system is defined as partial Gibbs free energy of the system (in the case of a charged species—except of the electric part of the free energy) related to this particular kind of species:

$$\mu_I = \left(\frac{dG}{dn_I} \right)_{p,T,n_{j \neq I}} \quad (2.4)$$

Here, G , p , and T stand for the Gibbs free energy of the phase, the pressure, and the absolute temperature. Thus, the chemical potential of species I^z is a partial derivative of the Gibbs free energy over the number of moles of species I^z at a constant pressure, temperature, and the numbers of moles of all other kinds of species present in the system. The value of G , as that of any energy quantity, cannot be determined to an absolute value. It is only determined in relation to some standard state, and one can only measure ΔG the difference in G between the current state of the system and the standard state. Thus, $G = G^0 + \Delta G$. One could think that differentiation eliminates G^0 and therefore we may have the absolute value of μ_I . This, however, is not true, because $G = U - TS$ (U stands for the internal energy and S for the entropy of the system), and $G^0 = U^0 - TS^0$, while U^0 and S^0 are extensive values which are proportional to the mass of the system. Therefore, $(dG^0/dn_I)_{p,T,n_{j \neq I}} \neq 0$ and chemical potential can only be determined in relation to some standard state (some reference point):

$$\mu_I = \mu_I^0 + RT \ln a_I \quad (2.5)$$

Here, μ_I^0 is the standard value of the chemical potential, that is, the chemical potential of species I^z in the standard state, R is the gas constant, and a_I is the activity of species I^z in the phase. The standard state can be chosen at our own will; however, some choices may be more convenient than others.

Very often, it is said that activity is a kind of “active concentration,” that is, C_I concentration value is “corrected” to comply with strict thermodynamic relations. The correction is represented by γ_I *activity coefficient*, so that

$$a_I = \gamma_I C_I \quad (2.6)$$

Sometimes one claims that Eq. (2.6) defines activity as “concentration multiplied by activity coefficient.” In fact, the reverse is true: Eq. (2.6) defines activity coefficient, while activity is defined as a function which satisfies the following equation:

$$a_I = \exp((\mu_I - \mu_I^0)/RT) \quad (2.7)$$

Obviously, Eq. (2.7), which defines activity, is just a rewritten Eq. (2.5).

Combining Eqs. (2.3) and (2.5), we obtain for the electric potential difference between the electrode and solution (the boundary potential):

$$\varphi_b = \phi^{\text{electrode}} - \phi^{\text{solution}} = -\frac{\mu_I^{0,\text{electrode}} - \mu_I^{0,\text{solution}}}{z_I F} - \frac{RT}{z_I F} \ln \frac{a_I^{\text{electrode}}}{a_I^{\text{solution}}} \quad (2.8)$$

Equation (2.8) is known as *Nernst equation*. If for whatever reason (to be discussed in later chapters) the activity of I^{z_I} in the electrode phase is constant, the interfacial potential follows a very simple formula:

$$\varphi = \varphi^0 + \frac{RT}{z_I F} \ln a_I^{\text{solution}} \quad (2.9)$$

Term φ^0 includes the constant terms $-(\mu_I^{0,\text{electrode}} - \mu_I^{0,\text{solution}}/z_I F)$ and $-(RT/z_I F) \ln a_I^{\text{electrode}}$. The potential difference φ is called electrode potential. Thus, the electrode potential is regularly dependent on the activity of ion I^{z_I} , and this makes the prerequisite for use of the electrode as a sensor of species I^{z_I} .

2.3 Diffusion Potential

2.3.1 The Physical Nature of the Diffusion Potential

Unlike boundary potentials arising at interfaces between contacting phases, diffusion potentials arise within homogeneous phases with non-uniform distribution of electrolytes. If an electrolyte is non-uniformly distributed within a solution, the electrolyte diffuses from layers with higher value of the chemical potential of the electrolyte to layers with lower chemical potential, very often, just from layers with higher concentration to layers with lower concentration of the electrolyte. In general, I^+ and X^- ions forming the electrolyte have different diffusion coefficients D_I , D_X and, respectively, also different mobilities u_I , u_X , see Eq. (2.10):

$$u_n = D_n/RT \quad (2.10)$$

This difference results in small, but regular charge separation, and therefore in a potential difference called diffusion potential—because it originates, ultimately, due to diffusion.

Let us try to understand the origin of the diffusion potential using a very simple model presented in Fig. 2.2. A 1:1 electrolyte producing I^+ cations and X^- anions with diffusion coefficients D_I and D_X is non-uniformly distributed within the volume of the phase. The electrolyte concentration along the x -axis decreases as shown in Fig. 2.2.

Now assume that at time $t = 0$, the phase is “frozen,” that is, ions are not allowed to move. We can (in one’s mind) slice the phase into thin layers with uniform distribution of the electrolyte within each layer, thus representing the continuous profile of the electrolyte concentration with a stepped line. Let us assume there is no regular charge separation: neither within each of the slices, nor

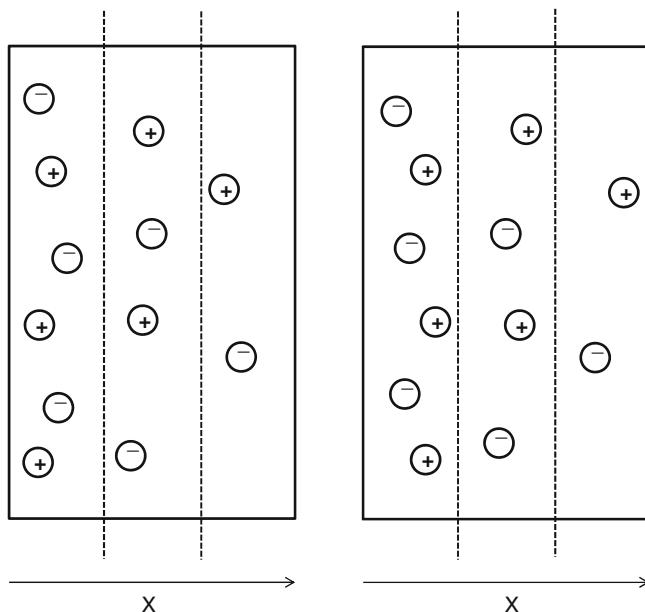


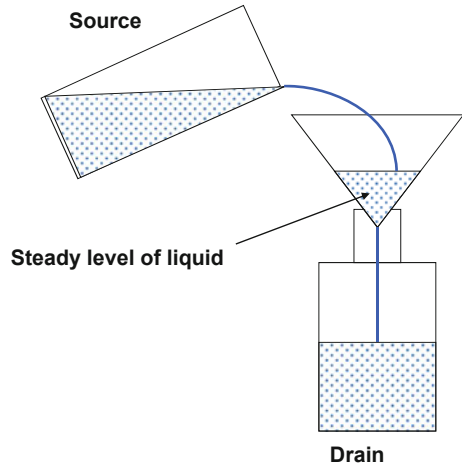
Fig. 2.2 Origin of the diffusion potential. *Left*: “frozen” phase, in one’s mind divided into thin layers. The concentration decreases from the *left* layer to the *right* layer; each layer is electrically neutral; ions are randomly distributed. *Right*: ions allowed to diffuse from *left* to *right*. Each layer remains electrically neutral, but cations are slightly shifted to the right relative to anions

within the whole phase.³ If we allow ions to move, they will diffuse along the x -axis from left to right. Let us assume $D_I > D_X$. In such a case, in the beginning of the diffusion process, cations within each slice will slightly pass the anions. This will produce some regular charge separation along the x -axis within each of the slices. The resulting regular Coulombic forces will speed up the anions and slow down the cations within each slice, preventing further charge separation. Thus established, regular charge separation produces a minute potential difference within each slice, which taken over the whole phase may reach up to several dozens of mVs, according to model calculations [2–8]. This is how diffusion potential arises.

There is a fundamental difference between interfacial and diffusion potentials. Interfacial potentials (when established) refer to equilibrium states and result from differences in equilibrium values: the chemical potentials of charged species in the contacting phases. Stable values of interfacial potentials, in principle, can last forever. Diffusion potentials refer to non-equilibrium states and result from differences in non-equilibrium values: mobilities of ions. Steady values of diffusion

³ Due to thermal movement, some random, chaotic charge separation always exists on short distances. However, being averaged over space and time, it produces zero effect.

Fig. 2.3 Simple example of a steady state: using a funnel when filling a glass



potentials refer to steady states. Let us take a look at these states. Under equilibrium state, there are no fluxes of matter or energy within the system.⁴ If the system is not at equilibrium, there are fluxes of matter driven by gradients of chemical potentials of the species. Now, if the flux is constant over space (e.g., diffusion flux over the x -axis) while the profile of the driving force is constant over time, we have the so-called steady state.

There is a very simple example of steady state, see Fig. 2.3. Let us assume, you pour a liquid from one large glass to another one. To avoid spilling, you use a funnel. It is easy to ensure a constant level of liquid in the funnel: when the flux of liquid coming from the source glass to funnel equals that from the funnel to the drain glass. You have established a constant level of the liquid in the funnel and constant flux along the whole system, from source to drain. Note: you will need some time to adjust the stream before the steady state is established, and you cannot maintain it forever: either the source empties, or the drain overfills. In general, a long-lasting steady state requires either a large source and a large drain, or a very small flux.

2.3.2 *The Mathematical Description of the Diffusion Potential*

There are different approaches aimed at mathematical description of the diffusion potential. We will discuss here the simplest case, which is when diffusion takes place along only one direction—along x -axis. This simplest case is the most

⁴ Some local fluctuations and local fluxes always exist except at absolute zero; however, they do not produce any macroscopic effect due to averaging over space and time.

relevant for all further discussions. We will use the *Nernst–Planck equation* for the flux of the I^z charged species along the x -axis:

$$J_I = -u_I C_I \frac{d\tilde{\mu}_I}{dx} = -u_I C_I \left(RT \frac{d \ln a_I}{dx} - z_I F \frac{d\phi}{dx} \right) \quad (2.11)$$

Although we omit its derivation, the equation's meaning is very clear: the flux depends on how fast the species moves (u_I), on the concentration of the species (C_I), and on the driving force of the flux: the gradient of $\tilde{\mu}_I$ the electrochemical potential along x coordinate. The negative sign before the right-hand part in Eq. (2.11) appears because the species moves from high to low values of $\tilde{\mu}_I$.

We discuss potentiometric sensors, so the measurements are performed under zero-current conditions: $I = 0$. On the other hand, in a system containing k sorts of charged species, the current density relates to the respective fluxes in a very simple way:

$$I = F \sum_{n=1}^k z_n J_n \quad (2.12)$$

Thus,

$$\sum_{n=1}^k \left(z_n u_n C_n \left(RT \frac{d \ln a_n}{dx} + z_n F \frac{d\phi}{dx} \right) \right) = 0 \quad (2.13)$$

By rearranging Eq. (2.13), we obtain for the differential of the diffusion potential:

$$d\phi = - \frac{RT \sum_{n=1}^k d(z_n u_n C_n \ln a_n)}{F \sum_{n=1}^k (z_n^2 u_n C_n)} \quad (2.14)$$

The value of the diffusion potential is given by

$$\varphi_d = - \frac{RT}{F} \int_{\text{left}}^{\text{right}} \frac{\sum_{n=1}^k (z_n u_n C_n d \ln a_n)}{\sum_{n=1}^k (z_n^2 u_n C_n)} \quad (2.15)$$

Integration requires knowledge on the profiles of activities and concentrations along the x -axis for all charged species present in the system. Generally speaking, this is not possible. Recently, advanced models have been developed which allow for numerical simulations of species concentration profiles and the electric potentials in real time and space, under certain assumptions [4–7, 9–11]. However, there are situations for which Eq. (2.15) can be simplified and easily solved for the respective special cases.

It is of importance to understand that diffusion potentials, as well as interfacial potentials cannot be rigorously measured and we can only approximate their values.

2.3.3 The Segmented Model of the Overall Membrane Potential

The overall membrane potential is the potential difference generated on a membrane dividing two solutions. This difference is zero in symmetric systems when a uniform membrane divides two identical solutions. A non-zero membrane potential arises in two cases: (1) solutions are non-identical, and (2) the membrane is non-uniform. It is convenient to split the overall membrane potential in three components: two boundary potentials at the membrane/solution interfaces and diffusion potential within the membrane, as shown in Fig. 2.4.

The solid horizontal lines show the potentials in the solutions far from the membrane. Within the space-charge regions 1 and 2—on both sides of the membrane, there are steep drops of the potential. These are boundary potentials φ_b^1 , φ_b^2 . The thickness of the space-charge regions is very much exaggerated in the figure. In fact, these are a few nm on the aqueous side, and up to 100–300 nm on the membrane side (for polymeric membranes with ionophores). This is why vertical dotted lines which show the physical borders of the membrane are shifted from the center of the space regions. Gently sloped solid line within the membrane bulk shows φ_d —the diffusion potential. The boundary potentials, typically, have opposite signs and partly eliminate each other. Therefore, φ_m —the overall membrane potential—is much smaller than any of the boundary potential drops.

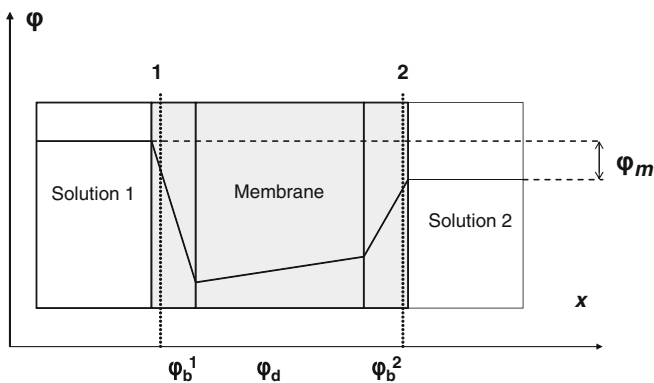


Fig. 2.4 The segmented model of the overall membrane potential

2.4 Galvanic Cells without Liquid Junction and with Liquid Junction, Advantages and Disadvantages Thereof

As mentioned in Chap. 1, potential of an individual electrode cannot be measured. One can only measure the difference of the potentials of two electrodes contacting via solution, as shown in Fig. 1.2. This construct containing the sensor electrode (also known as the indicator electrode [ISE]), the other (reference) electrode, and solution is called galvanic cell. Systems containing only one electrode in contact with the respective solution are often called half-cells.

The potential difference between the sensor electrode and the reference electrode (RE) is called electromotive force (EMF) of the cell:

$$E = \varphi - \varphi_{\text{RE}} \quad (2.16)$$

2.4.1 Cells without Liquid Junction

Let us imagine, we have two ideally working electrodes (i.e., both electrodes obey the Nernst equation). One electrode is cation-responding, and the other one is anion-responding. For further clarity, let these electrodes respond, for example, to potassium cation and to chloride anion:

$$\varphi_K = \varphi_K^0 + \frac{RT}{z_K F} \ln a_K \quad (2.17)$$

$$\varphi_{\text{Cl}} = \varphi_{\text{Cl}}^0 + \frac{RT}{z_{\text{Cl}} F} \ln a_{\text{Cl}} \quad (2.18)$$

If we immerse these two electrodes into a pure KCl solution, that is, solution containing only KCl and water, and connect the electrodes to a measuring device (as shown in Fig. 2.5, left), we will measure the EMF:

$$E = \varphi_K^0 + \frac{RT}{z_K F} \ln a_K - \varphi_{\text{Cl}}^0 - \frac{RT}{z_{\text{Cl}} F} \ln a_{\text{Cl}} \quad (2.19)$$

Since $z_K = 1$, $z_{\text{Cl}} = -1$, Eq. (2.19) transforms into

$$E = \varphi_K^0 - \varphi_{\text{Cl}}^0 + \frac{RT}{F} \ln a_K + \frac{RT}{F} \ln a_{\text{Cl}} = E^0 + \frac{RT}{F} \ln(a_K a_{\text{Cl}}) = E^0 + \frac{2RT}{F} \ln a_{\pm\text{KCl}} \quad (2.20)$$

Here, $E^0 = \varphi_K^0 - \varphi_{\text{Cl}}^0$ is the so-called standard EMF value, and $a_{\pm\text{KCl}} = \sqrt{a_K a_{\text{Cl}}}$ is the so-called mean activity of KCl. The mean activity of an electrolyte is a thermodynamically determined quantity. It can be experimentally measured by

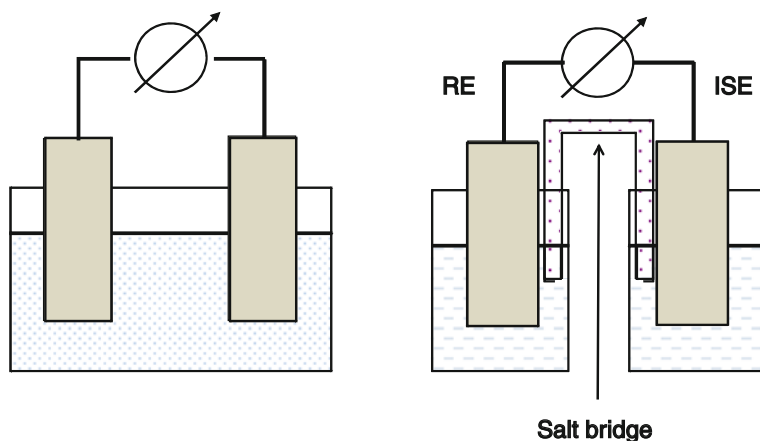


Fig. 2.5 *Left*—cell without liquid junction, *right*—cell with liquid junction

various independent techniques, such as isopiestic measurements, cryoscopy, ebullioscopy, extraction measurements, etc.

If we have two electrodes both responding to ions of the same charge, for example, two anions like chloride and nitrate, immersed in a mixed solution containing NaCl and NaNO₃, the respective EMF obeys the following expression:

$$\begin{aligned}
 E &= \varphi_{\text{Cl}} - \varphi_{\text{NO}_3} = \left(\varphi_{\text{Cl}}^0 - \frac{RT}{F} \ln a_{\text{Cl}} \right) - \left(\varphi_{\text{NO}_3}^0 - \frac{RT}{F} \ln a_{\text{NO}_3} \right) \\
 &= \varphi_{\text{Cl}}^0 - \varphi_{\text{NO}_3}^0 - \frac{RT}{F} \ln \frac{a_{\text{Cl}}}{a_{\text{NO}_3}}
 \end{aligned} \quad (2.21)$$

We can multiply the numerator and the denominator in the last term in Eq. (2.21) by the same quantity, for example, by a_{Na} and then the EMF is

$$E = \varphi_{\text{Cl}}^0 - \varphi_{\text{NO}_3}^0 - \frac{RT}{F} \ln \frac{a_{\text{Cl}} a_{\text{Na}}}{a_{\text{NO}_3} a_{\text{Na}}} = \varphi_{\text{Cl}}^0 - \varphi_{\text{NO}_3}^0 - \frac{2RT}{F} \ln \frac{a_{\pm \text{NaCl}}}{a_{\pm \text{NaNO}_3}} \quad (2.22)$$

Thus, again we obtain an expression containing only thermodynamically defined quantities.

Galvanic cells shown in Fig. 2.5 left—when both electrodes are immersed into the same solution—are called cells without liquid junction. The whole system, comprised of both electrodes and solution, is at equilibrium. Therefore, the EMF of a galvanic cell without liquid junction is thermodynamically well defined. This is a significant advantage of this kind of cell, and therefore, measurements with cells without liquid junction are routinely used in thermodynamic studies.

However, the vast majority of measurements with ISEs are made for analytical rather than for thermodynamic objectives, and for analytical goals, this kind of cell is not suitable. Let us discuss this issue using the same pair of electrodes—those responding to K⁺ and to Cl⁻. Furthermore, let us assume we wish to know the

potassium ion concentration: C_K . In a pure KCl solution, $C_K = C_{Cl} = C_{KCl} = a_{\pm KCl}/\gamma_{\pm KCl}$. Having $a_{\pm KCl}$ from the EMF measurements (see Eq. 2.20), and an independently known value of $\gamma_{\pm KCl}$, one can obtain the target quantity C_K . However, in mixed aqueous solutions, leaving alone real-world samples of various origins, measurements with cells without liquid junction are not practical. Let us assume we now have a mixed solution of KCl and NaCl. In this solution, the activity and concentration of our target ion (K^+) relate to one another as $a_K = C_K\gamma_K = C_{KCl}\gamma_K$. Thus, only KCl directly contributes to K^+ -ion activity, in full analogy with pure KCl solution (although the presence of NaCl also indirectly affects a_K because γ_K the potassium-ion activity coefficients in pure and mixed solutions with the same C_K are not the same). The respective relation for Cl^- is very different from that in a single salt solution $a_{Cl} = C_{Cl}\gamma_{Cl} = (C_{KCl} + C_{NaCl})\gamma_{Cl}$; thus, Cl^- -ion activity is directly affected by both salts: KCl and NaCl. The mean activity of KCl in mixed KCl + NaCl solution relates to the concentrations of the respective electrolytes as follows:

$$a_{\pm KCl} = \sqrt{C_{KCl}\gamma_K(C_{KCl} + C_{NaCl})\gamma_{Cl}} \quad (2.24)$$

One can see that $a_{\pm KCl}$ —the value obtained from measurements using cell without liquid junction—is not unambiguously related to K^+ ion concentration if some other electrolyte is also present in the sample.

Below, an example is given on how large the error caused by use of cell without junction may be for analysis of a mixed solution. Once again, let us consider galvanic cell consisting of K^+ and Cl^- electrodes, both responding to the respective ions, and assume that the standard EMF value of the cell is 200.0 mV, and the slope is 118.0 mV/log $a_{\pm KCl}$. If the electrodes are immersed into pure 0.01 M KCl solution with $\gamma_{\pm KCl} = 0.91$, the measured EMF is as follows:

$$E = 200.0 + 118.0 \cdot \log(0.01 \cdot 0.91) = -40.8 \text{ mV}$$

If the same electrodes are immersed into mixed solution containing the same 0.01 M KCl, and also 0.1 M NaCl, with $\gamma_{\pm KCl} = 0.79$ (this value is calculated by Debye-Hückel theory, see Sect. 2.5.), the measured EMF is as follows:

$$E = 200.0 + 118.0 \cdot \log\left(\sqrt{0.01(0.01 + 0.1)} \cdot 0.79\right) = 13.0 \text{ mV}$$

The difference between the values is 53.8 mV, and K^+ ion concentration in the latter case (mixed solution) is 2.9 times overestimated.

Obviously, for measurements of a target analyte in a mixed sample, we must have another kind of galvanic cell. This other kind of cell is called cells with liquid junction and is described below.

2.4.2 Cells with Liquid Junction

Obviously, if we wish to measure an individual species concentration via the potential of respective electrode, the potential of the other electrode must be constant. In our previous example, this means that Cl^- -responding electrode has to have a constant potential. If this is achieved, the EMF varies exclusively due to the variation of K^+ -responding electrode potential, and it delivers information on the K^+ ion concentration in the sample. The other electrode (Cl^- electrode in our example) is then called reference electrode (*RE*). Attempts to make electrodes with constant potentials whatever the sample composition are well known, and there is some progress in solving this problem [12]. The reliability of these REs so far remains insufficient. The commonly used approach is, therefore, different. The electrode to be used as the RE is placed in a separate vessel, and in this way, the constancy of its potential is guaranteed. The two half-cells—the sample vessel with the ISE and the reference vessel with the RE—are connected with one another via the so-called salt bridge, as shown schematically in Fig. 2.5, right.

Earlier, the common RE used to be the so-called saturated calomel electrode: $\text{Hg}/\text{Hg}_2\text{Cl}_2$ in saturated KCl. Because of the toxicity of mercury metal and of mercury salts, this electrode was replaced by silver chloride electrode, and nowadays, Ag/AgCl electrode immersed in 3 M KCl or in saturated KCl has become the most common RE. The concentration of a saturated solution is constant even if the vessel is not hermetically closed. This advantage, however, is largely depreciated by the temperature dependence of the solubility. Therefore, 3 M KCl is predominating as the RE solution.

It is more practical to immerse RE directly into sample or calibrator solutions, rather than use the setup shown in Fig. 2.5. The respective constructs, the so-called *single-junction RE* and *double-junction RE*, are discussed in more detail in Sect. 9.1.

The region of the contact of the salt bridge with the sample solution is called *liquid junction*. This term reflects the lack of a phase boundary between the sample solution and the bridge solution. The compositions of the salt bridge electrolyte and the sample are, generally speaking, different. Therefore, the respective electrolytes diffuse from the bridge to the sample and vice versa, driven by the gradients of their chemical potentials. Thus, in between the bulk of the sample solution and the bulk of the bridge solution, a layer arises with composition, which gradually varies from the composition of the sample to the composition of the bridge solution. This layer is called *diffusion layer*, because all of the electrolytes present in the system diffuse across this layer according to the respective gradients of chemical potentials.

Over time of the contact, the diffusion layer expands, and the sample gets contaminated by the species from the salt bridge solution, while the latter gets contaminated by the species from the sample. Therefore, normally the salt bridge is relatively thin tubing, and various measures can be taken to minimize the aforementioned mutual contamination.

Electrolytes diffuse from the RE to sample and vice versa. However, mobilities of ions differ; some ions move faster than the other. Because of this, a potential difference arises over the diffusion layer. This potential is called *liquid junction potential*, and it is of diffusion nature (see also Sect. 2.3.). Thus, the EMF of a cell with liquid junction combines not only the potentials of the ISE and the RE, but also the liquid junction (diffusion) potential:

$$E = \varphi_{\text{ISE}} - \varphi_{\text{RE}} + \varphi_d \quad (2.25)$$

The very idea of the cell is therefore somewhat compromised: we want to measure the variation of the ISE potential against a constant RE potential, but we actually have an additional term which also contributes to the measured signal. Obviously, to achieve our goal, we must make the liquid junction potential constant or simply minimize its value, which is given by [13]:

$$\varphi_d = -\frac{RT}{F} \sum_{n=1}^k \int_{\text{sample}}^{\text{bridge}} \frac{t_n}{z_n} d \ln a_n \quad (2.26)$$

Thus, the liquid junction potential can be presented as a sum of integrals for each kind of the charged species (from 1 to k) present in the diffusion layer. The limits of integration are obviously the bulk of the sample and the bulk of the bridge—the domains with constant compositions not affected by diffusion.

The values of a_n —the activities of the species—vary from the respective values in the sample to those in the bridge. Term t_n is called *transference number*, and it is defined as the part of q_n the electric charge transferred by the n th sort of species to the total charge transferred across the diffusional layer by all the species present:

$$t_n = \frac{|q_n|}{\sum_{n=1}^k |q_n|} \quad (2.27)$$

According to this definition, $\sum_{n=1}^k t_n = 1$. The electric charge transferred by a species equals J_n the flux of the species multiplied by z_n : $q_n = z_n F J_n = z_n^2 F u_n C_n$.⁵ Thus, t_n transference number of species n can be calculated as

$$t_n = \frac{z_n^2 u_n C_n}{\sum_{n=1}^k z_n^2 u_n C_n} \quad (2.28)$$

⁵ This equation appears very different from Eq. 2.11. The difference comes from the procedure of the measurements of the transference numbers. These are performed in a uniform solution (no activity gradients, so $d \ln a_i / dx = 0$), and the results are normalized to 1 unit of the electric field: $d\varphi/dx = 1$, for example, 1 V/m, or 1 V/cm, or whatever. In fact, this normalization does not really matter because in Eq. 2.28, the respective terms eliminate anyway.

Bearing in mind Eq. (2.28), one can easily see that Eq. (2.26) is equivalent to Eq. (2.15).

Let us assume that we have only one uni-univalent electrolyte IX in the diffusion layer, so that the diffusing species are I^+ and X^- . Then the liquid junction potential is

$$\varphi_d = -\frac{RT}{F} \int_{\text{sample}}^{\text{bridge}} \frac{u_I C_I}{(u_I C_I + u_X C_X)} d \ln(C_I \gamma_I) + \frac{RT}{F} \int_{\text{sample}}^{\text{bridge}} \frac{u_X C_X}{(u_I C_I + u_X C_X)} d \ln(C_X \gamma_X) \quad (2.29)$$

Due to the macroscopic electroneutrality, $C_I = C_X$ everywhere over the diffusion layer. Thus, if the mobilities of I^+ and X^- are equal, $u_I = u_X$, the liquid junction potential is almost eliminated because the two integrals in Eq. (2.29) differ only inasmuch as activity coefficients differ.

Filling the salt bridge with electrolyte consisting of ions with nearly equal mobilities is the most common approach aimed at minimization of the liquid junction potential. Such electrolytes are called *equitransferring electrolytes*. Among electrolytes with nearly equal mobilities of the cation and the anion are KCl, LiCH_3COO , NH_4NO_3 . The most commonly used electrolyte for salt bridges is 3 M KCl. If ions with equal mobilities predominate over other species in the diffusion layer, the respective transference numbers approach 0.5, while transference numbers of all other species approach zero. This is the reason to use high concentration of equitransferring electrolytes in salt bridges. Furthermore, if only two sorts of species (K^+ and Cl^-) predominate in diffusion, the liquid junction potential remains constant as long as the system is in steady state, even though the diffusion layer widens over time.

Minimization of the liquid junction potential makes cells with liquid junction practical, and the activity of the target analyte can be calculated from the measured EMF by equation

$$E = E^0 + 2.3026 \frac{RT}{z_I F} \log a_I + \varphi_{LJ} \quad (2.30)$$

where the last term is either neglected or calculated according to Henderson formalism. The real-world electrodes never obey Eq. (2.30) exactly: the slope $S = dE/d \log a_I$ differs from the theoretical value $2.3026 RT/z_I F$ which, at 25 °C, equals $59.2/z_I \text{ mV}/\log a_I$. Normally, the experimental slope values are slightly below this number.

More important, however, is another issue. Unlike $a_{\pm IX}$ —the mean activity of electrolyte, activity of I^+ single ion cannot be measured independently (the problem of single-ion activity is discussed in Sect. 2.5.) One may think that the use of thermodynamically undetermined values—single-ion activities and diffusion potentials—makes cells with liquid junction somewhat “fishy.” Below we will try to see whether this is true, using as example the same pair of electrodes, responding to K^+ and to Cl^- ions.

Let us imagine a cell with liquid junction, such as that shown in Fig. 2.5, right: the K^+ —responding electrode (ISE) is placed into right part of the system, with low concentration of KCl; and the Cl^- —responding electrode (RE) is placed into left part, with high concentration of KCl. Both electrodes obey the Nernst equation, so that the EMF of the cell is

$$E = \varphi_K - \varphi_{Cl} + \varphi_d = \varphi_K^0 - \varphi_{Cl}^0 + \frac{RT}{F} \ln a_K^{\text{right}} + \frac{RT}{F} \ln a_{Cl}^{\text{left}} + \varphi_d \quad (2.31)$$

For the liquid junction potential, using Eq. (2.26), we can write

$$\varphi_d = -\frac{RT}{F} \int_{\text{left}}^{\text{right}} \left(\frac{t_K}{z_K} d \ln a_K + \frac{t_{Cl}}{z_{Cl}} d \ln a_{Cl} \right), \quad (2.32)$$

and eliminating t_{Cl} as $t_{Cl} = 1 - t_K$ we rearrange it as follows:

$$\begin{aligned} \varphi_d &= -\frac{RT}{F} \int_{\text{left}}^{\text{right}} t_K d \ln a_K + \frac{RT}{F} \int_{\text{left}}^{\text{right}} d \ln a_{Cl} - \frac{RT}{F} \int_{\text{left}}^{\text{right}} t_K d \ln a_{Cl} \\ &= -\frac{RT}{F} \int_{\text{left}}^{\text{right}} t_K d \ln(a_K a_{Cl}) + \frac{RT}{F} \ln \frac{a_{Cl}^{\text{right}}}{a_{Cl}^{\text{left}}} \end{aligned} \quad (2.33)$$

By combining Eqs. (2.31) and (2.33), we obtain for the EMF of the cell:

$$E = \varphi_K^0 - \varphi_{Cl}^0 + \frac{RT}{F} \ln(a_K^{\text{right}} a_{Cl}^{\text{right}}) - \frac{RT}{F} \int_{\text{left}}^{\text{right}} t_K d \ln(a_K a_{Cl}), \quad (2.34)$$

which finally gives

$$E = \varphi_K^0 - \varphi_{Cl}^0 + \frac{2RT}{F} \ln(a_{\pm KCl}^{\text{right}}) - \frac{2RT}{F} \int_{\text{left}}^{\text{right}} t_K d \ln(a_{\pm KCl}) \quad (2.35)$$

Equation (2.35) contains parameters which can be independently measured: mean activities of electrolyte (KCl in our example) and transference number of K^+ . If we eliminate t_K as $t_K = 1 - t_{Cl}$, we would get a similar expression containing t_{Cl} . Nobody claims it is easy to measure transference numbers along the whole diffusion layer. The point is, however, that these values, in principle, can be measured. Thus, when the EMF of a cell with liquid junction is considered as a whole, it is in no way “thermodynamically worse” than that of a cell without liquid junction. Uncertainties and problems with thermodynamics arise from our methods of interpreting the EMF. Once we wish to split the whole EMF into separate electrode potentials, we immediately encounter problems of the single-ion activity

and the diffusion potential. However, our practical analytical goals force us to do so, and this is why we must somehow deal with these problems.

2.5 The Mean Electrolyte Activity and the Single-Ion Activity. The Elements of the Debye–Hückel Theory

For a solution containing two components, solvent and $I_{v+}X_{v-}$ electrolyte, using the Gibbs–Duhem equation, one can obtain for the activities at equilibrium:

$$\frac{a_I^{v+} a_X^{v-}}{a_{IX}} = K, \quad (2.36)$$

K is constant, and its value depends on the standard state chosen for the electrolyte. Since the standard state can be chosen at will, we chose the standard states for ions as

$$\left. \begin{aligned} \lim_{C_{IX} \rightarrow 0} a_I &= C_I = v_+ C_{IX} \\ \lim_{C_{IX} \rightarrow 0} a_X &= C_X = v_- C_{IX} \end{aligned} \right\} \quad (2.37)$$

According to this choice, the ion activity approaches the ion concentration along with dilution of the solution. This choice is the most convenient from the practical point of view. For the electrolyte, the standard state is chosen in such a way that $K = 1$, so that single-ion activities and the so-called full electrolyte activity relate to each other according to

$$a_I^{v+} a_X^{v-} = a_{IX} \quad (2.38)$$

As to mean activity of the electrolyte and mean activity coefficient, these are defined as

$$\left. \begin{aligned} a_{\pm IX} &= a_{IX}^{1/v} = (a_I^{v+} a_X^{v-})^{1/v} \\ \gamma_{\pm IX} &= \gamma_{iX}^{1/v} = (\gamma_I^{v+} \gamma_X^{v-})^{1/v} \end{aligned} \right\}, \quad (2.39)$$

with $v = v_+ + v_-$.

As already mentioned above, full and mean electrolyte activities are thermodynamically well-defined quantities, and their values can be experimentally measured by various independent techniques. On the contrary, the single-ion activity cannot be measured, and only combinations of single-ion activities like multiples of cation and anion activities, or ratios of two cations or two anions activities are accessible: $a_I a_X = a_{IX}$, $a_I/a_J = a_{IX}/a_{JX}$, $a_X/a_Y = a_{IX}/a_{IY}$.

To access single-ion activities, one has to introduce some extra-thermodynamic assumptions. These are either arbitrarily chosen rules for the fragmentation of full electrolyte activities into single-ion activities, or theoretical calculations based on some models aimed at consideration of the non-ideality of real systems.

The most common fragmentation rule for aqueous solutions is the so-called McInnes assumption—ion activity of K^+ cation and that of Cl^- anion in KCl solutions are equal to one another and therefore equal also to the mean activity of KCl:

$$a_K = a_{Cl} = \sqrt{a_K a_{Cl}} = a_{\pm KCl} \quad (2.40)$$

This assumption can be utilized for calculation of other single-ion activities. Let us illustrate this using the calculation of Na^+ cation activity in NaCl solution. Indeed, according to Eq. (2.38),

$$a_{Na}^{NaCl} = \frac{(a_{\pm NaCl}^{NaCl})^2}{a_{Cl}^{NaCl}}$$

Next, we replace the Cl^- anion activity in NaCl solution with that in the KCl solution of the same concentration, and using the McInnes assumption, we finally get

$$a_{Na}^{NaCl} = \frac{(a_{\pm NaCl}^{NaCl})^2}{a_{\pm KCl}^{KCl}}$$

In the same way, one can use the McInnes assumption for calculation of activities of various cations and anions. Less common is the so-called Guggenheim assumption: $a_{Ca} = a_{Cl} = \sqrt[3]{a_{Ca} a_{Cl}^2} = a_{\pm CaCl_2}$. One can use it in the same way as the McInnes assumption to calculate ion activities in different solutions.

Fragmentation rules do not help in the most typical cases: mixed solutions containing several electrolytes. The single-ion activity values for these systems can be calculated using the Debye-Hückel theory. This theory accounts to electrostatic interactions only. Under the first approximation of the theory, ions are considered infinitely small. According to this approximation, the I^z ion activity coefficient is determined by J —the so-called ionic strength of the solution:

$$\log \gamma_I = -Az_I^2 \sqrt{J} \quad (2.41)$$

For a solution containing n sorts of ions, the ionic strength is dependent on the concentrations and charges of all sorts of ions present in the solution:

$$J = \frac{1}{2} \sum_{k=1}^n C_k z_k^2 \quad (2.42)$$

For instance, the ionic strength of 0.01 M KCl equals 0.01 M, for 0.01 M $CaCl_2$ $J = 0.03$ M, and for mixed solution of 0.1 NaCl + 0.01 K_2SO_4 $J = 0.13$ M. The A constant in Eq. (2.41) is dependent on e —the elementary charge value, N_A —the Avogadro number, ϵ_0 —the vacuum dielectric permittivity, ϵ —the relative dielectric permittivity of the solution, k —the Boltzmann constant, and T —the absolute temperature:

$$A = \frac{e^3 \sqrt{N_A}}{2.3026\pi 4 \sqrt{2(\epsilon_0 \epsilon kT)^{3/2}}}$$

For aqueous solutions at 25 °C, $A \approx 0.512$. The first approximation of the Debye–Hückel theory can be used only for 1:1 electrolytes and only up to $J = 0.001$ M. The second approximation of the theory considers the sizes of the ions. This improvement yields for the single-ion activity coefficient:

$$\log \gamma_I = - \frac{Az_I^2 \sqrt{J}}{1 + a_{Kjel} B \sqrt{J}} \quad (2.43)$$

Here, a_{Kjel} is the Kjelland parameter which is roughly equal to the hydrated (or solvated) ion radius. Values of a_{Kjel} for a number of ions are summarized in [14], see also Table 9.1 in Sect. 9.3. The B constant is as follows:

$$B = (2e^2 N_A / \epsilon_0 \epsilon kT)^{1/2}$$

For aqueous solutions at 25 °C, $B \approx 0.328$. Equation (2.43) can be used for monovalent ions up to $J = 0.1$ M and for divalent to $J = 0.01$ M.

The dielectric permittivity in the vicinity of an ion is different from the average value of the whole solution. This effect was considered in the third approximation of the Debye–Hückel theory which yields

$$\log \gamma_I = - \frac{Az_I^2 \sqrt{J}}{1 + a_{Kjel} B \sqrt{J}} + 0.1z_I J \quad (2.44)$$

Equation (2.44) is suitable even for divalent ions at ionic strength up to 0.1 M. More advanced theories have been invented by Pitzer and by Robinson and Stokes. However, at ionic strengths below 0.3 M, these more complicated theories yield data close to those of the Debye–Hückel theory and therefore hardly needed for the ISE practice.

It appears a paradox: single-ion activity cannot be measured, but comments are available on whether a theory, that is, the Debye–Hückel theory can or cannot be used for a particular situation. The point is that the theory allows for calculation of a cation and also of an anion activity, and then the multiple can be compared with the thermodynamically rigorous full electrolyte activity value. This is how the reliability of such theories is evaluated.

References

1. K.N. Mikhelson, J. Bobacka, A. Ivaska, A. Lewenstam, M. Bochenska, *Anal. Chem.*, 2002, 74, 518.
2. K.N. Mikhelson, A.L. Smirnova, *Sens. Actuators B*, 1992, 10, 47.
3. K.N. Mikhelson, *Sens. Actuators B*, 1994, 18, 31.

4. T. Sokalski, A. Lewenstam, *Electrochem. Commun.* 2001, 3, 107.
5. T. Sokalski, P. Lingenfelter, A. Lewenstam, *J. Phys. Chem.*, 2003, 107, 2443.
6. J. Bobacka, A. Ivaska, A. Lewenstam, *Chem. Rev.*, 2008, 108, 329.
7. J.J. Jasielec, R. Filipek, K. Szyszkiewicz, J. Fausek, M. Danielewski, A. Lewenstam, 2012, in press. (Full reference will be provided later).
8. K.N. Mikhelson, A. Lewenstam, S.E. Didina, *Electroanalysis*, 1999, 11, 793.
9. W. Kucza, M. Danielewski, A. Lewenstam, *Electrochem. Commun.*, 2006, 8, 416.
10. P. Lingenfelter, I. Bedlechowicz-Sliwakowska, T. Sokalski, M. Maj-Zurawska, A. Lewenstam, *Anal. Chem.*, 2006, 78, 6783.
11. T. Sokalski, W. Kucza, M. Danielewski, A. Lewenstam, *Anal. Chem.*, 2009, 81, 5016.
12. A. Michalska, *Electroanalysis*, 2012, 24, 1253.
13. G. Scatchard, *J. Amer. Chem. Soc.*, 1953, 75, 2883.
14. J. Dvorak, J. Koryta, V. Bohackova, *Elektrochemie*, 1975, Academia, Praha.

Chapter 3

Ion-Selective Electrode Characteristics

This chapter is devoted to practically relevant characteristics of ISEs and to the methods of the experimental assay of these characteristics. For the practical use of ISEs, we have to know the working range and the response slope of the sensor, its' selectivity, response time, and the stability of these characteristics over time and their reproducibility from one replica electrode to another one.

The methods of the experimental assay of these characteristics are the same whatever is the ISE, whether it is with a polymeric, or a glass, or a crystalline membrane. Therefore, these methods are discussed in this chapter, which precedes chapters devoted to certain types of ISEs.

3.1 Ion-Selective Electrode Working Range and Response Slope

Basically, the ISE working range and response slope are determined directly from the calibration curve. The working range is characterized by the lower and the upper detection limits of the ISE. Traditionally, these limits were defined by IUPAC [1] and Buck and Lindner [2] as the values of the concentrations (activities) of the target analyte where the error of the analysis equals 100 %. This definition implies that the measured concentration (activity) is twice larger or twice lower than the target value. Bearing in mind the Nernst equation and the IUPAC definition of the detection limit, one can see that ΔE deviation of the measured EMF from the straight line in the detection limit is:

$$\Delta E = \pm \frac{RT}{z_1 F} \ln \frac{a^{\text{measured}}}{a^{\text{target}}} = \pm \frac{RT}{z_1 F} \ln 2 \quad (3.1)$$

The “+” sign refers to the lower and the “-” sign to the upper detection limit. Thus, at room temperature, for an electrode selective to a univalent ion, the lower detection limit refers to the deviation of approx. +18 mV, and in the case of a divalent ion—to approx. +9 mV. These deviations are significantly higher than the typical value of the experimental error. Therefore, the advantage of in this way

defined detection limits is low sensitivity to the inevitable random errors of the EMF measurements, see Fig. 3.1.

The linear range can be considered as the linear part of the calibration curve, that is, the part where the deviations from the linearity do not exceed the measurement error. Therefore, in contrast to the working range, the linear range is very sensitive to the value of the measurement error, and it is always narrower than the working range.

The working (and also the linear range) of an ISE may depend on the particular electrolyte, that is, on the nature of the anion for a cation-selective electrode and the nature of the cation for an anion-selective electrode. This is especially important for ISEs with ionophore-based membranes. In electrolyte solutions with lipophilic anions, the upper detection limit of cationic electrodes shifts to lower concentrations when compared with electrolytes containing only hydrophilic anions, for details see Sect. 4.4.4.

Recently, the traditional IUPAC definition of the detection limit was put under question. This happened for two reasons. One reason is connected to the progress in the improvement of the lower detection limit [3, 4]. Various approaches allow for the drastic expansion of the working range, see Sect. 7.2. However, the ISE response within this expanded range, typically, is not linear, and the calibration curve contains a super-Nernstian part (see Fig. 3.2). The traditional definition of the detection limit is not consistent with the super-Nernstian response curve. Indeed, the ISE presented in Fig. 3.2 is responding down to 10^{-10} M, and the readings deviate from the ideal Nernstian line to the negative direction which is in contrast to the calibration curve with an ordinary detection limit.

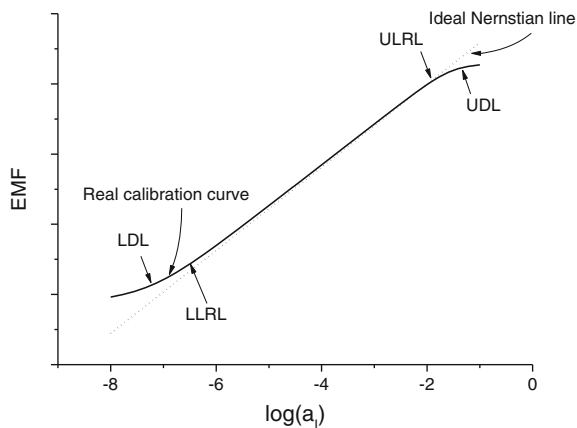
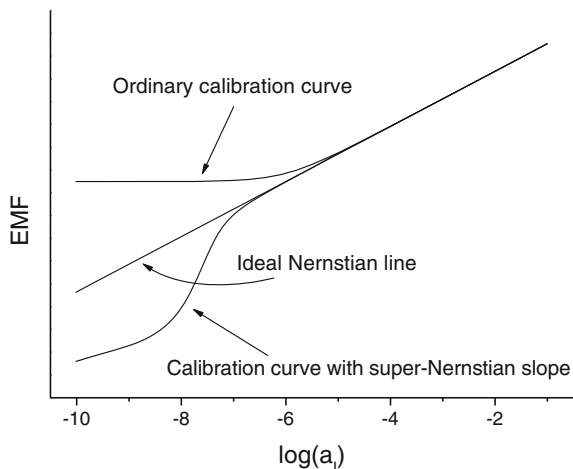


Fig. 3.1 Example of the ISE response span and slope. The ideal *Nernstian straight line* is plotted with the slope $S = dE/d \log a_i = 59.2$ mV. The *real calibration curve* has the slope $S = 57.2$ mV within the linear range from $\log a_i = -6.2$ (lower linear range limit—*LLRL*) to $\log a_i = -2.0$ (upper linear range limit—*ULRL*). The lower detection limit (*LDL*) is $\log a_i = -6.8$, and the upper detection limit (*UDL*) is $\log a_i = -1.2$

Fig. 3.2 Schematic plot of the ideal Nernstian response, a calibration curve with the ordinary lower detection limit, and a calibration curve with a super-Nernstian part



The other reason is that the IUPAC definition of the detection limit is not consistent with the respective definitions used in other branches of science, where the detection limit is affixed to a certain ratio of the reading value over the standard measurement error. Nevertheless, the traditional definition remains widely recognized and used.

3.2 Potentiometric Selectivity Coefficient

The potentiometric selectivity of an electrode is its ability to respond only to the target analyte ion in the presence of other ions. In other words, if the activity of the target ion is the same, the electrode potential and the measured EMF (ideally) are also the same whatever is the composition of the sample. Importantly, the potential of an ideally selective electrode is constant at a constant activity of the analyte, but not necessarily at a constant concentration. If the concentration of the target analyte ion is the same, but concentrations of other ions vary from sample to sample, the activity coefficients of all the ions also vary. Therefore, the activity of the analyte ion, and the respective electrode potential, also varies even in the hypothetical case of the ideal selectivity. The practical approaches to overcome this problem are discussed in [Sect. 9.1](#).

The selectivity of the real-world electrodes is far from being ideal. The glass pH electrode and, to lesser extent, the fluoride-selective electrode with membrane made of mono-crystalline LaF_3 doped with EuF_2 can be considered as exceptions. The selectivity of these electrodes to the pH and to F^- ions is extremely high. The selectivity of other electrodes is limited. Normally, the selectivity of an electrode is quantified on the basis of the Nikolsky equation. This equation already appeared in [Eq. \(1.5\)](#) and is presented here for the readers' convenience:

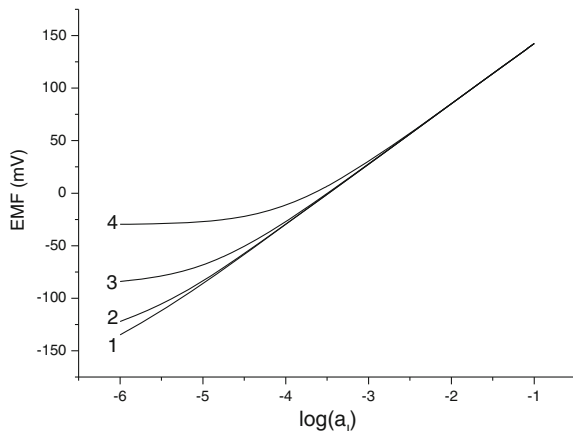


Fig. 3.3 The ISE response in mixed solutions IX + JX electrolytes with constant activity of J^+ interfering ions: $a_J = 0.1$. The ISE obeys the Nikolsky Eq. (3.2) with the following parameters: $E^0 = 200$ mV, $S = 57.5$ mV/ $\log a_I$. Curve 1 refers to pure IX solutions, curves 2–3 to solutions with $a_J = 0.1$ M. Selectivity coefficients are 10^{-5} (curve 2), 10^{-4} (curve 3), 10^{-3} (curve 4)

$$E = E^0 + S \log(a_I + K_{IJ} a_J) \quad (3.2)$$

The quantitative measure of the selectivity is the selectivity coefficient: the parameter K_{IJ} in the Eq. (3.2). In fact, this equation can only be applied if both I^z , the primary (target analyte) ion, and $J^{z'}$, the interfering ion have equal charges. The role of the selectivity coefficient is illustrated by Fig. 3.3. One can see how the selectivity affects the ISE response range in mixed solutions. Even in the case of relatively high selectivity, $K_{IJ} = 10^{-3}$, the linear range of the ISE in mixed solution with 0.1 M interfering ions is drastically narrower than in pure IX solutions.

Quantification of the selectivity to differently charged ions relies on different equations. Historically, the selectivity to I^{2+} divalent cations (or anions) in the presence of J^+ monovalent cations (anions) has been described by equation recommended in 1975 by IUPAC [1]:

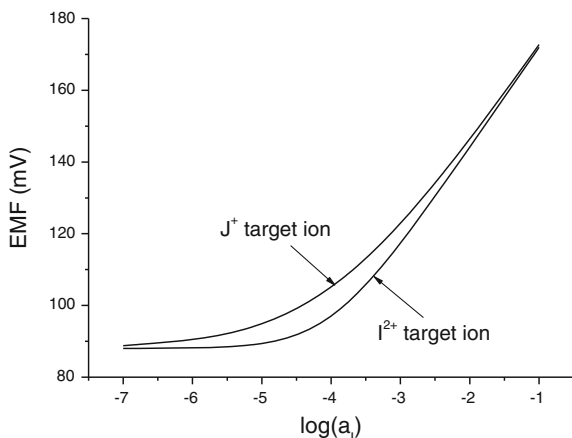
$$E = E^0 \pm \frac{RT}{2F} \ln(a_I + K_{IJ}^{\text{IUPAC}} a_J^2) \quad (3.3)$$

Another equation to describe the same case was proposed by Buck and Stover [5]:

$$E = E^0 \pm \frac{RT}{F} \ln(a_I^{1/2} + K_{IJ}^{\text{Buck}} a_J) \quad (3.4)$$

Sign + refers to cation-responding ISEs, and sign – to anion responding. These equations neither have clear theoretical background, nor fit experimental data, although are often called “semi-empirical.” Both Eqs. (3.3) and (3.4) look similar to the Nikolsky equation and transform into the Nernst equation if either a_I or a_J is zero, that is, in pure solutions of IX_2 or JX electrolytes. Unlike the Nikolsky

Fig. 3.4 Calibration curves calculated by IUPAC Eq. (3.3) for mixed solutions of IX_2 and 0.1 M JX electrolytes, considering as the target analyte either I^{2+} or J^+ ions



equation, Eqs. (3.3) and (3.4) are sensitive to whether I^{2+} divalent ion is the target and J^+ monovalent ion is the interference, or vice versa [6], see Fig. 3.4.

One can see that the respective curves calculated for mixed solutions do not coincide, except of the domains of full I^{2+} or full J^+ response.

First Morf [7] and later (in a different way) Bakker et al. [6] derived another equation to describe the potentiometric selectivity toward divalent primary ions in the presence of monovalent interference:

$$E = E^0 + \frac{RT}{F} \ln \left(\sqrt{a_I + \frac{1}{4} K_{IJ}^{M-B} a_J^2} + \sqrt{\frac{1}{4} K_{IJ}^{M-B} a_J^2} \right) \quad (3.5)$$

The selectivity coefficient here (K_{IJ}^{M-B}) is denoted here with upper index $M - B$, after Morf and Bakker, in order to distinguish between selectivity coefficients which appear in Eqs. (3.3) and (3.4).

The equation for the response to a monovalent primary ion in the presence of a divalent interference also was derived by Bakker et al. [6]:

$$E = E^0 + \frac{RT}{F} \ln \left(\frac{a_I}{2} + \frac{1}{2} (a_I^2 + 4K_{IJ}^B a_J)^{1/2} \right) \quad (3.6)$$

Equations (3.5) and (3.6) are symmetric and are not sensitive to which ion is considered target and which one is interference. Unfortunately, the theoretical derivation of Eqs. (3.5) and (3.6) relied on the complete dissociation of the electrolytes in the membrane phase. This assumption is hardly true for real ISE membranes, especially for divalent ions. However, these equations are suitable for the practical use.

3.3 Measurements of the Selectivity Coefficients

Describing the principles of the experimental estimation of the selectivity coefficients, we will rely on the Nikolsky equation. The measurements of the selectivity coefficients for ions of non-equal charges are performed in analogous ways. For more detailed discussion on various methods of the selectivity coefficients measurements, see [8, 9].

3.3.1 Separate Solutions Method

Currently, the *separate solutions method* (sometimes called the *bi-ionic potentials method*) is predominating among other experimental techniques aimed at the assay of the selectivity coefficients. The basic idea of the method is very simple. If we measure the ISE potentials in a series of pure IX electrolyte solutions (I^+ is the target ion), and the electrode obeys the Nikolsky equation, the EMF follows the equation below:

$$E_I = E^0 + S \log a_I \quad (3.7)$$

The EMF measured for pure JX, the electrolyte containing J^+ interfering ions, according to the Nikolsky equation is as follows:

$$E_J = E^0 + S \log (K_{IJ} a_J) \quad (3.8)$$

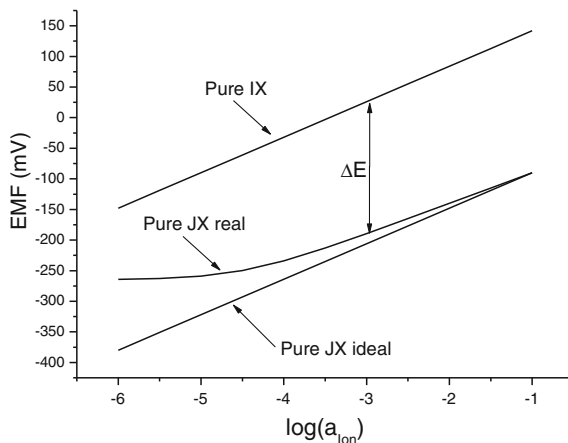
For the EMF values registered separately in pure IX and JX solutions with equal values of the primary and interfering ion activities ($a_I = a_J$), we have:

$$\log K_{IJ} = \frac{(E_J - E_I)}{S} \quad (3.9)$$

Thus, calibrating the ISE in two pure electrolyte solutions: IX and JX, one can obtain both the calibration parameters of the electrode (E^0 , S) and also the selectivity coefficient. The method is illustrated by Fig. 3.5.

The problem is that the real-world ISEs do not obey the Nikolsky equation quantitatively. That is, the respective calibration curves are not parallel, see Fig. 3.5, and the values of the selectivity coefficients depend on the particular values of $a_I = a_J$ chosen for the calculations. Normally, the calibration curve obtained in pure IX (target ion) electrolyte is linear, and the slope is close to the theoretical Nernstian value: $S \approx 2.303 RT/z_I F$. Special protocols of the ISE conditioning and of measurements allow for nearly Nernstian slope also in the JX (interfering ion) electrolyte, see Sect. 3.3.4. Otherwise, the calibration curve measured in JX electrolyte is nonlinear, and if it contains a linear part, the slope is rather sub-Nernstian. The curves converge in the diluted solutions, like shown in Fig. 3.5. Therefore, the values of the selectivity coefficients measured using the

Fig. 3.5 Separate solutions method. The data refer to $K_{IJ} = 10^{-4}$



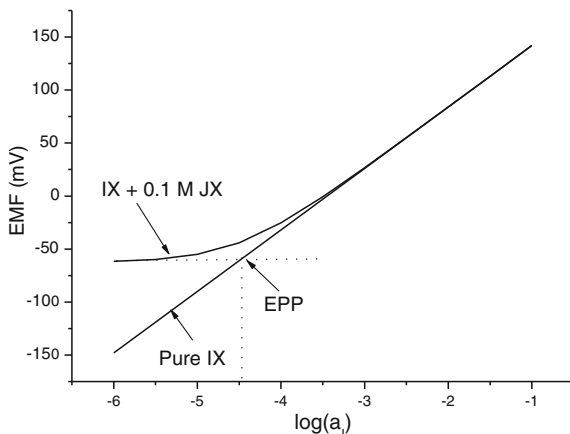
respective deltas of the EMFs are strongly dependent on the concentrations of the electrolytes. More of this, it becomes unclear which value of S must be set into Eq. (3.9): the slope obtained in pure IX or that obtained in pure JX. Normally, the slope measured in IX is set in calculations. The values of the selectivity coefficients measured at higher concentrations are more “optimistic,” while measurements at lower concentrations show worse selectivity of the ISE. Typically, the selectivity coefficients are roughly independent on the ions concentrations in the cases of moderate selectivity, when $\log K_{IJ} > -2$. The origin of the variability of the K_{IJ} values and the way of how to obtain the so-called unbiased selectivity coefficients is discussed below.

The practical solution of the problem of the non-constancy of the K_{IJ} values is quite obvious. If a study is undertaken for a certain kind of samples (e.g., technological fluids in a certain industrial process, or soils originating from the same region, or waste waters from the same factory), the compositions of the samples vary in a relatively narrow range. One therefore has to measure the selectivity under the particular conditions typical for this kind of samples. In this way, obtained selectivity coefficients can be used to see whether the ISE will provide with reliable data. In some cases, when the activity of the interfering ion is known, it is possible to introduce the correction for the interference using the value of the selectivity coefficient.

3.3.2 Fixed Interference Method

The separate solutions method relies on measurements in pure solutions. Therefore, it is often criticized as being non-adequate since the selectivity is the ability of an ISE to distinguish between ions in mixtures. Measurements in mixed solutions are performed with either (1) variable concentration of the target analyte ions

Fig. 3.6 Fixed interference method. The data refer to $a_I = 0.1 \text{ M}$, $K_{IJ} = 3 \cdot 10^{-4}$



and a constant concentration of the interference, the so-called *fixed interference method* (FIM), or (2) in another way round: with variable concentration of the interference at a constant level of the primary ion. The first option is represented in Fig. 3.6.

As shown in the figure, the linear range of the ISE response in pure solutions of IX (primary ion electrolyte) is wider than that in mixed solutions containing also JX interfering ion electrolyte. With dilution in IX, the curve measured in mixed solutions deviates more and more from the Nernstian line and finally gets flat at low concentrations of IX. The calibration plot contains two straight lines: the Nernstian (or near-Nernstian) response to the target ion and the horizontal line when the ISE potential is determined by the interfering ion. The intercept point of these two lines refers to equal values of the EMF obtained for pure IX solution and for mixed solution with $a_I \ll K_{IJ}a_J$. Thus, for the EMF in this point (the equipotential point—EPP), the Nikolsky equation gives:

$$E = E^0 + S \log a_I^{\text{EPP}} \quad (3.10)$$

and also

$$E = E^0 + S \log (K_{IJ}a_J) \quad (3.11)$$

The selectivity coefficient equals the ratio of the respective ion activities:

$$K_{IJ} = \frac{a_I^{\text{EPP}}}{a_J} \quad (3.12)$$

One can also solve the Nikolsky equation for the selectivity coefficient in all the points where the deviations from the linear response significantly exceed the experimental error. Then, the selectivity coefficient can be calculated according to the following equation:

$$K_{IJ} = \frac{10^{\frac{E-E^0}{S}} - a_I}{a_J} \quad (3.13)$$

Here, E stands for the EMF value measured for the particular values of a_I , a_J in mixed solution.

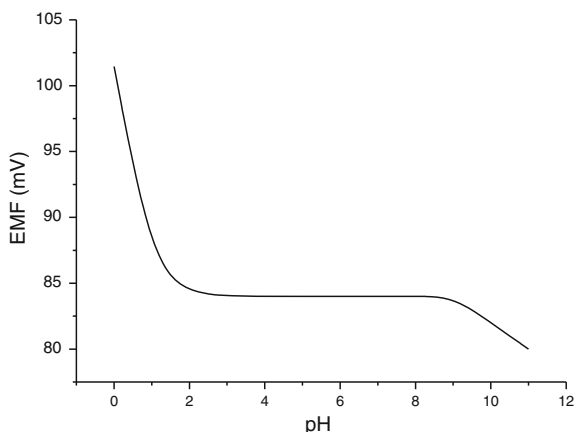
Although the mixed solutions method is often considered as more reliable than the separate solutions method, obtaining constant values of the selectivity coefficients requires special measures described in Sect. 3.3.4. Otherwise, the FIM method suffers the same problem as the SSM method: the selectivity coefficients depend on the measurements conditions. Calculations using Eq. (3.13) show more “optimistic” values of the selectivity coefficients for lower concentrations of the primary ion in mixed solution. It may seem this trend is in contrast to that typical for the separate solutions method. In fact, the numerical values of K_{IJ} obtained by FIM using a certain a_J value approach those obtained by SSM with the same activity of the interfering ion. If measurements are made in several series of mixed solutions which differ in the value of the fixed concentration of the interference, the results are completely consistent with those obtained by the separate solutions method. Like in the case of SSM, the results obtained for higher values of the interfering ion concentration yield better selectivity coefficients. The fixed interference method consumes more time and labor and therefore is less in use than the separate solutions method.

Practical recommendations to circumvent the problem of the variability of the selectivity coefficients are the same as in the case of the separate solutions method. The particular value of the fixed concentration of the interference in mixtures should not be chosen arbitrarily, but should be typical for the particular kind of samples to be analyzed.

The other option of the mixed solution method: when the primary ion concentration is fixed, and the interfering ion concentration is varied, nowadays is used almost exclusively to characterize the working pH range of an ISE. In this case, the selectivity coefficient is only rarely calculated, rather the range of the pH when the ISE potential remains unaltered is reported. For instance, the data presented in Fig. 3.7 suggest the working pH range of the ISE is 2–9.

The lower pH limit strongly depends on the nature and the composition of the ISE membrane. In many cases, it is determined by the interference from hydrogen ions with the ISE response. However, the upper pH limit for most of ISEs (except of the pH electrodes) is roughly the same: pH 9–10. In the case of crystalline electrodes selective to heavy metal cations, this is, at least partly, due to the solution chemistry: ions produce hydroxides and therefore concentrations of free ions decrease. In the case of ISEs with solvent-polymeric membranes selective to alkaline and alkaline-earth cations, and to various anions, the upper pH limit may be due to saponification of the membrane plasticizers and therefore is virtually independent on the nature of the ionophore.

Fig. 3.7 The working pH range



3.3.3 Matched Potentials Method

The matched potential method (MPM) does not rely on any theory and does not assume a certain equation describing the ISE response in a mixed solution. The method is based on a procedure of measurements of the potential differences caused by increase in the target analyte activity in solution and that due to increase in the interfering ion activity. The MPM measurements procedure is as follows: First, a suitable starting solution is chosen. Often, this solution is close to the lower detection limit. Then, the potential change is measured caused by increase in the target ion activity by an increment Δa_I . Next, the ISE is placed back into an identical starting solution, and interfering ions are added until the same potential change is registered. The selectivity coefficient is then calculated as the ratio of the respective activity increments resulting in the same potential change:

$$K_{IJ} = \frac{\Delta a_I}{\Delta a_J} \quad (3.14)$$

On the one hand, the MPM allows for artificial circumventing non-Nernstian slopes and the differences between the charges of the ions in question. On the other hand, lacking theoretical background, the K_{IJ} value obtained by the MPM also lacks predictive ability about the EMF measured with solutions other than those for which it was determined [8–10]. Therefore, the MPM method is practically not in use anymore.

3.3.4 Unbiased Selectivity and the Bakker Protocol

The selectivity coefficients of ISEs with various types of membranes (glass, crystalline, or polymeric) depend on the measurement conditions, in the first place,

on the concentrations of the ions in solutions. Different hypothesis have been proposed to explain this non-constancy [11]. A fundamental reason can be a non-adequacy of simple equations, like the Nikolsky equation, for the description of the electrode potentials in mixed solutions. Indeed, the simplifications used in the derivations of these equations may depreciate the final mathematical forms [12, 13]. There are also experimental sources for the variation of the selectivity coefficients. The point is that the ion exchange at the membrane/solution interface causes small deviations of the composition of the solution in the vicinity of the membrane when compared with the composition of the solution in the bulk [11]. Let us consider first the measurements of the selectivity coefficients by the separate solutions method. The method suggests that the ISE selective to I^{z_i} ions is immersed into a pure solution containing J^{z_j} ions. In reality, the latter solution is a pure electrolyte only in the bulk, while in the vicinity of the ISE membrane, the solution is slightly depleted in J^{z_j} ions and slightly enriched in I^{z_i} ions, because of the ion-exchange process at the membrane/solution interface. Thus, the membrane is effectively in contact with a mixed solution. The more selective is the ISE to the respective I^{z_i} primary ions, the bigger is the impact from these “extra” ions to the membrane potential. This is why the variability of the selectivity coefficients is more pronounced when J^{z_j} interfering ions are highly discriminated by the membrane, while in the case of only moderate selectivity, the K_{IJ} values may be roughly constant.

If the selectivity is quantified by means of the mixed solution method, the whole pattern is pretty much the same. The I^{z_i} primary ions coming from the membrane to the solution slightly increase the values of a_i^{surf} —the primary ions activity in the vicinity of the membrane surface, when compared with a_i —the respective bulk values. The effect intensifies in solutions diluted with respect to the I^{z_i} primary ions.

For ISEs with solvent-polymeric membranes, there is an additional reason for the variability of the selectivity coefficients. Such membranes produce I^{z_i} primary ions and thus contaminate the solutions not only due to the ion-exchange processes, but also due to the trans-membrane flux of ions from the internal solution of the ISE to the sample or calibrator. This effect was proved to determine also the lower detection limit of ISEs in pure solutions [3, 14, 15], see Sect. 7.2.

Thus, the classical methods of the measurements of the selectivity coefficients deliver values biased by the consequences of the ion-exchange processes at the membrane/solution interface and of trans-membrane fluxes of ions. On the basis of this conclusion, Bakker proposed a method of measurements of the so-called *unbiased selectivity coefficients*, also called the *Bakker protocol* [16, 17]. The method suggests using membranes not containing the primary ions. For instance, for K^+ electrodes instead of using the most common cation-exchanger potassium tetrakis(p-Cl-phenyl)borate, one has to use the respective sodium or lithium salt. The measurements must be done in two stages, utilizing two sets of the respective replica electrodes with the membranes of the same composition. The procedure is illustrated by Fig. 3.8.

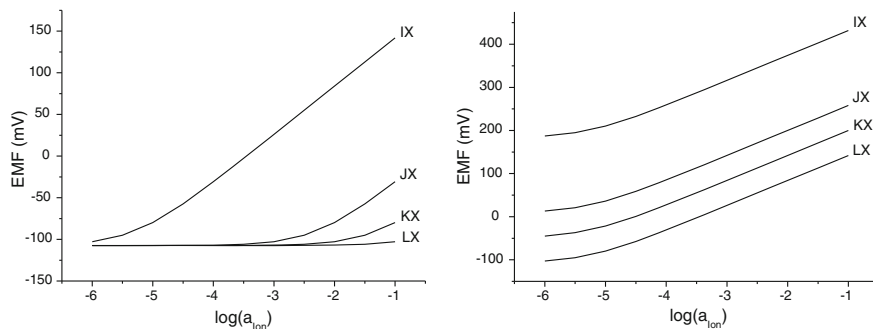


Fig. 3.8 Unbiased selectivity measurements of the selectivity coefficients to I^+ primary ion over J^+ , K^+ , and L^+ interferences, first stage (*left*), and second stage (*right*). The curves refer to the following values of the selectivity coefficients: $K_{IJ} = 10^{-3}$, $K_{IK} = 10^{-4}$, $K_{IL} = 10^{-5}$. The lower detection limit is $\log a_I = -5.3$. Notice the difference in the EMF scales in the *left* and *right* plots

The left plot in the figure represents the first stage of the Bakker protocol: the traditional SSM measurements of the selectivity. This stage provides with the order of ions arranged according to their interference with the response to the primary target analyte—from strongly interfering to highly discriminated ions. As one can see, even in JX solutions, in those containing J^+ ion, which shows relatively strong interference: $K_{IJ} = 10^{-3}$, the response is strongly nonlinear, and there is practically no response to more discriminated ions: K^+ and L^+ . However, one can clearly see the selectivity sequence:

$$I^+ > J^+ > K^+ > L^+$$

Thus, on the second stage, replica electrodes with the same kind of membranes, not being in contact with the primary ions, are filled with LX solution containing L^+ —the most discriminated ion. Next, calibrations are performed in other electrolytes from most discriminated to most interfering and, finally, in solutions containing the primary ions. Under this protocol, neither the trans-membrane flux, nor the ion exchange at the membrane/solution interface distort the ISE potential, and one can obtain calibration curves shown in Fig. 3.8, right plot. The curves show Nernstian slopes and the selectivity coefficient values not dependent on the ions concentrations. Furthermore, the selectivity coefficients obtained in accordance with the Bakker protocol are consistent with the respective thermodynamic parameters characterizing the affinity of the competing ions to the aqueous phase and to the membrane phase: the ionic distribution coefficients, the ion-to-ionophore complex formation constants, etc. [17].

3.4 Response Time

The practical response time of an ISE shows how fast the steady value of the EMF is established when the previous sample or calibrator is replaced with the next one. This characteristic is of great importance since it determines the throughput of a measuring device having an ISE as sensor. Therefore, the response time of a novel ISE is normally specified by the inventor. In early days of the ISE research, a lot of work has been done to study the regularities of the response time [7, 18–21]. Also, the term was defined more exactly, for instance, τ_{90} , τ_{95} , the times sufficient for, respectively, 90 or 95 % of the full potential change. Without these specifications, the random noise of the potential hinders the measurements of the response time, since, due to the noise, the readings are never ideally steady. This idea is illustrated by Fig. 3.9.

The curve refers to a flow through K^+ ISE with valinomycin in the membrane, filled with 0.01 M KCl, with Ag/AgCl internal electrode. The EMF is measured against Ag/AgCl electrode in 3 M KCl. The initial solution was 0.1 M KCl. At time 220 s, the flow cell was emptied with an air bubble passed using a syringe and then filled with 0.01 M KCl, also using a syringe. These manipulations took 10 s and caused overshoot in the response curve. The ISE potential reached 95 % of the signal change at time 305 s, and the full change was reached at about 350 s. Thus, in this example, $\tau_{95} \approx 45$ s, the “total” response time was even longer: about 90 s. Similar times refer to the back process: from 0.01 to 0.1 M KCl. However, large impact to these times comes from the procedure of replacement of the solution, use of faster diluting/concentrating devices results in $\tau_{95} \leq 5$ s. Furthermore, already in

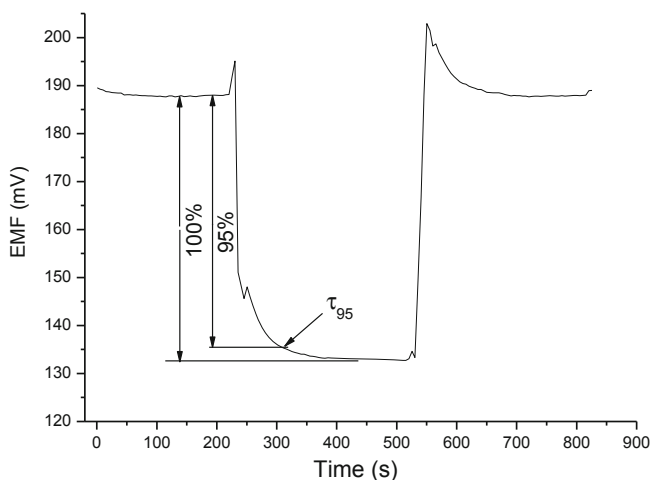


Fig. 3.9 Response curve of a K^+ -ISE when 0.1 M KCl is replaced with 0.01 M KCl, and then back with 0.1 M KCl

late 1980s, it was shown that using special devices for very fast sample change allows obtaining the ISE response time in millisecond range [21].

Theories developed in [7, 18–21] considered various processes determining the response time: (1) electrochemical reaction at the membrane/solution interface, (2) diffusion within the membrane phase, and (3) diffusion of the electrolytes across the so-called stagnant layer in the aqueous phase in the vicinity of the membrane.

The practical response time therefore does not tell how fast the interfacial equilibrium is established. The latter process depends on the exchange current densities at the membrane/solution interface and the double-layer capacitance. Electrochemical impedance studies of glass and crystalline membranes showed very fast charge transfer processes [22]. For ionophore-based membranes, the exchange current densities are 10^{-5} A/cm² and higher, while the double-layer capacitance is about 10^{-7} F/cm², thus giving τ_{RC} —the time constant not more than 0.01 s [23, 24]. The full establishing of the electrochemical equilibrium at the membrane/solution interface takes therefore $t_{\text{equilibr}} = 5\tau_{RC} \leq 0.05$ s. Of course, for a “bad” electrode, it may take much more time to reach the interfacial equilibrium.

Diffusion of ions within the membrane phase takes place within the transient part of the response—when the ISE loses the response to its primary ion in favor of the interference. Therefore, within the linear part of the response, the diffusion of the electrolytes across the “stagnant” layer is the major factor of the response time. Thus, generally speaking, the practical response time of a “good” electrode is determined by the hydrodynamic conditions in the cell when one solution is replaced with another one. Stirring helps obtaining shorter response times.

Long-term kinetics like that studied by Belyustin for glass electrodes does rely on the processes deep in the glass membrane phase [25, 26]. However, this long-term kinetics happens within days and weeks and does not alter practical response time of ISEs.

3.5 Stability and Piece-to-Piece Reproducibility of the ISE Response

Measurements with ISEs rely on calibration. Drift of an ISE readings immersed in the same sample over time suggests that either the standard potential (E^0) or the slope (S) obtained during the calibration cannot be used for the converting of the measured EMF into the analyte activity (or concentration). Thus, insufficient stability of the ISE response puts its practical usefulness under question.

Normally, the slope is much more stable over time than the standard potential. The change of the slope is mostly regular: slow decrease over the ISE lifetime, because of slow leaching of ionophores from membrane to aqueous solutions [27, 28].

For the ISEs with solvent-polymeric ionophore-based membranes, the slope, normally, changes gradually from its initial near-Nernstian value of $\pm(57\text{--}58)$ or

$\pm(26-27)$ mV/log a_I (for monovalent or divalent ions, respectively, “+” for cations and “-” for anions), down to $\pm(50-52)$ or $\pm(22-24)$ mV/log a_I during several months, up to one year, thus determining the ISE lifetime. However, there are examples of ionophore-based membranes with lifetime of several years [29]. The lifetime of crystalline and glass electrodes, if properly handled, is practically non-limited, and the slope does not change over time.

The membrane potential is non-zero only if there is some asymmetry in the system: either the solutions on the two sides of the membrane are not the same or the membrane itself is non-uniform. Good, commercially available electrodes have no “frozen” gradients across membranes and show only negligible asymmetry potential. Therefore, the potential of such a conventional ISE immersed into a solution of composition same as that of the internal filling equals the potential of the internal electrode versus the reference electrode used for the measurements. For instance, an ISE filled with 0.01 M KCl and equipped with Ag/AgCl internal electrode, when immersed into 0.01 M KCl shows about 135–138 mV versus Ag/AgCl reference electrode in 3 M KCl. This value is simply the EMF of a cell comprising Ag/AgCl electrode in 0.01 M KCl versus the same reference electrode. Therefore, ISE membranes themselves impact to the E^0 drifts only if become non-uniform during use. This may happen because of sorption of some undesirable species by the membrane surface or deeper—into the outer layers of membrane. Otherwise, the stability of the E^0 of the conventional ISEs with an internal filling solution (most often, a suitable chloride salt, for example, KCl in K^+ -ISEs and NaCl in Na^+ -ISEs) and an internal electrode (most often—Ag/AgCl) depends primarily on the constancy of the internal filling composition. Therefore, large ISEs with the internal filling volume of 1–3 ml are typically more stable over time than small ones with only 0.1–0.2 ml of the internal solution. Water mostly leaves the internal solution due to evaporation if the ISE is not hermetically closed. In the case of solvent-polymeric membranes, also a trans-membrane diffusion of water is possible, either from the internal solution to sample or vice versa—dependent on the difference in water activities in the respective solutions. Although this effect is small, it sometimes may impact to the instability of the standard potential. Some impurities present in samples may diffuse across the membrane from sample to the internal solution and accumulate there, causing significant drifts of the E^0 . For instance, even small flux of Br^- or I^- ions across an ISE membrane (so small that it does not deteriorate the ISE slope) may cause a significant change of the E^0 due to the change of the internal Ag/AgCl electrode potential in the presence of these ions. Obviously, these diffusion-induced effects happen only with ISEs with solvent-polymeric membranes and do not happen with crystalline and glass ISEs. On the other hand, the latter two types of ISEs are more sensitive to the adsorption on the membrane surface and formation of surface oxide layers. Therefore, glass and crystalline ISEs require refreshment of the membrane surface, by etching or polishing, respectively.

From the practical point of view, it is advisable to replace the internal solution with a fresh portion every two weeks or more often dependent on the volume of the internal solution and on how tight the electrode is closed up. Then, the E^0 value

or, rather, the potential in a certain “control” solution remains virtually the same (± 0.5 mV) during the whole lifetime of the ISE.

In various special devices, like in clinical analyzers, the changes of the E^0 are compensated by the measurements procedure. The reliability of the data is guaranteed by measuring the potential in a certain control solution after every three samples, or even after each sample—if this is required. For more details about ISEs in clinical analyzers, see Sect. 8.4.

The solid-contact electrodes, those without internal filling, intrinsically, are better suited for high stability of the standard potential over time. Indeed, the solid-contact ISEs with glass and crystalline membranes show excellent stability over time [30, 31]. However, for ISEs with ionophore-based membranes, securing a good stability of the E^0 remains a challenging task [32, 33]. For more details, see Sect. 8.2.

The piece-to-piece reproducibility of the ISE potentials is not an issue for a user having only one electrode. However, for a scientist or a manufacturer, a poor piece-to-piece reproducibility indicates some problem with electrodes. Piece-to-piece reproducibility is also important when ISEs are used for in-line monitoring of an industrial process. Then, it may be critical to replace a malfunctioning sensor with a new one without wasting time for calibration. For this task, it is critical to have the same values of the ISE calibration parameters: the standard potential and slope.

Conventional ISEs with internal filling solution and internal electrode show piece-to-piece reproducibility of the standard potential of about ± 1 mV and better, the piece-to-piece reproducibility of the slope is about ± 0.2 mV. Solid-contact ISEs with glass and crystalline membranes also show excellent piece-to-piece reproducibility. For solid-contact glass electrodes with Li-Sn alloy as the internal system, it is even possible to use “factory calibration” which remains stable for several years [30]. Unfortunately, the piece-to-piece reproducibility of solid-contact ISEs with polymeric membranes with ionophores, so far, does not allow replacing one electrode with a replica one without calibration. Although slope values within a batch of ISEs normally vary within the same narrow range of ± 0.2 mV, the standard potentials may deviate from one another in ± 15 mV or even more.

References

1. IUPAC Analytical Chemistry Division Recommendations for nomenclature of Ion-selective Electrodes, *Pure Appl. Chem.*, 1976, 48, 127.
2. R.P. Buck, E. Lindner, Recommendations for nomenclature of ion-selective electrodes, *Pure Appl. Chem.*, 1994, 66, 2527.
3. T. Sokalski, A. Ceresa, T. Zwickl, E. Pretsch, *J. Am. Chem. Soc.*, 1997, 119, 11347.
4. E. Bakker, P. Bühlmann, E. Pretsch, *Electroanalysis*, 1999, 11, 915.
5. R.P. Buck, F.S. Stover, *Anal. Chim. Acta*, 1978, 101, 231.
6. E. Bakker, R.K. Meruva, E. Pretsch, M.E. Meyerhoff, *Anal. Chem.*, 1994, 66, 3021.
7. W.E. Morf, *The principles of Ion-selective Electrodes and of Membrane Transport.*, Budapest, Akad. Kiado, 1981.
8. E. Bakker, E. Pretsch, P. Bühlmann, *Anal. Chem.*, 2000, 72, 1127.
9. E. Lindner and Y. Umezawa, *Pure Appl. Chem.*, 2008, 80, 85.

10. C. Macca, *Anal. Chim. Acta*, 1996, 321, 1.
11. A. Lewenstam, A. Hulanicki, *Sel. Electrode Rev.*, 1990, 12, 161.
12. K.N. Mikhelson K.N., *Electroanalysis*, 2003, 15, 1236.
13. K.N. Mikhelson, *Meth. Objects Chem. Anal. (Kiev)*, 2006, 1, 73.
14. Y. Mi, S. Mathison, R. Goines, A. Logue, E. Bakker, *Anal. Chim. Acta*, 1999, 397, 103.
15. R.E. Gyurcsanyi, E. Pergel, R. Nagy, I. Kapui, B.T.T. Lan, K. Toth, I. Bitter, E. Lindner, *Anal. Chem.*, 2001, 73, 2104.
16. E. Bakker, *J. Electrochem. Soc.*, 1996, 143, L83.
17. E. Bakker, *Anal. Chem.*, 1997, 69, 1061.
18. P.L. Markovic, J.O. Osburn, *AICHE J.*, 1973, 19, 504.
19. W.E. Morf, E. Lindner, W. Simon, *Anal. Chem.*, 1975, 47, 1596.
20. R.P. Buck, *Crit. Rev. Anal. Chem.*, 1975, 5, 323.
21. E. Lindner, K. Toth, E. Pungor, *Dynamic characteristics of ion-selective electrodes*, CRC Press, 1988, 136 p.
22. G.A. Rechnitz, H.F. Hameka, *Fres. Z. Anal. Chem.*, 1965, 214, 252.
23. K.N. Mikhelson, J. Bobacka, A. Lewenstam, A. Ivaska, *Electroanalysis*, 2001, 13, 876.
24. K.N. Mikhelson, J. Bobacka, A. Ivaska, A. Lewenstam, M. Bochenska, *Anal. Chem.*, 2002, 74, 518.
25. A.A. Belyustin, *Sov. J. Glass Phys. Chem.*, 1981, 7, 257.
26. A.A. Belyustin, M.M. Shultz, *Sov. J. Glass Phys. Chem.*, 1983, 9, 3.
27. U. Oesch, W. Simon, *Helv. Chim. Acta*, 1979, 62, 754.
28. P. Bühlmann, Y. Umezawa, S. Rondinini, A. Vertova, A. Pigliucci, L. Bertese, *Anal. Chem.*, 2000, 72, 1843.
29. J.J. Griffin, G.D. Christian, *Talanta*, 1983, 30, 201.
30. M.M. Shultz, O.S. Ershov, G.P. Lepnev, T.M. Grekovich, A.S. Sergeev, *J. Appl. Chem. USSR*, 1979, 52, 2487.
31. Yu. G. Vlasov, Y. E. Ermolenko, O. A. Iskhakova, *J. Anal. Chem. USSR*, 1979, 34, 1175.
32. N.M. Ivanova, M.B. Levin, K.N. Mikhelson, *Russ. Chem. Bull*, 2012, 5, 926.
33. A. Michalska, *Electroanalysis*, 2012, 24, 1253.

Chapter 4

Ionophore-Based ISEs

This chapter describes ISEs with membranes based on ionophores. Ionophores are organic lipophilic substances which selectively bind ions. The nature of these interactions makes the basis of the potentiometric selectivity of ISEs with membranes containing ionophores. A large variety of ionophores enables selective sensing of various analytes, mostly ions but sometimes also neutral species. The fundamentals of the ionophore-based potentiometric and optical sensors, as well as brief characterization of a large number of ionophores, are presented in review papers [1, 2]. Although published more than a decade ago, these reviews remain highly relevant. Currently, most of the progress in ISEs theory and its applications is related to ionophore-based membranes. This makes these membranes, probably, the most important kind, and therefore, we start our in-depth discussion of ISEs with this particular kind of sensor membranes: ionophore-based electrodes.

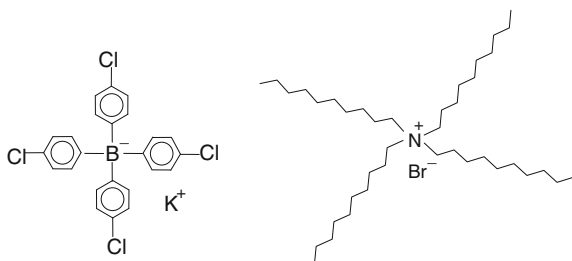
Originally, ionophore-based membranes were comprised of liquids, namely solutions of ionophores in suitable organic solvents. However, already for several decades, solvent-polymeric membranes with polymeric matrixes normally containing plasticizers, and doped with ionophores and ion exchangers, strongly predominate over liquid membranes in most applications. The chapter starts with description of the membrane materials, followed by a brief description of the theory of the response and the selectivity of this kind of ISEs.

4.1 Ion Exchangers and Charged Ionophores

The type of the electrode response (cationic or anionic) and the selectivity of the electrode are determined by ionophores and ion exchangers contained by the electrode membrane. Among the first ion exchangers were potassium salts of the tetraphenylboric acid derivatives (lipophilic anions) [3] and also salts of tetraalkylammonium, tetraalkylphosphonium, and tetraalkylarsonium (lipophilic cations) [4], see Fig. 4.1.

Generally speaking, ion exchangers are lipophilic salts (sometimes acids or bases) which, at least to some extent, dissociate in the membrane phase. The products of the

Fig. 4.1 Typical ion exchangers: potassium tetrakis(p-Cl-phenyl)borate (*left*) and tetradecylammonium bromide (*right*)



dissociation are R^{zR} : a lipophilic organic cation or anion and I^{zI} : a hydrophilic ion. The lipophilicity is a measure of the affinity of the species to organic phases. Quantitatively, the lipophilicity is defined as decimal log of the partition coefficient of the species between water and normal octanol [5]. Partition coefficients of individual ions (see below) cannot be measured. However, partition coefficients of salts formed by a lipophilic R^{zR} anion or cation and a water-soluble cation or anion are determined primarily by the lipophilicity of R^{zR} . The latter must be enough to prevent significant leak of the salt from the membrane phase to the aqueous phase. Ion exchangers and neutral ionophores suitable for the analysis of ordinary aqueous solutions must have the lipophilicity of 7.4 or more, and those for measurements in blood must show the lipophilicity of at least 11 [6]. Thus, the affinity of R^{zR} lipophilic ions to organic phases is very strong. Therefore, these ions are confined to the membrane phase and (ideally) do not participate in the charge transfer across the membrane/solution interface. The other product of the dissociation, I^{zI} hydrophilic ion, can be either of inorganic or of organic nature: its hydrophilicity can vary within a broad range, but anyway, I^{zI} ion is capable of crossing the interface and distribute reversibly between the two phases: membrane and solution.

Very often the term “ion exchanger” is used for R^{zR} ion—the lipophilic product of the dissociation. For instance, potassium tetrakis(p-Cl-phenyl)borate is a typical cation exchanger in the strict sense of the term. However, tetrakis(p-Cl-phenyl)borate anion is also often called ion exchanger. The lipophilic ions form the so-called ion-exchange sites in membranes. Dependent on whether these ions are covalently bonded to the polymeric matrix of the membrane, or can diffuse freely, the respective membranes are called membranes with fixed or with mobile ion-exchanger sites. Due to the macroscopic electroneutrality, the total number of hydrophilic ions in a membrane is equivalent to the total number of sites, regardless of the dissociation degree.

Historically, I^{zI} hydrophilic ions (e.g., cations) which counterbalance the charge of (e.g., anionic) R^{zR} sites were called counter-ions, while ions of the same charge as R^{zR} sites (anions in this case), which may co-extract by membrane together with I^{zI} cations, were called co-ions [7]. Nowadays, the term counter-ion often refers to ions of the same charge as the analyte, which interfere with the electrode response to I^{zI} . Ideally, the presence of ion-exchanger sites in a membrane prevents from co-extraction of aqueous electrolyte, in other words, from co-ions penetration.

The ability of ion exchangers to prevent from co-extraction is also called Donnan exclusion [8]. When the Donnan exclusion holds, the charge transfer across the membrane/solution interface is due to the ion-exchange process, while interfacial partition of the electrolyte as a whole plays only a minor role and often can be neglected. In the latter ideal case, pure ion-exchange is the sole electrochemical process at the membrane/solution interface, and one can expect full Nernstian potentiometric response of the respective electrode. The origin of the response will be discussed in detail below, see Sect. 4.4.

Let us look in more detail on how the Donnan exclusion works. For simplicity, we consider interfacial distribution of an IX 1:1 salt which can dissociate producing I^+ cation and X^- anion. At equilibrium, the activity of IX in the membrane phase is proportional to that in the aqueous phase and to k_{IX} the partition coefficient:

$$a_I^{\text{mem}} a_X^{\text{mem}} = k_{IX} a_I^{\text{aq}} a_X^{\text{aq}} \quad (4.1)$$

For simplicity, we now replace the activities of the species in the membrane phase with the respective concentrations (upper indexes denoting the membrane phase now omitted):

$$C_I C_X = k_{IX} a_I^{\text{aq}} a_X^{\text{aq}} \quad (4.2)$$

On the other hand, if the membrane contains IR salt with R^- lipophilic anion, the macroscopic electroneutrality requires the following:

$$C_I = C_R + C_X \quad (4.3)$$

The combination of these equations allows obtaining for the concentration of X^- in the membrane phase:

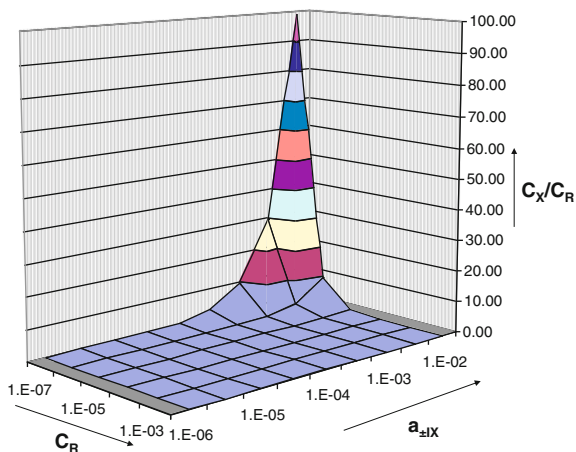
$$C_X = \left(\sqrt{C_R^2 + 4k_{IX} a_I^{\text{aq}} a_X^{\text{aq}}} - C_R \right) / 2 \quad (4.4)$$

Thus, the concentration of co-extracted X^- ions in the membrane phase depends on the R^- concentration in the membrane, on the activity of IX electrolyte in the aqueous phase, and on the value of the partition coefficient. One can see that as long as $C_R^2 \gg 4k_{IX} a_I^{\text{aq}} a_X^{\text{aq}}$ the concentration of X^- ions in the membrane is negligible, $C_X \ll C_R$ and effectively only I^+ cations cross the interface. This is the Donnan exclusion.

Donnan exclusion fails in the following cases: (1) too low ion-exchange capacity (too low R^- concentration), (2) too high concentration of IX electrolyte in the aqueous phase, or (3) too high partition coefficient value. Then, it may happen that $C_X \cong C_R$ and even $C_X \gg C_R$. These regularities are presented in Fig. 4.2. For most applications, the R^- sites concentration of 0.01 or even 0.001 M is enough.

The selectivity of ISEs with membranes based on ion exchangers is normally low and obeys the so-called Hofmeister series. That is, ISEs are more selective to hydrophobic ions and less selective to hydrophilic ions. Basically, this is because

Fig. 4.2 Donnan exclusion. The dependence of the C_X/C_R ratio on the R^- site concentration in membrane and the activity of IX electrolyte in solution. The data refer to $k_{IX} = 10^{-6}$

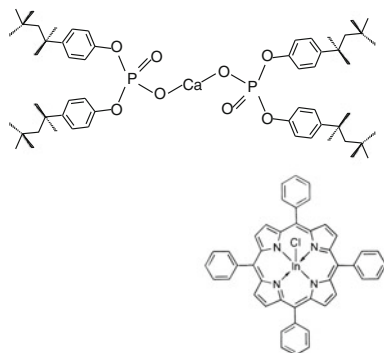


ion exchangers interact with ions only electrostatically, and the interaction is relatively weak. The detailed explanation of the origin of the Hofmeister series for ISE selectivity is given in Sect. 4.4.2.

Let us turn now to ionophores. Ionophores which are in use for solvent-polymeric membranes are divided into two groups: neutral ionophores (neutral carriers, neutral ligands) and charged ionophores (charged carriers, charged ligands) [1, 2, 9]. We will start the discussion with charged ionophores. Being charged, these ionophores impart some ion-exchange capacity to membranes and therefore prevent from co-extraction of electrolyte and ensure ion-exchange equilibrium at the membrane/solution interface. The first charged ionophore was calcium didecylphosphate used in Ca^{2+} -ISEs [10]. Since then, more charged ionophores have been invented, for example, bis[4-(1,1,3,3-tetramethylbutyl)phenyl]phosphate, also selective to Ca^{2+} ions [11], a number of metal porphyrine complexes [12–16] and guanidinium bases [17] for various non-Hofmeister anionic electrodes, see Fig. 4.3. It must be noted that metal porphyrines may also be neutral and, in this case, act as neutral ionophores [18].

The interaction of charged ionophores with ions in membranes is not of the pure electrostatic nature. Therefore, this interaction is much stronger and more selective than in the case of ion exchangers. From the formal point of view, these differences are quantified by the respective ion-to-ionophore association constants. It is not possible to define a threshold value of the association constant in such a way that lipophilic species with association constants below the threshold value are ion exchangers and those above the threshold are charged ionophores. In this sense, there is no way to set a formal difference between ion exchangers and charged ionophores. However, this does not cause a problem. Although only little data are available on the respective association constants [19–21], the data on the ISE selectivity allow for conclusion that the difference in association constants between ion exchangers and charged ionophores is about several orders of magnitude. Thus, the two groups are far from one another in terms of the association

Fig. 4.3 Structures of some complexes of ions with charged ionophores. Target ions given in *parenthesis*. Calcium bis[4-(1,1,3,3-tetramethyl butyl)phenyl]phosphate (Ca^{2+}), *top*; In^{III} teraphenylporphyrine chloride (NO_2^-), *bottom*



constants values, and the question of where exactly the “threshold” must be laid is irrelevant. From the practical point of view, it is widely recognized that a charged ionophore is a species which allows for obtaining non-Hofmeister selectivity, so that the selectivity to the respective ion is in contrast to its position in the Hofmeister series.

4.2 Neutral Ionophores

Neutral ionophores are non-electrolytes, these are nonionic species which are neither intrinsically charged nor dissociate producing charged species. Neutral ionophores are highly lipophilic molecules capable of selective binding of ions with formation of ion-to-ionophore complexes. Among the first and still widely used neutral ionophores were valinomycin for potassium-selective ISEs [22] and nactines for ammonium electrodes [23]. These two, together with crown and bis-crown ethers, belong to ionophores of macrocyclic structure. Later on, a number of synthetic neutral ionophores were invented. These were macrocyclic compounds: crown and bis-crown ethers, acyclic lipophilic diamides (podands), various calixarenes as neutral ionophores for cations. A large number of acyclic ionophores (podands) have been invented by Simon group in ETH Zürich: these ionophores are normally called by their respective ETH numbers.¹ All these ionophores selectively bind cations and are used in membranes for cation-selective electrodes.

Neutral ionophores binding anions are less numerous. These are lipophilic fluoro ketones like trifluoroacetyl-p-heptylbenzene selective to CO_3^{2-} [24–29] for carbonate, phosphate, and sulfate electrodes, salofenes [30, 31], thiourea derivatives selective to Cl^- [32, 33], mercurocarborands [34]. Examples of the neutral ionophore structures are presented in Fig. 4.4.

¹ ETH comes from Swiss-German name for the Swiss Federal Institute of Technology, Zurich.

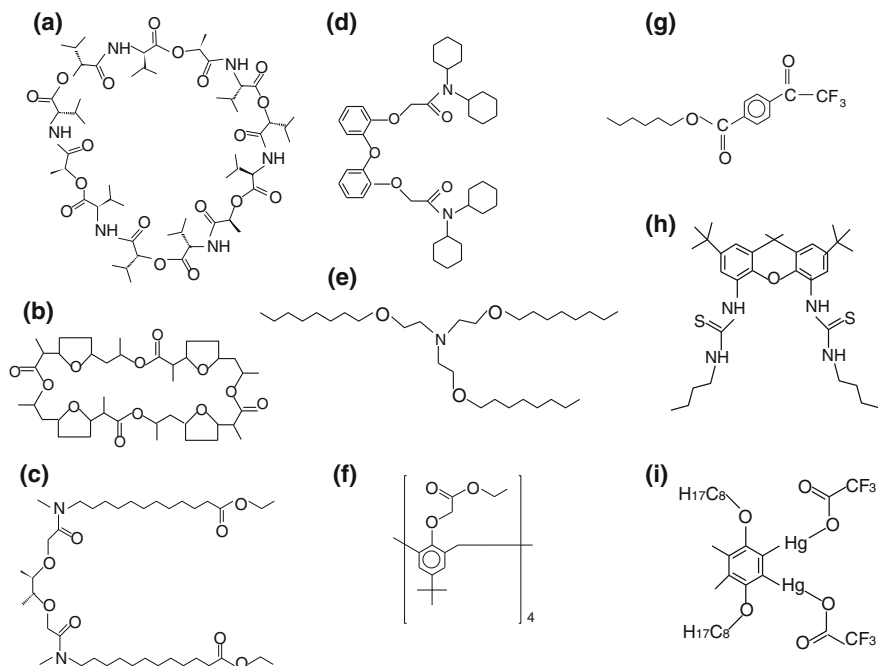


Fig. 4.4 Structures of some neutral ionophores. Target ions given in *parenthesis*. **a** valinomycin (K^+), **b** tetranactin (NH_4^+), **c** ETH 1001 (Ca^{2+}), **d** ETH 231 (Ba^{2+}), **e** Tris(2-octyl-oxy-ethyl)amine (H^+), **f** tert(4)butylcalixarene (Na^+), **g** *p*-hexyltrifluoroacetylbenzoate (CO_3^{2-}), **h** bis(thiourea)derivative (Cl^-), **i** organomercury compound (Cl^-)

Unlike ion exchangers and charged ionophores, neutral ionophores impart no ion-exchange capacity to membranes. Therefore, to exclude co-extraction of aqueous electrolytes, electrode membranes based on neutral ionophores must be doped with ion exchangers. However, in the early years of ISEs with neutral ionophore membranes, these membranes did not contain intentionally added ion exchangers. Surprisingly, the electrodes responded with almost full Nernstian slope [35]. The slope clearly indicated unipolar conductivity of membranes: only cations were permeable across them.² A number of theories were proposed to explain this fact. One explanation was rather straightforward. It was assumed that the whole membrane comprises the space-charge region, that is, macroscopic electroneutrality fails, and the membranes are positively charged [36]. This assumption means that the two electrical double layers, on the both sides of the membrane, overlap. According to the Gouy–Chapman theory, one can relate l , the effective thickness of the space-charge layer (the diffuse part of the electric double layer), to the concentration of ions in the respective phase and the dielectric permittivity of the phase:

² At that times only cation-binding neutral ionophores were known.

$$l = \frac{1}{F} \sqrt{\frac{RT\varepsilon_0\varepsilon}{2C}} \quad (4.5)$$

Here, l stands for the effective thickness of the space-charge region (meters), C is the dissociated electrolyte concentration (mol/m^3), ε is the relative dielectric permittivity of the phase, and $\varepsilon_0 = 8.85 \times 10^{-12}$ F/m (Farad per meter) is the vacuum dielectric constant. R , T , F are gas constant, absolute temperature, and Faraday constant. For a membrane with the thickness 0.4 mm (meaning $l = 0.2$ mm), Eq. (4.7) suggests $C = 1 \times 10^{-12}$ mol/m^3 or 10^{-15} M. Assuming the diffusion coefficients of about 10^{-8} cm^2/s [1], the resistivity of such a phase would be in three or more orders of magnitude higher than the experimental value for a site-free membrane. Thus, the space-charge theory is not supported by the experimental data.

A rather elegant theory was proposed by Simon group in ETH Zürich [37] and by Stefanova group at St. Petersburg University [38]. It was suggested that anions are co-extracted by neutral ionophore membranes in quantities equivalent to that of cations. However, the anion mobility in membranes is much lower than that of complexed cations because anions are immobilized in water droplets (inverted micelles) in the membrane phase. Indeed, when being in contact with aqueous solutions, membranes sorb water and become cloudy. This is because of Rayleigh scattering of light by the droplets. Since the scattering refers to the visible range, one can conclude that at least some of the droplets are rather large having diameter commensurable with the wavelength of visible light, that is, about 400–700 nm. The mobility of anions entrapped by water droplets is limited by the mobility of the droplets, and the latter move very slow due to their large size. Cations form lipophilic complexes with neutral ionophores. Therefore, cations are located in the organic phase and can diffuse within membranes relatively freely. In this way, the membrane as a whole is neutral, containing cations and anions in equivalent quantities, but cations move across the membrane much faster than anions. This is how the authors of [37, 38] explained the cationic response of membranes based on neutral ionophores containing no intentionally added ion-exchanger sites.

It was also suggested that the cationic response of these membranes is due to inevitably present lipophilic ionic impurities [39]. These are impurities present in polymers or those originating from plasticizers. The latter are often esters and, due to hydrolysis, produce organic acids and alcohols. Acids at least to some extent dissociate producing lipophilic anions (cation-exchanger sites) and hydrogen ions which are replaced by cations selectively interacting with the ionophore. This opinion got broad experimental support [40–42] and nowadays is generally accepted. Obviously, the content of the intrinsic impurities is difficult to standardize in the ISE manufacturing process. Also, the resistivity of such membranes is often too high, making the signal noisy and sensitive to external electrostatic field, so that screening the cell by use of a Faraday cage is needed for measurements. Therefore, modern ISE membranes based on neutral ionophores are always doped with deliberately added ion exchangers. This not only makes the response more stable and reproducible, but also allows for the optimization of the selectivity

[43–47], see Sect. 4.5.2. Addition of ion exchangers permits significant lowering of the resistance of membranes, facilitating the practical measurements with ISEs.

Some ionophores show a dualistic behavior working either as neutral or as charged ionophores dependent on external conditions. It was shown that some weak lipophilic acids, like monensin, as well as alkylphosphoric acids may act as charged or as neutral ionophores dependent on the pH of the solution [47].

A large number of charged and neutral ionophores are listed and briefly characterized in a review paper [2]. Although this review has been published more than a decade ago, it remains a very useful source of information when a suitable ionophore must be chosen for a certain application.

4.3 Polymers and Plasticizers in ISE Membranes

4.3.1 *Poly(vinylchloride) Plasticized Membranes*

The ionophore(s) content in ISE membranes is normally only 0.5–2 % of the whole membrane mass, while most of the membrane mass is made of polymer and (normally) also plasticizer. Polymers suitable for ISE membranes must meet a number of requirements. These polymers must be mechanically robust and in the same time elastic—either due to intrinsically low glass transition temperature (T_g) or due to a plasticizer added. Polymers must be processable, stable within a reasonable temperature range, for example, between 0 and 50 °C, must be chemically inert, must not lose their molecular mass spontaneously, must be non-soluble in water, and stable against hydrolysis, at least up to pH 8–9.

In many cases, particularly for poly(vinylchloride) (PVC) membranes, some of the requirements are fulfilled by adding plasticizers. The latter play a dualistic role: plasticizers allow for elasticity of membranes (and for sufficient mobility of ionophores and ions within the membrane phase) at temperatures below T_g , and on the other hand, plasticizers act as solvents for ionophores.

PVC remains the most popular polymer in ISE membranes, wherefore we will discuss this kind of membranes in utmost detail. PVC-based membranes always require a suitable plasticizer because the glass transition temperature of PVC is much higher than the temperature in ISE applications. Different kinds of PVC show T_g from 85 to 102 °C [48, 49]. The mobility of ions and ionophores in polymers at temperatures below T_g is extremely low hindering measurements with such membranes. Also, pure PVC cracks spontaneously. For suitable elasticity, it is enough to add 0.5 mass units of a plasticizer to 1 mass unit of PVC. Obviously, one can dissolve ionophore(s) in this amount of the plasticizer and thus dope the membrane with ionophores. However, even at the 1:1 mass ratio of the plasticizer to the polymer, the electrical resistivity of the membranes is too high, and therefore, the measured signals are noisy. On the other hand, the membrane with the ratio 5:1 is sticky and jelly-like, mechanically non-robust and hardly suitable for real-world sensors. In the pioneering works [50, 51], the plasticizer to PVC

ratio was 3:1 and 2:1, respectively. For decades, the choice of this ratio was rather traditional than scientifically sounded. Only a handful of examples are known when the optimization of the plasticizer to PVC ratio indeed allowed for significant improvement of the ISE performance. These reports highlight the improvement of the lower detection limit of the ISEs by the optimization of this ratio [52]. However, the large majority of PVC-based ISE membranes contain 30–33 % of PVC and 60–66 % of a plasticizer, thus the membranes with the 2:1 ratio predominate.

Plasticizers used in PVC membranes are non-volatile organic liquids compatible with PVC. These are mostly esters, like carboxylic acid esters or phosphorous and phosphonic acid esters, and also some ethers, in first place, 2-nitrophenyloctyl ether. Structures of the most popular plasticizers used in PVC membranes are presented in Fig. 4.5.

The number of plasticizers suitable for PVC membranes is obviously much smaller than that of solvents for liquid membranes. There were suggestions that solvation of ions by plasticizers may significantly modify the selectivity of ISEs [53, 54]. Attempts were made to develop special plasticizers for almost any analyte ion [55]. Indeed, trialkylphosphates or dioctylphenylphosphonate as plasticizers are advantageous for calcium electrodes [56, 57]. A very characteristic example is the water hardness sensor. Membrane containing didecylphosphoric acid in trihexylphosphate provides high selectivity to Ca^{2+} ions in the presence of Mg^{2+} and other alkali-earth cations, while the replacement of trihexylphosphate with n-decanol levels the selectivity between Ca^{2+} and Mg^{2+} ions, and the respective electrode is used as a water hardness sensor [10, 58]. However, all other

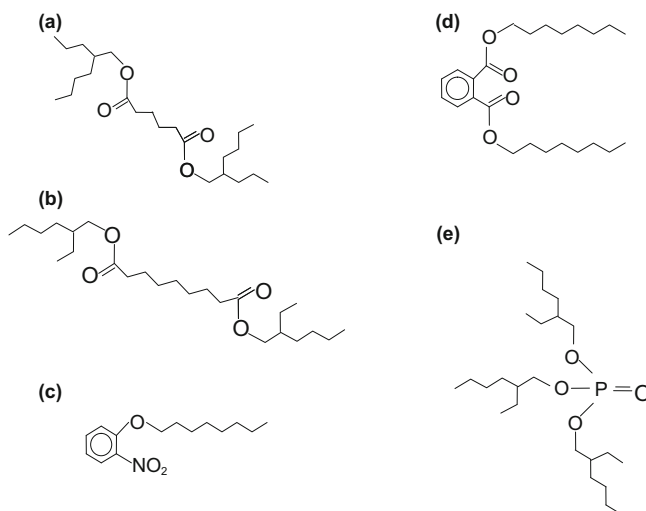


Fig. 4.5 Structures of some plasticizers used in PVC membranes. **a** bis(butylpentyl)adipate, **b** bis(2-ethylhexyl)sebacate, **c** 2-nitrophenyloctyl ether, **d** dioctylphthalate, **e** tri(2-ethylhexyl)phosphate

known PVC membranes can be made with one of the following plasticizers: bis(butylpentyl)adipate (BBPA), bis(2-ethylhexyl)sebacate (DOS), or 2-nitrophenyloctyl ether (oNPOE). The first two are used for ISEs selective for monovalent ions, and oNPOE is more suitable for divalent ion sensors [1, 2].

The point is that the potentiometric selectivity can be achieved if the target analyte is more eager to transfer from the aqueous solution phase to the membrane phase than other ions present in the sample. In principle, in terms of energy, a transfer from a polar phase (aqueous solution) to a low-polar membrane phase is unfavorable for any charged species. However, the energy loss is especially large for a divalent ion. Morf and Simon considered this issue using the Born equation for energy of the transfer of a charged species from vacuum to a phase with a dielectric constant ε [59]. Assuming I^{z+} ions form (in aqueous solution) $[IL]^{z+}$ complexes with L neutral ionophore, and then distribute between the two phases, they obtained for the distribution coefficient

$$\lg k_{IL} \sim \frac{z_{IL}^2}{r_{IL}} \left(\frac{1}{78.5} - \frac{1}{\varepsilon} \right). \quad (4.6)$$

Here, z_{IL} is the charge of the ion-ionophore complex, and r_{IL} stands for the complex effective radius, 78.5 is the dielectric constant of water. Equation (4.6) shows that the decrease in ε always causes a decrease in the affinity of the species to the membrane phase. Since the charge appears in Eq. (4.6) in the second power, the effect is more pronounced for divalent ions. Thus, low-polar plasticizers are especially unfavorable for divalent ions and therefore are more suitable for monovalent ions, while ISEs for divalent ions require membranes with polar plasticizers.

All in all, this concept proved to be fruitful, especially for sodium and calcium ISEs [60–62]. However, not all the ISEs follow this simple rule. For instance, the replacement of low-polar bis(hexyl)adipate in Na^+ ISEs with more polar 2-nitro-p-cumol does lead to the increase in the interference from Ca^{2+} ions. However, it does not alter the influence from Mg^{2+} , and the interference from Ba^{2+} is even decreased [63]. Apparently, this is due to different stoichiometry of the complexes of different ions with the same ionophore, so the effective radii of the respective complexes are also different.

Membranes plasticized with polar plasticizer oNPOE show dielectric constant $\varepsilon = 14$ which lies in between $\varepsilon = 2$ for pure PVC and $\varepsilon = 24$ for pure oNPOE. However, the relation between the dielectric constant of plasticized PVC membranes and that of the respective pure plasticizer is not always so trivial. The dielectric constant of pure DOS is $\varepsilon = 4$, but a PVC membrane plasticized with DOS has $\varepsilon = 6$, thus exceeds that of any of the components [64]. This fact can be explained as follows [65]. In pure PVC, the rotation of C–Cl bond around the C–C bond of the polymer backbone is “frozen,” but in plasticized PVC it becomes possible. Therefore, in plasticized PVC, the polar C–Cl bonds orientate in an electric field and decrease its intensity, which on the macroscopic level manifests in higher dielectric permittivity. This is why the dielectric constant of a membrane

containing low-polar plasticizer may exceed ε of the pure components. It was shown that the dielectric constants of plasticized PVC membranes lie within the range from 4 to 14 [64].

Plasticized PVC membranes are cast from the so-called membrane cocktails. These are solutions of PVC, plasticizer and ionophores in a volatile organic solvent. Most frequently the latter is tetrahydrofuran (THF), sometimes (seldom) cyclohexanone is used. The amount of THF in the cocktail is normally about 85 %, the rest, the so-called dry mass, is made of PVC, plasticizer and ionophores and ion exchangers (ionic additives). The cocktail can be cast onto a Petri dish, and in this way, a large “master” membrane with a diameter of 3–10 cm can be obtained after the evaporation of THF. The thickness of the membrane, obviously, depends on the dry mass of the cocktail and normally varies from 0.3 to 0.6 mm. Next, smaller discs with diameters of 5–10 mm can be cut from this master membrane with a suitable cork bore. The discs can be fixed in electrode body in different ways. The so-called Philips electrode body is the most popular, see Fig. 4.6. Membrane disc is fixed and sealed with a silicon O-ring in screw cap connected to the body. The latter contains internal reference electrode. In Fig. 4.6, the membrane is shown black to be seen clearly. The Philips body set also includes a special tool (similar to a cork bore) to cut membrane discs from master membrane.

Membrane discs can be glued to PVC bodies with a PVC-cyclohexanone slurry. In the case of solid-contact electrodes, no master membrane is prepared. Instead, portions of membrane cocktails can be drop-cast directly on the respective substrate. The area of the membrane formed after evaporation of THF must be slightly larger than that of the substrate, so that the membrane surely covers all the substrate and some part of the body as well. No glue is used in this case; however, poor adhesion of the membrane to the substrate and/or to the body may cause a

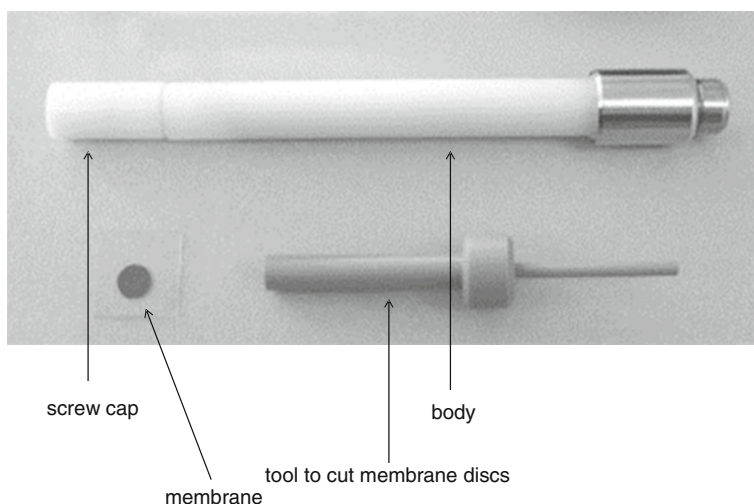


Fig. 4.6 Philips electrode body

shortened lifetime of the electrode. Sometimes membranes can even detach from the substrate.

Plasticized PVC membranes appear macroscopically uniform. However, studies of the component distribution over the membrane volume showed differently. By means of X-ray photoelectron spectroscopy and secondary ion mass spectroscopy [66], as well as by atomic force microscopy [67], it was shown that the layers in the outmost vicinity of the membrane surface are enriched by the plasticizer in comparison with its average content over the whole membrane. Experiments with small-angle neutron scattering revealed tiny PVC clusters the size of about 6 nm which do not dissolve in THF even after lengthy and vigorous mixing of the membrane cocktail [68]. Thus, plasticized PVC membranes are to some extent intrinsically non-homogeneous.

When solvent-polymeric membranes are in contact with aqueous solutions, another kind of non-homogeneity arises. It originates from water sorption by the membranes. Plasticized PVC membranes sorb water in relatively large quantities: from 0.5 to 2 % of the total mass of the membrane [69, 70]. Water in membranes aggregates into large clusters (inverted micelles) which cause scattering of the transmitting light. Because of this, membranes in contact with solutions become dim, sometimes even milk white. When taken out from solutions, membranes lose absorbed water. It evaporates from membranes within several minutes, up to about 1 h depending on the membrane composition and geometry and on the ambient temperature. After that, the membranes became fully transparent again. Water sorption strongly depends on the nature of the plasticizer, membranes plasticized with phosphates and phosphonates sorb water in larger quantities than other kinds of membranes [70].

Water uptake was studied by spectrophotometry and NMR [69, 71–74]. It was shown that water is non-uniformly distributed within the membrane. Membrane layers in the vicinity of the surface are enriched with water when compared with the membrane bulk [69]. The typical size of water clusters is about 16 nm, and the freezing point of water in the clusters may be below zero, within the range from 0 to $-15\text{ }^{\circ}\text{C}$ [72]. Water uptake takes place in two stages. During the first hour of contact, membrane sorbs water from solution and forms mobile particles with diffusion coefficients of about $D \approx 10^{-6}\text{ cm}^2/\text{s}$. After that, light-scattering clusters (water droplets) form with a much lower mobility: $D \approx 10^{-9}\text{ cm}^2/\text{s}$. The non-uniformity of the water distribution in the membrane is most pronounced during the first few hours of contact with the solution. However, even after 5 days of contact, the content of water in the layers of about $25\text{ }\mu\text{m}$ from the membrane/solution interface is about 20 % higher than the average value over the whole membrane [73, 74]. Analogous non-uniformity was also found for the distribution of ionophores [75].

Further studies of the water uptake were carried out for solid-contact ISEs with conducting polymers in the transducer layer in between ionically conducting PVC membranes and electronically conducting substrates (glassy carbon, graphite). These studies also revealed several kinds of water clusters with diffusion coefficients $D_1 = 4.7 \times 10^{-10}$, $D_2 = 5.1 \times 10^{-11}$, and $D_3 = 4.7 \times 10^{-12}\text{ cm}^2/\text{s}$ in the

poly(trioctylthiophene) layer, that is, in several orders of magnitude lower than in PVC [76, 77]. The absorbed water does not only make a dispersed phase within the membrane, but also form a continuous layer even on hydrophobic substrates like conducting polymers and graphite [76–79]. By the neutron reflectometry and the IR–ATR methods, it was shown that the water layer thickness is about 10 nm [76, 79].

These peculiarities hinder correct theoretical description of the electrochemistry of solvent-polymeric membranes. Most often, however, these peculiarities are neglected in theoretical considerations, and solvent-polymeric membranes are normally treated as liquid phases. The presence of the polymer matrix is only indirectly accounted for. For instance, in considerations of the ion transfer across the ISE membranes, the typical values of the ion diffusion coefficients are 10^{-8} cm²/s, while those in liquid membranes are in 1.5–2 orders of magnitude higher. The polymer therefore is considered as an inert network which impedes the movement of the species within the membrane, but otherwise does not participate in any chemical interactions.

4.3.2 Non-PVC Polymeric Membranes, ISEs with Ion-Exchanger Sites and Ionophores Covalently Bound to Polymer Backbone

One of the disadvantages of plasticized polymeric membranes, in particular, plasticized PVC membranes, is their sensitivity to elevated temperatures and organic solvents. Indeed, plasticizers simply dissolve in organic solvents, while at elevated temperatures, membranes get depleted in plasticizers and ionophores even in aqueous solutions. Under normal conditions: room temperature and only aqueous samples, the lifetime of ISEs with plasticized PVC membranes is about 1 year, although the shelf time may be up to 10 years [80]. Therefore, for many years, efforts were made and still are made aimed to replace PVC as the membrane matrix polymer with other polymers. The final goal would be a polymer with a low glass transition temperature and with covalently bonded ionophores. Such a membrane may be stable at elevated temperatures as well as in mixed aqueous-organic solutions.

Among polymers, apparently suitable as substitutes of PVC, are silicon rubbers, acrylic polymers, acrylsiloxanes, and urethanes. Low glass transition temperature allows, in principle, use of these polymers without plasticizers. Anyway, these membranes are normally doped with plasticizers which in these cases are mostly needed as solvents for ionophores [81]. Much less is published about ISEs with plasticizer-free membranes containing only a polymer and an ionophore. The latter can be distributed within the polymer bulk as individual molecules, or covalently bonded to the polymer backbone [82].

Historically, first attempts of substitution of PVC were focused on silicon rubbers [35]. Silicon rubbers adhere to various substrates much stronger than PVC, which is an important advantage, especially in production of solid-contact electrodes or ion-selective field effect transistors. Plasticizers must be added to these membranes to increase the solubility of ionophores, to ensure Nernstian response slope, and to reduce Ohmic resistance of the membranes. These goals can be achieved without a decrease in the adhesion of membranes to substrates [83, 84].

Later, photocured polymers, mostly of acrylic or urethane nature, and acrylic-siloxane polymers had become more popular as substitutes of PVC. In addition to good adhesion properties, these polymers allow for photolithographic technology of the sensor manufacturing. This, in turn, strongly facilitates mass production of small-sized sensors with good piece-to-piece reproducibility and low rejection. Calcium electrodes with acrylic membranes are capable of working in the presence of high contents of perchlorate [85]. Methacrylic membranes for ISEs selective to K^+ and to various inorganic anions have been described in [86]. Polyurethane and urethane-acrylic membranes were described in [81, 87–89], among them for carbonate ions [88] and for K^+ , NH_4^+ , Ca^{2+} [81, 89]. Self-plasticizing membranes with methacryl-acryl copolymer matrixes having glass transition temperatures from -20 to -44 °C can be used for K^+ , Na^+ , Ca^{2+} and also for pH ISEs [49, 90–93]. A method was developed to obtain acrylic membranes for K^+ and Ca^{2+} ISEs with a given ratio of the concentrations of the target analyte ion and interfering ion, to preset the dynamic range of the ISEs [94]. Ion diffusion coefficients and therefore also trans-membrane fluxes of electrolytes in acrylic polymers are much lower than those in plasticized PVC. This makes ISEs with acrylic membranes promising for measurements in strongly diluted samples [95]. It was also reported about a successful use of ionic liquids as plasticizers in ISEs with acrylic membranes [96–98].

Durability of ISE membranes can be improved by covalent binding of ionophores and/or ion-exchanger sites to polymeric backbone (PVC or other polymers). Poly-crown ethers were used as oligomeric ionophores in plasticized PVC membranes since late 1970s [99]. It was reported on ISEs with crown ethers and calixarenes covalently bonded to silicone rubbers [100–102] or to carboxylated PVC [103]. More recently, membranes with neutral ionophores bound to acrylic polymer backbone were obtained for Ca^{2+} [82] and Pb^{2+} [104] ISEs. Calcium ISEs with alkylphosphoric groups (charged ionophores) were immobilized on polystyrenbutadiene [105, 106] and on vinylchloride-vinylacetate copolymer [107]. Dodecacboran lipophilic anion known as a promising analog of tetraphenylborates (widely used cation exchangers) [108, 109] can also be covalently bound to acrylic backbone. In this way, a novel Ca^{2+} electrode was made with a polymeric cation exchanger [110]. Polyetherketon functionalized with sulfonated groups was successfully used in NH_4^+ ISEs with nonactin as neutral ionophore [111]. Also, acrylic polymers are sometimes used in solid-state reference electrodes [112, 113].

Fluorous polymers, plasticizers, and ionophores have been reported by Bühlmann [114–117]. The selectivities of ISEs with fluorous membranes significantly exceed those of their PVC analogs. The membranes consisting of these extremely hydrophobic compounds are especially promising for clinical and biological

applications since the ISEs with these membranes do not suffer from bio fouling. The respective sensors are also suitable for measurements at trace levels of analytes, for example, down to 4.1 ppt Ag^+ [117]. Originally, fluoros membranes were of liquid type, more recently it was reported on polymeric fluoros membranes with Teflon AF2400: poly[4,5-difluoro-2,2-bis(trifluoromethyl)-1,3-dioxole]-co-poly(tetrafluoroethylene) as polymer matrix [116].

A totally novel approach was proposed by Gyurcsanyi [118]. Ionophores are immobilized on the surface of gold nanopores. First promising results are obtained with Ag^+ —selective sensors with thiacalixarene derivative as neutral ionophore.

4.4 The Theory of the Ionophore-Based Membranes Response and Selectivity

4.4.1 Response and Selectivity of ISEs with Membranes Containing Ion Exchangers and Charged Ionophores

Discussion of the selectivity of ISEs with membranes containing ion exchangers and charged ionophores requires some mathematical apparatus; namely, we will consider the boundary potentials on the two sides of the membrane: the external (sample) side and the internal side, as well as the diffusion potential within the membrane. In this way, we will obtain an equation for the overall membrane potential (the electric potential difference across the whole membrane). To do this, we will use ideas and equations discussed in Chap. 2.

If the membrane/solution interface is at electrochemical equilibrium with regard to I^z species, the interfacial (boundary) potential:

$$\varphi_b = \varphi^{(\text{mem})} - \varphi^{(\text{aq})} = -\frac{(\mu_I^{0(\text{mem})} - \mu_I^{0(\text{aq})})}{z_I F} - \frac{RT}{z_I F} \ln \frac{a_I^{(\text{mem})}}{a_I^{(\text{aq})}} \quad (4.7)$$

This equation, the same as Eq. (2.8), is presented here for the readers' convenience. In most cases, the activities of all the species in the membrane phase are replaced with the concentrations of the respective free (non-complexed, non-associated) ions. Under this assumption, we can rewrite Eq. (4.7) in the following form:

$$\varphi_b = \varphi^{(\text{mem})} - \varphi^{(\text{aq})} = -\frac{(\mu_I^{0(\text{mem})} - \mu_I^{0(\text{aq})})}{z_I F} - \frac{RT}{z_I F} \ln \frac{C_I^{(\text{mem})}}{a_I^{(\text{aq})}} \quad (4.8)$$

Since the membrane, generally speaking, separates solutions with different compositions, the values of the species concentrations within the membrane phase may vary across the membrane. The membrane (or its part with non-uniform distribution of ions) constitutes therefore a diffusion layer. The diffusion of the species across this layer results in additional contribution to the membrane

potential: the diffusion potential. Although this phenomenon is discussed in Sect. 2.3.2, here we address this issue again, adopting our consideration closer to ionophore-based membranes.

The flux of I^{z_I} charged species caused by the gradient of the respective electrochemical potential across the membrane obeys the Nernst–Planck equation:

$$\begin{aligned} J_I &= -u_I C_I \frac{d}{dx} (\mu_I + z_I F \phi) = -u_I C_I \frac{d}{dx} (RT \ln a_I + z_I F \phi) \\ &= u_I C_I \frac{d}{dx} (RT \ln C_I + z_I F \phi) \end{aligned} \quad (4.9)$$

The electric current density (i) produced by the fluxes of charged species equals the sum of the respective fluxes multiplied by the respective charge numbers, and the whole sum is multiplied by the Faraday constant. Under the potentiometric conditions, the electric current density is zero, so

$$i = F \sum_I z_I J_I = 0 \quad (4.10)$$

Let us consider the case when the membrane containing R^- lipophilic sites is in contact with mixed solutions of IX , JX mono-monovalent hydrophilic electrolytes. We will also assume that the Donnan exclusion holds, and that the electrolytes in the membrane are present as ions R^- , I^+ , and J^+ , and ion-pairs IR , JR . This means that R^- , I^+ , and J^+ are the only charged species present in the membrane. Using Eq. (4.9), we obtain for this simple case:

$$-u_I C_I \frac{d}{dx} (RT \ln C_I + F \phi) - u_J C_J \frac{d}{dx} (RT \ln C_J + F \phi) + u_R C_R \frac{d}{dx} (RT \ln C_R - F \phi) = 0 \quad (4.11)$$

After combining all the terms containing the potential in the left-hand part and all other terms in the right-hand part, we get

$$F \frac{d\phi}{dx} (u_I C_I + u_J C_J + u_R C_R) = -RT \left(u_I \frac{dC_I}{dx} + u_J \frac{dC_J}{dx} - u_R \frac{dC_R}{dx} \right), \quad (4.12)$$

which immediately gives the differential form of the diffusion potential within the membrane:

$$\frac{d\phi}{dx} = -\frac{RT d(u_I C_I) + d(u_J C_J) - d(u_R C_R)}{F (u_I C_I + u_J C_J + u_R C_R)} \quad (4.13)$$

The macroscopic electroneutrality holds, so that $C_I + C_J = C_R$ in any layer within the membrane. The interaction between I^+ and R^- versus the interaction between J^+ and R^- is generally speaking different. Therefore, profiles of I^+ and J^+ species across the membrane caused by the difference of the solution compositions may also cause a profile of R^- distribution as well. Because of this, Eq. (4.13), although it looks

very simple, for integration thereof requires either the knowledge of the profiles of the species distribution across the membrane or some further simplifications.

One of these simplifications can be the assumption of the complete dissociation of the membrane electrolytes, so that only R^- , I^+ , and J^+ , that is, only charged species are present in the membrane, and no ion-pairs exist. In such a case, the replacement of I^+ with J^+ counter-ion or vice versa does not produce any driving force for R^- flux: the competing ions are identical for the sites. Then, at least in the steady state, the sites are distributed uniformly, there is no flux of R^- , and the concentration of sites everywhere within the membrane equals their total concentration: $C_R = C_R^{\text{tot}} = \text{Const}$. Thus, under the assumption of the complete dissociation of the electrolytes in the membrane, $C_I + C_J = C_R = C_R^{\text{tot}} = \text{Const}$. This allows for the integration of Eq. (4.13) which results in the equation for the diffusion potential within the membrane:

$$\varphi_d = -\frac{RT}{F} \ln \frac{(u_I C_I + u_J C_J)^{(r)}}{(u_I C_I + u_J C_J)^{(l)}} \quad (4.14)$$

Upper indices (l) and (r) denote the external and the internal sides of the membrane. The same result can be obtained in the case when I^+ and J^+ ions do form ion-pairs with R^- sites, but the respective association constants are the same. Here, once again, the competing ions are identical for the sites.

Using the so-called ionic distribution coefficients introduced by Eisenman [119] as $k_I = \exp(-(\mu_I^{0(\text{mem})} - \mu_I^{0(\text{aq})})/RT)$,³ one can express the concentration of J^+ ions in the membrane as a function of the I^+ and J^+ activities in the aqueous solution and of the concentration of I^+ ions in the membrane:

$$C_J = C_I \frac{a_J k_J}{a_I k_I} \quad (4.15)$$

By combining Eq. (4.8) written for the both sides of the membrane, with Eqs. (4.14) and (4.15), we obtain for the overall membrane potential:

$$\begin{aligned} \varphi_{\text{mem}} &= \varphi_b^{(l)} + \varphi_b^{(r)} + \varphi_d \\ &= -\frac{RT}{z_I F} \ln \frac{C_I^{(l)}}{a_I^{(l)}} - \frac{RT}{z_I F} \ln \frac{a_I^{(r)}}{C_I^{(r)}} - \frac{RT}{z_I F} \ln \frac{C_I^{(r)} \left(u_I + u_J \frac{a_J^{(r)} k_J}{a_I^{(r)} k_I} \right)}{C_I^{(l)} \left(u_I + u_J \frac{a_J^{(l)} k_J}{a_I^{(l)} k_I} \right)} \end{aligned} \quad (4.16)$$

³ Note, in contrast to the electrolyte distribution coefficient, the ionic distribution coefficient does not show the ratio of the activities of the species within the two contacting phases. This ratio for any charged species is also dependent on the value of the interfacial electrical potential. Only combinations of the ionic distribution coefficients like multiples of those for a cation and an anion, or ratios of these values for ions of the same charge are potential independent. These multiples and ratios are equivalent to the ordinary electrolyte distribution coefficients or to the ratios of the latter, respectively. Nevertheless, ionic distribution coefficients are useful, especially for the theoretical descriptions of the boundary and membrane potentials.

Trivial algebra allows obtaining from Eq. (4.16):

$$\varphi_{\text{mem}} = -\frac{RT}{z_I F} \ln \frac{\left(a_I^{(r)} + \frac{u_J k_J}{u_I k_I} a_J^{(r)} \right)}{\left(a_I^{(l)} + \frac{u_J k_J}{u_I k_I} a_J^{(l)} \right)} \quad (4.17)$$

Let us now assume that the right-hand side of the membrane is in contact with the internal solution of the ISE and the composition of this solution is constant, while the left-hand side solution comprises a sample or a calibrator. Then for the membrane potential, we get

$$\varphi_{\text{mem}} = \varphi_{\text{mem}}^0 + \frac{RT}{z_I F} \ln \left(a_I^{(l)} + \frac{u_J k_J}{u_I k_I} a_J^{(l)} \right) \quad (4.18)$$

Thus, in the case of the complete dissociation of electrolytes in the membrane, as well when the interactions between sites and both kinds of the competing ions are identical, the membrane potential follows the Nikolsky equation:

$$\varphi_{\text{mem}} = \varphi_{\text{mem}}^0 + \frac{RT}{z_I F} \ln(a_I + K_{IJ} a_J), \quad (4.19)$$

and the selectivity coefficient to the target (primary) I^+ ions in the presence of the interfering J^+ ions is

$$K_{IJ} = \frac{u_J k_J}{u_I k_I} \quad (4.20)$$

Thus, the selectivity coefficient depends on the ratios of the ion mobilities and the ion partition coefficients. The latter may vary in orders of magnitude, while the former may vary in times, at most. Therefore, the selectivity is normally governed by the so-called equilibrium factor: k_J/k_I . However, there are some examples of the selectivity determined by the mobilities ratio [120, 121].

Besides the assumption of the identical interactions between I^+ and J^+ ions with R^- sites (or the lack of interaction: the case of the complete dissociation), some other simplifications allow for the integration of the Eq. (4.13). One can consider the situation when R^- sites are immobilized by covalent binding with the matrix polymer, or the sites are just low mobile for any other reason, meaning $u_R \ll u_I, u_J$. In this case

$$\frac{d\phi}{dx} = -\frac{RT}{z_I F} \frac{d(u_I C_I) + d(u_J C_J)}{(u_I C_I + u_J C_J)} = -\frac{RT}{z_I F} d \ln(u_I C_I + u_J C_J) \quad (4.21)$$

The obtained form comprises a full differential, and the respective integral is the same as that given by Eq. (4.11). Consequently, Eqs. (4.13–4.17) are also valid in this case.

It is also possible that I^+ and J^+ ions have equal mobilities, while the mobility of R^- sites is different: $u_I = u_J \neq u_R$. If this is true, the differential form of the diffusion potential (Eq. 4.15) looks as follows:

$$\frac{d\phi}{dx} = -\frac{RT}{F} \frac{d(u_I(C_I + C_J)) - d(u_R C_R)}{(u_I(C_I + C_J)) + (u_R C_R)} \quad (4.22)$$

Because of the macroscopic electroneutrality, $C_I + C_J = C_R$, therefore Eq. (4.22) produces the equation for the diffusion potential within the membrane:

$$\varphi_d = -\frac{RT}{F} \frac{u_I - u_R}{u_I + u_R} \ln \frac{C_I^{(r)} + C_J^{(r)}}{C_I^{(l)} + C_J^{(l)}} \quad (4.23)$$

The combination of Eq. (4.23) for the diffusion potential, with Eq. (4.8) for the two boundary potentials, gives for the overall membrane potential the following expression:

$$\varphi_{\text{mem}} = \frac{u_I - u_R}{u_I + u_R} \frac{RT}{F} \ln \frac{a_I^{(l)} + \frac{k_I}{k_I} a_J^{(l)}}{a_I^{(r)} + \frac{k_I}{k_I} a_J^{(r)}} + \frac{2u_R}{u_I + u_R} \frac{RT}{F} \ln \frac{a_I^{(l)} C_I^{(l)}}{a_I^{(r)} C_I^{(r)}} \quad (4.24)$$

Here, only the first term in the right-hand side is Nikolsky like, while the second term contains parameters (free ion concentrations in the membrane) which are unknown variables. These variables can be calculated numerically if the respective parameters are known: the ionic distribution coefficients and ion-site association constants [19, 20, 122–127]. As to the Nikolsky-like term, one can see that the selectivity here is entirely determined by the ratio of the ionic distribution coefficients, while the mobilities show up only in the pre-logarithmic factors of the two right-hand terms of Eq. (4.24).

4.4.2 The Hofmeister Series

Whatever the simplifying assumption is which allows for the integration of the differential presented by Eq. (4.13), one can see that the selectivity is determined by the ratio of the ionic distribution coefficients and also by the ratio of the species' mobilities within the membrane. This consideration is useful for the understanding of the regulations in the selectivity of the ISE membranes containing ion exchangers and charged ionophores. The selectivity of ISEs with membranes containing only ion exchangers is relatively low and depends primarily on the free energy of the ion hydration. Below we will try to explain this. If we consider only the equilibrium factor of the selectivity (neglecting the mobilities' ratio), the selectivity is determined by the difference of the free energy of transfer of the two competing ions. Let them be I^+ primary (target) ion and J^+ interfering ion. When distributing from the aqueous solution to the membrane, both ions lose ΔG_I^h , ΔG_J^h , the free energies of hydration, and gain ΔG_I^s , ΔG_J^s , the free energies of solvation by the membrane components, and also ΔG_{IR} , ΔG_{JR} , the free energies of the association with R^- sites. Thus, the difference of the free energies

of the ion transfer which refers to the ability of J^+ interfering ion to replace I^+ primary ion in the membrane can be written as follows:

$$\Delta\Delta G_{I/J}^{\text{tr}} = \Delta G_J^{\text{tr}} - \Delta G_I^{\text{tr}} = -\Delta G_J^{\text{h}} + \Delta G_I^{\text{h}} + \Delta G_J^{\text{s}} - \Delta G_I^{\text{s}} + \Delta G_{\text{JR}} - \Delta G_{\text{IR}} \quad (4.25)$$

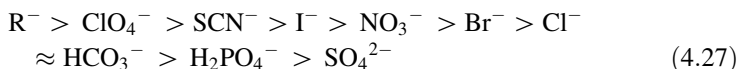
In practically relevant membranes, there are no specific interactions between ions and membrane solvent (plasticizer). Therefore, the values of the free energy of solvation are low for any ion. The interaction between ion exchangers and ions is mostly of pure electrostatic nature, and therefore, the ion-site association constants are relatively low [19–21]. Furthermore, these association constants are virtually independent of the nature of the ion: whichever I^+ or J^+ in our example. This is because R^- lipophilic sites are large and the distances between the centers of the ions in the ion-pairs depend primarily on the effective radius of R^- . Therefore, the electrostatic forces in IR and JR ion-pairs are roughly the same. For instance, ion-site association constant values for K^+ , Na^+ , Cs^+ , and NH_4^+ cations with CITPB $^-$ anion in bis(butylpentyl)adipate are 2.5×10^3 , 2.0×10^3 , 4.0×10^3 , and $3.2 \times 10^3 \text{ M}^{-1}$, respectively, thus only weakly dependent on the cation nature [20]. For a typical concentration of ion exchanger in PVC membranes about 0.01 M, these values mean that the fraction of ion-pairs varies from 18 % for NaCITPB to 27 % for CsCITPB.

The only significant impact to the difference of the free energies of the ion transfer comes from the difference in the free energies of hydration, while the other components are of minor importance, so

$$\Delta\Delta G_{I/J}^{\text{tr}} = \Delta G_J^{\text{tr}} - \Delta G_I^{\text{tr}} \approx -\Delta G_J^{\text{h}} + \Delta G_I^{\text{h}} \quad (4.26)$$

Therefore, the selectivity of ISEs with ion-exchanger-based membranes is governed primarily by the affinity of ions to the aqueous phase: an ion-exchanger-based membrane is more selective to the ion which leaves aqueous phase more easily. In this sense, ions form the so-called Hofmeister series. This series contains ions arranged in order of their free hydration energy, with low hydration on the left-hand side and high hydration on the right-hand side. Originally, Hofmeister revealed these series when studying the influence of inorganic salts on the solubility of proteins in water [128].

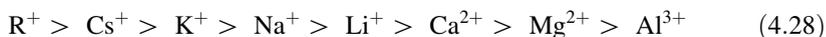
Anion-selective electrodes with membranes having only ion exchangers remain widely used. Therefore, we will first discuss the Hofmeister series for anions. It looks as follows:



In the series above, R^- represents organic anions. Many of them are lipophilic and prefer an organic phase over an aqueous phase. Therefore, ion-exchanger-based membranes are more selective to most of organic ions, even in the presence

of ClO_4^- or SCN^- . Inorganic ions, obviously, prefer to stay in a polar—aqueous—phase, rather than in membrane phase which is significantly less polar [64]. However, the free hydration energy of ions which measures the adherence of ions to water is dependent primarily on the so-called surface charge density of the ion. This is the ratio of the ion charge over the surface area of the ion considered a sphere with the effective radius. Obviously, the surface charge density of a small divalent or trivalent ion is high, while that of a large monovalent ion is low. Therefore, there is no surprise that perchlorate, thiocyanate, iodide—monovalent ions—which are only weakly hydrated due to relatively large size, belong to the left-hand side of the series. These ions are more eager to get into membrane phase than nitrate, bromide, chloride, and bicarbonate. It is therefore easy to ensure selectivity, for example, to perchlorate over nitrate and chloride, or to nitrate over sulfate. However, when having only the ion exchanger present in the membrane, one cannot make an electrode selective to hydrophilic ions like divalent carbonate, phosphate, or sulfate.

The Hofmeister series for cations is as follows:



R^+ represents organic cations. Cation-selective electrodes already in early years of ISEs with liquid and polymeric membranes have been based on ionophores specifically interacting with cations. However, when studying novel ionophores, it is strongly advisable to compare the selectivities of ISEs having ionophores in membranes with those of ISEs having only ion-exchanger sites. In this sense, Hofmeister series for cations is useful as reference.

4.4.3 Selectivity of the ISEs Based on Neutral Ionophores

The first theory of the response and the selectivity of ISEs with membranes containing neutral ionophores selectively binding cations was proposed by Ciani et al. [129]. Their studies were aimed at modeling living cell membranes, and ISE membranes served as model systems. The ISE membranes, therefore, have been assumed very thin, and this assumption allowed neglecting anions in membranes: membranes with thickness comparable with the respective Debye length may deviate from the electroneutrality condition. Thus, in [129], they considered a membrane containing L neutral ionophore and equilibrated with two mixed aqueous solutions of electrolytes IX and JX. Both I^+ and J^+ cations form 1:1 complexes with the neutral ionophore: IL^+ and JL^+ . Interestingly, Ciani, Eisenman, and Szabo assumed that the complexes are formed in the aqueous phase with K_{IL} , K_{JL} the respective formation constants, and the complexes distribute between the phases with k_{IL} , k_{JL} the respective ionic distribution coefficients. For this case, according to [129], the membrane potential can be described as follows:

$$\varphi_m = \frac{RT}{F} \ln \frac{a_I^{\text{ex}} + \frac{u_{\text{JL}} k_{\text{JL}} K_{\text{JL}}}{u_{\text{IL}} k_{\text{IL}} K_{\text{IL}}} a_J^{\text{ex}}}{a_I^{\text{in}} + \frac{u_{\text{JL}} k_{\text{JL}} K_{\text{JL}}}{u_{\text{IL}} k_{\text{IL}} K_{\text{IL}}} a_J^{\text{in}}} \quad (4.29)$$

Here, u_{IL} , u_{JL} stand for the mobilities of the complexes within the membrane phase. Thus, the membrane potential follows the Nikolsky equation, and the complex formation constants directly contribute to the selectivity coefficient:

$$K_{\text{IJ}} = \frac{u_{\text{JL}} k_{\text{JL}} K_{\text{JL}}}{u_{\text{IL}} k_{\text{IL}} K_{\text{IL}}} \quad (4.30)$$

If IL^+ and JL^+ complexes are isosteric, the respective distribution coefficients and mobilities must be roughly the same for both kinds of the species: $k_{\text{IL}} \approx k_{\text{JL}}$, $u_{\text{IL}} \approx u_{\text{JL}}$. Then, the selectivity coefficient is determined by the ratio of the complex formation constants in the aqueous phase:

$$K_{\text{IJ}} = K_{\text{JL}}/K_{\text{IL}} \quad (4.31)$$

Macrocyclic neutral ionophores do form isosteric complexes with ions of the same charge. Acyclic ionophores (podands) in most cases form complexes with two molecules of the ionophore per one ion. Effectively, these complexes are also isosteric, while the two molecules of the ionophore in the complex can be (formally) considered as a product of the ionophore dimerization. Thus, according to the Ciani, Eisenman, and Szabo theory, the selectivity of ISEs with neutral ionophores in membranes, at least for ions of the same charge and forming complexes of the same stoichiometry, must be independent of the membrane solvent. The latter seems, probably, the most striking result of the theory, and this result often gets experimental support.

Morf considered the formation of ion-to-ionophore complexes in the membrane phase, while ions distribute between the phases as individual species [130]. His equation for the membrane potential looks very similar to Eq. (4.29):

$$\varphi_m = \frac{RT}{F} \ln \frac{a_I^{\text{ex}} + \frac{u_{\text{JL}} k_{\text{JL}} K_{\text{JL}}}{u_{\text{IL}} k_{\text{IL}} K_{\text{IL}}} a_J^{\text{ex}}}{a_I^{\text{in}} + \frac{u_{\text{JL}} k_{\text{JL}} K_{\text{JL}}}{u_{\text{IL}} k_{\text{IL}} K_{\text{IL}}} a_J^{\text{in}}} \quad (4.32)$$

However, the distribution coefficients in Morf's Eq. (4.32) refer to ions (not to complexes), and the complex formation constants refer to the membrane phase.

In principle, if all the necessary equilibria (heterogeneous and homogeneous) are established, the mechanism of the complex formation and of the ion distribution does not matter. Indeed, the Gibbs free energy of ion transfer according to the Ciani, Eisenman, and Szabo theory combines the loss of the Gibbs free energy of the hydration of the free ion, the gain due to the complexation in the aqueous phase, the loss of the Gibbs hydration free energy of the complex, and the gain of the Gibbs free energy of the solvation of the complexed ion in the membrane phase:

$$\Delta G_I^{\text{aq} \rightarrow m} = -\Delta G_{I,h} + \Delta G_{\text{IL}}^{\text{aq}} - \Delta G_{\text{IL},h} + \Delta G_{\text{IL},s} \quad (4.33)$$

According to the alternative approach (like that considered by Morf),

$$\Delta G_I^{\text{aq} \rightarrow m} = -\Delta G_{I,h} + \Delta G_{I,s} + -\Delta G_{IL,h} + \Delta G_{IL,s} \quad (4.34)$$

It was mentioned above that according to the Ciani, Eisenman, and Szabo theory, the selectivity of the membranes with neutral ionophores does not depend on the membrane solvent. This conclusion is often but not always supported by experimental data. The explanation why and when the solvent influences the selectivity, and when it does not, has been proposed by Mikhelson [131–134]. Basically, if both the target analyte ion and the interfering ion form complexes of the same stoichiometry (and therefore isosteric), and these complexes predominate over non-complexed ions in the membrane, the complex solvation free energy contributions are eliminated. Then, solvent does not influence the selectivity to ions of the same charge. Obviously, this conclusion is similar to that proposed by Ciani, Eisenman, and Szabo, however, not limited to thin membranes. If the stoichiometry of the complexation is different for the primary and the interference ions, the nature of the solvent affects the selectivity.

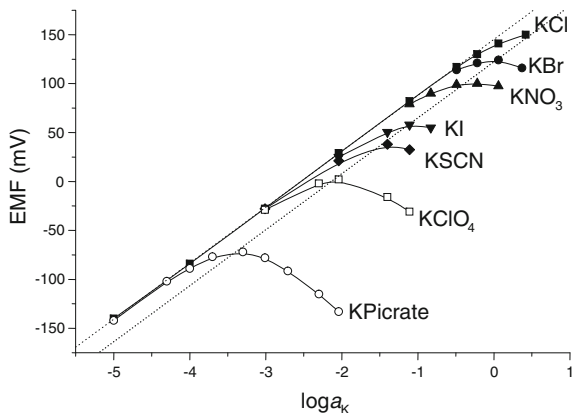
4.4.4 Co-Ion Interference with the Response of ISEs Based on Neutral Ionophores

ISEs with membranes based on neutral ionophores show interesting peculiarity. The span of the Nernstian response is strongly dependent on the nature of the co-ion [135]; namely, cation-selective ISEs show interference from anions present in solution, and anion-selective electrodes show interference from cations. An example of the anion interference with the potassium response of membranes based on valinomycin is shown in Fig. 4.7.

With the increase in the concentration of the electrolyte, the response to the potassium ions deviates more and more from the Nernstian law, and after passing a maximum turns into anionic response. It was shown that the ability of the anions to interfere is determined by their position in the Hofmeister series, that is, by their Gibbs free energy of hydration [130, 134, 136]. Less hydrated anions interfere even at low concentrations.

For the theory, the two phenomena, the anion interference with the cationic response and the cation interference with the anionic response, are absolutely symmetrical. Since most of the respective studies have been performed for cationic ISEs, the phenomenon is often called “anion interference with cationic response.” The trivial explanation in terms of high mobility of anions within membranes is not consistent with the data on the ion transference numbers in membranes [137]. Also, it is hardly possible that the anions in membranes are low mobile when in contact with diluted solutions, and the mobility is increasing with the solution concentration. The consistent theory of the co-ion interference was first proposed by Simon’s

Fig. 4.7 Anion interference with K^+ membranes containing valinomycin and KCITPB in DOP [123]. Adapted with permission from Mikhelson [123]. Copyright 1992 Elsevier



group [138]. According to [138], for the full Nernstian response to, for example, cations, the neutral ionophore must be present in some excess over the complexed ions. The concentration of the latter is roughly equal to the concentration of R^- ion-exchanger sites in the membrane since the concentration of non-complexed ions is very small: $C_{IL} \approx C_R$, $C_I \ll C_{IL}$. On the other hand, the concentration of the complexed ions is proportional to that of the free ionophore: $C_{IL} = C_I C_L K_{IL}$. Thus, $C_I = C_{IL} C_L^{-1} K_{IL}^{-1} \approx C_R C_L^{-1} K_{IL}^{-1}$. Therefore, as long as the Donnan exclusion holds, $C_I \approx \text{Const}$ and the boundary potential follows the Nernst equation, while the diffusion potential within the membrane is negligible. With the increase in the concentration of the solution, the membrane extracts the electrolyte in significant quantities (the Donnan exclusion failure) and more and more of the ionophore molecules are consumed by the extracted ions by complexation. Decrease in C_L , the free ionophore concentration, causes increase in C_I the free ion concentration in the membrane. Because of this, the boundary potential deviates from the Nernst equation, and eventually the response appears to be anionic. The latter limiting situation is characteristic to membrane with fully complexed ionophore. This means that the membrane contains a lipophilic cation (the cationic complex) in excess over R^- sites, so, effectively, the membrane works as anion exchanging.

The position of the maximum on the response curve depends on the stoichiometry of the ion-to-ionophore complexation and on the dissociation degree of the complexed electrolyte in the membrane in a complicated way [138, 139]. In the simplest case of 1:1 complexation, and low degree of association with anions, the activity of the target ion in the solution when the response curve reaches maximum is [139]

$$a_I^{\max} = \sqrt{\frac{4C_L^{\text{tot}}}{3K_e}} \quad (4.35)$$

Here, C_L^{tot} is the total concentration of the neutral ionophore in the membrane, and $K_e = k_{IX} K_{IL}$ is the co-extraction constant—the multiple of the electrolyte

distribution coefficient and the complex formation constant. It was shown that in the point of the maximum 1/3 of the total ionophore concentration refers to the complexes, and 2/3 is free [139]. Furthermore, the maxima on the curves belong to a straight line, parallel to the Nernstian response line, and shifted in $\Delta E = (2RT/F) \ln \sqrt{3} \approx 27.7$ mV to more negative values [139]. The experimental value for the valinomycin membrane (see Fig. 4.7) is 24.5 mV [136], supporting this theoretical conclusion. Equation (4.34) shows that the co-ion interference intensifies with the decrease in the hydrophilicity of the electrolyte (therefore, the anions interfere according to their position in the Hofmeister series) and with the increase in the complex formation constant.

A detailed comparison of the anion interference on the cationic response of ISEs with neutral and charged ionophores was performed by Bühlmann [140].

4.5 Generalized Theories of Ionophore-Based ISE Membranes

Theoretical considerations presented in Sects. 4.4.1–4.4.4 contain too many simplifications: the ion-site interactions are either negligible (complete dissociation), or the same for any kind of counter-ion, or sites are immobile, or mobilities of counter-ions are the same. These approaches are very useful giving intuitively clear simple descriptions of the respective limiting cases. On the other hand, these simplifications are hardly true for the real-world ISEs. Low polarity of membranes suggests a rather strong association than complete dissociation of the electrolytes in membranes, the sites, typically, are mobile. Therefore, attempts were made to develop a more realistic description of the ISE response and selectivity. Here, we will briefly outline several generalized approaches to the description of the ISE membrane response and selectivity. Even more advanced theories providing the description of the membrane potential in real time and space are discussed in Sect. 7.1.

4.5.1 The Sandblom–Eisenman–Walker Theory

The Sandblom–Eisenman–Walker theory was proposed already in the mid-1960s [119]. This theory was developed to access the influence of ion-site association with ion-exchanger-based membranes. The theory addressed the boundary potentials as well as the diffusion potential within the membrane. The whole system—membrane and solutions—was considered being in the steady state, while the membrane/solution interfaces were supposed to be at electrochemical equilibrium. Only limiting cases were solved: (1) complete dissociation and (2) strong association of the electrolytes in the membrane.

For the first limiting case, the complete dissociation, the description of the membrane potential in a mixed solution containing I^+ primary ions and n sorts of monovalent interferences, is Nikolsky like

$$\varphi_m = \varphi_m^0 + \frac{RT}{F} \ln \left(a_I + \sum_{i=1}^n \frac{u_J k_{J_i}}{u_I k_I} a_J \right) \quad (4.36)$$

Furthermore, Eq. (4.36) shows the additivity of the impacts from the interferences to the membrane potential. Thus, in the case of the complete dissociation, the selectivity coefficient is dependent on the species mobilities and on their ionic distribution coefficients.

Since real membranes are low-polar, the second limiting case, the strong association of the electrolytes in the membrane phase, appears more realistic. For this more complicated situation (and for only two competing ions: I^+ and J^+), Sandblom, Eisenman, and Walker obtained

$$\varphi_m = -\frac{RT}{F} \left\{ (1 - \tau) \ln \frac{a_I^{\text{in}} + \left[\frac{u_J + u_R}{u_I + u_R} \frac{k_I}{k_J} \right] a_J^{\text{in}}}{a_I^{\text{ex}} + \left[\frac{u_J + u_R}{u_I + u_R} \frac{k_I}{k_J} \right] a_J^{\text{ex}}} + \tau \ln \frac{a_I^{\text{in}} + \left[\frac{u_{JR}}{u_{IR}} \frac{k_I K_{JR}}{k_J K_{IR}} \right] a_J^{\text{in}}}{a_I^{\text{ex}} + \left[\frac{u_{JR}}{u_{IR}} \frac{k_I K_{JR}}{k_J K_{IR}} \right] a_J^{\text{ex}}} \right\} \quad (4.37)$$

Here, u_I , u_J , u_R , u_{IR} , u_{JR} are mobilities of I^+ , J^+ ions, of R^- ion-exchanger sites and of IR, JR ion-pairs; K_{IR} , K_{JR} stand for the ion-pairs association constants. Upper indexes *in* and *ex* denote the internal and the external solutions.

Equation (4.37) constitutes a sum of two Nikolsky-like logarithmic terms with weighting factor:

$$\tau = \frac{u_R(u_{JR}K_{JR} - u_{IR}K_{IR})}{(u_I + u_R)u_{JR}K_{JR} - (u_J + u_R)u_{IR}K_{IR}} \quad (4.38)$$

The first logarithmic term in Eq. (4.37) shows, basically, the impact of the ionic distribution coefficients to the selectivity. The presence of the ion exchanger manifests in the first term only via u_R : the R^- mobility value. The second term is directly related to the association—via K_{IR} , K_{JR} ion-pair association constants and u_{IR} , u_{JR} mobilities. Thus, Eq. (4.37) is crucially different from the Nikolsky-like equations with only one parameter. According to the Sandblom, Eisenman, and Walker theory, the selectivity of an associated membrane is characterized by three parameters: $K_D^{(1)} = (u_J + u_R)k_J / (u_I + u_R)k_I$, $K_D^{(2)} = (u_{JR}k_J K_{JR}) / (u_{IR}k_I K_{IR})$, and τ . This may explain the variability of the selectivity coefficients calculated by the Nikolsky equation: a one-parameter equation is not suitable for ISEs with strong association of the electrolytes in membranes.

4.5.2 Phase-Boundary Potential Approaches, Ionic Additives, Selectivity Optimization

Large variety of the compositions of the ionophore-based membranes, in combination with large variety of analytes and interferences, sometimes causes peculiar dependences of the membrane potential on the activities of ions. Apparently, non-Nernstian responses with slopes approaching one-half, two-thirds, and other multiples of $RT/z_I F$ are frequently observed, especially for membranes with charged ionophores [141]. A consistent theoretical explanation of these facts, taking into account the boundary potentials as well as the diffusion potential within membrane, may be mathematically too complicated and intuitively not clear. On the other hand, accounting for only the boundary potentials allows for rationalization of many of these peculiar facts, like the apparently non-Nernstian slopes [47, 141] and non-monotonous curves for Ca ISEs when the pH is varied [45]. Furthermore, the boundary potential approach allowed inventing the so-called *ionic additives method* for the improvement of the selectivity of the ISEs with membranes containing charged ionophores [43–47]. This fact deserves special consideration presented below.

The selectivity coefficient of an ISE with a membrane containing a neutral ionophore is directly proportional to K_{JL}/K_{IL} , the ratio of the complex formation constants of L, the ionophore with I^+ and J^+ , the primary and the interfering ions, see Eq. (4.32). However, in the case of an ISE with a membrane containing R^- charged ionophore, the selectivity coefficient is proportional to $\sqrt{K_{JR}/K_{IR}}$ —the square root of the association constants ratio. Thus, the selectivity of ion complexation by a neutral ionophore fully translates into the potentiometric selectivity, whereas the selectivity of the association translates into the potentiometric selectivity only partly. For instance, if $K_{JR}/K_{IR} = 10^{-4}$, the respective increment in the selectivity is only 10^{-2} . Let us see why this happens.

The boundary potential between the membrane and IX solution is

$$\varphi_b^{IX} = \varphi^{\text{mem}} - \varphi^{\text{aq}} = \frac{RT}{z_I F} \ln k_I + \frac{RT}{z_I F} \ln \frac{a_I}{C_I} \quad (4.39)$$

Here, a_I is the activity of I^+ ion in solution, and its activity in the membrane is approximated by C_I —the free I^+ concentration. An analogous equation can be written for the interfering ion. We now assume that the selectivity is measured by the SSM method ($a_I = a_J$), so that

$$\ln K_{IJ} = \frac{z_I F}{RT} (\varphi_b^{JX} - \varphi_b^{IX}) = \left(\frac{RT}{z_I F} \ln \frac{k_J}{k_I} - \frac{RT}{z_I F} \ln \frac{C_J a_I}{C_I a_J} \right) \frac{z_I F}{RT} = \ln \frac{k_J C_I}{k_I C_J} \quad (4.40)$$

In the membrane equilibrated with IX solution, the concentration of IR ion-pairs is $C_{IR} = C_I C_R K_{IR}$. The macroscopic electroneutrality holds, so $C_I = C_R$. Due to the low polarity of membranes, the associates predominate over free ions, so that the concentration of IR ion-pairs approaches the total concentration of the

charged ionophore: $C_{\text{IR}} \approx C_{\text{R}}^{\text{tot}}$. Thus, $C_{\text{I}} \approx \sqrt{C_{\text{R}}^{\text{tot}}/K_{\text{IR}}}$. The same reasoning is true for J^+ ions, so that

$$K_{\text{IJ}} \approx k_{\text{J}} K_{\text{JR}}^{1/2} / k_{\text{I}} K_{\text{IR}}^{1/2} \quad (4.41)$$

Because of this relation, for a long time, it was assumed that charged ionophores are intrinsically inferior to neutral ionophores when it comes to ISEs.

Now, we will turn to membranes also containing S^+ —a bulky ionic additive with the charge sign opposite to the sign of the ionophore. The ionic additives are added in excess over I^+ ions, but in such a way that $C_{\text{S}}^{\text{tot}} < C_{\text{R}}^{\text{tot}}$. The electroneutrality condition for such a membrane looks like: $C_{\text{I}} + C_{\text{S}} = C_{\text{R}}$, and due to the excess of S^+ it turns $C_{\text{S}} \approx C_{\text{X}}$. Since the ionic additives practically do not associate with R^- , $C_{\text{S}} \approx C_{\text{S}}^{\text{tot}}$. Therefore, $C_{\text{IR}} \approx C_{\text{R}}^{\text{tot}} - C_{\text{R}} \approx C_{\text{R}}^{\text{tot}} - C_{\text{S}}^{\text{tot}}$, and $C_{\text{I}} \approx (C_{\text{R}}^{\text{tot}} - C_{\text{S}}^{\text{tot}})/C_{\text{S}}^{\text{tot}} K_{\text{IR}}$.

With the same reasoning for J^+ ions, we come to

$$K_{\text{IJ}} = \frac{k_{\text{J}} K_{\text{JR}}}{k_{\text{I}} K_{\text{IR}}} \quad (4.42)$$

This is how ionic additives allow for the full translation of the selectivity of the association with the potentiometric selectivity. This approach works for various charged ionophores, in particular for metal porphyrine complexes [12]. It is also valid for divalent analytes and helps improving the selectivity to Ca^{2+} ions in more than two orders of magnitude [44, 46, 142].

Membranes containing neutral ionophores are doped with ionic additives (ion-exchanger sites) with a charge sign opposite that of the target analyte ion. In early years of the ionophore-based ISE research, it was assumed that the neutral ionophore must be in excess over sites, otherwise the ratio of the neutral ionophore concentration over the concentration of sites does not play significant role. However, within the frames of the phase-boundary model, it was shown theoretically, and supported experimentally, that the variation of this ratio may produce non-monotonous selectivity curves [1, 143–146]. In other words, this ratio is critical for the optimization of the electrode selectivity. The respective optimal values of ISEs based on charged and neutral ionophores are summarized in Table 4.1, in accordance with [146].⁴

4.5.3 Multispecies Approximation

Detailed description of the membrane potential and selectivity requires detailed consideration of the species present in ISE membranes. To do so, Mikhelson

⁴ The table assumes the target and the interfering ions being cations. The situation for anion-selective ISEs is completely symmetric.

Table 4.1 Optimal values of R^{z_R} ionic site concentration over L^{z_L} the ionophore concentration ratios for I^{z_I} primary and J^{z_J} interfering ions forming, respectively, IL_{n_I} and JL_{n_J} complexes with charged or neutral ionophores, in accordance with [146]

Charge		Stoichiometry		Ratio sites over ionophore, mole percentage			
Z_I	Z_J	n_I	n_J	Charged $Z_L = -1$	Ionophore	Neutral $Z_L = 0$	Ionophore
				Z_R	$C_R^{\text{tot}}/C_L^{\text{tot}}$	Z_R	$C_R^{\text{tot}}/C_L^{\text{tot}}$
+2	+2	1	2	-1	41	-1	141
		2	3	+1	23	-1	77
		3	4	+1	46	-1	54
+2	+1	1	1	-1	62	-1	162
		2	2	+1	27	-1	73
		3	3	+1	54	-1	46
+1	+1	1	2	+1	29	-1	71

invented an approach called *multispecies approximation* [122–127]. To the best of our knowledge, this approximation is the only one capable of description of the membrane potential for any dissociation degree of the membrane electrolytes.

The approximation is as follows. For each component present in membranes, as many as possible, individual forms are taken into consideration. For instance, for a potassium-selective membrane containing valinomycin (L) and tetrakis(p-Cl-phenyl)borate (R^-), it is assumed that potassium is present as K^+ -free ions, KL^+ -complexed ions, and also KR and KLR neutral associates. In turn, valinomycin is present as L-free ionophore, KL^+ and KLR, while tetrakis(p-Cl-phenyl)borate exists as R^- -free anion, and KR and KLR neutral species. Thus, in this case, six sorts of species are taken into consideration. For higher valencies and for higher complexation stoichiometries, the number of sorts of species increases sharply. The general model also includes S^+ ionic additives and accounts for the possibility of the Donnan exclusion break, so that X^- ions from solution can penetrate into membrane. The model is schematically presented in Fig. 4.8.

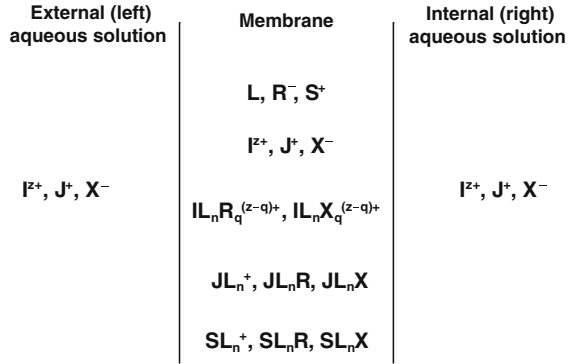
It is assumed that the total concentrations of the ionophores and additives are determined by the membrane preparation. This allows using the respective mass balances:

$$C_L^{\text{tot}} = C_L + \sum_{n=1}^k \left[\sum_{q=0}^z n(C_{IL_nR_q} + C_{IL_nX_q}) + \sum_{q=0}^1 n(C_{JL_nR_q} + C_{JL_nX_q}) + \sum_{q=0}^1 n(C_{SL_nR_q} + C_{SL_nX_q}) \right] \quad (4.43)$$

$$C_R^{\text{tot}} = C_R + \sum_{n=0}^k \sum_{q=1}^z q C_{IL_nR_q} + \sum_{n=0}^k C_{JL_nR} + \sum_{n=0}^k C_{SL_nR} \quad (4.44)$$

$$C_S^{\text{tot}} = \sum_{n=0}^k \sum_{q=0}^1 C_{SL_nR_q} \quad (4.45)$$

Fig. 4.8 Schematic representation of the multispecies approximation. The stoichiometry coefficients are $n = 0, 1, \dots, k$, and $q = 0, 1, \dots, z$



The macroscopic electroneutrality holds, so that

$$\sum_{n=0}^k \left(\left[\sum_{q=0}^z ((z-q)C_{IL_n R_q} + (z-q)C_{IL_n X_q}) \right] + C_{JL_n} + C_{SL_n} \right) = C_R + C_X \quad (4.46)$$

The system of Eqs. (4.43–4.46), together with the ion-exchange equation $C_J = C_I((a_J k_J)^z / a_I k_I)^{1/z}$ and the co-extraction equation $C_X = (a_I (a_X)^z / k_{IX} C_I)^{1/z}$, fully determines the membrane composition. However, this system cannot be solved analytically and requires computer simulations. The model assumes the so-called group mobilities, that is, the mobilities of all cationic species are the same: u_+ , and the mobilities of all anionic species are also the same: u_- .

For a membrane containing a neutral ionophore and an ion exchanger, when the Donnan exclusion holds, the model yields for the membrane potential:

$$\begin{aligned} \varphi_m = & -\frac{RT}{F}(1-2\tau) \left[\ln \frac{a_I^{\text{in}} + K_{IJ}^{\text{in}} a_J^{\text{in}}}{a_I^{\text{ex}} + K_{IJ}^{\text{ex}} a_J^{\text{ex}}} + \ln \frac{\sum_{n=0}^k (C_L^{\text{in}})^n K_{IL_n}}{\sum_{n=0}^k (C_L^{\text{ex}})^n K_{IL_n}} \right] \\ & - 2\frac{RT}{F} \tau \ln \left[\frac{a_I^{\text{in}} / C_I^{\text{in}} + a_J^{\text{in}} / C_J^{\text{in}}}{a_I^{\text{ex}} / C_I^{\text{ex}} + a_J^{\text{ex}} / C_J^{\text{ex}}} \right] \end{aligned} \quad (4.47)$$

The weighting factor (τ) depends on the species mobilities: $\tau = u_- / (u_+ + u_-)$. Equation (4.47) contains three logarithmic terms, and only the first one is Nikolsky like with the selectivity coefficient:

$$K_{IJ} = \frac{k_J \sum_{n=0}^k (C_L)^n K_{JL_n}}{k_I \sum_{n=0}^k (C_L)^n K_{IL_n}} \quad (4.48)$$

The second term represents the impact to the membrane potential from the non-uniform distribution of the free neutral ionophore molecules in the membrane. This non-uniformity arises in an initially uniform membrane due to the difference in the solution compositions—external and internal. Also, it may be arranged artificially, and this allows for the studies of the ion-to-ionophore interactions in ISE membranes, see Sect. 4.6.

Equations (4.47) and (4.48) helped rationalizing various shapes of the dependences of the selectivity coefficient on the concentration of the neutral ionophore, including those with minima and maxima, see Fig. 4.9.

The multispecies approach was also successfully applied to the membranes with ionic additives [19, 20, 122–127]. In particular, it was shown that the role of the ionic additives may be more complicated than in accordance with the phase boundary potential models, and the mobilities of the species modify the respective dependences. Curves presented in Fig. 4.10 illustrate this conclusion. One can see how much the improvement of the selectivity caused by an ionic additive depends on the τ value.

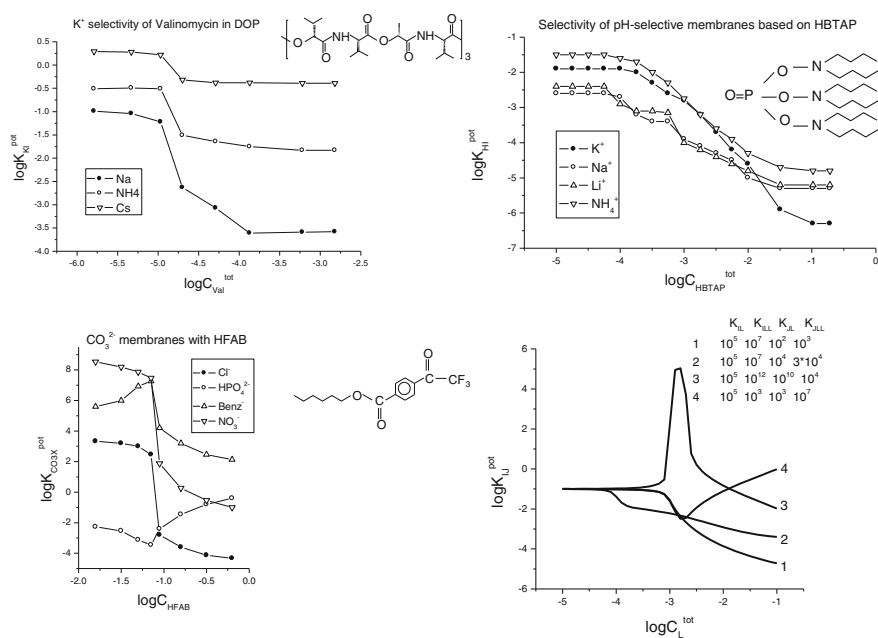
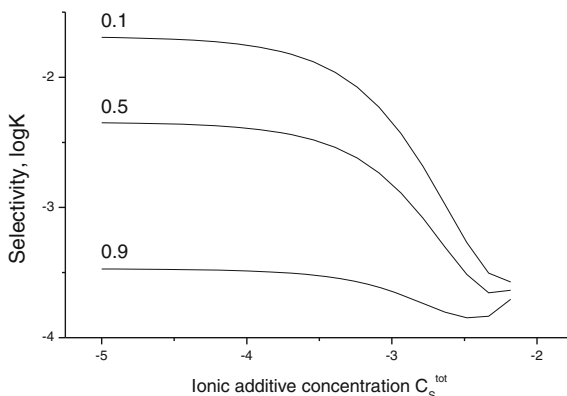


Fig. 4.9 Dependence of the selectivity coefficient on the concentration of the neutral ionophores. Experimental curves, *top* and *bottom, left*: valinomycin (Val), K⁺ ISEs [122], hexabutyltri-amido phosphate (HBTAP), H⁺-ISEs [123], *p*-hexyltrifluoroacetylbenzoate (HFAB), CO₃²⁻-ISEs [122], the ionophore structures shown next to the respective graphs. Calculated curves, *bottom right*, the complex formation constant values shown next to graph. Adapted with permission from Mikhelson and Smirnova [122]. Copyright 1992 Elsevier

Fig. 4.10 Dependence of the selectivity on the concentration of S^+ ionic additive for different values of $\tau = u_-/(u_+ + u_-)$ [126]. Adapted with permission from Mikhelson and Lewenstam [126]. Copyright 2000 American Chemical Society



4.6 Studies of the Species Interactions in Ionophore-Based Membranes

4.6.1 Complexation of Ions by Neutral Ionophores

Selective complexation of analyte ions by neutral and charged ionophores is commonly recognized as primarily responsible for the selectivity of sensors. Data on the interactions of ions and ionophores in membranes are therefore of great academic and practical interest. In early years of ISEs study, some attempts were made to measure complex stability constants in model solutions, mostly in water–ethanol mixtures [147–150]. The data obtained showed only a poor correlation with the potentiometric selectivity. Later on, a number of methods allowing measuring of complex stability constants in situ have been invented [151–154]. These methods suffer from two intrinsic drawbacks. First, an additional reference is required. The reference is either a chromoionophore [151] or a pH ionophore [152, 153], which supposedly does not interact with the ion of interest, or it is an ion (e.g., tetrabutylammonium) which supposedly does not interact with the ionophore under study [154]. Since the respective interactions may occur (at least to some extent), the usage of references may bias the results. Second, the complex stoichiometry has to be known or postulated beforehand or can be determined only indirectly by means of an iteration procedure [154].

A different approach to measure complex stability constants in ISEs membranes containing neutral ionophores relies on recording electrical potential of segmented sandwich membranes [155]. The sandwich consists of two ordinary membranes attached to one another (see Fig. 4.11). The only difference between the membranes is the ionophore content. An artificial gradient of a neutral ionophore in the segmented membrane dividing two identical aqueous solutions with two identical electrodes immersed (e.g., Ag/AgCl) evokes a nonzero electromotive force in the galvanic cell. Initially, the effect was studied “as such” [155, 156]. Later, it was

utilized to reveal the free ionophore fraction in membranes [132], and finally to measure stability constants of ion-to-ionophore complexes [156–164].

In principle, an EMF signal caused by uneven distribution of a mobile ionophore species across a sandwich membrane is intrinsically unsteady. Initially, there are two flat concentration levels of the ionophore in two respective segments of the sandwich (see Fig. 4.11), horizontal lines 1 and 2. Diffusion of the ionophore from A, the segment with a higher concentration to B, the segment with a lower concentration change the initial step-like profile of the ionophore distribution. The measured EMF is steady (giving a “plateau”) when boundary conditions on both sides of the sandwich membrane remain unaltered by the diffusion (see Fig. 4.11, curve 3). When the diffusion front reaches the membrane boundaries (curve 4 in Fig. 4.11), the EMF starts to decrease. Diffusion of the ionophore eventually levels its distribution (horizontal line 5 in Fig. 4.11) and reduces the EMF to zero. A typical example of the respective kinetic curves obtained first by Stefanova and Suglobova for valinomycin membranes [156] is presented in Fig. 4.12.

As one can see from Fig. 4.12, the plateau time gets increased with a decrease in the gradient of the ionophore in the membrane (except for curve 1, which refers to a very low initial concentration of valinomycin). When the segments’ geometry and contact area are well defined, it is possible to obtain the diffusion coefficients of the ionophore in the membrane from the kinetic curve. Data obtained for valinomycin in PVC membranes plasticized with dibutyl phthalate: $D \cong 10^{-8} \text{ cm}^2/\text{s}$ [165] agree well with the values obtained by radiotracers [166]. Here, however, we concentrate on the complex formation constants. From now on (in the text and in the figures), by EMF, we mean only the “plateau” values and use the Mikhelson’ multispecies approach (see Sect. 4.5.3) and, respectively, Eq. (4.47) for the interpretation of the data [167].

The second term in the Eq. (4.47) represents the contribution from possible non-uniform distribution of the neutral ionophore in a segmented sandwich membrane in contact with two identical pure solutions of electrolyte IX. In the

Fig. 4.11 Schematic representation of a segmented sandwich membrane

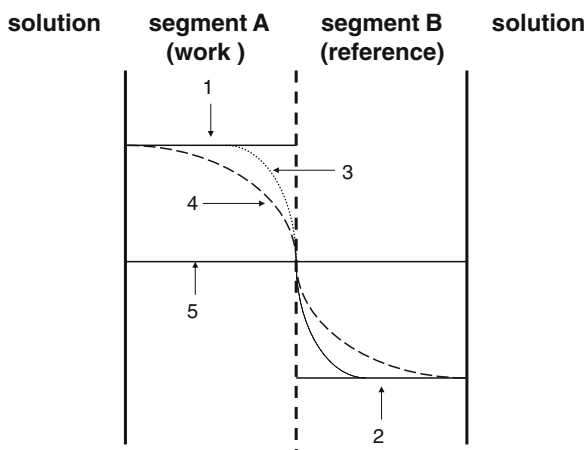
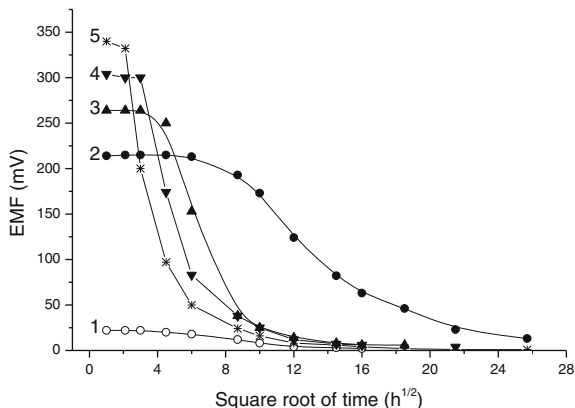


Fig. 4.12 Kinetics of sandwich membrane potential: valinomycin in DBP. $C_{\text{val}}^{\text{tot}}$ (mM): (1) 0.022, (2) 2.24, (3) 11.2, (4) 28.0, and (5) 270 [156, 167]. Adapted with permission from Shultz et al. [167]. Copyright 2002 American Chemical Society



segments, the total content of L neutral ionophore is different, while the total content of R^- ion-exchanger sites is the same. When only one sort of IL_n^+ complexes is predominating, Eq. (4.47) gets very much reduced:

$$E_m = -\frac{RT}{F} \ln \left(\frac{1 + (C_L^{\text{in}})^n K_{IL_n}}{1 + (C_L^{\text{ex}})^n K_{IL_n}} \right) \quad (4.49)$$

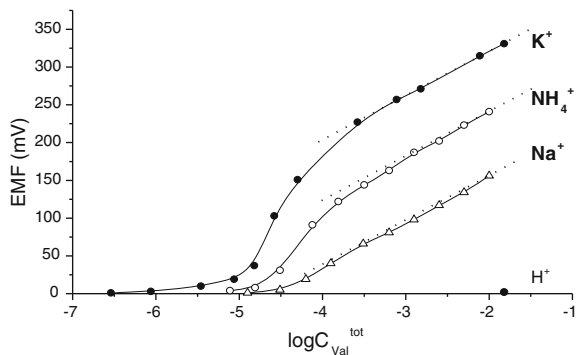
If on one (internal) side, in the reference segment, $C_L^{\text{in,tot}} = 0$, while $(C_L^{\text{ex}})^n K_{IL_n} \gg 1$, we can obtain from (4.49):

$$E_m = n \frac{RT}{F} \ln C_L^{\text{ex}} + \frac{RT}{F} \ln K_{IL_n} \quad (4.50)$$

According to Eq. (4.50), the EMF is linearly dependent on the free ionophore concentration in the external (working) segment of the sandwich. If n stoichiometry coefficient is known, the free ionophore concentration can be calculated as $C_L^{\text{ex}} = C_L^{\text{ex,tot}} - n C_R^{\text{tot}}$. In membranes with large excess of neutral ionophore over sites $C_L^{\text{ex,tot}} \gg C_R^{\text{tot}}$, and therefore concentration of the free ionophore approaches, the total concentration: $C_L^{\text{ex}} \approx C_L^{\text{ex,tot}}$. Thus, a domain of the plot EMF versus $\log C_L^{\text{ex,tot}}$ has to appear, where EMF linearly depends on $\log C_L^{\text{ex,tot}}$. The respective slope nRT/F gives n : the stoichiometry coefficient of the complex. In this way, variation of the ionophore concentration in a wide range allows to obtain the stoichiometry of the complex without a priori knowledge. Extrapolation of the straight line to $\ln C_L^{\text{ex,tot}} = 0$ provides information on the complex formation constant. Examples of the respective experimental curves are given in Figs. 4.13, 4.14.

Detailed description of the advantages and limitation of the segmented sandwich method of the study of the complexation of ions by neutral ionophores is presented in [167].

Fig. 4.13 Segmented sandwich potential curves obtained with valinomycin membranes [167]. Adapted with permission from Shultz et al. [167]. Copyright 2002 American Chemical Society



4.6.2 Quantification of Ion-Site Association in Membranes

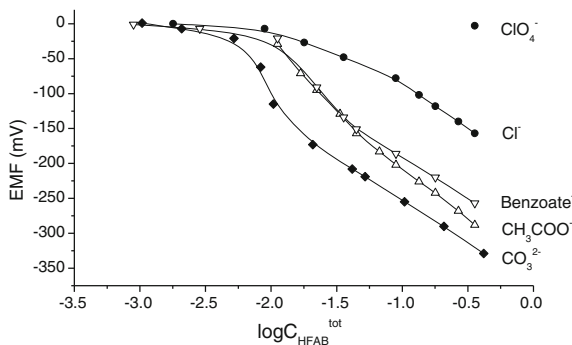
It appears that, in full analogy with neutral ionophores, arranging of artificial gradient of charge ionophore or ion-exchanger sites in membrane will provide with the data on ion-site association. However, the potential of such segmented sandwich membrane does not allow for measurements of ion-site association constants. It is only possible to distinguish between strong and weak association, and it was shown that even tetraphenylborate salts are mostly associated with ISE membranes [161].

A modification of segmented sandwich membrane method which, in principle, may allow for direct measurements of ion-site association constants in real membranes was briefly discussed for the first time in [19]. The theory of the modified method relies on computer simulations using the multispecies approach. The simulations revealed another experimental setup which allows for the quantification of ion-site association with real membranes. The essence of the modified setup is that the total concentration of sites in the working segment must be constant and be the same as in the reference segment. However, the working segment must contain lipophilic ionic additive charged oppositely to the sites, and the concentration of the additive must be varied.

The results of simulations of segmented sandwich membrane potentials are presented in Fig. 4.15. Interaction between S^+ additive and R^- sites was assumed rather weak: $K_{SR} = 1$. This assumption may be realistic for bulky S^+ additive and R^- sites with low density of charge.

One can see that the variation of the concentration of the ionic additive allows obtaining EMF response, increasing with the increase in the content of the additive and also with the increase in the association constant. At relatively high values of K_{IR} , like $10^6 M^{-1}$, the simulated curves contain linear domain with Nernstian slope. When the values of association constants are even higher, $K_{IR} \geq 10^{12} M^{-1}$, the simulated curves tend to come close to one another, and the whole response curve is Nernstian. The overall sandwich membrane potential in the linear domain obeys simple equation below [19, 20]:

Fig. 4.14 Segmented sandwich potential curves obtained with membranes containing *p*-hexyltrifluoroacetylbenzoate [167]. Adapted with permission from Shultz et al. [167]. Copyright 2002 American Chemical Society



$$E = \frac{RT}{F} \left(\frac{1}{2} \ln K_{IR} + \ln C_S^{\text{tot}} - \frac{1}{2} \ln C_R^{\text{tot}} \right) \quad (4.51)$$

Thus, the modified setup for the segmented sandwich membrane method allows for measurement of the ion-site association constants in real membranes. This simple behavior can be anticipated only for membranes with strong ion-site association, and weak interaction between the main sites (or charged ionophores) and lipophilic additive. Otherwise one cannot expect linear domains in the curves of segmented sandwich membrane potential. Interpretation of experimental results obtained for membranes with $K_{IR} < 10^6 \text{ M}^{-1}$, or with commensurable values of K_{IR} and K_{SR} , may require nonlinear fitting of the data. Simulated EMF curves presented in Fig. 4.15 tend to coincide at very high association constants, so the EMF is not more sensitive to the value of K_{IR} . Thus, the method is limited to membranes with moderate ion-site association.

The method was applied for estimation of the ion-site association constants in membranes containing tetradecylammonium bromide (TDABr) and tetrakis(*p*-Cl-phenyl)borates (CITPB⁻) [19, 20]. The results are presented in Figs. 4.16, 4.17.

Fig. 4.15 The results of simulations of segmented sandwich membrane potentials [20]. Adapted with permission from Peshkova et al. [20]. Copyright 2008 Elsevier

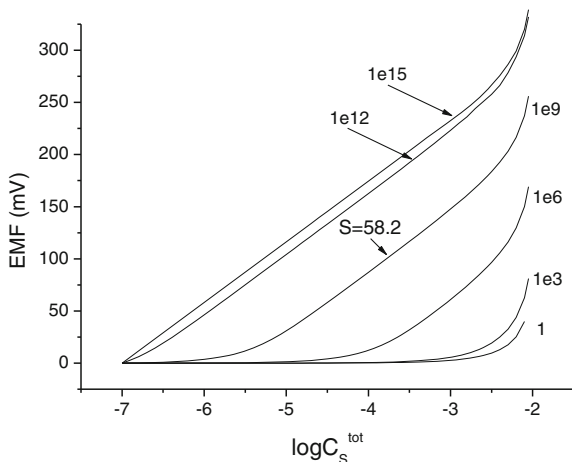
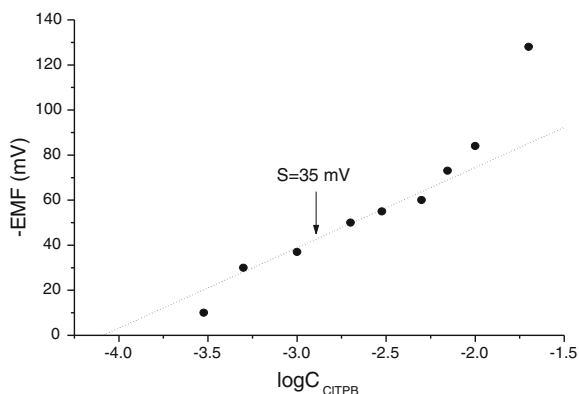


Fig. 4.16 EMF of sandwiches with 0.03 M of TDABr with variation of CITPB⁻ concentration in work segment [19]. Adapted with permission from Mikhelson [19]. Copyright 2003 Wiley



According to [20], the estimated values of the association constants of CITPB⁻ ion pairs in membranes plasticized with bis(butylpentyl)adipate are as follows: $K_{KClCITPB} = 2.5 \times 10^3$, $K_{NaCITPB} = 2.0 \times 10^3$, $K_{CsCITPB} = 4.0 \times 10^3$, $K_{NH_4CITPB} = 3.2 \times 10^3 M^{-1}$, $K_{TDDACITPB} = 2.5 \times 10^2 M^{-1}$. For membrane plasticized with *o*-nitrophenyl octyl ether, $K_{KClCITPB} = 1.6 \times 10^3 M^{-1}$, $K_{TDDACITPB} = 10 M^{-1}$. The association constant of TDABr in dioctylphthalate was estimated as $K_{TDABr} = 10^{6.5} M^{-1}$ [19].

Measuring association by the above described modified segmented sandwich method is time and labor consuming. However, the data obtained can be used as reference in the simplified method proposed later by Egorov [21].

4.7 Potentiometric Sensing of Nonionic Species

Ion-selective electrodes are essentially electrochemical sensors, and therefore, it may appear that ISEs are sensitive only to ions. This, however, is not always true. Nonionic species present in samples may interfere with the ISE response, and this makes some problems, especially in clinical applications [168]. On the other hand, the sensitivity to nonionic species may be used for sensing thereof. The nature of the effect can be rationalized with the same reasoning as used in Sect. 4.6 concerning segmented sandwich membranes.

If N, a nonionic species is capable of partitioning into the membrane phase, and bind the potential-determining ion, the result is effectively the same as in the segmented sandwich membrane, see Fig. 4.18. This type of response is most often observed for membranes containing Ba²⁺ ionophores.

In contrast to a segmented sandwich membrane with artificially non-uniform distribution of the ionophore, here the gradient of N, —nonionic species, arises naturally: because it is present only in the sample, not in the internal solution, and therefore penetrates into the membrane only from one side. Due to binding of ions with N in the membrane, N molecules act as water-soluble ionophore. Because of

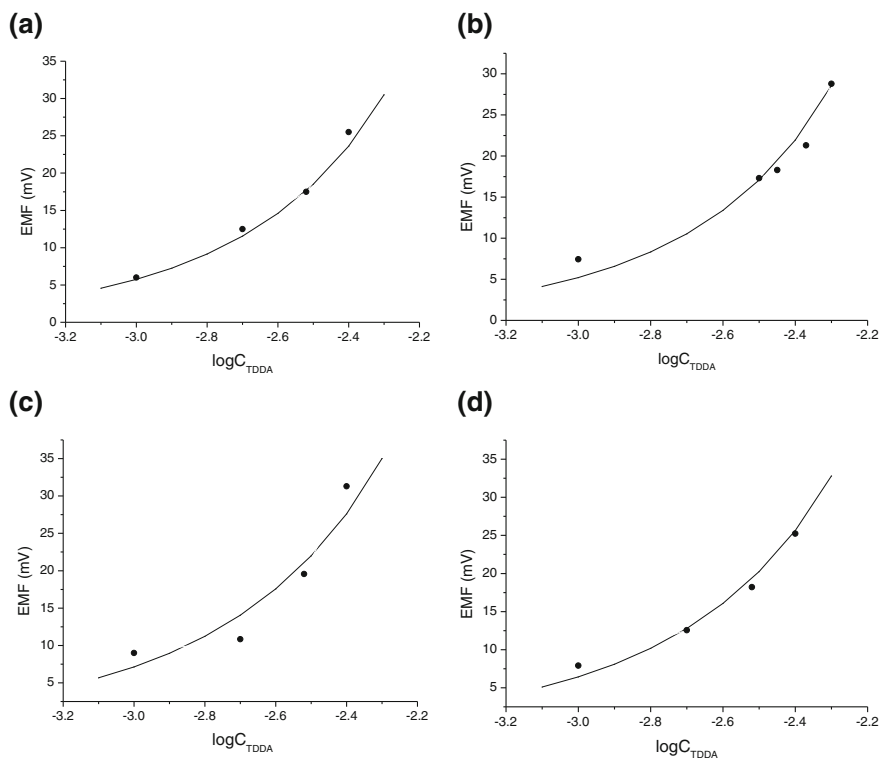


Fig. 4.17 Potentials of segmented sandwich membranes plasticized with BBPA, equilibrated with KCl (a), NaCl (b), CsCl (c), and NH_4Cl (d) [20]. Adapted with permission from Peshkova et al. [20]. Copyright 2008 Elsevier



Fig. 4.18 Schematic representation of the mechanism of ISE response to nonionic species

this, a nonzero membrane potential is established, and the respective EMF delivers information on the concentration of N species.

In this way, a number of environmentally relevant species can be measured, in the first place—phenol derivatives [169] and a large number of nonionic surfactants [170, 171].

4.8 Studies of the Interfacial Kinetics at the Membrane/Solution Boundary

The most convenient and most informative method of studying the charge transfer kinetics at the membrane/solution interface relies on measurements of the electrochemical impedance of membrane/solution systems [172]. The method, in principle, provides with the information on the processes in the membrane bulk, in boundary layers, and directly at the interface. The registered impedance spectrum is interpreted with the help of the respective equivalent circuits.

Among the equivalent circuits proposed for an ion-selective membrane in contact with aqueous solutions, the most common is circuit **A** presented in Fig. 4.19 [173, 174]. In the circuit, R_s^l and R_s^r stand for solution resistance, R_{ct}^l and R_{ct}^r for charge transfer resistance, C_{dl}^l and C_{dl}^r for double-layer capacity, Z_w^l and Z_w^r for Warburg impedance, R_b is the membrane bulk resistance, and C_g is the geometric capacity of the membrane. Superscripts l and r denote left and right sides of the membrane. It is advisable to make the cell symmetric, that is, the

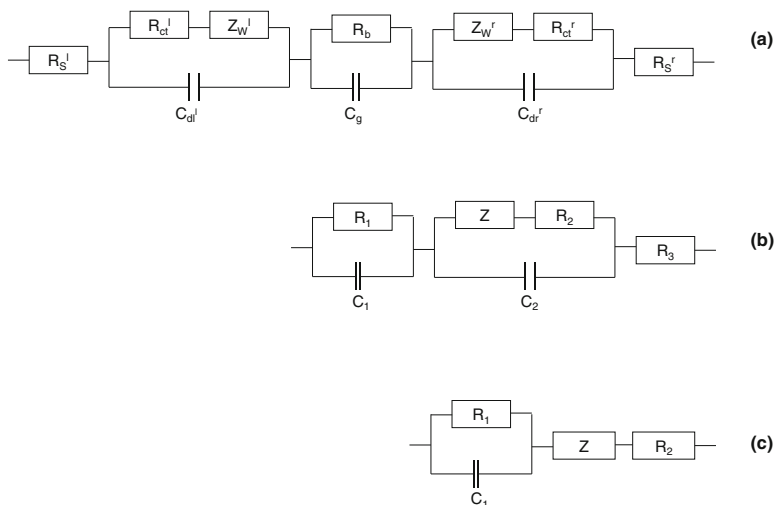


Fig. 4.19 Equivalent circuits used to interpret impedance data. **a** The Randles circuit assumed for membrane dividing two solutions. **b** Circuit for fitting EIS with two semicircles. **c** Circuit for fitting EIS with one semicircle

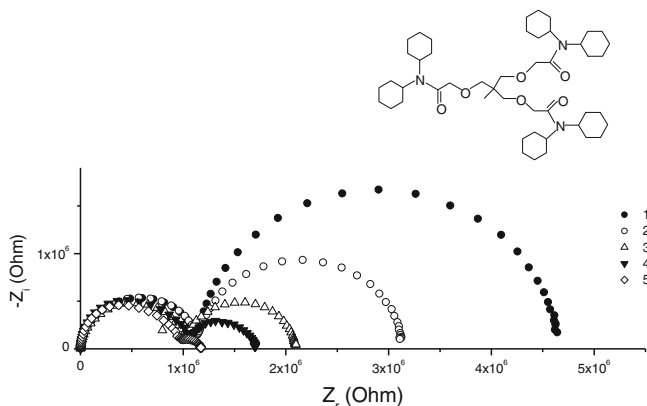


Fig. 4.20 The impedance spectra of Li ISEs in LiCl supported with 0.01 M MgCl_2 . LiCl concentrations: 10^{-6} M (1), 3×10^{-6} M (2), 10^{-5} M (3), 3×10^{-5} M (4), 10^{-4} M (5). The ionophore structure shown above the spectrum [163]. Adapted with permission from Mikhelson et al. [163]. Copyright 2002 American Chemical Society

solutions must be identical, and the surface area of both—left and right—sides of the membrane must be the same.

Depending on their shape, the experimentally recorded spectra can be fitted to circuits **B** and **C**, also presented in Fig. 4.19. The symmetry of the cell suggests that the respective values for both sides of the membrane are the same. Consequently, the relation between cell parameters (circuit **A**) and those derivable by experimental impedance spectra (circuits **B** and **C**) is as follows: $R_S = R_3/2$, $R_{ct} = R_2/2$, $C_{dl} = 2C_2$, $Z_w = Z/2$, $R_b = R_1$, and $C_g = C_1$.

The impedance method was widely used for studies of ionophore-based membranes, but most studies clearly show only one (bulk) semicircle, followed by the Warburg diffusion wave at lower frequencies [142, 173–177]. Only a few reports on well-resolved Faradaic impedance semicircles are known [163, 178–180]. In Fig. 4.20, the impedance spectra are presented, obtained for Li^+ -selective electrodes with neutral ionophore [163].

In the spectra, one can see a high-frequency and also a low-frequency semicircle. The latter is regularly dependent on LiCl, NaCl, and KCl concentrations in solutions. The regularity suggests the Faradaic nature of the semicircle. The results allowed estimation of the standard exchange current densities for Li^+ , Na^+ , and K^+ as 1.7×10^{-5} , 2.9×10^{-7} and 1.6×10^{-7} A/cm². The respective capacity C_2 lies in the range 4×10^{-8} – 7×10^{-8} F and in a few cases reaches values up to 1.2×10^{-7} F. These values suggest for the double-layer capacity C_{dl} , the value of 3×10^{-8} – 6×10^{-8} F/cm². Using the Gouy–Chapman theory, these values allowed estimation of the thickness of the double layer at the interface between an aqueous solution and a polymeric membrane containing ionophores as 100–300 nm. These results also tell about the transient time of the charge transfer process. This time lies in the range from 10^{-5} to 10^{-3} s, dependent on the nature of the membrane

and the ion in question. In particular, the interfacial electrochemical equilibrium establishes in about 10^{-4} to 10^{-2} s, which is much less than the practical response time of ISEs.

References

1. E. Bakker, P. Bühlmann, E. Pretsch, *Chem. Rev.*, 1997, 97, 3083.
2. P. Bühlmann, E. Pretsch, E. Bakker, *Chem. Rev.*, 1998, 98, 1593.
3. G. Baum, M. Linn, *Anal. Chim. Acta*, 1973, 65, 393.
4. C.J. Coetzee, H. Freiser, *Anal. Chem.*, 1968, 40, 1128.
5. A. Leo, C. Hansch, D. Elkins, *Chem. Rev.*, 1971, 71, 515.
6. O. Dinten, U. Spichiger, N. Chaniotakis, P. Gehrig, E. Rusterholz, W.E. Morf, W. Simon, *Anal. Chem.*, 1991, 63, 596.
7. F. Helferich, Ionenaustausher, Chemie GMBH, Weinheim, 1959.
8. F.G. Donnan, *Chem. Rev.*, 1924, 1, 73.
9. R.D. Johnson, L.G. Bachas, *Anal Bioanal Chem.*, 2003, 376, 328.
10. J.W. Ross, *Science*, 1967, 156, 1378.
11. A. Craggs, G.J. Moody, J.D.R. Thomas, *Analyst*, 1979, 104, 412.
12. E. Bakker, E. Malinowska, R.D. Schiller, M.E. Meyerhoff, *Talanta*, 1994, 41, 881.
13. I.H.A. Badr, M. Diaz, M.F. Hawthorne, L.G. Bachas, *Anal. Chem.*, 1999, 71, 1371.
14. S. Amemiya, P. Bühlmann, Y. Umezawa, R.C. Jagessar, D.H. Burns, *Anal. Chem.*, 1999, 71, 1049.
15. R.S. Hutchins, P. Bansal, P. Molina, M. Alajari, A. Vidal, L.G. Bachas, *Anal. Chem.*, 1997, 69, 1273.
16. M. Pietrzak, M.E. Meyerhoff, *Anal. Chem.*, 2009, 81, 3637.
17. S.S. Koseoglu, C.-Z. Lai, C. Ferguson, P. Bühlmann, *Electroanalysis*, 2008, 20, 331.
18. V.V. Egorov, E.M. Rakhman'ko, A.A. Rat'ko, *J. Anal. Chem.*, 2002, 57, 55.
19. K.N. Mikhelson, *Electroanalysis*, 2003, 15, 1236.
20. M.A. Peshkova, A.I. Korobeynikov, K.N. Mikhelson, *Electrochim. Acta*, 2008, 53, 5819.
21. V.V. Egorov, P.L. Lyaskovski, I.V. Ilinchik, V.V. Soroka, V.A. Nazarov, *Electroanalysis*, 2009, 21, 2061.
22. L. Pioda L., W. Stankova, W. Simon, *Anal. Lett.*, 1969, 2, 665.
23. R.P. Scholer, W. Simon, *Chimia*, 1970, 24, 372.
24. H.B. Herman, G.A. Rechnitz, *Anal. Chim. Acta*, 1975, 76, 155.
25. N.V. Garbuzova, A.L. Grekovich, L.I. Ishutkina, V.S. Karavan, E.A. Materova, *Ion-exchange Ionometry*, 1979, 2, 156 (Russ.).
26. A.L. Smirnova, A.L. Grekovich, E.A. Materova, *Sov. Electrochem.*, 1985, 21, 1221 (Russ.).
27. A.L. Smirnova, A.L. Grekovich, E.A. Materova, *Sov. Electrochem.*, 1985, 21, 1335 (Russ.).
28. A.L. Smirnova, V.N. Tarasevitch, E.M. Rakchmanko, *Sensors and Actuators B*, 1994, 18-19, 392.
29. S. Makarychev-Mikhailov, A. Legin, J. Mortensen, S. Levitchev, Yu. Vlasov, *Analyst*, 2004, 129, 213.
30. M.M.G. Antonisse, D.N. Reinhoudt, *Electroanalysis*, 1999, 11, 1035.
31. W. Wróblewski, K. Wojciechowski, A. Dybko, Z. Brzózka, R.J.M. Egberink, B. Snellink-Ruël, D.N. Reinhoudt, *Anal. Chim. Acta*, 2001, 432, 79.
32. M.J. Berrocal, A. Cruz, I.H.A. Badr, L.G. Bachas, *Anal. Chem.*, 2000, 72, 5295.
33. A.S. Watts, V.G. Gavalas, A. Cammers, P. Sanchez Andrada, M. Alajari, L.G. Bachas, *Sensors and Actuators B*, 2007, 121, 200.
34. I.H.A. Badr, M. Diaz, M.F. Hawthorne, L.G. Bachas, *Anal. Chem.*, 1999, 71, 1371.
35. B.P. Nikolsky, E.A. Materova, *Ion-selective Electrodes*, Khimia, Leningrad, 1980 (Russ.).

36. R.P. Buck, *Anal. Chem.*, 1976, 48, 23R.
37. A.P. Thoma, A. Viviani-Nauer, S. Arvanitis, W.E. Morf, W. Simon, *Anal. Chem.*, 1977, 49, 1567.
38. B.P. Nikolsky, E.A. Materova, O.K. Stefanova, V.E. Yurinskaya, *Radiochemistry*, 1982, 6, 808 (Russ.).
39. O. Kedem, M. Perry, R. Bloch, *Proc. IUPAC ISE-Symp. Cardiff, UK*, 1973, 44.
40. A. Van den Berg, P.D. Van der Wal, M. Skowronska-Ptasinska, E.J.R. Sudholter, D.N. Reinhoudt, P. Bergveld, *Anal. Chem.*, 1987, 59, 2827.
41. S. Yajima, K. Tohda, P. Bühlmann, Y. Umezawa, *Anal. Chem.*, 1997, 69, 1919.
42. Y. Qin, E. Bakker, *Anal. Chem.*, 2001, 17, 4262.
43. R. Eugster, P.M. Gehrig, W.E. Morf, U.E. Spichiger, W. Simon, *Anal. Chem.*, 1991, 63, 2285.
44. U. Shaller, E. Bakker, U.E. Spichiger, E. Pretsch, *Anal. Chem.*, 1994, 66, 391.
45. U. Schaller, E. Bakker, E. Pretsch, *Anal. Chem.*, 1995, 67, 3123.
46. M. Nägele, Y. Mi, E. Bakker, E. Pretsch, *Anal. Chem.*, 1998, 70, 1686.
47. S. Amemiya, P. Bühlmann, Y. Umezawa, *Anal. Chem.*, 1998, 70, 445.
48. G.J. Moody, B. Saad, J.D.R. Thomas, *Analyst*, 1987, 112, 1143.
49. E. Malinowska, L. Gawart, P. Parzuchowski, G. Rokicki, Z. Brzozka, *Anal. Chim. Acta*, 2000, 421, 93.
50. R. Bloch, A. Shatkay, H.A. Saroff, *Biophys. J.*, 1967, 7, 865.
51. G.J. Moody, R.B. Oke, J.D.R. Thomas, *Analyst*, 1970, 95, 910.
52. M. Puntener, M. Fibbioli, E. Bakker, E. Pretsch, *Electroanalysis*, 2002, 14, 1329.
53. A.L. Grekovich, E.A. Materova, K.N. Mikhelson, *Ion-exchange Ionometr.*, 1979, 2, 111 (Russ.).
54. A.L. Grekovich, O.A. Goncharuk, K.N. Mikhelson, *Ion-exchange Ionometr.*, 1979, 2, 125 (Russ.).
55. R. Eugster, T. Rosatzin, B. Rusterholz, B. Aebersold, U. Pedrazza, D. Rüegg, A. Schmid, U.E. Spichiger, W. Simon, *Analyt. Chim. Acta*, 1994, 289, 1.
56. G.J. Moody, J.D.R. Thomas, *Ion-Selective Electrodes Rev.*, 1979, 1, 3.
57. S.E. Didina, A.L. Grekovich, *Ion-exchange Ionometr.*, 1986, 5, 99 (Russ.).
58. S.K.A.G. Hassan, G.J. Moody, J.D.R. Thomas, *Analyst*, 1980, 105, 147.
59. W.E. Morf, W. Simon, *Helv. Chim. Acta*, 1971, 54, 2683.
60. D. Ammann, E. Pretsch, W. Simon, *Anal. Lett.*, 1974, 7, 23.
61. M. Güggi, W. Oeme, E. Pretsch, W. Simon, *Helv. Chim. Acta*, 1976, 59, 2417.
62. U. Fiedler, *Anal. Chim. Acta*, 1977, 89, 101.
63. E.A. Materova, Z.S. Alagova, G.I. Shumilova, L.P. Vatlina, I.K. Stekolnikova, *Herald Leningrad Univ.*, 1980, 22, 112 (Russ.).
64. R.D. Armstrong, G. Horvai, *Electrochim. Acta*, 1990, 35, 1.
65. M. Kisbenyi, *J. Polymer. Sci. C.*, 1971, 33, 113.
66. Q. Ye, G. Horvai, K. Toth, I. Bertoti, M. Botreau, T.M. Duc, *Anal. Chem.*, 1998, 70, 4241.
67. Q. Ye, Z. Keresztes, G. Horvai, *Electroanalysis*, 1999, 11, 729.
68. Q. Ye, S. Borbely, G. Horvai, *Anal. Chem.*, 1999, 71, 4313.
69. J.D. Harrison, X. Li, *Anal. Chem.*, 1991, 63, 2168.
70. N.V. Rozhdstvenskaya, O.K. Stefanova, *Sov. Electrochem.*, 1982, 18, 1379(Russ.).
71. A.D.C. Chan, X. Li, J.D. Harrison, *Anal. Chem.*, 1992, 64, 2512.
72. A.D.C. Chan, J.D. Harrison, *Anal. Chem.*, 1993, 65, 32.
73. Z. Li, X. Li, S. Petrovic, J.D. Harrison, *Anal. Chem.*, 1996, 68, 1717.
74. Z. Li, X. Li, M. Rothmaier, J.D. Harrison, *Anal. Chem.*, 1996, 68, 1726.
75. E. Lindner, T. Zwickl, E. Bakker, B.T.T. Lan, K. Toth, E. Pretsch, *Anal. Chem.*, 1998, 70, 1176.
76. T. Lindfors, F. Sundfors, L. Höfler, R.E. Gyurcsanyi, *Electroanalysis*, 2009, 21, 1914.
77. F. Sundfors, L. Höfler, R.E. Gyurcsanyi, T. Lindfors, *Electroanalysis*, 2011, 23, 1769.
78. L. Gorski, A. Matusевич, M. Pietrzak, L. Wang, M. E. Meyerhoff, E. Malinowska, *J. Solid State Electrochem*, 2009, 13, 157.

79. R. De Marco, J.-P. Veder, G. Clarke, A. Nelson, K. Prince, E. Pretsch, E. Bakker, *Phys. Chem. Chem. Phys.*, 2008, 10, 73.
80. J.J. Griffin, G.D. Christian, *Talanta*, 1983, 30, 201.
81. S.S. Levitchev, A.L. Smirnova, A.V. Bratov, Yu.G. Vlasov, *Fres. J. Anal. Chem.*, 1997, 361, 252.
82. Y. Qin, S. Peper, A. Radu, A. Ceresa, E. Bakker, *Anal. Chem.*, 2003, 75, 3038.
83. J.H. Shin, D.S. Sakong, H. Nam, G.S. Cha, *Anal. Chem.*, 1996, 68, 221.
84. B.K. Oh, C.Y. Kim, H.J. Lee, *Anal. Chem.*, 1996, 68, 503.
85. T. Dimitrakopoulos, J.R. Farrel, P.J. Iles, *Electroanalysis*, 1996, 8, 391.
86. T.M. Ambrose, M.E. Meyerhoff, *Electroanalysis*, 1996, 8, 1095.
87. S.Y. Yun, Y.K. Hong, B.K. Oh, *Anal. Chem.*, 1997, 69, 868.
88. S.S. Levitchev, A.L. Smirnova, V.L. Khitrova, *Sens. Actuators B*, 1997, 44, 397.
89. N.Yu. Abramova, A.V. Bratov, Yu.G. Vlasov, *Russ. J. Appl. Chem.*, 1997, 70, 1107 (Russ.).
90. L.Y. Heng, E.A.H. Hall, *Anal. Chim. Acta*, 2001, 443, 25.
91. L.Y. Heng, E.A.H. Hall, *Anal. Chem.*, 2000, 72, 42.
92. L.Y. Heng, E.A.H. Hall, *Anal. Chim. Acta*, 2000, 403, 77.
93. A. Rzewuska, M. Wojciechowski, E. Bulska, E.A.H. Hall, K. Maksymiuk, A. Michalska, *Anal. Chem.*, 2008, 80, 321.
94. A. Michalska, K. Pyrzynska, K. Maksymiuk, *Anal. Chem.*, 2008, 80, 3921.
95. A. Michalska, C. Appaih-Kusi, L.Y. Heng, S. Walkiewicz, E.A.H. Hall, *Anal. Chem.*, 2004, 2031.
96. N.V. Shvedene, D.V. Chernyshov, M.G. Khrenova, A.A. Formanovsky, V.E. Baulin, I.V. Pletnev, *Electroanalysis*, 2006, 18, 1416.
97. D.V. Chernyshov, M.G. Khrenova, I.V. Pletnev, N.V. Shvedene, *Mendeleev Communications*, 2008, 18, 88.
98. D.V. Chernyshov, V.M. Egorov, N.V. Shvedene, I.V. Pletnev, *ACS Appl. Mater. Interfaces*, 2009, 1 2055.
99. K. Kimura, T. Maeda, H. Tamura, T. Shono, *J. Electroanal. Chem.*, 1979, 95, 91.
100. Y. Tsujimura, T. Sunagawa, M. Yokoyama, K. Kimura, *Analyst*, 1996, 121, 1705.
101. R.J.W. Lugtenberg, R.J.M. Egberink, J.F.J. Engbersen, D.N. Reinhoudt, *J. Chem. Soc. Perkin Trans.* 1997, 2, 1353.
102. K. Kimura, T. Sunagawa, S. Yajima, S. Miyake, M. Yokoyama, *Anal. Chem.* 1998, 70, 4309.
103. S. Daunert, L.G. Bachas, *Anal. Chem.* 1990, 62, 1428.
104. M. Püntener, T. Vigassy, E. Baier, A. Ceresa, E. Pretsch, *Anal. Chim. Acta*, 2004, 503, 187.
105. L. Ebdon, A.T. Ellis, G.C. Cornfield, *Analyst*, 1979, 104, 730.
106. L. Ebdon, A.T. Ellis, G.C. Cornfield, *Analyst*, 1982, 107, 288.
107. P.C. Hobby, G.J. Moody, J.D.R. Thomas, *Analyst*, 1983, 108, 551.
108. S. Peper, Y. Qin, P. Almond, M. McKee, M. Telting-Diaz, T. Albrecht-Scmitt, E. Bakker, *Anal. Chem.*, 2003, 75, 2131.
109. Z. Mousavi, J. Bobacka, A. Lewenstam, A. Ivaska, *J. Electroanal. Chem.*, 2006, 593, 219.
110. Y. Qin, E. Bakker, *Anal. Chem.*, 2003, 75, 6002.
111. A. Gonzalez-Bellavista, J. Macanas, M. Munoz, E. Fabregas, *Anal. Chim. Acta*, 2006, 577, 85.
112. A. Kisiel, A. Michalska, K. Maksymiuk, E.A.H. Hall, *Electroanalysis*, 2008, 20, 318.
113. A. Michalska, *Electroanalysis*, 2012, 24, 1253.
114. P.G. Boswell, P. Bühlmann, *J. Am. Chem. Soc.*, 2005, 127, 8958.
115. P.G. Boswell, C. Szijjarto, M. Jurisch, J.A. Gladysz, Jo. Rabai, P. Bühlmann, *Anal. Chem.* 2008, 80, 2084.
116. C.Z. Lai, S.S. Koseoglu, E.C. Lugert, P.G. Boswell, J. Rabai, T.P. Lodge, P. Bühlmann, *J. Am. Chem. Soc.* 2009, 131, 1598.
117. C.Z. Lai, M.A. Fierke, R. Correa da Costa, J.A. Gladysz, A. Stein, P. Bühlmann, *Anal. Chem.* 2010, 82, 7634.
118. G. Jagerszki, A. Takacs, I. Bitter, R.E. Gyurcsanyi, *Angew. Chem. Int. Ed.* 2011, 50, 1656.

119. J.P. Sandblom, G. Eisenman, J.L. Walker, *J. Phys. Chem.*, 1967, 71, 3871.
120. C. Fabiani, R. Danesi, G. Scibona, B. Scuppa, *J. Phys. Chem.*, 1974, 78, 7974.
121. C. Fabiani, *Anal. Chem.*, 1976, 48, 865.
122. K.N. Mikhelson, A.L. Smirnova, *Sensors and Actuators B*, 1992, 10, 47.
123. K.N. Mikhelson, *Sensors and Actuators B*, 1994, 18, 31.
124. K.N. Mikhelson, A. Lewenstam A., *Sensors and Actuators B*, 1998, vol. 48, p. 344-350.
125. Mikhelson K.N., Lewenstam, S.E. Didina, *Electroanalysis*, 1999, 11, 793.
126. K.N. Mikhelson, A. Lewenstam, *Anal. Chem.*, 2000, 72, 4965.
127. K.N. Mikhelson, Multispecies description of ion-selective electrodes, *Encyclopedia of Sensors*, American Scientific Publishers, Eds. Craig A. Grimes, Elizabeth C. Dickey, and Michael V. Pishko, 2006, 6, p. 335.
128. F.Hofmeister, *Arch. Exp. Pathol. Pharmacol.*, 1888, 24, 247.
129. S. Ciani, G. Eisenman, G. Szabo, *J. Membrane Biol.*, 1969, 1, 1.
130. W.E. Morf, *The Principles of Ion-selective electrodes and of Membrane Transport*, Akademiai Kiado, Budapest, 1981.
131. K.N. Mikhelson, A.L. Grekovich, E.A. Materova, S.Yu. Filippov, *Sov. Electrochemistry*, 1982, 18, 53 (Russ., Engl. transl.).
132. K.N. Mikhelson, A.L. Grekovich, E.A. Materova, *Sov. Electrochemistry*, 1982, 18, 1099 (Russ., Engl. transl.).
133. K.N. Mikhelson, A.L. Grekovich, E.A. Materova, L.P. Dement'eva, *Sov. Electrochemistry*, 1982, 18, 1102 (Russ., Engl. transl.).
134. K.N. Mikhelson, A.L. Grekovich, E.A. Materova, *Sov. Electrochemistry*, 1983, 19, 226 (Russ., Engl. transl.).
135. J.H. Boles, R.P. Buck, *Anal. Chem.*, 1973, 45, 2057.
136. K.N. Mikhelson, A.L. Grekovich, *Ion-Exchange and Ionometry*, 1979, 2 171 (Russ.).
137. V.E. Yurinskaya, O.K. Stefanova, E.A. Materova, *Sov. Electrochemistry*, 1980, 16, 860.
138. R. Buchi, E. Pretsch, W.E. Morf, W. Simon, *Helv. Chim. Acta.*, 1976, 59, 2407.
139. Z.S. Alagova, V.A. Gindin, K.N. Mikhelson, G.I. Shumilova, *Sov. Electrochemistry*, 1988, 24, 17.
140. P. Bühlmann, S. Amemiya, S. Yajima, Y. Umezawa, *Anal. Chem.*, 1998, 70, 4291.
141. E.D. Steinle, S. Amemiya, P. Bühlmann, M.E. Meyerhoff, *Anal. Chem.*, 2000, 72, 5766.
142. K.N. Mikhelson, J. Bobacka, A. Lewenstam, A. Ivaska, *Electroanalysis*, 2001, 13, 876.
143. P.C. Meier, W.E. Morf, M. Läubli, W. Simon, *Anal. Chim. Acta*, 1984, 156, 1.
144. R. Eugster, P.M. Gehrig, W.E. Morf, U.E. Spichiger, W. Simon, *Anal. Chem.*, 1991, 63, 2285.
145. S. Amemiya, P. Bühlmann, E. Pretsch, B. Rusterholz, Y. Umezawa, *Anal. Chem.* 2000, 72 1618.
146. E. Bakker, P. Bühlmann, E. Pretsch, *Talanta*, 2004, 63, 3.
147. E. Eyal, G.A. Rechnitz, *Anal. Chem.* 1971, 43, 1090.
148. P.U. Fröh, J.T. Clerc, W. Simon, *Helv. Chim. Acta* 1971, 54, 1445.
149. N.N.L. Kirsch, W. Simon, *Helv. Chim. Acta* 1976, 59, 357.
150. N.N.L. Kirsch, R.J.J. Funck, E. Pretsch, W. Simon, *Helv. Chim. Acta* 1977, 60, 2326.
151. E. Bakker, M. Willer, M. Lerchi, K. Seiler, E. Pretsch, *Anal. Chem.* 1994, 66, 516.
152. E. Bakker, E. Pretsch, *J. Electrochem. Soc.* 1997, 144, L125.
153. E. Bakker, E. Pretsch, *Anal. Chem.* 1998, 70, 295.
154. A. Cereza, E. Pretsch, *Anal. Chim. Acta* 1999, 395, 41.
155. O.K. Stefanova, *Elektrokhimia* 1979, 15, 1707 (Russ.).
156. O.K. Stefanova, E.D. Suglobova, *Elektrokhimia* 1979, 15, 1822.
157. S.B. Mokrov, O.K. Stefanova, E.A. Materova, E.E. Ivanova, *Herald Leningr. Univ.* 1984, 16, 41 (Russ.).
158. S.B. Mokrov, O.K. Stefanova, *Elektrokhimia* 1985, 21, 540.
159. S.B. Mokrov, O.K. Stefanova, *Elektrokhimia* 1990, 26, 294-299 (Russ.).
160. V.M. Lutov, K.N. Mikhelson, *Sens. Actuators, B* 1994, 19, 400.
161. Y. Mi, E. Bakker, *Anal. Chem.* 1999, 71, 5279.

162. Y. Qin, Y. Mi, E. Bakker, *Anal. Chim. Acta*, 2000, 421, 207.
163. K.N. Mikhelson, J. Bobacka, A. Ivaska, A. Lewenstam, M. Bochenska, *Anal. Chem.*, 2002, 74, 518.
164. M.A. Peshkova, N.V. Timofeeva, A.L. Grekovich, S.M. Korneev, K.N. Mikhelson, *Electroanalysis*, 2010, 22, 2147.
165. S.B. Mokrov, V.V. Malev, O.K. Stefanova, *Elektrokhimika* 1990, 26, 1087-1091 (Russ).
166. U. Oesch, W. Simon, *Anal. Chem.*, 1980, 52, 692.
167. M.M. Shultz, O.K. Stefanova, S.B. Mokrov, K.N. Mikhelson, *Anal. Chem.*, 2002, 74, 510.
168. E. Malinowska, M.E. Meyerhoff, *Anal. Chem.*, 1998, 70, 1477.
169. N.N. Markuzina, S.B. Mokrov, O.K. Stefanova, S.N. Sementsov, *Rus. J. Appl. Chem.*, 1993, 66, 2315 (Russ.).
170. T. Ito, H. Radecka, K. Tohda, K. Odashima, Y. Umezawa, *J. Amer. Chem. Soc.*, 1998, 120, 3049.
171. N.M. Mikhaleva, E.G. Kulapina, *J. Anal. Chem.*, 2005, 60, 646.
172. K.N. Mikhelson, *Chem. Analityczna – Anal. Chem. (Warsaw)*, 2006, 51, 853.
173. K. Cammann, *Anal. Chem.* 1978, 50, 936.
174. R.P. Buck, *Ion-selective Electrode Rev.* 1982, 4, 3.
175. K. Cammann, G.A. Rechnitz, *Anal. Chem.* 1976, 48, 856.
176. S.-L. Xie, K. Cammann, *J. Electroanal. Chem.* 1987, 229, 243.
177. A.L. Smirnova, S.S. Levitchev, V.L. Khitrova, A.L. Grekovich, Yu.G. Vlasov, A. Schwake, K. Cammann, *Electroanalysis* 1999, 11, 763.
178. G. Horvai, E. Graf, K. Toth, E. Pungor, R.P. Buck, *Anal. Chem.* 1986, 58, 2735.
179. K. Toth, E. Graf, G. Horvai, E. Pungor, R.P. Buck, *Anal. Chem.* 1986, 58, 2741.
180. W. Zhang, U.E. Spichiger, *Electrochim. Acta*, 2000, 45, 2259.

Chapter 5

Glass Electrodes

This chapter is devoted to glass electrodes for the pH and metal ion measurements, as well as to RedOx-sensitive glass electrodes.

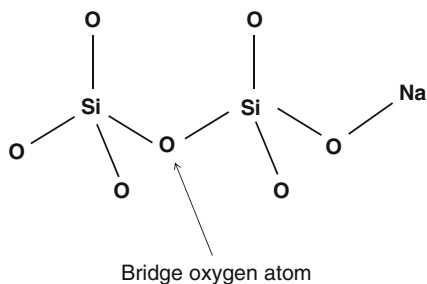
5.1 Materials of the Glass Electrode Membranes

Ion-selective electrodes with glass membranes are the oldest [1–5] (see also Sects. 1.2–1.4) and until now the most frequently used among other ISEs. This is because glass electrodes are by far the best sensors of the pH, and the pH is the most frequently measured parameter of the chemical composition of various types of samples. Besides measurements of the pH, measurements of activities of several metal cations (in the first place— Na^+) can also be performed with the respective glass electrodes.

Silicon dioxide (SiO_2) is the main component of the electrode glasses. Silicate glass membranes are very stable against aggressive chemicals like concentrated acids (except of HF) or organic solvents. Therefore, electrodes with glass membranes can be used under harsh conditions, including those in chemical and biochemical industries. Phosphoric glasses are also known but only seldom in use because these kinds of glasses are relatively soluble in water and therefore unstable in most real applications.

Although glasses are amorphous, a short-range ordering exists in glass membranes. In quartz, silicon dioxide forms tetrahedral lattice. A similar although less regular structure is characteristic also for the electrode glasses. As shown in Fig. 5.1, oxygen atoms are of two types: bridge and non-bridge atoms. The former are bound to two silicon atoms, the latter to only one silicon atom, while the other is a metal atom. The metal atoms in the structure originate from the respective metal oxides: Li_2O , Na_2O , and K_2O . Electrode glasses are always doped with some of these metal oxides because pure SiO_2 is non-conducting. Metal oxides are introduced into melted silicon dioxide, and the whole melt has to be cooled fast in order to maintain in the hard glass the uniform distribution of the components, which is characteristic of the melted oxide mixture.

Fig. 5.1 Silicon dioxide tetrahedral lattice in glass. Most of oxygen atoms are bound to silicon atoms (*bridge oxygen atoms*), but some of oxygens are bound to a silicon atom and to a metal atom



When a glass membrane is in contact with an aqueous solution, water molecules enter glass and attack Si–O and also O–M bonds in $\equiv\text{Si}-\text{O}-\text{Si}\equiv$ and $\equiv\text{Si}-\text{O}-\text{M}$ fragments. Hydrogen atoms partly replace silicon and metal atoms, producing $\equiv\text{Si}-\text{O}-\text{H}$ groups. These groups, in turn, are subjects for the water molecule attack as well and undergo the hydrolysis process, resulting in $\equiv\text{Si}-\text{O}^-$ groups and H_3O^+ ions released into solution, see Fig. 5.2. These both processes are reversible (this feature is not shown in Fig. 5.2 to avoid overloading) and govern the glass electrode response to pH and metal cations.

The respective ion-exchange sites in glass are represented by $(\text{SiO}_{3/2})\text{O}^-$ groups: the products of the partial dissociation of the $\equiv\text{Si}-\text{O}-\text{H}$ and $\text{Si}-\text{O}-\text{M}$ groups. The $\equiv\text{Si}-\text{O}-\text{H}$ bond is much more covalent than the $\equiv\text{Si}-\text{O}-\text{M}$ bond. Therefore, hydrogen atoms are strongly preferred by the glass phase. This is why electrodes with membranes made of binary glasses containing only SiO_2 and Na_2O or Li_2O (the typical compositions are 22 mol % Na_2O , 78 mol % SiO_2 and 27 mol % Li_2O , 73 mol % SiO_2) show Nernstian response to the pH in an enormously broad range: from pH 1 to pH 9. Some multi-component glasses allow for pH measurements from pH – 1 to even 14, but in this case, the alkaline pH is adjusted by means of bases with large organic cations.

Some compositions of the pH-selective glass membranes are presented in Table 5.1, composed on the basis of a similar table by Belyustin [6]. As one can

Fig. 5.2 Schematic illustration of the ion-exchange process (*top*) and the hydrolysis process (*bottom*)

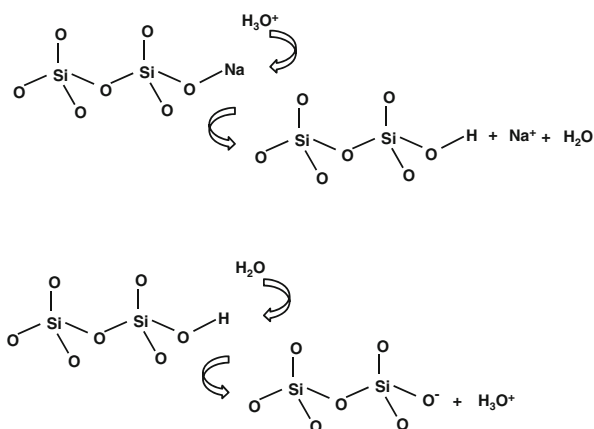


Table 5.1 Compositions of glasses for the pH electrodes

Marking	Composition	Author, year, reference
<i>Sodium silicate glasses (wt. %)</i>		
“Hughes’s glass”	20 Na ₂ O–8 CaO–72 SiO ₂	Hughes 1928 [37]
McInnes and Dole glass, Corning 015	22 Na ₂ O–6 CaO–72 SiO ₂	MacInnes, Dole 1929, 1930 [38, 39]
<i>Lithium silicate glasses (mol %)</i>		
LiCa	18.1 Li ₂ O–9.6 CaO–72.3 SiO ₂	Sokolov, Passinskii 1932 [40]
LiBa	26 Li ₂ O–3.6 BaO–70.4 SiO ₂	Avseevich 1938–1948 [41, 42]
LiMg	26.5 Li ₂ O–12.3 MgO–61.2 SiO ₂	Cary, Baxter 1949 [43]
LiCa	25 Li ₂ O–7 CaO–68 SiO ₂	Perley 1948, 1949 [44, 45]
Present day glasses for pH electrodes	21–33 Li ₂ O, 2–4 Cs ₂ O, 3–5 La ₂ O ₃ (Nd ₂ O ₃ , Er ₂ O ₃), 2–4 CaO (BaO)–SiO ₂ (the rest)	Manufacturers all over the world

see, a large variety of the pH glass membrane compositions have been invented already by 1950s. Besides SiO₂ and Na₂O (Li₂O), glass membranes contain also alkaline earth metal oxides. More recent progress has been motivated by the success of the Perley’s glass and relies on doping glass membranes with rare earth metal oxides.

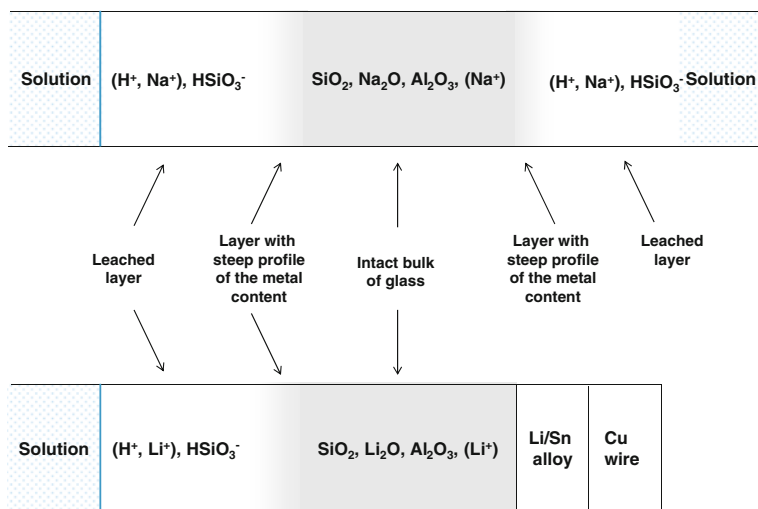
Addition of Al₂O₃ or B₂O₃ to an electrode glass composition causes significant changes in the electrode selectivity. Qualitatively, the same kind of processes like those taking place with the ≡Si–O–H and Si–O–M groups also takes place with =Si–O–Al–H, =Si–O–B–H, and =Si–O–AlM, =Si–O–B–M groups: ion exchange and hydrolysis. However, quantitatively the situation is very different. Aluminum and boric hydroxides (when tetra-coordinated) are relatively strong acids, and glasses containing these dopants show dramatically lower selectivity to hydrogen ions than glasses for the pH control. This makes possible using the respective electrodes for measuring metal ion activities in solutions. However, the excess of the metal ions over hydrogen must be about 1,000; otherwise, the electrode responds to pH. Examples of the compositions for some metal cation sensing glass membranes are given in Table 5.2, composed on the basis of [6].

Kiprianov added halogen (fluoride) as LiF (up to 3.5 %) to the glass compositions [7, 8]. The resulting melts are less viscose, which is technologically advantageous. The selectivity to K⁺ ions and the chemical robustness of the electrodes are improved as compared to the ISEs without fluoride in membranes.

Not only the surface of the glass undergoes hydration process. In fact, hydration spreads into the glass phase forming the so-called hydrated surface layers. There are two main types of surface layers: (1) a layer with smooth profile with a steep gradient of the metal (e.g., Na) concentration starting from the very glass/solution

Table 5.2 Compositions of glasses for metal ion sensing

Marking, target ions	Composition (mol %)	Author, year reference
<i>Sodium (potassium) silicate glasses</i>		
Schott, Na ⁺ , K ⁺ , Ag ⁺	Na ₂ O–B ₂ O ₃ –Al ₂ O ₃ –SiO ₂ + additives	Horovitz, Schiller 1923–1925 [46, 47]
D _a and its options, Na ⁺	(11–25) Na ₂ O–(9–12) B ₂ O ₃ –(3–5) Al ₂ O ₃ –SiO ₂ (the rest)	Schultz et al. 1953–1955 [48, 49]
Potassium analogs of D _a	(15–25) K ₂ O–(9–12) B ₂ O ₃ –(3–5) Al ₂ O ₃ – SiO ₂ (the rest)	Schultz et al. 1955–1958 [50, 51]
NAS-1118, Na ⁺	11 Na ₂ O–18 Al ₂ O ₃ –71 SiO ₂	Eisenman, since 1957, [52, 53]
NAS-2704, K ⁺	27 Na ₂ O–4 Al ₂ O ₃ –69 SiO ₂	Eisenman, since 1957, [52, 53]
ESL-51, Na ⁺ , Gomel Instrumentation Factory, Belarus	24 Na ₂ O–5 B ₂ O ₃ –9 Al ₂ O ₃ –62 SiO ₂ and 21 Na ₂ O–3 B ₂ O ₃ –12 Al ₂ O ₃ –64 SiO ₂	Schultz et al. [54]
<i>Lithium silicate glasses</i>		
39278, Na ⁺	26.2 Li ₂ O–12.4 Al ₂ O ₃ –61.4 SiO ₂	Beckman [55]
BH-67A, Na ⁺	Li ₂ O–Al ₂ O ₃ –SiO ₂	Electronic Instruments Ltd., UK [56]
ESL-10, Na ⁺ , Li ⁺ , Gomel Instrumentation Factory, Belarus	16 Li ₂ O–8 Al ₂ O ₃ –76 SiO ₂	Belyustin et al. [57]

**Fig. 5.3** Glass membranes of a classical glass electrode (*top*) and a solid-contact glass electrode (*bottom*). Species ensuring the conductivity are shown in parenthesis; the thickness of the surface layers is exaggerated for clarity

boundary and (2) a layer containing a relatively lengthy leached layer (5–100 nm in Li-glasses and up to 2–3 μm in Na-glasses), with an underlying layer with a steep gradient of the metal concentration. These layers formed in a membrane of a classical glass electrode with internal solution, and that in a solid-contact glass electrode, are shown schematically in Fig. 5.3. For the discussion of solid-contact ISEs, see Sect. 8.2.

The conductivity of glasses is of ionic in nature, due to the diffusion of H^+ and Na^+ (Li^+) ions in the leached layers and Na^+ (Li^+) ions in the intact bulk of the glass membrane. Special type of glasses—electronically conducting glasses—is briefly discussed in Sect. 5.3.

5.2 The Theories of the pH and Metal Ion Glass Electrode Response and Selectivity

5.2.1 The Nikolsky “Simple” Theory

The so-called simple theory has been proposed by Nikolsky already in 1937 [3]. Below, we will briefly describe this theory like it was done by Nikolsky himself. The theory was aimed at rationalization of the following experimental observations, well established by that time:

1. glass electrodes show linear response to pH with the slope close to Nernstian value in a broad pH range:

$$\frac{dE}{dpH} \approx -\frac{RT}{F} \quad (5.1)$$

2. the response deviates from linearity at high pH values (in alkaline region)
3. the magnitude of the deviations in alkaline region depends on the composition of glass
4. anions do not interfere with the electrode potential.

Observation (3) deserves special consideration. Table 5.1 provides with some details on this observation. One can see that the interference from an ion is determined by the ion’s size. Glasses doped with lithium oxide, that is, the oxide of the smallest metal among other metals, suffer significant interference only from the lithium ion, while larger ions sodium and potassium show low interference. Glasses doped with sodium oxide discriminate K^+ , but Li^+ and Na^+ interfere with the pH response. Now, glasses doped with potassium oxide discriminate only rather large cations like barium and tetraethylammonium. These facts suggest that the ability of an ion to interfere depends on its ability to enter the glass phase and replace the metal dopant atom in the membrane structure. This is nothing else as

Table 5.3 Dependence of the cation interference with the glass electrode response to pH on the nature of the metal oxide in the membrane

Metal oxide	Interfering ions	Discriminated ions
Li ₂ O	Li ⁺	Na ⁺ , K ⁺
Na ₂ O	Li ⁺ , Na ⁺	K ⁺
K ₂ O ^a	Li ⁺ , Na ⁺ , K ⁺	Ba ²⁺ , Et ₄ N ⁺

^a Nowadays, this kind of glasses is not in use for the pH measurements

ion-exchange process between the two phases: solution and membrane (Table 5.3).

By the mid-1930s, it was also known that glass electrodes are low polarizable. This suggests fast charge-transfer process at the membrane/solution interface. Thus, the ion-exchange process which makes possible the interfacial charge transfer must also be fast and must reach equilibrium within a short time period after the phases are put into contact.

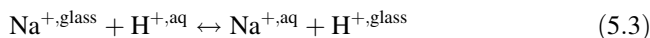
In principle, adsorption of ions at the membrane surface could result in similar effects. However, according to the Freundlich equation describing the potential effect of ion adsorption, the electrode should respond as below:

$$\frac{dE}{\ln C_H} = \left(1 - \frac{1}{n}\right) \frac{RT}{F}. \quad (5.2)$$

Given the factor $1/n$ in Eq. (5.2) is normally about 0.6, the adsorption theory predicts the response with a half-Nernstian or even lower slope which is not confirmed by the experimental data.

Based on these considerations, Nikolsky assumed that the main reason for the glass electrode response to the pH is ion exchange at the membrane/solution interface, and the selectivity of this response originates from large shift of the respective equilibrium, see Eq. (5.3), in favor of hydrogen ions. The formal apparatus of the Nikolsky “simple” theory is presented below.

It is assumed that the interfacial ion exchange takes place and reaches equilibrium:



Then, one can easily obtain for the boundary potential:

$$\begin{aligned} F(\varphi^{\text{glass}} - \varphi^{\text{aq}}) &= \mu_{\text{H}^+}^{0, \text{aq}} - \mu_{\text{H}^+}^{0, \text{glass}} + RT \ln \frac{a_{\text{H}^+}^{\text{aq}}}{a_{\text{H}^+}^{\text{glass}}} \\ &= \mu_{\text{Na}^+}^{0, \text{aq}} - \mu_{\text{Na}^+}^{0, \text{glass}} + RT \ln \frac{a_{\text{Na}^+}^{\text{aq}}}{a_{\text{Na}^+}^{\text{glass}}}. \end{aligned} \quad (5.4)$$

The equilibrium constant of the ion-exchange reaction (5.3) is as follows:

$$K_{\text{H}/\text{Na}}^{\text{exch}} = \exp(\mu_{\text{H}^+}^{0, \text{glass}} - \mu_{\text{H}^+}^{0, \text{aq}} + \mu_{\text{Na}^+}^{0, \text{aq}} - \mu_{\text{Na}^+}^{0, \text{glass}}/RT) = \text{Const.} \quad (5.5)$$

Next comes the assumption which Nikolsky himself considered as obvious: The sum of the concentrations (or that of the mole fractions of hydrogen and the metal ions) is constant and equals that of R^{-1} ion-exchange sites in glass:

$$N_0 = N_{H^+} + N_{Na^+}. \quad (5.6)$$

With full respect to Nikolsky, the author of this book does not consider this obvious. This assumption is true for the respective total values: total sites, total hydrogen, and total sodium (or other metal), whatever in associated forms, HR and NaR, or in ionic forms, R^- , H^+ , and Na^+ . When referred to only ionic forms, Eq. (5.6) is only true if the dissociation degrees of HR and NaR ion pairs are always equal. The latter suggests either equal dissociation constants of HR and NaR, which is hardly true, or very high dissociation constants of both HR and NaR so that the ionic forms strongly predominate over the associated forms. Otherwise, N_0 varies along the ion-exchange process. Anyway, assuming Eq. (5.6) is true, we obtain for the ratio of the cation activities in the glass phase:

$$\frac{a_{Na^+}^{glass}}{a_{H^+}^{glass}} = \frac{N_{Na^+}}{a_{H^+}^{glass}} = \frac{N_0 - N_{H^+}}{a_{H^+}^{glass}} \cdot f_{Na^+}^{glass} = K_{H/Na}^{exch} \frac{a_{Na^+}^{aq}}{a_{H^+}^{aq}}. \quad (5.7)$$

Here, $f_{Na^+}^{glass}$, $f_{H^+}^{glass}$ stand for the Na^+ and H^+ ion activity coefficients in the glass phase. Assuming both these values are equal to 1, that is, activities in the glass phase are replaced with the respective concentrations, we get

$$\frac{a_{H^+}^{aq}}{a_{H^+}^{glass}} = \frac{a_{H^+}^{aq} + K_{H/Na}^{exch} a_{Na^+}^{aq}}{N_0}. \quad (5.8)$$

The combination of Eqs. (5.4) and (5.8) yields

$$(\varphi^{glass} - \varphi^{aq}) = \frac{\mu_{H^+}^{0,aq} - \mu_{H^+}^{0,glass}}{F} + \frac{RT}{F} \ln \frac{a_{H^+}^{aq} + K_{H/Na}^{exch} a_{Na^+}^{aq}}{N_0}. \quad (5.9)$$

Now, we can write for the emf of a galvanic cell containing the glass electrode and a suitable reference electrode as shown in the equation below:

$$E = E^0 + \frac{RT}{F} \ln(a_{H^+}^{aq} + K_{H/Na}^{exch} a_{Na^+}^{aq}) \quad (5.10)$$

Equation (5.10) is the well-known Nikolsky equation. Equations by form the same as the one derived in [3] are the most frequently used in the ISE theory and practice, whatever is the nature of the membrane. However, the physical meaning of the selectivity coefficient (the parameter $K_{H/Na}$ or, more generally, $K_{I/J}$) is different dependent on the nature of the membrane (glass, polymeric, crystalline). According to the Nikolsky “simple” theory, the potentiometric selectivity

¹ Here, the symbol R^- stands for ionogenic group in glass: $\equiv Si-O^-$ or $=Al-O^-$ or $=B-O^-$ or whatever else, dependent on the glass composition.

coefficient equals the ion-exchange constant at the membrane/solution interface. More advanced theories consider more factors influencing the selectivity.

5.2.2 The Eisenman Theory

In the transient part of the response, when the pH response vanishes at high pH and turns to a metal cation response, the experimental curves deviate from what should be according to the Nikolsky equation. The transient part is more expanded in comparison with that predicted by Eq. (5.10), see also Fig. 5.4. This fact motivated further experimental research into the mechanism and the evolution of the theoretical description of the glass electrode response. An important contribution was made by Eisenman [5, 9, 10]. Eisenman assumed power function for the dependence of the ion activities in glass on their mole fractions: $a_i^{\text{glass}} = N_i^n$. Under this assumption, the equation for the EMF is

$$E = E^0 + n \frac{RT}{F} \ln \left((a_{\text{H}^+}^{\text{aq}})^{1/n} + (K_{\text{H}/\text{Na}}^{\text{pot}} a_{\text{Na}^+}^{\text{aq}})^{1/n} \right). \quad (5.11)$$

The n value is selected empirically in order to fit the experimental data.

The Eisenman theory differs from the Nikolsky “simple” theory also regarding the physical meaning of the selectivity coefficient. Eisenman has considered the overall membrane potential, including also the diffusion potential contribution [5, 10]. Therefore, the selectivity coefficient in Eq. (5.11) is dependent not only on the ion-exchange constant but also on the ion mobilities ratio:

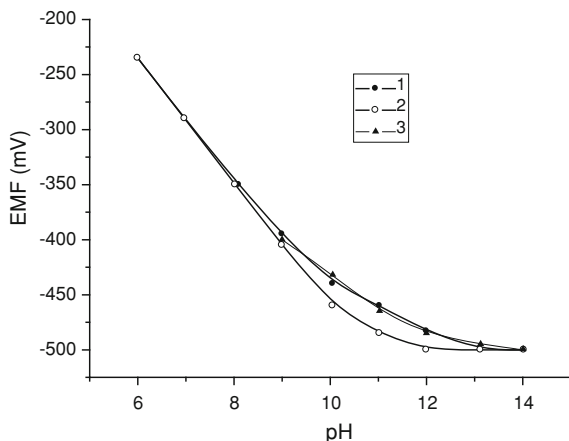


Fig. 5.4 Experimental and calculated curves for the pH electrode with membrane containing 22 % Na_2O , 9.4 % B_2O_3 , and 68.6 % SiO_2 [18]. Sodium activity is $a_{\text{Na}} = 2.14$. Curve 1: experimental values, Curve 2: calculated with Eq. (5.10) using $K_{\text{H}/\text{Na}}^{\text{exch}} = 1.4 \times 10^{-11}$, Curve 3: calculated with Eq. (5.15) using $\alpha_{\text{H},1/2} K_{\text{H}/\text{Na}}^{\text{exch}} = 1.4 \times 10^{-11}$, $\alpha_{\text{H},1} = 9 \times 10^{-4}$

$$K_{\text{H/Na}}^{\text{pot}} = \frac{u_{\text{Na}}}{u_{\text{H}}} K_{\text{H/Na}}^{\text{exch}}. \quad (5.12)$$

Since the ion mobilities are assumed constant, the consideration of the diffusion potential within the membrane does not alter the shape of the response curve. However, the difference in ion mobilities may contribute to the value of the selectivity coefficient as compared to only the ion-exchange constant.

It is worth to mention that before Eisenman, the same has been done by Stefanova [11]. Furthermore, several distinctively different mechanisms of ion transfer within the glass phase have been considered, aimed at rationalization of surprisingly high selectivity of silicate glasses to pH (higher than could be expected from low acidity of SiO_2) [12–15]. These papers, however, have been published only in Russian and for years remained unknown for the international scientific community, until Morf briefly analyzed these approaches in his book [16].

5.2.3 The Nikolsky–Shultz Generalized Theory

Nikolsky together with Shultz developed the so-called Nikolsky–Shultz generalized theory. This theory is known in two versions, based on two distinctively different approaches. Below, the Nikolsky–Shultz generalized theory is described like it was summarized by Belyustin [17]. Both versions of the generalized theory accounted for differences in the strength of the interactions between the ions and different ionogenic groups (ion-exchange sites) in glass. However, one approach relied mostly on quasi-thermodynamic improvements in the Nikolsky “simple” theory, while the other one directly considered the difference in the dissociation degrees for different ion-exchange sites.

Within the frames of the first approach, Nikolsky and Shultz introduced $\alpha_{\text{H}^+,i}$, $\alpha_{\text{M}^+,i}$ —the so-called partial activity coefficients. It was assumed that the ion activities in glass can be represented by the sums of the multiples of the respective partial activity coefficients and mole fractions of the respective sites:

$$a_{\text{H}^+}^{\text{glass}} = \sum_i \alpha_{\text{H}^+,i} N_{\text{H}^+,i}, \quad a_{\text{M}^+}^{\text{glass}} = \sum_i \alpha_{\text{M}^+,i} N_{\text{M}^+,i}.$$

Thus, for each of the i sorts of the ion-exchange sites in glass, the partial activity coefficients of H^+ and M^+ ions are different and however do not depend on $N_{\text{H}^+,i}$, $N_{\text{M}^+,i}$ —the mole fractions of the cations bound to these kind of sites. Thus, the assumption on the constant values of the overall activity coefficients in glass utilized in the Nikolsky “simple” theory is replaced here by the assumption on the constancy of the partial activity coefficients. For each sort of the sites, the sum of the mole fractions referring to H^+ and M^+ ions is constant:

$$N_{\text{H}^+,i} + N_{\text{M}^+,i} = N_{0,i} = \text{Const}. \quad (5.13)$$

The latter statement, like in the case of the Nikolsky “simple” theory, suggests equal dissociation degrees for H^+ and M^+ ions bounded to a particular sort of the sites. The final form obtained for the EMF using this approach is

$$E = E^0 + \frac{RT}{F} \ln \sum_i \frac{a_{H^+}^{aq} + \alpha_{H^+,i} K_{H/M} a_{M^+}^{aq}}{\alpha_{H^+,i} N_{0,i}}. \quad (5.14)$$

The physical meaning of the other approach is different and perfectly clear. Each ionogenic group in glass, whatever in H^+ or M^+ form, dissociates $R_iH \leftrightarrow R_i^- + H^+$ and $R_iM \leftrightarrow R_i^- + M^+$, and these dissociation equilibria are characterized by the respective dissociation constants:

$$k_{H^+,i} = \frac{a_{R_i^-}^{glass} a_{H^+}^{glass}}{a_{R_iH}^{glass}}, \quad k_{M^+,i} = \frac{a_{R_i^-}^{glass} a_{M^+}^{glass}}{a_{R_iM}^{glass}}.$$

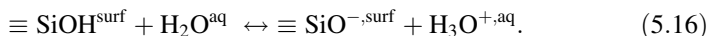
The values of $k_{H,i}$, $k_{M,i}$ are specific and may differ significantly. The approach results in equation

$$E = E^0 + 0.5 \frac{RT}{F} \ln(a_{H^+}^{aq} + K_{H/M} a_{M^+}^{aq}) + 0.5 \frac{RT}{F} \sum_i \frac{a_{H^+}^{aq} + \alpha_{H^+,i} K_{H/M} a_{M^+}^{aq}}{k_{H^+,i} N_{0,i}}. \quad (5.15)$$

This equation allowed for rational explanation of the expanded transient parts in the calibration curves (for one sort of anionic sites in glass), see Fig. 5.4, and also for step-wise EMF—pH curves in the case of two sorts of anionic sites, see Fig. 5.5 [18]:

5.2.4 The Baucke Theory, Comparison with the Nikolsky Theory

A different theory has been developed by Baucke [19–24]. Brief description of this theory is presented below, on the basis of [24]. According to the Baucke theory, glass electrodes work primarily due to a dissociation mechanism, that is, due to the hydrolysis process shown in Fig. 5.2, bottom. Baucke considers the following ionogenic groups in glass: $\equiv Si-O-H$, $\equiv Si-O-Na$, and $\equiv Si-O^-$. Furthermore, the groups located at the glass surface are not the same as those in the glass bulk. At the surface, the $\equiv Si-O-H$ groups are hydrolyzed by water molecules producing hydrogen ions into the aqueous phase:



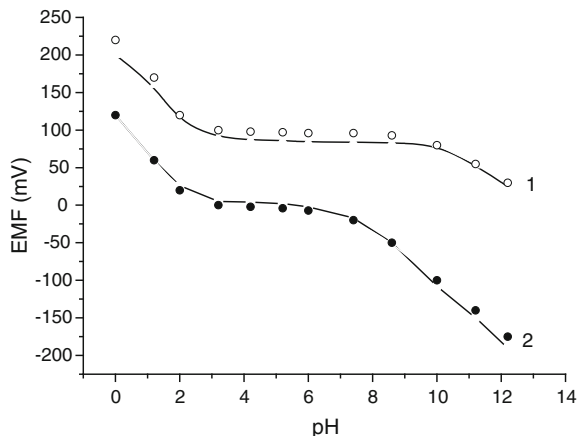


Fig. 5.5 Experimental (circles) and calculated using Eq. (5.15) (solid lines) step-wise E–pH curves for the electrodes with membranes containing 22 % Na₂O, 2 % Al₂O₃, and 76 % SiO₂ [18]. Curve 1: 21 % Na₂O, 2.4 % Al₂O₃; curve 2: 76.6 % SiO₂ (2). Sodium activity is $a_{\text{Na}} = 0.08$. Parameter values: $K_{\text{H}/\text{Na}}^{\text{exch}} = 1.4 \cdot 10^{-11}$, $\alpha_{\text{H},1} = 1$, $\alpha_{\text{H},2} = 10^{-10}$

The equilibrium constant of the reaction (5.16) is expressed as below:

$$K_{D,H} = \frac{a_{\text{R}}^{\text{surf}} a_{\text{H}_2\text{O}}^{\text{aq}}}{a_{\text{RH}}^{\text{surf}} a_{\text{H}_2\text{O}}^{\text{aq}}}. \quad (5.17)$$

Here, as before, R^- stands for $\equiv\text{Si}-\text{O}^-$ groups, however, located at the surface rather than in the glass bulk. The value of $K_{D,H}$ is smaller than that of the analogous homogeneous reaction in the bulk of the glass phase because the negative charge of the glass surface hinders the hydrogen ion coming out the glass phase.

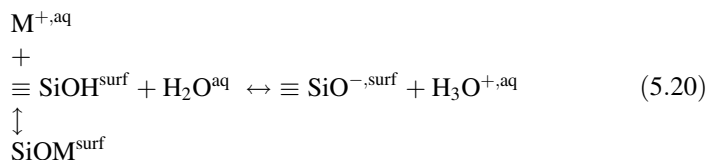
The other process which is taken into account by Baucke is the formation of associates of metal cations from aqueous solution and $\equiv\text{Si}-\text{O}^-$ anions at the glass surface:



The respective association constant is

$$K_{A,M} = \frac{a_{\text{RM}}^{\text{surf}}}{a_{\text{R}}^{\text{surf}} a_{\text{M}}^{\text{aq}}}. \quad (5.19)$$

The equilibria (5.16) and (5.18) can be combined into a crossed equilibrium below:



Thus, the anionic form of the surface groups $\equiv\text{Si-O}^-$ binds the partial equilibria (5.16) and (5.18) together. Baucke therefore characterizes the selectivity by selectivity product: $K_{D,H}K_{A,M}$. Unfortunately, the two components of the selectivity product: $K_{D,H}$ and $K_{A,M}$ cannot be measured independently. However, the value of the selectivity product has been measured by ion bombardment for spectrochemical analysis (IBSCA) technique and proved to be very close to the respective value obtained from the potentiometric measurements. The interpretation of the latter, obviously, suggests an equation which describes the electrode response in mixed solutions. The respective equation for the membrane potential [20] is, formally, equivalent to the Nikolsky equation:

$$\varphi = \varphi^0 + \frac{RT}{F} \ln(a_{\text{H}_3\text{O}^{\text{aq}}} + K_{D,H}K_{A,M}a_{\text{M}^{\text{aq}}}). \quad (5.21)$$

It may appear that the physical meaning of the Baucke's selectivity product is critically different from that of the Nikolsky's selectivity coefficient (or ion-exchange constant in the Nikolsky "simple" theory). In fact, the key factor of the Baucke theory is $a_{\text{R}}^{\text{surf}}$ —the activity of the surface anionic groups eliminates from the selectivity product value:

$$K_{D,H}K_{A,M} = \frac{a_{\text{R}}^{\text{surf}} a_{\text{H}_3\text{O}^{\text{aq}}} a_{\text{RM}}^{\text{surf}}}{a_{\text{RH}}^{\text{surf}} a_{\text{H}_2\text{O}^{\text{aq}}} a_{\text{R}}^{\text{surf}} a_{\text{M}^{\text{aq}}}^{\text{aq}}} = \frac{a_{\text{H}_3\text{O}^{\text{aq}}} a_{\text{RM}}^{\text{surf}}}{a_{\text{RH}}^{\text{surf}} a_{\text{H}_2\text{O}^{\text{aq}}} a_{\text{M}^{\text{aq}}}^{\text{aq}}}. \quad (5.22)$$

This equilibrium constant refers to the reaction below:



One can see that the reaction (5.23) considered in the Baucke theory is, effectively, an ion-exchange reaction. However, it is different from that considered by Nikolsky [3]. One source of difference comes from the consideration of associated rather than dissociated forms of hydrogen and metal cations on the glass surface. When it comes to the generalized Nikolsky–Shultz theory, this difference disappears (see Sect. 5.2.3). Another source of difference between the Nikolsky theory and the Baucke theory is that the reaction (5.23) directly accounts for the hydrolysis process at the glass surface, which is somewhat hidden in the Nikolsky's approach.

The direct consideration of the hydrolysis process at the glass/solution interface appears important novelty of the Baucke theory. Indeed, consideration of the hydrolysis as a process located at the surface allows obtaining the following expression for the electrode potential within the range of the pH response:

$$\varphi = \varphi^0 + \frac{RT}{F} \ln \frac{a_{\text{R}}^{\text{surf}}}{a_{\text{RH}}^{\text{surf}} a_{\text{H}_2\text{O}^{\text{aq}}}} + \frac{RT}{F} \ln a_{\text{H}_3\text{O}^{\text{aq}}}. \quad (5.24)$$

Activities of water in the solution and that of $\equiv\text{Si-OH}$ groups at the glass surface are virtually constant [19–24] but $a_{\text{R}}^{\text{surf}}$ —the surface activity of $\equiv\text{Si-O}^-$ —varies with the variation in the solution composition. From the practical point

of view, the respective contribution to the electrode slope is relatively small: of about -0.1 to -1 mV. However, from the academic viewpoint, the explanation of slightly sub-Nernstian slope of glass pH electrodes (which is a well-known experimental fact) is very significant and must be considered an important achievement.

Let us discuss why the Nikolsky's approach, whatever for full dissociation or for partial association, predicts full Nernstian slope within the pH or a metal ion response range. The concept of ion exchange suggests macroscopic equality of the quantities of ions exchanging between the contacting phases.² Therefore, a pure ion-exchange process like $H^{+,glass} \leftrightarrow H^{+,aq}$ or $Na^{+,glass} \leftrightarrow Na^{+,aq}$ can change neither the exchanging ion activity, nor the dissociation degree of the ionogenic groups in glass. The point is that consideration of processes *within phases*, not *at the surface*, inevitably results in the mass balance and in the macroscopic electroneutrality condition, presented below for H^+ —response range in terms of the species concentrations (for better clarity):

$$C_R^{tot,glass} = C_R^{glass} + C_{RH}^{glass} C_R^{glass} = C_H^{glass} \quad (5.25)$$

The concentration of the associated form is proportional to the respective species concentrations and the association constant: $C_{RH}^{glass} = C_R^{glass} C_H^{glass} K_{RH}$. One can easily obtain for hydrogen ion concentration in the glass phase:

$$C_H^{glass} = \left(-1 + \sqrt{1 + 4C_R^{tot,glass}} \right) 2K_{RH}. \quad (5.26)$$

According to Eq. (5.26), the concentration of hydrogen ions in the glass phase equilibrated with an aqueous solution is constant whatever is the composition of the solution (within the pH response range), predicting the full Nernstian slope.

The same result can be obtained for the metal ion response range. As to the transient response range, within the Nikolsky approach, the variable slope originates from variable ratio of the hydrogen and the metal ion concentrations in the membrane phase. The response is therefore described by Eqs. (5.10) or (5.15)—dependent on whether the model assumes complete or incomplete dissociation.

Apparently, the Nikolsky approach although originally developed for glasses is more adequate for the ionophore-based membranes where the extraction and ion-exchange processes do affect the contacting phases, not only the surface of the membrane, even during the normal measurement procedures. On the other hand, the long-term kinetics of the glass electrode response reveals significant, sometimes even crucial, effects caused by processes deep in the glass phase [25–30].

² It is important to mention that microscopic non-equality of ion exchange and the respective deviation from the electroneutrality within the space-charge region at the membrane/solution interface always takes place. Furthermore, the boundary potential originates from this minute non-equality, see Sect. 2.2. However, this microscopic non-equality does not affect the macroscopic compositions of the respective phases and even those of the surface layers outside the space-charge region.

The thickness of the layers modified by the ion-exchange processes is up to 20 μm [25–30]. Also, the enormous amount of studies performed using the Nikolsky's concept revealed practically and academically important regularities of the electrode properties as a function of the glass composition [6, 17].

Therefore, considering the Nikolsky theory and the Baucke theory as antagonistic to one another appears counter-productive. Rather, these two approaches are complementary to one another and must be unified under an umbrella of a generalized theory.

5.3 Glass Electrodes for RedOx Sensing

As mentioned above (see Sect. 5.1), the electrode glasses are, normally, ionic conductors. However, Pisarevskii showed that glasses doped with transient metal oxides ($\text{Fe}^{\text{II}}/\text{Fe}^{\text{III}}$, $\text{Ti}^{\text{III}}/\text{Ti}^{\text{IV}}$) are semiconductors of p-type or n-type dependent on the nature of the transient metal (Fe or Ti) and also on their concentrations [31–36]. These glasses possess significant electronic conductivity, and the electrodes with membranes made of these glasses can be used for RedOx sensing.

The concentrations of the respective transient metal oxides must be tuned to ensure the electronic conductivity and, at the same time, the glass-like state of the membrane (to suppress crystallinity), while the ionic conductivity is suppressed by the so-called mixed-alkali effect. The intrinsic electronic conductivity of these glasses allows for solid-contact construct of the electrode, with vacuum-sputtered silver on the internal side of the glass membrane. The electrode is stuffed with graphite to ensure contact between the sputtered silver layer and wire.

In a number of reversible RedOx systems like $\text{Fe}^{2+}/\text{Fe}^{3+}$, $\text{Fe}(\text{CN})_6^{4-}/\text{Fe}(\text{CN})_6^{3-}$, and quinone/hydroquinone glass, RedOx electrodes behave in the same way as platinum or other noble metals. These electrodes also work in systems like $\text{Eu}^{2+}/\text{Eu}^{3+}$ and $\text{Ce}^{3+}/\text{Ce}^{4+}$ —“difficult” for measurements with noble metal electrodes. On the other hand, glass RedOx electrodes are insensitive to oxygen and some other gases.

To describe the RedOx glass electrode behavior, Pisarevskii invented the concept of the RedOx selectivity, that is, the selectivity toward one RedOx system in the presence of other ones [32–35]. Obviously, under total equilibrium, no RedOx selectivity exists: The electrode potential is governed by the formal activity of electron in the sample, which, in turn, is a net effect of the interactions between all the RedOx systems involved. Therefore, the Pisarevskii's concept is intrinsically irreversible: The electrode is selective to the system which is faster than the others, and this is due to the catalytic properties of the electrode surface toward this particular system. The respective formalism is Nikolsky-like with the selectivity coefficient determined by equilibrium parameters: $E^{0,1}$, $E^{0,2}$ —the standard potentials of the two “competing” RedOx systems and also by kinetic parameters: α —the transfer coefficient and $j^{0,1}$, $j^{0,2}$ —the respective standard exchange current

densities. The deviation of the potential caused by the presence of RedOx system 2 (mixed potential) from the equilibrium value obtained for pure system 1 obeys the equation below:

$$\Delta E = E^{1,2}_{\text{mixed}} - E^1 = \frac{RT}{F} \frac{j^{0,2}}{j^{0,1}} \exp \frac{\alpha_2 F (E^{0,1} - E^{0,2})}{RT} \left(\frac{a_{\text{Ox},1} a_{\text{Red},2}}{a_{\text{Red},1} a_{\text{Ox},2}} \right)^{\alpha_2}. \quad (5.27)$$

Equation (5.27) holds for the situations when $E^{0,1} - E^{0,2} > 4RT/F$, $\Delta E < RT/F$. One can see that if $j^{0,2} \ll j^{0,1}$ the presence of RedOx system 2 does not influence the electrode potential.

Glass RedOx electrodes show a pronounced selectivity to systems with low oxidation potential. This selectivity allows for measurements under ambient conditions because the atmospheric oxygen does not interfere with the electrode potential. The glass RedOx electrodes proved to be critically useful for a number of applications, like the measurements of the chemical or the biologic oxygen demand [32, 33, 35, 36].

References

1. M. Cremer, Z. Biol., 1906, 47, 562.
2. F. Haber, Z. Klemensiewicz, Z. Phys. Chem., 1909, 67, 385.
3. B.P. Nicol'sky, Acta Physicochim. URSS, 1937, 7, 597.
4. M. Dole, The glass electrode. Methods, applications, and theory. Wiley, N.Y., 1941.
5. G. Eisenman (ed), Glass electrodes for hydrogen and other cations. Principles and practice. Dekker, N.Y., 1967.
6. A.A. Belyustin, J. Solid State Electrochem., 2011, 15, 47.
7. A.A. Kiprianov, N.G. Karpukhina, V.A. Molodozhen, Herald St. Petersburg Univ., 1998, ser. 4, 53 (Russ).
8. N.G. Karpukhina, A.A. Kiprianov, Fiz. Khim. Stekla, 2001, 27, 101 (Russ.).
9. G. Eisenman, Biophys. J., 1962, 2, 259.
10. G. Eisenman, Adv. Anal. Chem. Instrum., 1965, 4, 213.
11. O.K. Stefanova, M.M. Shultz, E.A. Materova, B.P. Nikolsky, Herald Leningrad Univ., 1963, ser. 4, 93 (Russ).
12. M.M. Shultz, Dokl. Acad. Nauk USSR, 1970, 194, 377 (Russ.).
13. M.M. Shultz, O.K. Stefanova, Herald Leningrad Univ., 1972, ser. 4, 22 (Russ).
14. M.M. Shultz, O.K. Stefanova, Herald Leningrad Univ., 1972, ser. 4, 80 (Russ).
15. M.M. Shultz, O.K. Stefanova, Herald Leningrad Univ., 1976, ser. 4, 88 (Russ).
16. W.E. Morf, The principles of Ion-Selective Electrodes and of Membrane Transport, Akademiai Kiado, Budapest, 1981.
17. A.A. Belyustin, M.M. Shultz, in Academician B.P. Nikolsky, Life, Works, School, A.A. Belyustin, F.A. Belinskaya (Eds), St.Petersburg. Univ. Publ. House, St.Petersburg, 2000, p. 196 (Russ.).
18. B.P. Nikolsky, M.M. Shultz, A.A. Belyustin, Herald Leningrad Univ., 1963, Ser. 4, 86 (Russ.).
19. F.G.K. Baucke, Anal. Chem., 1994, 66, 4519.
20. F.G.K. Baucke, Fres. J. Anal. Chem., 1994, 349, 582.
21. F.G.K. Baucke, J. Electroanal. Chem., 1994, 367, 131.
22. F.G.K. Baucke, Ber. Bunsenges. Phys. Chem., 1996, 100, 1466.

23. F.G.K. Baucke, *J. Phys. Chem. B*, 1998, 102, 4835.
24. F.G.K. Baucke, *J. Solid State Electrochem.* 2011, 15, 23.
25. A.A. Belyustin, *Russ. Chem. Rev.*, 1980, 49, 920.
26. A.A. Belyustin, I.V. Valova, *Fiz. Khim. Stekla*, 1980, 6, 449 (Russ.).
27. A.A. Belyustin, I.V. Valova, *Fiz. Khim. Stekla*, 1980, 6, 456 (Russ.).
28. I.S. Ivanovskaya, A.A. Belyustin, I.D. Pozdnyakova, *Sens. Actuators B*, 1995, 24–25, 304.
29. A.A. Belyustin, I.S. Ivanovskaya, Kh.L. Bichiya, *Sens. Actuators B*, 1998, 48, 485.
30. A.A. Belyustin, *Electroanalysis*, 1999, 11, 799.
31. B.P. Nikolsky, M.M. Shultz, A.M. Pisarevskii, US Patent 3773642, 1973.
32. B.P. Nikolsky, M.M. Shultz, A.M. Pisarevskii, FRG Patent 2134101, 1973.
33. M.M. Shultz, A.M. Pisarevskii, I.P. Polozova, *Oxidation Potential. Theory and Practice*, Khimia Publ. House, Leningrad, 1984 (Russ.).
34. A.A. Belyustin, A.M. Pisarevskii, G.P. Lepnev, A.S. Sergeev, M.M. Schultz, *Sens. Actuators B*, 1992, 10, 61.
35. A.M. Pisarevskii, I.P. Polozova, O.I. Starushko, L.A. Khorseeva, *Ion-exchange Ionometry*, 1982, 3, 184 (Russ.).
36. A.M. Pisarevskii, I.P. Polozova, F. Hockridge, *Russ. J. Appl. Chem.*, 2005, 78, 102.
37. W.S. Hughes, *J. Chem. Soc., London*, 1928, 491.
38. D.A. McInnes, M. Dole, *Ind Eng Chem Anal*, 1929, Ed 1, 57.
39. D.A. McInnes, M. Dole, *J. Amer. Chem. Soc.*, 1930, 52, 29.
40. S.I. Sokolov, A.G. Passinskii, *Z. Phys. Chem. A*, 1932, 160, 366.
41. G.P. Avseevich, *Ucheniye Zapiski Leningr. Univ.*, 1949, 108, 3 (Russ.).
42. G.P. Avseevich, *Ucheniye Zapiski Leningr. Univ.*, 1951, 150, 50 (Russ.).
43. H.H. Cary, W.P. Baxter, US Patent No 2462843 (1949).
44. G.A. Perley, US Patent No 2444845, (1948).
45. G.A. Perley, *Anal. Chem.*, 1949, 21, 395.
46. K. Horovitz, *Z. Physik.*, 1923, 15, 369.
47. H. Schiller, *Ann. Phys.*, 1924, 74, 105.
48. M.M. Schultz, T.M. Ovchinnikova, *Vestnik Leningr. Univ.*, 1954, Ser. Math. Fiz. Khim., 2, 129 (Russ.).
49. M.M. Schultz, L.G. Aio, *Vestnik Leningr. Univ.*, 1955, Ser. Math. Fiz. Khim., 8, 153 (Russ.).
50. B.P. Nikolskii, M.M. Schultz, N.V. Peshkxonova, *Zh. Fiz. Khim.*, 1958, 32, 19 (Russ.).
51. B.P. Nikolskii, M.M. Schultz, N.V. Peshkxonova, *Zh. Fiz. Khim.*, 1958, 32, 262 (Russ.).
52. G. Eisenman, D.O. Rudin, J.U. Casby, *Science*, 1957, 126, 831.
53. G. Eisenman, Particular properties of cation-selective glass electrodes containing Al₂O₃, Ref. 5, pp 268–283.
54. M.M. Schultz, V.A. Dolidze, E.P. Sarukhanova, V.A. Bagaturova, USSR Patent No 206023, 1967.
55. J.E. Leonard, Beckman reprint R-6148, 1959.
56. G. Mattock, *Analyst*, 1962, 87, 930.
57. A.A. Belyustin, I.V. Valova, V.A. Dolidze, G.I. Orlova, E.P. Sarukhanova, Ts.M. Siradze, M.M. Schultz, *Anal. Instrum.-making industry*, 1975, 3, 112 (Russ.).

Chapter 6

Ion-Selective Electrodes with Crystalline Membranes

6.1 Materials of Crystalline Electrode Membranes

Crystalline membranes are made of polycrystalline or monocrystalline materials. Most of the polycrystalline membranes comprise mixed crystals of low-soluble silver salts and heavy metal sulfides. Due to the similarity in the chemical compositions, also chalcogenide glasses will be briefly discussed in this chapter although these materials comprise amorphous phases.

Some activity related to potentiometric sensing using crystalline electrodes has been reported already in the 1920s and 1930s [1–4]. However, the first really working electrode with crystalline sensing element was proposed by Pungor in the early 1960s [5]. This electrode was very different from the modern crystalline electrodes. The sensing material, solid silver iodide powder, was embedded in inert polyethylene matrix. Since that time, a large number of ISEs based on low-soluble salt precipitates embedded in polyethylene or polypropylene matrixes were invented.

The next and very important step was proposed by Frant and Ross in 1966 [6]. These authors invented a fluoride-selective electrode with a homogeneous solid membrane made of a monocrystalline LaF_3 . The selectivity of this ISE to its target analyte— F^- anion is extremely high, so that only the pH glass electrodes are more selective to their target ion. Among possible interferences, only hydroxyl anion interferes significantly with the fluoride electrode response.

Although the fluoride electrode with a monocrystalline membrane shows such impressive properties, this ISE comprises rather exception than a rule. Crystalline membranes of electrodes for measuring other ions are made of mixed polycrystalline materials. These are mostly pressed polycrystalline pellets [7–9]. The pellets typically consist of silver sulfide and another low-soluble silver salt (a halide or a thiocyanate). Without silver sulfide, the electrodes have relatively high resistance and show significant interference from the ambient light so that stable readings require maintaining constant illumination. Silver sulfide is not purely ionic conductor, having also some electronic conductivity. This is why the presence of Ag_2S allows for decrease in the membrane resistance. Otherwise, silver

sulfide is often considered as inert matrix since it is much less soluble than other silver salts used in membranes [7].

Electrodes with such membranes show anionic response and are suitable for measuring the activities of S^{2-} , Cl^- , Br^- , I^- , SCN^- . Another combination of low-soluble salts—silver sulfide mixed with a low-soluble metal sulfide—allows for sensing of a number of heavy metals like Hg^{2+} , Ag^+ , Cu^{2+} , Pb^{2+} , Cd^{2+} , and some others. Thus, crystalline membranes provide a basis for potentiometric measurements of a number of analytes, including anions and also cations. The systems consisted of various crystalline membranes, and aqueous solutions are schematically presented in Fig. 6.1.

Materials of crystalline membranes, whatever poly- or monocrystalline, possess a number of advantages. These membranes show significantly lower resistance than those made of glass or of plasticized polymers. The conductivity of the membranes is mostly ionic in nature and is due to the Frenkel-type defects. The number of the defects and therefore also the conductivity can be further increased by doping the membranes with suitable dopants. This approach is especially characteristic to the fluoride-selective electrode: The LaF_3 monocrystal is normally doped with EuF_2 , sometimes with another difluoride salt, for example, CaF_2 [10]. Silver sulfide crystals are present in two modifications: β -form with monoclinic lattice having ionic conductivity due to Ag^+ ion migration along Frenkel-type defects in the structure and α -form with cubic lattice having electronic conductivity. Therefore, crystalline membranes typically containing some α - Ag_2S also possess some electronic conductivity. This feature can be either advantageous or disadvantageous. On the one hand, some impact from the electronic conductivity

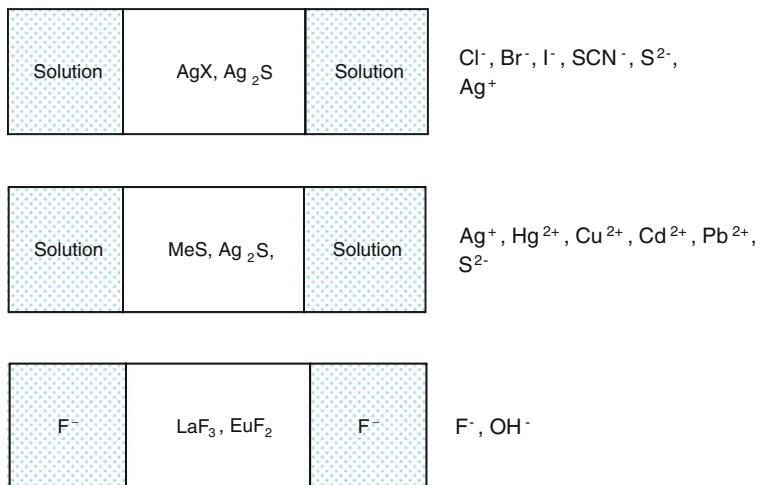


Fig. 6.1 Schematic representation of crystalline membranes in contact with aqueous solutions and ions measurable with the respective electrodes. From *top* to *bottom*: polycrystalline membrane for anion sensing, polycrystalline membrane for heavy metal cation sensing, F^- ion-selective monocrystalline membrane

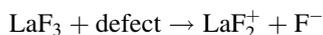
allows for making stable and reproducible solid-contact electrodes. These are produced by vacuum sputtering of metal silver on the inner side of the pellet, and the wire is soldered to this thin silver layer. Since pellets always contain a silver salt, these solid-contact electrodes' functioning principle is similar to the classical second-kind electrodes. On the other hand, when the electronic component's conductivity is too high, the electrode shows a mixed response to ions and to RedOx-active species. Therefore, although the very idea of the crystalline membranes appears quite simple, the compositions of the pellets are thoroughly optimized in order of getting electrodes responding only to ions.

Crystalline membranes are chemically inert, and therefore, in principle, the respective ISEs can be used for measurements in non-aqueous media. In fact, however, these electrodes are only seldom used for this kind of analysis. In view of the measurements in the non-aqueous solutions, the "weak spot" of crystalline electrodes is the body and, even worse, the glue used to fix the membrane pellet in the body. Both the plastic body and the epoxy glue are damaged by organic solvents or organic components in mixed aqueous-organic solutions, so the ISEs either do not work at all or show significantly shortened lifetime. Another problem of the measurements in mixed aqueous-organic solutions, and especially in organic solutions, arises from the uncertainties about the ionic activity coefficients in these media.

The raw materials for crystalline membranes are significantly more expensive than those for silicate glass membranes, but much cheaper than those for membranes based on neutral and charged ionophores.

6.2 Fluoride Electrode Based on Lanthanum Fluoride Monocrystal

The LaF_3 crystals form a hexagonal lattice, and each La^{3+} cation in the lattice is surrounded with five F^- anions. Next six closest neighbors to the lanthanum cation are also F^- anions. Thus, the lattice consists of alternating layers of LaF_2^+ and F^- anions [11, 12]. Fluoride anions can relatively move easily across the crystal phase jumping from one Frenkel defect to another one, like schematically shown below:



The specific conductivity of the undoped LaF_3 lies within the range from 2.9×10^{-7} to 3.6×10^{-7} S/cm. A crystal doped with 0.5 % w/w of EuF_2 shows a much higher specific conductivity of 1.9×10^{-6} to 2.4×10^{-6} S/cm, and further doping up to 1 % w/w of EuF_2 allows for further increase in the conductivity of 4.3×10^{-6} S/cm [11].

In pure fluoride solutions, F-ISE shows response with a slope close to the Nernstian value within a concentration range from 1 to 10^{-6} M [7, 13]. However, in fluoride buffer solutions, the lower detection limit is shifted to 10^{-10} M of the free F^- anion concentration [14]. The selectivity coefficient to fluoride anion

against hydroxyl is about 0.1 [6], so the interference from hydroxyl ion is very strong. On the other hand, hydroxyl anion is virtually the only one directly influencing the response of the LaF_3 F-ISE. However, many ions, for example, Al^{3+} , Fe^{3+} , Be^{2+} , may cause some errors in an indirect way: by forming complexes with F^- anions in solutions. Therefore, in spite of the excellent selectivity of the electrode, one has to be careful when interpreting the emf readings in terms of the fluoride concentration. To avoid errors, the use of BRUIS buffer is recommended [15]. The buffer contains acetic acid, sodium chloride, 1,2-cyclohexanediaminetetraacetic acid, and water, with the pH adjusted at 5–5.5 with NaOH. The buffer allows maintaining constant ionic strength, while Al^{3+} and Fe^{3+} ions are strongly complexed by the 1,2-cyclohexanediaminetetraacetate anions so that the free F^- anion concentration approaches the respective total value. According to further studies performed in [16], a modification of the standard BRUIS with ammonium citrate can be advised.

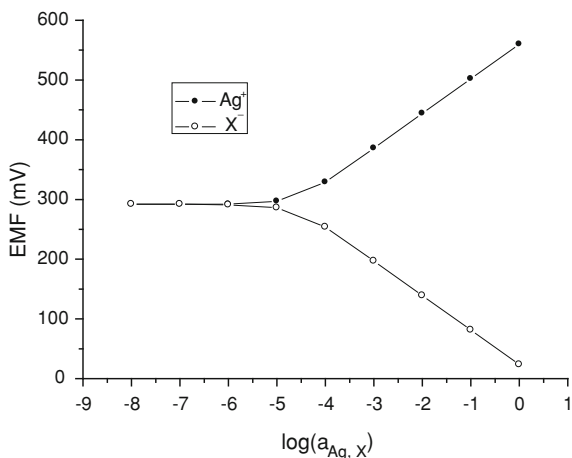
Unfortunately, the attempts to make a solid-contact ISE with LaF_3 monocrystalline membrane having a stable potential over long time periods and with good piece-to-piece reproducibility so far are unsuccessful. The fundamental reason for this is the total lack of electronic conductivity in LaF_3 crystal.

6.3 Analytical Characteristics of ISEs with Polycrystalline Membranes

6.3.1 *Electrode Response and Detection Limit*

The analytical performance of ISEs with polycrystalline membranes in some respects is very different from that of ionophore-based and silicate glass membranes. In the first place, similar to the silver chloride and other second-kind electrodes, even the anionic crystalline electrodes show response to silver ions. When thinking about the response of crystalline electrodes based on low-soluble silver salts, it is always advantageous to consider Ag^+ as potential-determining species. The cationic (i.e., heavy metal sensing electrodes) are analogs of the classical third-kind electrodes and respond to the respective cations and also to sulfide anions. Basically, this is because the crystalline electrodes are capable of responding to all those kinds of ions that are the components of the membrane [17]. This ability is schematically illustrated in Fig. 6.2. Unlike the classical second- and third-kind electrodes, ISEs with crystalline membrane pellets are much less sensitive to RedOx components in solution and to illumination. The finite solubility of the salts determines the detection limit of the ISEs—in contrast to the ISEs with ionophore-based membranes with detection limit determined by the trans-membrane fluxes of the electrolytes. This makes another specialty of the crystalline membranes. Yet another specialty is the lack of the internal diffusion potential in crystalline membranes—because the ion locations are fixed by the

Fig. 6.2 The emf response of an ISE with crystalline membrane containing low-soluble salt AgX (the data refer to AgCl)



crystalline lattice—and there are no concentration gradients within the whole membrane [11].

As already mentioned, it is widely recognized that the detection limits of ISEs with polycrystalline membranes are determined primarily by the solubilities of the respective salts. Below, we will briefly discuss this issue following Morf's book [17]. Two processes are taken into account: (1) the dissolution of the membrane material governed by the solubility products of the respective salts and (2) leaching out of silver ions originating from co-precipitated soluble salts or reversibly adsorbed components, or produced by the oxidation of the membrane material. The leached cation activity ($a_{\text{Ag}}^{\text{leached}}$) at the membrane surface is found to be roughly constant for a given set of experimental parameters, but may be changed by a different preparation technique or conditioning of the membrane [18]. Additionally, it may depend on the stirring rate of the sample [19]. Under assumption that the $a_{\text{Ag}}^{\text{leached}}$ value is constant, the following relationship can be obtained to describe the deviations of the activities of ions in the vicinity of the membrane surface— $a_{\text{Ag}}^{\text{surf}}$, $a_{\text{X}}^{\text{surf}}$ —from their values in the bulk of a non-buffered solution— $a_{\text{Ag}}^{\text{bulk}}$, $a_{\text{X}}^{\text{bulk}}$:

$$a_{\text{Ag}}^{\text{surf}} - a_{\text{Ag}}^{\text{bulk}} = z(a_{\text{X}}^{\text{surf}} - a_{\text{X}}^{\text{bulk}}) + a_{\text{Ag}}^{\text{leached}} \quad (6.1)$$

On the other hand, the multiple of the equilibrium values of Ag^+ and X^{z-} activities gives the solubility product:

$$a_{\text{Ag}}^z a_{\text{X}} = SP_{\text{Ag}_z\text{X}} \quad (6.2)$$

Here a_{Ag} , a_{X} are the equilibrium values of Ag^+ and X^{z-} activities and $SP_{\text{Ag}_z\text{X}}$ is the solubility product of Ag_zX low-soluble salt. By combination of Eqs. (6.1) and (6.2), one can obtain the value of X^{z-} activity in the vicinity of the membrane [17]:

$$(a_X^{\text{surf}})^{\frac{z+1}{z}} - (a_X^{\text{surf}})^{\frac{1}{z}} (a_X^{\text{bulk}} - a_{\text{Ag}}^{\text{leached}}) - \frac{SP_{\text{Ag}_z\text{X}}^{1/z}}{z} = 0 \quad (6.3)$$

Two distinctly different limiting cases are as follows: leaching of silver ions from the membrane can be neglected and leaching is governing the potential deserve separate discussion.

Case 1: $z = 1$ and $SP_{\text{AgX}} \gg a_{\text{Ag}}^{\text{leached}}$

This case is true, for example, for AgCl membrane. Then, according to [17], the electrode potential is

$$\varphi = \varphi_{\text{Ag}}^0 + \frac{RT}{F} \ln \frac{a_{\text{Ag}}^{\text{bulk}} + \sqrt{(a_{\text{Ag}}^{\text{bulk}})^2 + 4SP_{\text{AgX}}}}{2} \quad (6.4)$$

Thus, Nernstian response to Ag^+ ions is expected only for samples with $a_{\text{Ag}}^{\text{bulk}} \gg 4SP_{\text{AgX}}$. The response to X^- anions is described in a symmetric way:

$$\varphi = \varphi_X^0 - \frac{RT}{F} \ln \frac{a_X^{\text{bulk}} + \sqrt{(a_X^{\text{bulk}})^2 + 4SP_{\text{AgX}}}}{2} \quad (6.5)$$

Curves shown in Fig. 6.2 illustrate the regularities given by Eqs. (6.4) and (6.5). The potentials are calculated by Eqs. (6.4) and (6.5), and the emf assumes saturated Ag/AgCl reference electrode. The parameters used for the calculations are close to those characteristic for the AgCl membranes: $\varphi_{\text{Ag}}^0 = 560$ mV versus Ag/AgCl in saturated KCl, $\log SP_{\text{AgX}} = -9.25$.

Case 2: $(a_{\text{Ag}}^{\text{leached}})^{z+1} \gg SP_{\text{Ag}_z\text{X}}$

This situation must be true for Ag_2S and may be also true for AgI membranes [17]. The electrode potential is

$$\varphi = \varphi_{\text{Ag}}^0 + \frac{RT}{F} \ln (a_{\text{Ag}}^{\text{bulk}} + a_{\text{Ag}}^{\text{leached}}) \quad (6.6)$$

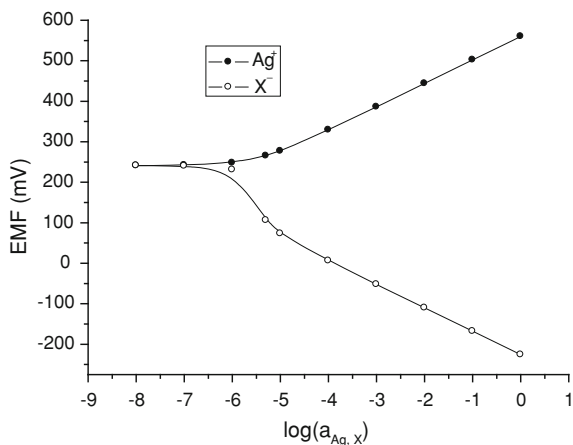
The response to anions depends on the relationship between the anion activity and that of the leached silver cations:

$$\text{for } a_X^{\text{bulk}} < a_{\text{Ag}}^{\text{leached}}/z : \varphi = \varphi_{\text{Ag}}^0 + \frac{RT}{F} \ln (a_{\text{Ag}}^{\text{leached}} - za_X^{\text{bulk}}) \quad (6.7)$$

$$\text{for } a_X^{\text{bulk}} > a_{\text{Ag}}^{\text{leached}}/z : \varphi = \varphi_X^0 - \frac{RT}{zF} \ln (a_X^{\text{bulk}} - a_{\text{Ag}}^{\text{leached}}/z) \quad (6.8)$$

The response curves calculated using Eqs. (6.7) and (6.8) are presented in Fig. 6.3. The calculations assume $z = 1$, $a_{\text{Ag}}^{\text{leached}} = 10^{-5.5}$. The response to Ag^+ ions looks similar to that shown in Fig. 6.2. However, the anionic response curve is more complicated: Sharp change in the potential can be seen at $a_X^{\text{bulk}} \approx a_{\text{Ag}}^{\text{leached}}/z$. Morf interpreted this effect as titration of the leached Ag^+ ions with the X^{z-} anions [17].

Fig. 6.3 The emf response of an ISE with crystalline membrane containing extremely low-soluble salt AgX, with the effect of leaching of silver ions



6.3.2 Crystalline Electrodes Responding to Heavy Metal Cations

The response of electrodes with crystalline membranes containing Ag₂S and a heavy metal sulfide, for example, CdS, can be treated as follows [7]. The silver ion activity in aqueous solution without a soluble silver salt is determined by the solubility of Ag₂S:

$$a_{\text{Ag}}^{\text{aq}} = \sqrt{SP_{\text{Ag}_2\text{S}}/a_{\text{S}}^{\text{aq}}} \quad (6.9)$$

The sulfide ion activity, in turn, is determined by the activity of MeX—the soluble heavy metal salt, for example, Cd(NO₃)₂:

$$a_{\text{S}}^{\text{aq}} = SP_{\text{CdS}}/a_{\text{Me}}^{\text{aq}} \quad (6.10)$$

Combination of the Eqs. (6.9) and (6.10) yields

$$a_{\text{Ag}} = \left(a_{\text{Cd}} \frac{SP_{\text{Ag}_2\text{S}}}{SP_{\text{MeS}}} \right)^{1/2} \quad (6.11)$$

and the electrode potential obeys the equation below:

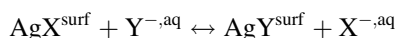
$$\varphi = \frac{\mu_{\text{Ag}}^{0,\text{aq}} - \mu_{\text{Ag}}^{0,\text{surf}}}{F} + \frac{RT}{2F} \ln \frac{SP_{\text{Ag}_2\text{S}}}{SP_{\text{MeS}}} + \frac{RT}{2F} \ln a_{\text{Me}}^{\text{aq}} \quad (6.12)$$

In this way, one can measure a number of heavy metal cations using ISEs with crystalline membranes. There are, however, some limitations. The solubility product of the MeX salt must be much higher than that of Ag₂S: $SP_{\text{MeX}} \gg SP_{\text{Ag}_2\text{S}}$. Otherwise, the membrane surface is completely covered with MeS due to the excess of Me²⁺ in solution. On the other hand, SP_{MeX} must be low enough to

prevent significant contamination of the sample with Me^{2+} cations originating from MeS dissolution.

6.3.3 Selectivity of ISEs with Crystalline Membranes

Let us discuss the selectivity issue using, as an example, a crystalline membrane containing low-soluble salt AgX and responding to X^- primary (target analyte) ions, in contact with a mixed electrolyte solution containing salts MX and MY . The latter salts are soluble; however, AgY salt is low-soluble. The X^- and Y^- anions can replace one another in the membrane via dissolution–precipitation processes so that a mixed phase is formed containing both AgX and AgY . The equilibrium between the mixed phase and solution can be written in the form of ion-exchange reaction [20]:



The equilibrium constant of this reaction is

$$K_{\text{XY}} = \frac{N_{\text{AgY}}^{\text{surf}} a_{\text{X}^{-,\text{aq}}}}{N_{\text{AgX}}^{\text{surf}} a_{\text{Y}^{-,\text{aq}}}} \quad (6.13)$$

Here, $N_{\text{AgX}}^{\text{surf}}$, $N_{\text{AgY}}^{\text{surf}}$ are the mole fractions of the respective salts in the surface layer. The sum of the mole fractions is constant:

$$N_{\text{AgX}}^{\text{surf}} + N_{\text{AgY}}^{\text{surf}} = 1 \quad (6.14)$$

The boundary potential can be expressed as

$$\varphi_b = -\frac{\mu_{\text{Ag}^+}^{0,\text{Ag}} - \mu_{\text{Ag}^+}^{0,\text{aq}}}{F} + \frac{\text{RT}}{F} \ln SP_{\text{AgX}} + \frac{\text{RT}}{F} \ln \frac{N_{\text{AgX}}}{a_{\text{X}^{-,\text{aq}}}} \quad (6.15)$$

Combining Eqs. (6.13–6.15), one can obtain a Nikolsky-like description of the response of a crystalline electrode in mixed solutions:

$$\varphi_b = -\frac{\mu_{\text{Ag}^+}^{0,\text{Ag}} - \mu_{\text{Ag}^+}^{0,\text{aq}}}{F} + \frac{\text{RT}}{F} \ln SP_{\text{AgX}} - \frac{\text{RT}}{F} \ln(a_{\text{X}^{-,\text{aq}}} + K_{\text{XY}}^{\text{pot}} a_{\text{Y}^{-,\text{aq}}}) \quad (6.16)$$

Here, the ISE selectivity coefficient equals the exchange constant: $K_{\text{XY}}^{\text{pot}} = K_{\text{XY}}$. This results from the assumption of the total equilibrium at the membrane/solution interface. Consideration of only the boundary potential neglecting the diffusion potential in the membrane is justified for crystalline membranes. From the thermodynamic point of view, K_{XY} exchange constant is determined by the chemical potentials of the respective species (the electric contributions referring to X^- and Y^- anions eliminate each other):

$$K_{XY} = \exp((\mu_{\text{AgY}}^{\text{surf}} + \mu_{\text{X}}^{\text{aq}} - \mu_{\text{AgY}}^{\text{surf}} - \mu_{\text{Y}}^{\text{aq}})/RT) \quad (6.17)$$

Adding and subtracting the chemical potential of silver in the aqueous phase, we rewrite Eq. (6.17) as follows:

$$K_{XY} = \exp((\mu_{\text{AgY}}^{\text{surf}} + \mu_{\text{X}}^{\text{aq}} + \mu_{\text{Ag}}^{\text{aq}} - \mu_{\text{AgX}}^{\text{surf}} - \mu_{\text{Y}}^{\text{aq}} - \mu_{\text{Ag}}^{\text{aq}})/RT) \quad (6.18)$$

Now, assuming the AgX and AgY sub-phases in the mixed AgX + AgY phase are at equilibrium, we finally obtain

$$K_{XY} = \exp((\mu_{\text{X}}^{\text{aq}} + \mu_{\text{Ag}}^{\text{aq}} - \mu_{\text{Y}}^{\text{aq}} - \mu_{\text{Ag}}^{\text{aq}})/RT) = SP_{\text{AgX}}/SP_{\text{AgY}} \quad (6.19)$$

Thus, under the assumption of the total interfacial equilibrium, the selectivity coefficient of a crystalline ISE to X^- anions in the presence of Y^- anions equals the ratio of the target ion salt solubility product to that of the interfering ion salt. In the case of more complex salts, like Ag_2S , the solubility products appear in the respective powers: $K_{XY} = SP_{\text{AgX}}/SP_{\text{Ag}_2\text{X}}^{1/z}$.

In the case of a cation-responding crystalline membrane ISEs, the selectivity can be treated in the same way, and the selectivity coefficient under the total equilibrium assumption is also determined by the ratio of the respective solubility products.

6.3.4 Diffusion Layer Model by Lewenstam and Hulanicki

The equilibrium approaches like the one discussed above neglect the effects of non-equilibrium processes which sometimes govern the ISE response, especially at short times after the sample solution is changed. The equilibrium between the AgX and AgY sub-phases within the mixed phase is under question. The dissolution-precipitation processes may lead to complete covering of one low-soluble salt with another one so that the surface comprises pure AgX or pure AgY, instead of the formation of the mixed phase. Interestingly, these processes are often governed by diffusion in the aqueous phase rather than by the reaction rates in the solid phases. Therefore, a detailed elaboration, an “improvement” in the equilibrium approach, is hardly useful. Instead, a totally different model has been invented by Lewenstam and Hulanicki [20, 21]. This model covers situations when the equilibrium is established, and also situations determined by diffusion. In the latter case, the model predicts several distinctively different types of the ISE behavior dependent on whether (1) $K_{XY} \gg 1$, or (2) $K_{XY} \approx 1$, or (3) $K_{XY} \ll 1$. In the most typical cases, when $K_{XY} \gg 1$, the ISE obeys a Nikolsky-like equation with the selectivity coefficient determined by the ratio of the ion diffusion coefficients in the aqueous phase: $K_{XY}^{\text{pot}} = D_{\text{Y}}^{\text{aq}}/D_{\text{X}}^{\text{aq}}$. The diffusion layer model explained a number of effects known from experiments and allowed developing procedures of fast measurements when, for example, chlorides were successfully measured in the

presence of bromides [21, 22]. Furthermore, the Meyerhoff's idea of ISEs for polyions assay is largely based on the diffusion layer model by Lewenstam and Hulanicki, although realized for ISEs with ion-exchanger solvent polymeric membranes [23–25]. Critical comparison of the total equilibrium models, diffusion layer models, and advanced non-equilibrium models is presented in [26].

6.4 Chalcogenide Glass ISEs

This section could be placed either in Chap. 5 together with other glass electrodes or here—under crystalline ISEs. I decided to have this section here because the chemical composition of chalcogenide glass membranes is closer to those of crystalline membranes containing low-soluble heavy metal salts, and also, the analytes measured by chalcogenide glass ISEs are primarily the heavy metal cations.

Chalcogenide membranes often contain sulfur as a metal sulfide, but other elements of the VI group of the periodic table, Se and Te, are also often in use. Another difference when compared with crystalline membranes comes from the presence of the III–V group elements: B, Al, Ga, Ge, Sn, As, Sb, Bi in chalcogenide glasses. Alloys containing these elements show large glass domains, combine ionic and electronic conductivity, and can be doped with metals: Tl, Ag, Cu, Hg, Fe, and others. The dopant cations turned out being the potential-determining species at the membrane/solution interface of the chalcogenide glass electrodes.

Chalcogenide glass membranes are superior to polycrystalline membranes in regard to the detection limits and to some other characteristics. The presence of some electronic component's conductivity also facilitates making solid-contact ISEs with chalcogenide glass membranes.

ISEs with chalcogenide glass membranes were invented in early 1970s [27]. Much of the research in this field was performed by Vlasov's group [28–30]. ISEs for measuring the concentrations of Ag^+ [31], Pb^{2+} [29, 32–34], Sn^{2+} [35], Cu^{2+} [29, 36], Cd^{2+} [29, 37], Fe^{3+} [10, 38], Zn^{2+} , Mn^{2+} [39], and other ions [40] have been invented. Of special interest is the possibility to measure Na^+ ions with a chalcogenide glass electrode [41]. The relationship between the ionic response, surface ion exchange, and bulk membrane transport in chalcogenide membranes was studied in [42].

Besides sensors with traditional thick membranes, thin-film microsensors are known for measuring Pb^{2+} [43] and also Cu^{2+} , Cd^{2+} , Tl^+ [44].

More recently, chemical sensors selective to various heavy metal ions with membranes based on chalcogenide glasses containing GeSe_2 as glass former, Sb_2Se and Sb_2Te_3 as network modifier, and heavy metal chalcogenides MeCh ($\text{Me} = \text{Zn}, \text{Cd}, \text{Sn}, \text{Pb}$; $\text{Ch} = \text{Se}, \text{Te}$) were described in [45].

Due to RedOx processes changing the ratio of Fe^{3+} to Fe^{2+} ions in samples, measurements of Fe^{3+} and the interpretation of the results turned to be difficult.

This complication was one of the motivations for the development of the so-called *electronic tongue*, see Sect. 7.4. ISEs with chalcogenide glass membranes constitute the base of these promising analytical devices.

References

1. G. Trümpfer, Z. Phys. Chem. 1921, 99, 9.
2. H.J.C. Tendeloo, J. Biol. Chem., 1936, 113, 333.
3. I.M. Kolthoff, H.L. Sanders, J. Am. Chem. Soc., 1937, 59, 416.
4. B.P. Nikolsky, V.M. Vdovenko, Doklady Akademii Nauk USSR, 1937, 16, 101 (*Russ.*).
5. E. Pungor, E. Hollos-Rokosinyi, Acta Chem. Hung., 1961, 27, 63.
6. M.S. Frant, J.W. Ross, Science, 1066, 154, 1553.
7. R.A. Durst, ed., Ion-selective Electrodes, NBS spec. publ. 314, 1969, Washington, DC.
8. E.H. Hansen, C.G. Lamm, J. Ruzicka, Anal. Chim. Acta, 1972, 59, 403.
9. J. Vesely, Coll. Czech. Chem. Comm., 1974, 39, 710.
10. Yu.G. Vlasov, Yu.E. Ermolenko, V.V. Kolodnikov, M.S. Miloshova, Russ. J. Anal. Chem., 1980, 35, 691.
11. J. Koryta, K. Stulik, Ion-selective electrodes, Academia, Praha (1984).
12. J. Dvorak, J. Koryta, Elektrochemie, 3, Academia, Praha (1983).
13. W.E. Bazzelle, Anal. Chim. Acta, 1971, 54, 29.
14. E.W. Baumann, Anal. Chim. Acta, 1971, 54, 189.
15. M.S. Frant, J.W. Ross, Anal. Chem., 1968, 40, 1169.
16. E. Nicholson, E.J. Duff, Anal. Lett., 1981, 14, 887.
17. W.E. Morf, The principles of ion-selective electrodes and of Membrane Transport, Akademiai Kiado, Budapest (1981).
18. W.E. Morf, G. Kahr, W. Simon, Anal. Chem., 1974, 46, 1538.
19. R.P. Buck, Anal. Chem., 1976, 48, 23R.
20. A. Hulanicki, A. Lewenstam, Anal. Chem., 1981, 53, 1401.
21. A. Hulanicki, A. Lewenstam, Talanta, 1977, 24, 171.
22. A. Lewenstam, A. Hulanicki, T. Sokalski, Anal. Chem., 1987, 59, 1539.
23. S.-C. Ma, V.C. Yang, M.E. Meyerhoff, Anal. Chem., 1992, 64, 694.
24. S.-C. Ma, V.C. Yang, B. Fu, M.E. Meyerhoff, Anal. Chem., 1993, 65, 2078.
25. E. Bakker, M.E. Meyerhoff, Anal. Chim. Acta, 2000, 416, 121.
26. J. Bobacka, A. Ivaska, A. Lewenstam, Chem. Rev., 2008, 108, 329.
27. C.T. Baker, I. Trachtenberg, J. Electrochem. Soc., 1971, 118, 571.
28. Y.G. Vlasov, E.A. Bychkov, in J.R.D. Thomas (Ed.), Ion-Selective Electrode Reviews, vol. 9, Pergamon Press, Oxford, UK (1987), 5-93.
29. Yu.G. Vlasov, Fres. Z. Anal. Chem., 1989, 335, 92.
30. Yu.G. Vlasov, E.A. Bychkov, A.V. Bratov, Analyst, 1994, 119, 449.
31. Yu.G. Vlasov, E.A. Bychkov, Sens. Actuators B, 1987, 12, 275.
32. Yu.G. Vlasov, E.A. Bychkov, A.V. Legin, Talanta, 1994, 6, 1059.
33. Y.G. Vlasov, A.V. Legin, E.A. Bychkov, Sens. Actuators B, 1995, 24, 309.
34. V. Vassilev, K. Tomova, S. Boycheva, J. Non-Cryst. Solids, 2007, 353, 2779.
35. V. Vassilev, K. Tomova, S. Boycheva, V. Parvanova, J. Non-Cryst. Solids, 2009, 355, 1566.
36. A.M. Bolotov, E.A. Bychkov, Yu.G. Vlasov, S.B. Rozenkov, F. Khalifa, Sov. J. Glass Phys. Chem., 1992, 18, 382.
37. M.M. Essi, Chalcogenide Letters, 2011, 8, 341.
38. Yu.G. Vlasov, E.A. Bychkov, A.V. Legin, M.S. Miloshova, Russ. J. Anal. Chem., 1990, 45, 1381.
39. K.A. Legin, A.M. Bolotov, A.V. Legin, Yu.G. Vlasov, Russ. J. Appl. Chem., 2004, 77, 716.

40. A. Pradel, O. Valls, C. Cali, G. Taillades, A. Bratov, C. Dominguez, M. Ribes, *Journal of Optoelectronics and Advanced Materials*, 2001, 3, 641.
41. Yu.G. Vlasov, E.A. Bychkov, *Anal. Lett.*, 1989, 22, 1125.
42. Yu.G. Vlasov, E.A. Bychkov, *J. Electroanal. Chem.*, 1994, 378, 201.
43. Yu. Mourzina, M.J. Schöning, J. Schubert, W. Zander, A.V. Legin, Yu.G. Vlasov, P. Kordos, H. Lüth, *Sens. Actuators B*, 2000, 71, 13.
44. Yu. Mourzina, M.J. Schöning, J. Schubert, W. Zander, A.V. Legin, Yu.G. Vlasov, H. Lüth, *Anal. Chim. Acta*, 2001, 433, 103.
45. S. Boycheva, V. Vassilev, *NATO Science for Peace and Security Series B: Physics and Biophysics*, 2011, 175.

Chapter 7

Modern Trends in the ISEs Theory and Applications

This chapter relates to four modern but already well-developed areas in ISEs: real time and space modeling, trace analysis, ISEs under nonzero current, and electronic tongue. Novel materials used in ISEs are discussed in the respective chapters.

7.1 Real Time and Space Modeling of ISEs

The multispecies approximation described in Sect. 4.2.5 was among the first approaches to develop ISE theories using computer simulations of the membrane potential. The multispecies approach is limited to a quasi-steady state of the membrane, see Sect. 4.2.5.

More recently, a number of attempts have been made aimed at description of the membrane potential in the real time and space. Morf invented a model describing the propagation of ions within an ionophore-based membrane [1]. This description does not account for the non-compensated charges in the double layer at the interface.

More advanced theory is developed in Lewenstam' group [2–7]. This theory does not rely on equilibrium nor on steady state. The core of the Lewenstam' theory is the numerical solution of the system of the Nernst–Planck and the Poisson equations:

$$J_k(x, t) = -D_k \left[\frac{\partial C_k(x, t)}{\partial x} - z_k C_k(x, t) \frac{F}{RT} E(x, t) \right] \quad (7.1)$$

$$I(t) = F \sum_k z_k J_k(x, t) + \varepsilon \frac{\partial E(x, t)}{\partial t} \quad (7.2)$$

Equation (7.1) describes $J_k(x, t)$ the place (x) and time (t)-dependent flux of the species k as a function of D_k , $C_k(x, t)$ and $E(x, t)$,—the diffusion coefficient, the species concentration, and the electric field. In Eq. (7.2), the Poisson equation rewritten for $I(t)$ the time-dependent total current density, z_k stands for the species charge and ε for the dielectric permittivity. This allows for tracing the formation of

the boundary and the diffusion potentials in membranes over time and space. Furthermore, the theory provides with guidelines for the optimization of the membrane and of the internal solution compositions for the improvement of the ISE sensitivity. In this way, the theory is applied for the optimization of the membrane and of the internal solution compositions of ISEs for trace analysis (see Sect. 7.2) [6, 7]. The comparative review of different theoretical descriptions of the ISE membrane potential and selectivity is given in [8].

On the other hand, even this very much advanced theory describes the membrane as an ideal system: the species concentration is used instead of activity, the diffusion coefficients are assumed constant, and no local changes of the dielectric permittivity (e.g., close to the interface) are discussed. Furthermore, these advanced theories assume the electrolytes in membranes fully dissociated. Therefore, the effects of the association with membranes, so far, are treated only on the basis of the multispecies approximation described in Sect. 4.5.3.

7.2 ISEs in Trace Analysis

For a long time, ISEs could not be used for the measurements at concentrations below 10^{-5} , at best below 10^{-6} M. The decisive step in the understanding of the nature of the lower detection limit of ISEs, and of what can be done to improve it, was made by Sokalski and co-workers [9]. After this pioneering work describing large improvement of the low detection limit of ISEs with ionophore-based membranes studies aimed at potentiometric measurements in sub-nanomolar concentration range became a mainstream of the ISE research. Deviations from Nernstian response of ISEs in micromolar and sub-micromolar concentration range are caused by the local increase in the concentration of the analyte in the sample in the vicinity of the sensor membrane, see Fig. 7.1. It is now generally recognized that this local increase in the analyte concentration is caused by trans-membrane fluxes of ions co-extracted from the internal filling solution to the sample and by the fluxes caused by the replacement of the primary ions in the membrane with the interfering ions due to ion exchange [10–12]. These fluxes have been registered experimentally by the electrochemical scanning microscopy method [13]. The internal reference system of a solid contact ISE, for example, based on a conducting polymer also may be a source of analyte ions which eventually contaminate sample solutions, although to somewhat lesser extent than in the case of ISEs with internal aqueous solution [14–17].

The resulting deviation is insignificant if the bulk concentration of the sample is larger than the impact from the trans-membrane flux. With dilution, the deviation increases, and at sample concentrations below 10^{-5} M, the ions brought by the trans-membrane flux determine the surface concentration of the analyte.

The driving force for these fluxes are large differences in the activities of the target analyte in diluted samples and in internal solutions containing analyte ions in millimolar concentration or at even higher level. The first approach aimed at

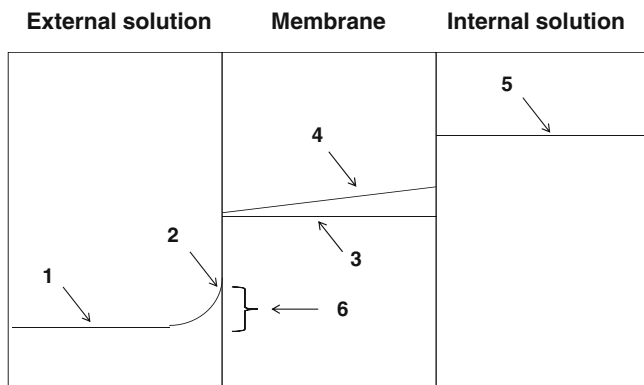


Fig. 7.1 Schematic representation of the electrolyte profiles in a membrane/solution system. (1) The electrolyte concentration in the sample bulk; (2) the electrolyte concentration in the vicinity of the membrane; (3) the “ideal” flat analyte ion concentration profile determined by the ion-exchanger concentration; (4) the real analyte ion profile (caused by the co-extraction); (5) the electrolyte concentration in the internal solution; (6) the deviation of the surface concentration of the analyte from its bulk value

reduction in the trans-membrane fluxes was invented in the late 1990s [9]. It relied on maintaining the activity of the target analyte in the internal filling solution of an ISE at a very low level by means of a suitable buffer while maintaining also a sufficiently high activity of an interfering ion. Under these conditions, the analyte ions in the ISE membrane layers close to the internal surface are largely replaced by the interference, producing a gradient of the concentration of the analyte ions across the membrane. This gradient, ideally, eliminates ion fluxes directed to the sample and in this way ensures Nernstian response of the ISE down to very low concentrations. If no suitable buffer exists, low activity of analyte in the internal solution may be kept by using, for example, ion-exchange resins [18, 19].

The disadvantage of this (chemical) approach is that the trans-membrane fluxes of ions are eliminated, rigorously speaking, at only one concentration of the analyte in the sample. From the practical view point, this means that the slope in even more diluted solutions is super-Nernstian because then the flux is directed toward the internal solution and the sample in the vicinity of the membrane is depleted of the analyte ions (see also Fig. 3.3).

More advanced approaches are based on the theory of diffusion and suggest modifications in the membrane geometry or composition [20]. The magnitude of the trans-membrane flux can be decreased by lowering the respective driving force: the gradient of the analyte ion concentration, using therefore thicker membranes [21, 22]. Also, the flux can be decreased by reducing ion diffusion coefficients, that is, by higher content of polymer in the membrane [23]. Transportation of ions across membranes can be also minimized by means of dispersing of silica gel microparticles in the membrane [24]. This is how the deviations from Nernstian response in diluted samples can be minimized at the cost of increasing the sensor

resistance. Also, when microparticles are incorporated, membranes show some loss of selectivity [23]. The acceleration of the ion transport in the sample phase can be achieved using rotating disc electrode (the electrode rotates during experiments inducing a flux of analyte to the electrode) or simply by stirring [25]. Variety of these approaches was critically analyzed and evaluated [12].

An alternative way of the elimination of the trans-membrane fluxes (or, rather, of the consequences of these fluxes) is based on galvanostatic polarization of the ISE. This (electrochemical) approach has been first proposed by Buck [26], and since then, it was utilized by several groups of researchers [15, 16, 27–30]. By applying a suitable current, one can eliminate the trans-membrane ion flux. Galvanostatic polarization seems to be more flexible approach aimed at the improvement of the low detection limit, when compared with the modification of the composition of the internal solution, or of the composition and/or the geometry of the membrane.

When the analyte concentration in the sample is below 10^{-5} M, the gradient of the analyte ion concentration across the membrane is determined by the concentration of the internal electrolyte which is, typically, 10^{-3} M or higher. Therefore, the steady trans-membrane flux across the membrane to solutions with concentrations of 10^{-5} M or lower is also the same. In turn, the steady electric current compensating this flux must be the same [28]. However, waiting for the steady state may take several hours and therefore is not practical. If the steady state is not reached, then for each particular concentration of the analyte a particular, specific compensating current is needed. This is why the galvanostatic polarization using a certain constant current density works ideally only in a very narrow concentration range. Outside this range, a sub- or a super-Nernstian slope is registered, similarly to chemical approach which relies on buffering the internal solution. Therefore, obtaining linear Nernstian response in a broad concentration range in practically acceptable time requires specific compensating current magnitudes tuned for particular concentrations of the analyte in the sample.

Tuned galvanostatic polarization has been successively used by Mikhelson et al. first for Ca^{2+} electrodes [31] and later also for Cd^{2+} electrodes [32] with PVC membranes containing neutral ionophores. The polarizing current density was optimized for each concentration of the analyte ion, see Fig. 7.2. The ISEs were polarized for certain time (always the same). The potential value registered in 0.2 s after the current is turned off was used as the analytical signal (plotted in Fig. 7.2, curve 2). The same approach helped enlarging the working range of Pb^{2+} ISE with crystalline membrane [33]. Since the optimal density of the compensating current is dependent on the analyte concentration, it is known only for calibrators, but not known for samples. This problem was successfully solved on the basis of the regularities governing the relation between the analyte concentration in sample and the respective optimal current density revealed in [31, 32]. It was shown that the optimal current density is proportional to the delta of the logs of the analyte ion activity in the sample in question and that at the lower detection limit:

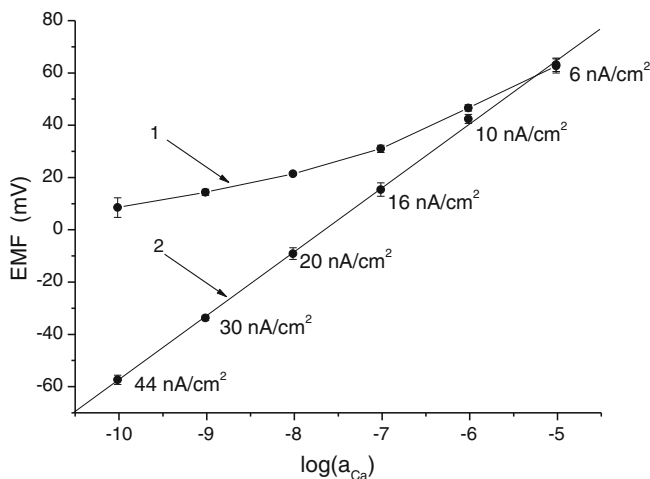


Fig. 7.2 Data obtained for Ca ISE based on the ionophore ETH 1001. Traditional zero current calibration plot (1) and calibration plot of electrodes polarized with optimized currents (2) [31]. Adapted with permission from Peshkova et al. [31]. Copyright 2008 American Chemical Society

$$i_{\text{opt}} = \beta(\log a_I - \log a_I^{\text{LDL}}) \quad (7.3)$$

Two practically feasible procedures which deliver both the optimal current density and the analyte ion concentration have been proposed and gave good results [31–33].

7.3 Use of ISEs Under Nonzero Current Conditions

Improvement of the lower detection limit is not the only area where ISEs are used under nonzero current conditions. Ionophores are widely used in voltammetric [34–36], conductometric [34, 37, 38], and optical sensors [39–41]. This suggests that the chemical interactions which provide a basis for the response of these different sensors do not require the traditional (for ISEs) limitation: measurements under zero current. For decades, polarization of ISEs was widely used for studying the mechanism of the response [42–45]. However, except of a few works by Nieman with fluoride mono-crystalline and calcium polymeric electrodes [46–49], polarization was never used to improve the analytical behavior of ISEs. Nieman made a rapid series of current measurements at various voltage pulse magnitudes (0–5 V) lasting 100 μs and then extrapolated the current–voltage curve to zero voltage. According to Nieman, the measured signal is concentration rather than activity dependent, making adjustment of the ionic strength unnecessary. This idea did not get further development. The situation changed drastically in the late 1990s

when they started using galvanostatically polarized ISEs for trace analysis (see Sect. 7.2).

Another promising area of polarized ISEs refers to the modification of the type of the electrode response (cationic or anionic) and that of the selectivity. Basically, the type of the ISE response and the selectivity are determined by the membrane composition. Shvarev found that when an ISE is under nonzero current conditions, it is possible to impose a certain type of the response and also modify the selectivity by passing current across the electrode membrane [50]. This can be done with ISEs having membranes with neutral ionophores and lipophilic background electrolyte (e.g., tetradodecyl ammonium tetrakis(p-Cl-phenyl) borate), but without ion-exchanger sites [50]. The concentration of the analyte ion in the membrane is when adjusted by passing current of a tuned density for a certain time. Polarization of a membrane containing Na^+ -selective neutral ionophore Na-X (see Sect. 4.2) with low cathodic current: about -3 mcA/cm^2 results in pseudo-Nernstian response to Na^+ ions with the selectivity coefficient determined by the ionic partition coefficients and ion-to-ionophore complexation constants:

$$K_{\text{NaK}} = \frac{k_K K_{\text{KL}}}{k_{\text{Na}} K_{\text{NaL}}} \quad (7.4)$$

When the electrode is polarized with cathodic current of higher density (approx. -30 mcA/cm^2), the concentration of the extracted ions exceeds the ionophore content, and the selectivity is determined by ionic partition coefficients only, like in the case of an ionophore-free membrane:

$$K_{\text{NaK}} = \frac{k_K}{k_{\text{Na}}} \quad (7.5)$$

The change of the sign of the current allows replacing a cationic response with anionic. As shown in [50], use of small anodic current (about $+3 \text{ mcA/cm}^2$) results in a response to Cl^- anions.

Nonzero current measurements are also suitable for sensing polyions, for example, heparin ($z \approx -70$) and protamine ($z \approx 20$). The classical equilibrium measurements do not allow sensing these ions because the large denominator in RT/zF —the Nernst factor, results in negligible slope. Therefore, Meyerhoff invented a non-equilibrium procedure of measurements when the process is under the diffusion control, and the potential difference upon addition of Y^- polyionic analyte obeys equation below [51–53]:

$$\Delta E = \frac{RT}{F} \ln \left(1 - \frac{z_Y D_{\text{aq}} \delta_m}{C_R D_m \delta_{\text{aq}}} C_Y \right) \quad (7.6)$$

Here, z_Y is the charge of species Y^- , C_Y is its concentration in the sample, C_R is the concentration of R^+ ion-exchanger sites in the membrane, D_{aq} and D_m are the ion diffusion coefficients in the aqueous phase and in the membrane phase, δ_{aq} and δ_m are the thicknesses of the diffusion layers in these phases.

The linearity and the reproducibility of the response of ISEs under diffusional control were poor [51–53]. However, applying alternating galvanostatic and potentiostatic pulses allowed obtaining very good reproducibility of the response to polyions. Furthermore, the calibration curve was linear with the slope like for a monovalent ion [54]:

$$E = \frac{RT}{F} \ln C_Y \quad (7.7)$$

Nonzero current measurements provide therefore with new opportunities also for polyion sensing.

7.4 Multisensor Arrays, Electronic Tongue

The variability of the traditionally measured selectivity coefficients hinders correction for interferences even in artificial mixed solutions containing only a handful of ions. The use of the unbiased selectivity coefficients requires special protocols which are difficult to follow dealing with real samples. Therefore, for real samples, the correction of the data for un-sufficient selectivity of electrodes is even more challenging, and hardly feasible at all.

An alternative approach may help solving this problem. This approach relies on measurements with arrays of sensors having moderate selectivity and processing the data with chemometrical methods.

Initially, the studies concentrated on the imitation of the functioning of the olfaction organs of mammals [55]. Attempts of development of the so-called *electronic nose* started in early 1980s [56]. These systems are nowadays widely used for the analysis of multicomponent gas mixtures [55].

In analogy to the electronic nose, the respective systems for the analysis of liquid samples (described first in [57]) are called *electronic tongue* [57–59]. In contrast to the traditional approach when attempts are made to use sensors with as highest selectivity as possible, the electronic tongue system relies on sensors with only moderate selectivity and having the so-called cross-sensitivity. In this way, each sensor in the array, in principle, delivers information on the concentrations of a number of analytes. The next step is to decode the signals obtained from the sensor array.

The sensors in the array can be of different nature—not necessarily ISEs. However, studies with ISEs were, probably, most successful, and therefore ISEs predominate among various types of sensors used for the electronic tongue systems [60–62]. In turn, although different types of ISEs can be utilized in electronic tongue, electrodes with chalcogenide glass membranes (see Sect. 6.4) are particularly suitable for these devices.

The number of sensors in the array can vary, but most typical number is about 10–20. In contrast to the classical measurements with ISEs, the electronic tongue system can work without a reference electrode. In such a setup, the potential

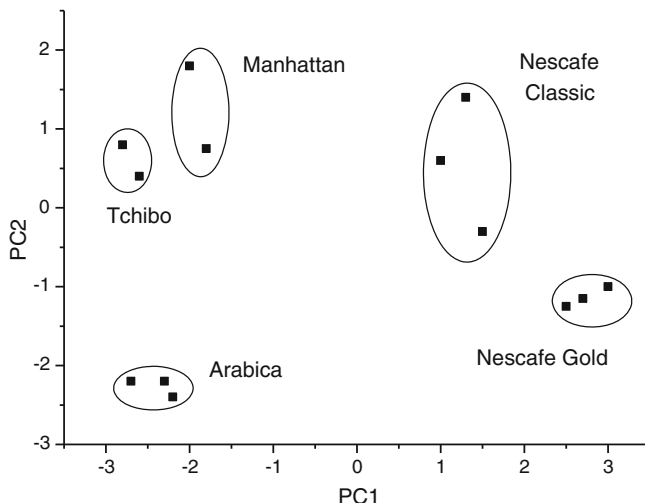


Fig. 7.3 Principal component plot identifying different sorts of coffee based on analysis with electronic tongue [67]. Adapted with permission from Legin et al. [59] Copyright 1997 Elsevier

difference is measured for all pairs of the electrodes in the array [63]. This is advantageous since reference electrodes often cause problems with the measurements.

The signals obtained from the sensor array are processed using various chemometrical methods: multilinear and nonlinear regressions, partial least squares, artificial neural networks [64]. The interpretation and representation of the data is often based on the principal component analysis method. This allows for the characterization of the samples not only in terms of the concentrations of the particular analytes, but also for the recognition of the nature of the sample: different types of samples fall into different places in the principal components plot. In this way, it is possible to distinguish between different sorts of juices [59, 65], mineral waters [66], coffee [67], tea [68], milk and dairy products [69, 70]. Example of identification of various sorts of coffee using electronic tongue and processing the data with artificial neural network is shown in Fig. 7.3. Electronic tongue is successfully used in a number of clinical applications: in artificial kidney [71, 72], in blood [73], and in urine analysis [74].

References

1. W.E. Morf, E. Pretsch, N.F. De Rooij, *J. Electroanal. Chem.*, 2007, 602, 43.
2. T. Sokalski, A. Lewenstam, *Electrochem. Commun.* 2001, 3, 107.
3. T. Sokalski, P. Lingenfelter, A. Lewenstam, *J. Phys. Chem.*, 2003, 107, 2443.
4. W. Kucza, M. Danielewski, A. Lewenstam, *Electrochem. Commun.*, 2006, 8, 416.

5. P. Lingenfelter, I. Bedlechowicz-Sliwakowska, T. Sokalski, M. Maj-Zurawska, A. Lewenstam, *Anal. Chem.*, 2006, 78, 6783.
6. T. Sokalski, W. Kucza, M. Danielewski, A. Lewenstam, *Anal. Chem.*, 2009, 81, 5016.
7. J.J. Jasielec, R. Filipek, K. Szyszkiewicz, J. Fausek, M. Danielewski, A. Lewenstam, 2012, in press. (Full reference will be provided later).
8. J. Bobacka, A. Ivaska, A. Lewenstam, *Chem. Rev.*, 2008, 108, 329.
9. T. Sokalski, A. Ceresa, T. Zwickl, E. Pretsch, *J. Amer. Chem. Soc.* 1997, 119, 11347.
10. Y. Mi, S. Mathison, R. Goines, A. Logue, E. Bakker, *Anal. Chim. Acta* 1999, 397 103.
11. R. Berezki, B. Takacs, J. Langmaier, M. Neely, R.E. Gyurcsanyi, K. Toth, G. Nagy, E. Lindner, *Anal. Chem.* 2006, 78, 942.
12. Z. Szigeti, T. Vigassy, E. Bakker, E. Pretsch, *Electroanalysis* 2006, 18, 1254.
13. R.E. Gyurcsanyi, E. Pergel, R. Nagy, I. Kapui, B.T.T. Lan, K. Toth, I. Bitter, E. Lindner, *Anal. Chem.* 2001, 73, 2104.
14. A. Michalska, J. Dumanska, K. Maksymiuk, *Anal. Chem.* 2003, 75, 4964.
15. A. Michalska, *Electroanalysis* 2005, 17, 400.
16. K.Y. Chumbimuni-Torres, N. Rubinova, A. Radu, L.T. Kubota, E. Bakker, *Anal. Chem.* 2006, 78, 1318.
17. A. Michalska, *Electroanalysis*, 2012, 24, 1253.
18. W. Qin, T. Zwickl, E. Pretsch, *Anal. Chem.* 2000, 72, 3236.
19. A. Malon, A. Radu, W. Qin, Y. Qin, A. Cereza, M. Maj-Zurawska, E. Bakker, E. Pretsch, *Anal. Chem.* 2003, 75, 3865.
20. T. Zwickl, T. Sokalski, E. Pretsch, *Electroanalysis* 1999, 11, 673.
21. A. Ceresa, T. Sokalski, E. Pretsch, *J. Electroanal. Chem.* 2001, 501.
22. T. Vigassy, C.G. Huber, R. Wintringer, E. Pretsch, *Anal. Chem.* 2005, 77, 3966.
23. M. Püntener, M. Fibbioli, E. Bakker, E. Pretsch, *Electroanalysis* 2002, 14, 1329.
24. T. Vigassy, R.E. Gyurcsanyi, E. Pretsch, *Electroanalysis* 2003, 15 375.
25. A. Radu, M. Telting-Diaz, E. Bakker, *Anal. Chem.* 2003, 75, 6922.
26. E. Lindner, R.E. Gyurcsanyi, R.P. Buck, *Electroanalysis* 1999, 11, 695.
27. E. Pergel, R.E. Gyurcsanyi, K. Toth, E. Lindner, *Anal. Chem.* 2001, 73, 4249.
28. W.E. Morf, M. Badertscher, T. Zwickl, N.F. de Rooij, E. Pretsch, *J. Electroanal. Chem.* 2002, 526, 19.
29. I. Bedlechowicz, T. Sokalski, A. Lewenstam, M. Maj-Zurawska, *Sens. Act. B* 2005, 108, 836.
30. I. Bedlechowicz-Sliwakowska, P. Lingenfelter, T. Sokalski, A. Lewenstam, M. Maj-Zurawska, *J. Anal. Bioanal. Chem.* 2006, 385, 1477.
31. M.A. Peshkova, T. Sokalski, K.N. Mikhelson, A. Lewenstam, *Anal. Chem.*, 2008, 80, 9181.
32. M.A. Peshkova, T. Sokalski, K.N. Mikhelson, A. Lewenstam, *Herald of St. Petersburg Univ.*, 2010, 4, 106 (Russ.).
33. G. Lisak, T. Sokalski, J. Bobacka, L. Harju, K. Mikhelson, A. Lewenstam, *Anal. Chim. Acta*, 2011, 707, 1.
34. K. Cammann, B. Ahlers, D. Henn, C. Dumschat, A.A. Shul'ga, *Sens. Actuators B*, 1996, 35-36, 26.
35. M. Senda, H. Katano, M. Yamada, *J. Electroanal. Chem.*, 1999, 468, 34.
36. S. Jadhav, E. Bakker, *Anal. Chem.*, 1999, 71, 3657.
37. A.A. Shul'ga, B. Ahlers, K. Cammann, *J. Electroanal. Chem.*, 1995, 395, 305.
38. A.E. Shvarev, D.A. Rantsan, K.N. Mikhelson, *Sens. Actuators B*, 2001, 76, 500.
39. E. Bakker, P. Bühlmann, E. Pretsch, *Chem. Rev.*, 1997, 97, 3083.
40. O.S. Wolfbeis, *Anal. Chem.*, 2002, 74, 91R.
41. K. Cammann, G.A. Rechnitz, *Anal. Chem.*, 1976, 48, 856.
42. K. Cammann, *Anal. Chem.*, 1978, 50, 936.
43. T. Kakiuchi, I. Obi, M. Senda, *Bull. Chem. Soc. Japan*, 1985, 58, 1636.
44. K.N. Mikhelson, J. Bobacka, A. Ivaska, A. Lewenstam, M. Bochenska, *Anal. Chem.*, 2002, 74, 518.
45. E.N. Samsonova, V.M. Lutov, K.N. Mikhelson, *J. Solid State Electrochem.*, 2009, 13, 69.
46. C.R. Powley, R.F. Geiger, T.A. Nieman, *Anal. Chem.*, 1980, 52, 705.

47. C.R. Powley, T.A. Nieman, *Anal. Chim. Acta*, 1982, 139, 61.
48. C.R. Powley, T.A. Nieman, *Anal. Chim. Acta*, 1982, 139, 83.
49. C.R. Powley, T.A. Nieman, *Anal. Chim. Acta*, 1983, 152, 173.
50. A. Shvarev, E. Bakker, *Anal. Chem.*, 2003, 75, 4541.
51. S.-C. Ma, V.C. Yang, M.E. Meyerhoff, *Anal. Chem.*, 1992, 64, 694.
52. S.-C. Ma, V.C. Yang, B. Fu, M.E. Meyerhoff, *Anal. Chem.*, 1993, 65, 2078.
53. E. Bakker, M.E. Meyerhoff, *Anal. Chim. Acta*, 2000, 416, 121.
54. A. Shvarev, E. Bakker, *J. Am. Chem. Soc.*, 2003, 125, 11192.
55. S.S. Schiffman, T.C. Pearce, *Handbook of Machine Olfaction. Electronic Nose technology*, Darmstadt, Wiley-VCH, 2003.
56. K. Persaud, G.H. Dodd, *Nature*, 1982, 299, 352.
57. K. Hayashi, M. Yamanaka, K. Toko, K. Yamafuji, *Sens. Actuators B.*, 1990, 2, 205.
58. C. Di Natale, A. D'Amico, Yu.G. Vlasov, A.V. Legin, *Proc. of the Int. Conf. Eurosensors IX*, Stockholm, 1995, 512.
59. A.V. Legin, A.M. Rudnitskaya, Yu.G. Vlasov, C. Di Natale, F. Davide, A. D'Amico, *Sens. Actuators B*, 1997, 44, 291.
60. Yu. Vlasov, A. Legin, A. Rudnitskaya, *Anal. Bioanal. Chem.*, 2002, 373, 136.
61. A. Legin, A. Rudnitskaya, Yu. Vlasov, *Integrated Analytical Systems. Comprehensive Analytical Chemistry*, 36, Amsterdam, Elsevier, 2003, 437.
62. A. Rudnitskaya, A. Legin, *J. Industr. Microbiol. Biotechnol.*, 2008, 35, 443.
63. A. Legin, A. Rudnitskaya, Yu. Vlasov, A. D'Amico, C. Di Natale, *Proc. 8th Inter. Conf. Electroanalysis. Bonn*, 2000, A27.
64. B. Lavine, J.J. Workman, *Anal. Chem.*, 2004, 76, 3365.
65. F. Winquist, P. Wide, I. Lundstrom, *Anal. Chim. Acta*, 1997, 357, 21.
66. A. Legin, A. Rudnitskaya, Yu. Vlasov, C. Di Natale, E. Mazzone, A. D'Amico, *Electroanalysis*, 1999, 11, 814.
67. T. Fukinaga, K. Toko, S. Mori, Y. Nakabayashi, M. Kanda, *Sens. Mater.*, 1996, 8, 47.
68. L. Lvova, A. Legin, Yu. Vlasov, G.S. Cha, H. Nam, *Sens. Actuators B*, 2003, 91, 32.
69. M. Hruskar, N. Major, M. Krpan, I.P. Krbavcic, G. Saric, K. Markovic, N. Vahcic, *Mljikarstvo*, 2009, 59, 193.
70. L.G. Dias, A.M. Peres, A.C.A. Veloso, F.S. Reis, M. Vilas-Boas, A.A.S.C. Machado, *Sens. Actuators B*, 2009, 136, 209.
71. A. Legin, A. Smirnova, A. Rudnitskaya, L. Lvova, Yu. Vlasov, *Anal. Chim. Acta*, 1999, 385, 131.
72. P. Ciosek, L. Grabowska, Z. Brzozka, W. Wroblewski, *Microchim. Acta*, 2008, 163, 139.
73. M. Gutierrez, S. Alegret, M. del Valle, *Biosens. Bioelectronics*, 2008, 23, 795.
74. L. Lvova, E. Martinelli, F. Dini, A. Bergamini, R. Paolesse, C. Di Natale, A. D'Amico, *Talanta*, 2009, 77, 1097.

Chapter 8

ISE Constructions

8.1 Conventional ISEs with Internal Filling Solution

The schematic sketch of a conventional ISE (an ISE with internal aqueous solution) is presented in Fig. 8.1, left. The main sensing element—the electrode membrane—is fixed in the end of a tubular body. The material of the body depends on the type of the membrane. For glass membrane electrodes, the body constitutes a glass tubing, and the membrane is formed in the end of the body by glass-blowing technique.

There to, the body tubing is immersed for a short while into the electrode glass melt, and then, the drop of the melt is blown into the typical spherical glass membrane. ISEs with crystalline and polymeric membranes, normally, have plastic bodies. Membranes are fixed in the end of the body with a suitable glue or with a clamping nut. In the latter case also, an O-ring made of an inert material (e.g., silicon rubber) is used for a hermetic seal. Typical constructions of the conventional ISEs are shown in Fig. 8.2.

Micro-ISEs for cellular studies (see Sect. 8.4) and electrodes in flow-through cells, in particular in clinical analyzers (see Sect. 8.5), are often of the conventional type, although solid-contact setup (see Sect. 8.2) appears more promising for these miniature devices.

Conventional ISEs contain an internal solution. This can be an ordinary liquid solution or a gel. For stable and reproducible electrical potential at the interface between the membrane and the internal solution, the latter must contain the ion to which the membrane is selective. For instance, for a glass pH electrode, this must be H^+ ; for a Pb^{2+} crystalline electrode, this is Pb^{2+} ; for a K^+ and NO_3^- polymeric electrodes, these are K^+ and NO_3^- , etc.

The membrane and the internal solution are ionic conductors, while the wire is electronic conductor. For a reversible transduction from the ionic conductivity in the internal solution to the electronic conductivity in the wire, an internal electrode is needed. To this end, one can use well-known classical first- and second-kind electrodes, as well as RedOx electrodes. Most often, a second-kind electrode, in particular—Ag/AgCl, is used as the internal electrode in the conventional ISEs. Then, the internal solution must also contain Cl^- ions. For the above listed

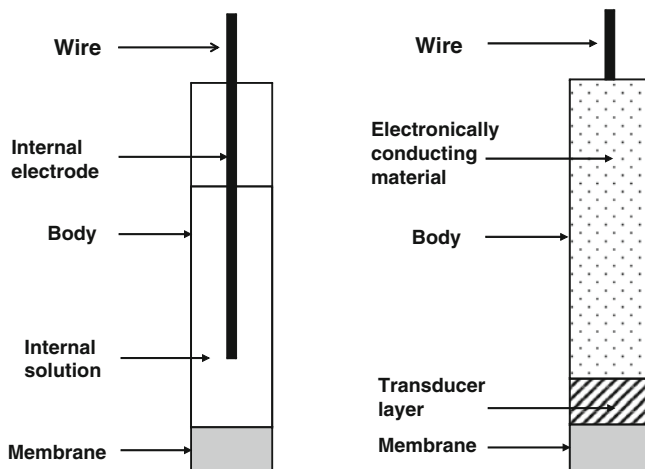


Fig. 8.1 Schematic sketch of a conventional ISE (*left*) and a solid-contact ISE (*right*)

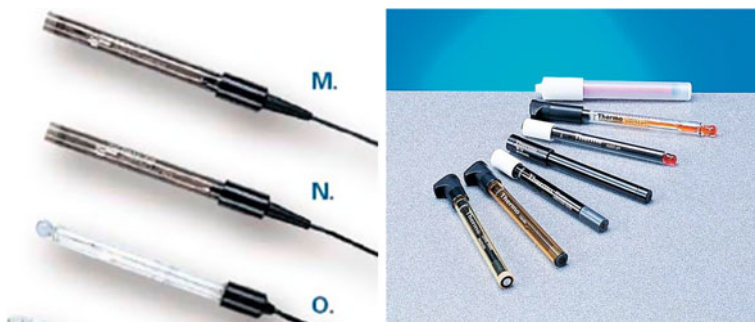


Fig. 8.2 *Left* the Denver Instruments ISEs with crystalline membrane (M), PVC membrane (N), and glass membrane (O). *Right* the Thermo Fisher ISEs

examples, the most typical internal solutions are as follows: 0.01 M HCl, 0.0001 M PbCl_2 , 0.01 M KCl, and 0.01 M NaNO_3 + 0.01 M NaCl, respectively. Potassium ion is controlled mostly in clinical and agricultural samples where the concentration of the target ion is relatively high (about 4.5 mM in blood and up to 0.1 M in carrot juice). Nitrate is measured predominantly in agriculture (e.g., in fertilized soils) and in some polymer production. The target ion concentrations in the samples are rather high. Therefore, the internal solutions in the respective ISEs contain high concentrations of the analyte ions. Lead-selective ISEs are mostly used in environmental control where lead must be measured at trace levels; therefore, the internal solution should not contain high concentrations of the target ions (see also Sect. 7.2). Furthermore, complexing agents can be added for further decrease in the analyte ion activity in the internal solutions in ISEs for trace analysis.

Internal solutions often contain some other additives, for example, to prevent freezing during electrode transportation in winter.

As example of the charge transfer in a conventional ISE, let us consider a K^+ ISE filled with KCl solution and equipped with Ag/AgCl internal electrode, see Fig. 8.3, top. Across the membrane/solution interface, charge is transferred by K^+ ions. The respective exchange currents are high, securing the electrochemical equilibrium at the interface [1, 2]. Within the internal solution, charge is carried by K^+ and Cl^- ions. At the interface between the internal solution and Ag/AgCl electrode, Ag atoms reversibly oxidize to Ag^+ cations, producing electrons: $Ag^{Ag} \leftrightarrow Ag^{+,aq} + e^-$. The silver cations with the chloride anions produce low-soluble salt: $Ag^{+,aq} + Cl^{-,aq} \leftrightarrow AgCl \downarrow$. Due to these reversible processes, the activity of silver ions in solution is determined by the chloride activity:

$$a_{Ag^+,aq} = SP_{AgCl} / a_{Cl^{-,aq}} \tag{8.1}$$

The internal Ag/AgCl electrode potential can be expressed as follows:

$$\begin{aligned} \varphi_{Ag/AgCl} &= -\frac{\mu_{Ag^+}^{0,Ag} - \mu_{Ag^+}^{0,aq}}{F} - \frac{RT}{F} \ln \frac{a_{Ag^+}^{Ag}}{a_{Ag^+}^{aq}} \\ &= -\frac{\mu_{Ag^+}^{0,Ag} - \mu_{Ag^+}^{0,aq}}{F} - \frac{RT}{F} \ln \frac{a_{Ag^+}^{Ag} a_{Cl^{-,aq}}}{SP_{AgCl}} \end{aligned} \tag{8.2}$$

If the chloride activity is well above $\sqrt{SP_{AgCl}}$, the electrode potential is very stable. This is why the concentration of Cl^- ions in the internal solution must be 10^{-4} M or higher.

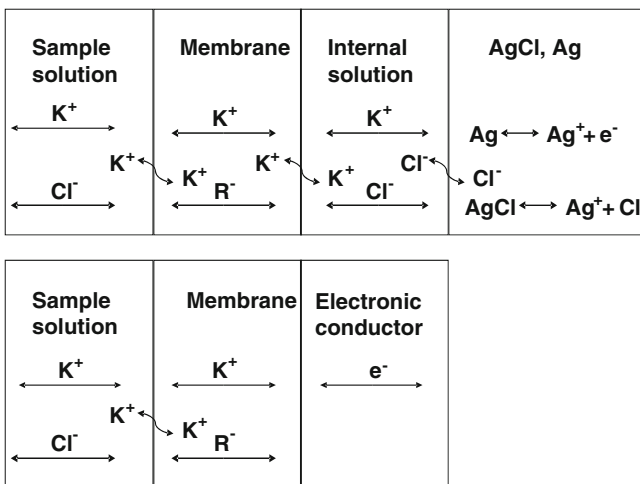


Fig. 8.3 Charge transportation in a conventional K^+ ISE (top) and a coated-wire K^+ ISE (bottom)

In this way, in the conventional ISEs, the reversible charge transfer is arranged, including the interface between ionically and electronically conducting phases. When all reactions involved are fast, the electrode behaves as ideally non-polarizable. This is why the conventional ISEs, if properly maintained, show excellent stability and reproducibility of the potentials. However, if electrode is not sealed hermetically, the internal solution must be from time to time replaced with a fresh portion.

8.2 Solid-Contact ISEs

8.2.1 Why Solid Contact?

It is difficult to make small-size conventional ISEs with internal solution and internal electrode. This hinders the ISE application in small volumes which would be especially advantageous for the analysis of clinical and biological samples. Furthermore, the conventional construction is non-compatible with the modern planar technologies. Therefore, for decades, researchers strived for the elimination of the internal solution and the internal electrode and for the replacement thereof with the so-called “solid contact”.

The solid-contact ISEs (see Fig. 8.1, right) comprise of an electronically conducting substrate covered with a transducer layer (see below) and a sensor layer (still called membrane) on the top of the transducer layer. The substrate may be a metal wire. In this way, it is possible to decrease the diameter of the ISE down to 0.6 mm and less. One can use a relatively large conducting plate as the substrate and cover it with the transducer layer and then with the sensor layer. After that, the three-layer construct can be cut into a number of pieces each being an individual solid-contact ISE. The latter approach utilizes the advantages of the planar technology and promises mass production of low-cost sensors.

Elimination of the internal reference system and replacement thereof with a solid contact appears a purely technical task. However, solving this task encounters fundamental problems. So far, these problems are solved for glass and crystalline electrodes and remain largely unsolved for polymeric membranes with ionophores. From the practical point of view, these problems result in insufficient long-term stability of the ISE potentials and in poor piece-to-piece reproducibility.

Since the interpretation of the measured signal—the EMF—relies on the calibration, the stability of the calibration parameters (E^0 and S) over time directly translates into the accuracy and the reliability of the analysis. Normally, the slope value is stable whatever the ISE construction: conventional or with a solid contact. However, the standard potentials of the solid-contact ISEs often change from day to day in a chaotic way. This causes unpredictable parallel shifts of the calibration curve, which, in turn, worsens the accuracy of the measurements. The low piece-to-piece reproducibility within a series of replica electrodes, from the practical

point of view, hinders the interchangeability of the ISEs. From the academic viewpoint, it indicates the insufficient knowledge of the regularities governing the electrode potential formation.

The ISE membrane is an ionic conductor, and the boundary potential at the membrane/solution interface is a well-defined value determined by the equilibrium distribution of ions between the phases. The substrate (a metal or a carbon-based material) is an electronic conductor connected (via a wire) to the measuring device. Therefore, the stability and reproducibility of the readings require a stable electrical potential at the interface between the ionically conducting membrane and electronically conducting substrate. This potential must be defined by a RedOx reaction at the interface between these phases (like the oxidation and reduction of silver in Ag/AgCl electrode). Furthermore, this RedOx reaction must be fast, and the two phases must be buffered with respect to the reactant: to re-establish the equilibrium in the case of some external perturbations [3]. Without a suitable RedOx reaction, the interface is blocked: Ions are confined to the membrane, and electrons cannot leave the substrate. Consequently, the interface between the membrane and the substrate constitutes a capacitor and behaves as an ideally polarizable electrode.¹ A fortuitous tiny charge causes a significant change in the potential of such an electrode.

8.2.2 Solid-Contact ISEs with Glass and Crystalline Membranes

The problem of the stabilization of the potentials of the solid-contact ISEs with glass and crystalline membranes has been solved successfully. The internal surface of the glass membrane is covered by a metal alloy, containing small amount of the respective alkali metal. The wire directly contacts the alloy. For instance, pH solid-contact electrodes with membranes containing Li₂O and a Sn alloy doped with Li show excellent stability over time [4, 5]. The potential at the interface between the membrane glass and the alloy is determined by the equilibrium of the oxidation/reduction in Li: $\text{Li}^{\text{Alloy}} \leftrightarrow \text{Li}^{+\text{,glass}} + e^{-\text{,alloy}}$. Thus, for these solid-contact ISEs, the concept of the classical first-kind electrode is exploited. The piece-to-piece reproducibility of these electrodes allows for factory calibration: The user gets the calibration parameters from the manual, and these parameters retain their values for years [4, 5].

¹ Ideally polarizable electrode is an electrode characterized by the absence of net current between the electrode surface and the electrolyte. Even tiny electric charge causes large change in the potential (large polarization) of such an electrode. On the contrary, the potential of an ideally non-polarizable electrode is virtually non-sensitive to any charge passed. The classical examples of the ideally polarizable and ideally non-polarizable electrodes are, respectively, mercury and platinum electrodes in a solution containing a RedOx couple.

The concept of the second-kind electrode is used as a basis for solid-contact ISEs with crystalline membranes [6]. These membranes contain Ag_2S or other low-soluble salt AgX with $\text{X}^- = \text{Cl}^-, \text{Br}^-, \text{J}^-, \text{SCN}^-$ —in ISEs selective to the respective anions. Electrodes selective to $\text{Cu}^{2+}, \text{Pb}^{2+}, \text{Cd}^{2+}, \text{Ag}^+, \text{Hg}^{2+}$ contain Ag_2S and a sulfide of the respective metal. The internal side of the membrane is covered with a thin layer (film) of vacuum-sputtered silver, and the wire is then soldered to this silver layer. The RedOx equilibrium is established between Ag^+ ions in the crystalline membrane and Ag atoms in the silver metal film. The solid-contact ISEs with chalcogenide glass membranes are arranged in an analogous way [7].

Detailed description of various solid-contact ISEs is presented in review papers [8–10].

8.2.3 *Ionophore-Based Solid-Contact ISEs Without Transducer Layer*

First attempts of making solid-contact ISEs with ionophore-based membranes were undertaken in 1970s. These were Selectrodes [11, 12] and the so-called coated-wire electrodes [13–15]. Selectrodes constitute porous graphite rods impregnated with a liquid membrane cocktail (without polymer). In the coated-wire electrodes, the membrane is deposited on the surface of a noble metal wire: Pt, Au, Ag—by dipping wire into membrane cocktail. The electrodes of both these types show practically the same working ranges and selectivities as conventional electrodes with the same membrane compositions. However, the potentials of these ISEs drift chaotically and relatively fast—up to 10 mV/h. The potentials of replica electrodes prepared in exactly the same way sometimes differ in the range of 20–100 mV.

The reason is that the membrane/graphite and membrane/wire interfaces are blocked (see above), and the respective potential is sensitive to even small accidental charges. This sensitivity is inversely dependent on the capacity of the interface:

$$d\varphi = C^{-1}dQ \quad (8.3)$$

Here, C is the capacitance and dQ is the accidental charge. This simple equation shows that increasing the capacitance, that is, by increasing the area of the contact, allows for some stabilization of the potential.

In reality, the membrane/graphite and membrane/metal interfaces are partly unblocked by oxygen and other RedOx agents penetrating through the membrane. The oxygen-induced RedOx processes provide for some stabilization of the potential so that the calibration parameters retain their values for some time (about one hour) [16, 17]. It was reported on the dependence of the coated-wire electrode potentials on the oxygen partial pressure in the ambient air [17].

The first-kind electrode concept is not promising for ISEs with the ionophore-based membranes. These membranes sorb water from solutions. Furthermore, water penetrates through the membrane and forms a thin layer on the metal surface. The metal ion concentration in this aqueous layer is not stable, causing instability of the electrode potential.

Grekovich suggested using the second-kind electrode concept. It was reported on solid-contact ISEs for Cl^- , Br^- , and SCN^- anions with high stability and reproducibility of the potentials [18]. Membranes containing PVC, plasticizer (dibutyl phthalate), and ion exchanger, TDAX tetradecyl ammonium salt ($\text{X}^- = \text{Cl}^-$, Br^- , SCN^-), were deposited on the respective second-kind electrode: Ag/AgCl , Ag/AgBr , or Ag/AgSCN . This approach is limited to anions producing low-soluble silver salts.

8.2.4 Solid-Contact ISEs with Electron–Ion-Exchanger Resins in the Transducer Layer

Doping the membrane with suitable RedOx agents may stabilize the solid-contact ISE potentials. Then, however, the RedOx agents must be confined to the vicinity of the electronic conductor. Otherwise, the ISE is sensitive to RedOx components in samples. Stefanova therefore suggested the use of electron–ion-exchanger resins EO-7 and EI-21 [19, 20]. The EO-7 resin constitutes a polymer with quinone–hydroquinone functional groups. The EI-21 resin is a polymeric cation exchanger with $-\text{SO}_3^-$ groups, containing Cu^{2+} counter-ions. Part of Cu^{2+} is electrochemically reduced to Cu which forms tiny copper metal particles. The electrodes are prepared by depositing the membrane cocktail containing also the resin and carbon black on graphite substrate. After the evaporation of the cocktail solvent (THF), a mixed-conducting layer forms on the top of the graphite rod. The ionic conductivity in this transducer layer is due to the presence of mobile ion-exchanger sites (e.g., ClTPB^-), ions, and charged ion–ionophore complexes. The electronic conductivity is due to electrons in Cu metal particles and in carbon black. The sensor membrane (without resin particles and carbon black) is deposited on the top of this transducer layer. The scheme of a potassium-selective solid-contact ISE of this type is shown in Fig. 8.4.

Ions K^+ and R^- move freely within the transducer layer, in the same way as in the membrane. Between the membrane proper and the resin, ion-exchange equilibrium is established: $2\text{M}^{+, \text{membrane}} + \text{Cu}^{2+, \text{resin}} \leftrightarrow 2\text{M}^{+, \text{resin}} + \text{Cu}^{2+, \text{membrane}}$. Together with RedOx equilibrium in the resin, $\text{Cu}^{\text{resin}} \leftrightarrow \text{Cu}^{2+, \text{resin}} + 2\text{e}^{-, \text{resin}}$, these processes ensure reversible transduction from ionic to electronic conductivity. Carbon black plays a dualistic role: connecting the resin particles with one another and with the substrate and increasing the capacitance of the interface between ionically conducting and electronically conducting phases. This mixed-conducting layer works as transducer from ionic to electronic conductivity.

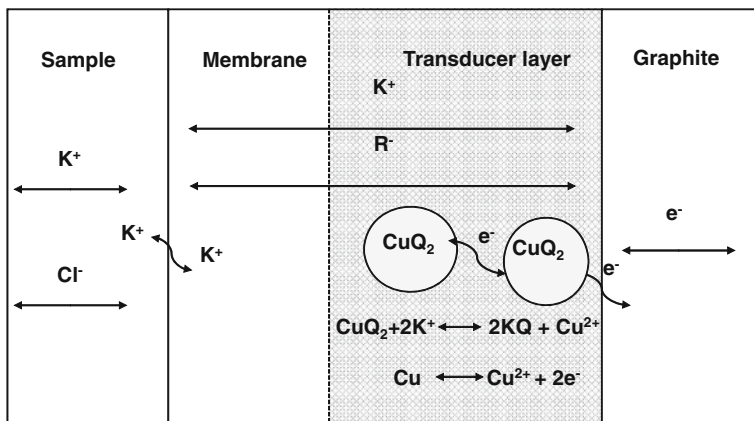


Fig. 8.4 Scheme of solid-contact ISE with EI-21 resin in the transducer layer. Q^- is the anionic functional group in the resin. Carbon black suspension is shown with gray dots

Solid-contact ISEs for K^+ , Na^+ , NH_4^+ , Ca^{2+} , NO_3^- , CO_3^{2-} ions with EI-21 resin in the transducer layer are much more stable than the analogous Selectrode or coated-wire ISEs. The electrode potentials in control solutions retain values within $\pm 1-2$ mV during several days. However, periods of stability alternate with sudden potential jumps in 2–5 mV within a few hours. The most probable reason for these jumps is extraction of some RedOx agents from samples. These agents diffuse across the membrane and reach the transducer layer with RedOx-sensitive components after a few days. At this time, the potential undergoes sharp change [21].

8.2.5 Solid-Contact ISEs with Conducting Polymers in the Transducer Layer

Conducting polymers (CP) appear very promising for the stabilization of the solid-contact ISEs potentials. Most of the conducting polymers are *p*-type semiconductors when oxidized and doped with anions to maintain the macroscopic electroneutrality. There are, however, also *n*-type CPs doped with cations. Thus, the doping/de-doping reaction is coupled with oxidation/reduction of the polymer. In this way, CPs work as transducers from ionic to electronic conductivity. Most popular CPs used in solid-contact ISEs are polythiophenes: polytrioctylthiophene (POT), polyethylenedioxythiophene (PEDOT), polyaniline (PANI), and polypyrrole (PPy). All these CPs belong to the *p*-type semiconductors.

Thorough discussion of the advantages and limitations of various CPs for the solid-contact ISE purposes is presented in Bobacka et al. [8]. The oxidation potential of POT is too high, and therefore, its oxidation degree is too low under normal conditions. Therefore, its conductivity and RedOx capacity are also low.

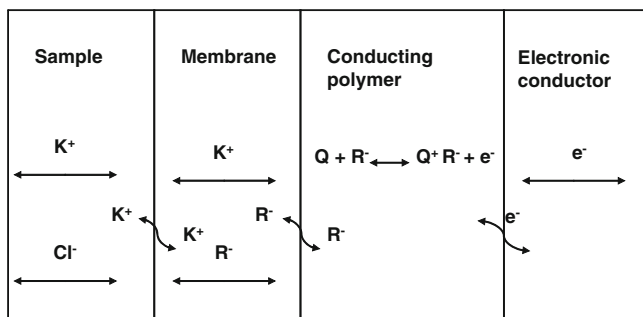


Fig. 8.5 Scheme of solid-contact ISE with a *p*-type conducting polymer in the transducer layer

Oxidized PEDOT, PANI, and PPy are stable under normal conditions; these CPs have high RedOX capacity and, consequently, less sensitive to external RedOX agents. However, CPs, especially PANI, are sensitive to pH. Therefore, oxygen, CO_2 , and even water may cause changes in the oxidation state of CPs. This is one of the reasons why the potentials of solid-contact ISEs are not as stable as one could expect. Lindfors [22] studied the light sensitivity of the solid-contact ISEs potentials with PPy, POT, PEDOT, and PANI in the transducer layer. ISEs with POT showed highest and those with PPy, the lowest sensitivity to light [22].

Scheme of a potassium-selective solid-contact ISE with a *p*-type conducting polymer in the transducer layer is shown in Fig. 8.5.

Many inorganic ions [8, 23, 24], ionic surfactants [25], and polyions [26] are measured with solid-contact ISEs containing CPs in the transducer layer. Using CPs, it is possible to make very small ISEs, for example, within a syringe needle [27] or even microelectrodes for measurements within a living cell [28]. It is also possible to avoid metal or carbon substrate: Full-plastic ISEs for K^+ and Ca^{2+} ions were described by Michalska and Maksymiuk [29].

8.2.6 Influence of Water Uptake on the Stability of Solid-Contact ISEs

Although conducting polymers and ion-to-electron-exchanger resins provide for reversible transduction from ionic to electronic conductivity, solid-contact ISEs with ionophore-based membranes are not as stable as electrodes with glass and crystalline membranes. A significant difference between these types of ISEs is the ability of polymeric membranes to sorb water. Water in membranes is present in significant quantities and forms aggregates with different sizes and diffusion coefficients [30–34]. Water uptake is strongly dependent on the nature of the polymer; POT sorbs much less water than plasticized PVC [34]. Furthermore,

water forms a continuous layer with the thickness of about 10 nm in between the membrane and the transducer layer [34–37]. Thus, an internal aqueous solution spontaneously forms in solid-contact ISEs with polymeric membranes. The volume of this solution does not exceed 0.05 μl , and therefore, its composition, although with some delay, strongly depends on the ambient conditions due to diffusion of electrolytes across the membrane. Therefore, the presence of the water layer worsens the stability of solid-contact ISEs.

Test for the presence of water layer was proposed in Fibbioli et al. [38]. The idea of the test is as follows. Let us have an ISE for I^+ ions in contact with IX electrolyte solution for some time. Then, we replace the IX solution with a JX solution, and J^+ ion is discriminated by the membrane. The potential of an electrode without water layer drops fast into the negative direction and maintains a stable value. When this electrode is removed from JX solution and placed back into IX solution, the potential returns to its initial value, like shown in Fig. 8.6, solid line. If a water layer is present, J^+ ions diffuse through the membrane to the water film, and I^+ ions diffuse from the film to solution. This results in depletion of the water layer in I^+ ions, while the solution in the utmost vicinity of the membrane also contains I^+ ions. Therefore, when such an ISE is immersed into JX solution, the potential drifts to more positive direction. When the ISE is placed back into IX electrolyte, the potential shows an overshoot because the water layer is depleted in I^+ ions, and then, the potential drifts to the initial value, see Fig. 8.6, dotted line.

In order to avoid the formation of the water layer, the water uptake must be reduced by decrease in the plasticizer content in membrane [39] or by replacement PVC with another polymer. It is also advisable to increase the hydrophobicity of the transducer layer and the substrate. To this end, very useful are dispersed carbon materials like carbon nanotubes [40, 41] and porous graphite [42, 43].

Fig. 8.6 Scheme of the water layer test. *Solid line* refers to an ISE without water layer, *dotted line*—with water layer

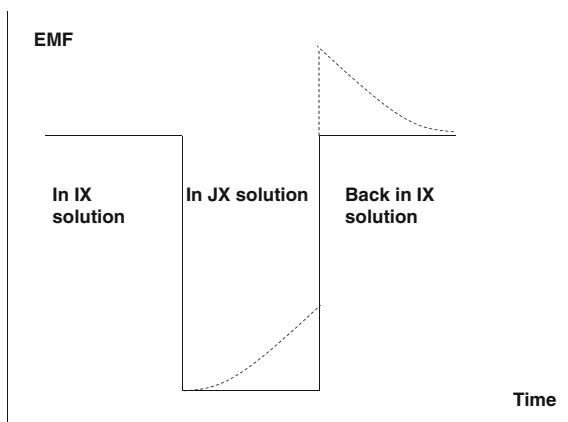
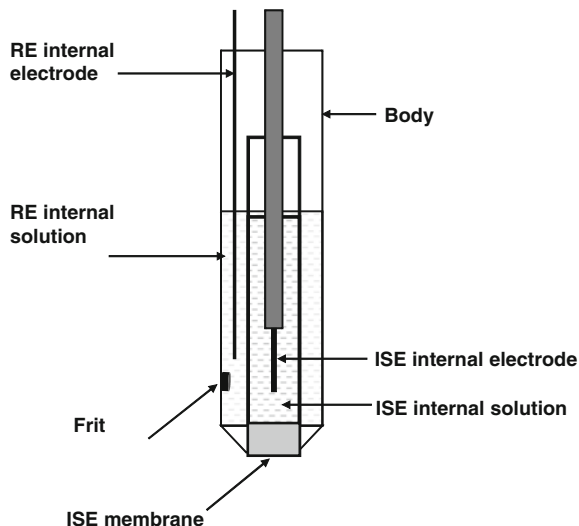


Fig. 8.7 Scheme of a combination electrode



8.3 Combination Electrodes

Combination electrodes constitute an ISE and a reference electrode (RE) combined in one body. The constructions of REs are discussed in detail in Sect. 9.1. A schematic sketch of a combination electrode is shown in Fig. 8.7. The body contains two compartments: for the ISE and for the RE; often, these are two coaxial cylinders: inner cylinder for the ISE and the room between the cylinders—for the RE. The ISE is in contact with the sample or calibrator solution through the membrane. The role of the liquid junction plays a frit made of a porous ceramics or glass.

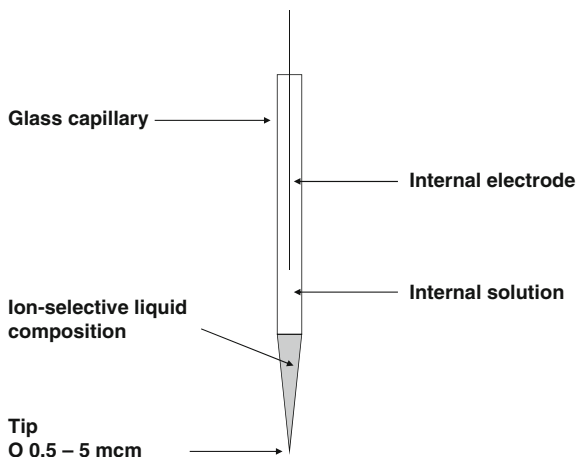
Combination electrodes are convenient in use, especially if only one ion must be controlled. It is not advisable to have several combination electrodes in one sample beaker because of the increased contamination of the sample with electrolytes from the REs. Therefore, if a number of ions must be measured in the same sample, it is better to use ordinary ISEs and an ordinary RE.

8.4 Micro-ISEs for Cellular Studies

Microelectrodes are used for measurements of ion concentrations in living cells. Obviously, these electrodes must be very small and therefore constitute glass capillaries, containing liquid membrane compositions in tip. Scheme of a microelectrode is shown in Fig. 8.8.

The tip diameter is about 0.5–5 μm . Because of high resistivity, polymeric membranes are not suitable for microelectrodes. Furthermore, in order to increase

Fig. 8.8 Scheme of a microelectrode



the dissociation degree of electrolytes in membrane, polar solvent oNPOE (see Sect. 4.3) predominates among other solvents used with ionophore-based membranes. From the manufacturing point of view, it is also necessary to use liquid membranes in microelectrodes because these are prepared by sucking the membrane composition into the capillary. Capillaries must be hydrophobic to avoid water leak between the membrane phase and glass. Thereto, the tip is silanized. Microelectrodes fundamentals and practice are thoroughly described by Ammann [44].

8.5 Flow-Through ISE Cells

Many applications of ISEs suggest measurements in flow. For instance, electrodes may be placed into a bypass in an industrial process. Application of ISEs for clinical analysis also requires flow-cells to decrease consumption of samples and also enhances the reliability of the measurements. This is often achieved by alternating samples and calibrators, and for this task, measurements in flow-cells are superior to those in beakers. A typical example of flow-through ISEs and assembled flow-cell for clinical analyzer is shown in Fig. 8.9, left.

In the electrode bodies are two channels: vertical channel for the membrane and internal reference system and horizontal channel for samples and calibrators. Once the cell is assembled, sample/calibrator channels of individual electrodes make a channel across the whole cell like shown in Fig. 8.9, right. Normally, 30–100 μl of sample or calibrator is enough to measure concentrations of several ions using a flow-through cell like shown in Fig. 8.9.

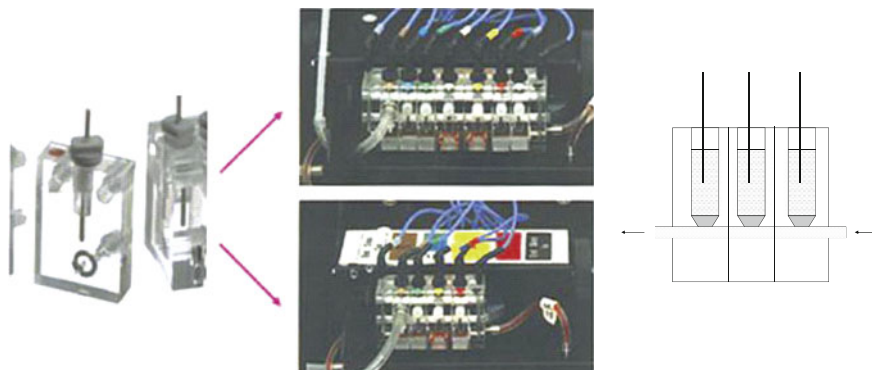


Fig. 8.9 *Left* flow-through cell with ISEs for clinical analyzer Konelab (Thermo Fisher). Electrodes (*left*) and assembled flow-through cells with five ISEs and a RE (*right, top*) and with three ISEs and a RE (*right, bottom*). Terminal electrodes are for conductivity measurements—to control whether the channel contains sample or is empty. Next to *left* terminal electrode, the RE is located. *Right* scheme of a flow-through cell

References

1. K.N. Mikhelson, J. Bobacka, A. Lewenstam, A. Ivaska, *Electroanalysis*, 2001, 13, 876.
2. K.N. Mikhelson, J. Bobacka, A. Ivaska, A. Lewenstam, M. Bochenska, *Anal. Chem.*, 2002, 74, 518.
3. B.P. Nikolskii, E.A. Materova, *Ion-Selective Electrode Rev.* 1985, 7, 3.
4. M.M. Shultz, O.S. Ershov, G.P. Lepnev, T.M. Grekovich, A.S. Sergeev, *Russ. J. Appl. Chem.*, 1979, 52, 2487 (Russ.).
5. A.A. Belyustin, A.M. Pisarevskii, G.P. Lepnev, A.S. Sergeev, M.M. Schultz, *Sens. Actuators B*, 1992, 10, 61.
6. Yu. G. Vlasov, Y. E. Ermolenko, O. A. Iskhakova, *J. Anal. Chem. USSR*, 1979, 34, 1175.
7. Yu.G. Vlasov, E.A. Bychkov, *Ion-Selective Electrode Rev.* 1987, 9, 3.
8. J. Bobacka, A. Ivaska, A. Lewenstam, *Chem. Rev.* 2008, 108, 329.
9. A. Michalska, *Electroanalysis*, 2012, 24, 1253.
10. N.M. Ivanova, M.B. Levin, K.N. Mikhelson, *Russ. Chem. Bull.*, 2012 (full reference will be provided).
11. J. Ruzicka, C.G. Lamm, *Anal. Chim. Acta*, 1971, 54, 1.
12. J. Ruzicka, E.H. Hansen, J.C. Tjell, *Anal. Chim. Acta*, 1973, 67, 155.
13. R. W. Cattrall, H. Freiser, *Anal. Chem.*, 1971, 43, 1905.
14. R.W. Cattrall, D.M. Drew, *Analyt. Chim. Acta.*, 1975, 77, 9.
15. R. W. Cattrall, I. C. Hamilton, *Ion-Selective Electrode Rev.*, 1984, 6, 125.
16. R.P. Buck, V.R. Shepard, *Anal. Chem.*, 1974, 46, 2097.
17. A. Hulanicki, M. Trojanovicz, *Anal. Chim. Acta*, 1976, 87, 411.
18. A.L. Grekovich, K.N. Mikhelson, S.E. Didina, N.V. Garbuzova, E.A. Materova, *Ion Exchange and Ionometry*, 1982, 3, 130 (Russ.).
19. O.K. Stefanova, N.V. Rozhdestvenskaya, V.F. Gorshkova, *Sov. Electrochem*, 1983, 19, 1225.
20. O.K. Stefanova, N.V. Rozhdestvenskaya, B.A. Mukhitdinova, E.E. Ergozhin, O.V. Sofronova, T.E. Barinova, *Sov. Electrochem.*, 1990, 26, 976.
21. G. A. Khripoun, E. A. Volkova, A.V. Liseenkov, K.N. Mikhelson, *Electroanalysis*, 2006, 18, 1322.
22. T. Lindfors, *J Solid State Electrochem*, 2009, 13, 77.

23. T. Lindfors, H. Aarnio, A. Ivaska, *Anal. Chem.*, 2007, 79, 8571.
24. A. Michalska, A. Ivaska, A. Lewenstam, *Anal. Chem.*, 1997, 69, 4060.
25. A. Kovacs, B. Csoka, G. Nagy, A. Ivaska, *Anal. Chim. Acta*, 2001, 437, 67.
26. K. Fordyce, A. Shvarev, *Anal. Chem.*, 2008, 80, 827.
27. S.V. Lamaka, M.G. Taryba, M.L. Zheludkevich, M.G.S. Ferreira, *Electroanalysis*, 2009, 21, 2447.
28. N. Rubinova, K. Chumbimuni-Torres, E. Bakker, *Sens. & Actuat. B*, 2007, 121, 135.
29. A. Michalska, K. Maksymiuk, *Anal. Chim. Acta*, 2004, 523, 97.
30. N.V. Rozhdestvenskaya, O.K. Stefanova, *Sov. Electrochem.*, 1982, 18, 1379.
31. J.D. Harrison, X. Li, *Anal. Chem.*, 1991, 63, 2168.
32. Z. Li, X. Li, S. Petrovic, J.D. Harrison, *Anal. Chem.*, 1996, 68, 1717.
33. Z. Li, X. Li, M. Rothmaier, J.D. Harrison, *Anal. Chem.*, 1996, 68, 1726.
34. T. Lindfors, F. Sundfors, L. Höfler, R.E. Gyurcsanyi, *Electroanalysis*, 2009, 21, 1914.
35. F. Sundfors, L. Höfler, R.E. Gyurcsanyi, T. Lindfors, *Electroanalysis*, 2011, 23, 1769.
36. L. Gorski, A. Matusevich, M. Pietrzak, L. Wang, M. E. Meyerhoff, E. Malinowska, *J Solid State Electrochem*, 2009, 13, 157.
37. R. De Marco, J.P. Veder, G. Clarke, A. Nelson, K. Prince, E. Pretsch, E. Bakker, *Phys. Chem. Chem. Phys.*, 2008, 10, 73.
38. M.Fibbioli, W.E. Morf, M. Badertscher, N.F. de Rooij, E. Pretsch, *Electroanalysis*, 2000, 12, 1286.
39. M. Puntener, M. Fibbioli, E. Bakker, E. Pretsch, *Electroanalysis*, 2002, 14, 1329.
40. G.A. Crespo, S. Macho, F.X. Rius, *Anal. Chem.* 2008, 80, 1316.
41. G.A. Crespo, S. Macho, J. Bobacka, F.X. Rius, *Anal. Chem.* 2009, 81, 676.
42. C.Z. Lai, M.A. Fierke, A. Stein, P. Bühlmann, *Anal. Chem.*, 2007, 79, 4621.
43. M.A. Fierke, C.Z. Lai, P. Bühlmann, A. Stein, *Anal. Chem.*, 2010, 82, 680.
44. D. Ammann, *Ion-selective Microelectrodes*, Springer, Berlin-Heidelberg-New York-Tokyo, 1986.

Chapter 9

The Basics of the Routine Analysis with ISEs

9.1 Reference Electrodes

It is not possible to measure a single electrode potential. Therefore, all electrode potentials are measured against some reference electrode (RE), and the respective EMFs are used for further processing. The primary RE which is supposed to have zero potential at all temperatures is the so-called *standard hydrogen electrode*. This is a piece of platinum with rough surface, immersed into acidic solution, and gaseous hydrogen is bubbling through the solution. Platinum works as catalyst for hydrogen oxidation reaction which takes place on the platinum surface:



The respective potential depends on the pH and also on the hydrogen partial pressure:

$$\varphi = \varphi^0 - \frac{RT}{F} \text{pH} - \frac{RT}{2F} \ln p_{\text{H}_2} \quad (9.1)$$

Thus, the primary reference for all potentiometric measurements is the potential of the hydrogen gas electrode immersed into solution with $\text{pH} = 0$, at pressure of 1 atm.

In practice, this electrode is inconvenient and therefore replaced in routine measurements with a suitable secondary RE. Earlier, calomel electrode, $\text{Hg}/\text{Hg}_2\text{Cl}_2$ in saturated KCl, was often in use. However, given its toxicity, mercury must be avoided, if possible. Therefore, most frequently used is silver chloride electrode (Ag/AgCl) immersed into 3 M KCl solution. This solution is connected with sample or calibrator via salt bridge. In the so-called *single-junction* REs, the bridge is filled with the same solution as that in the RE, for example, 3 M KCl. If the contamination of the sample with K^+ and/or Cl^- ions is of no importance for the results, a *single-junction RE* schematically shown in Fig. 9.1 is a suitable choice.

In many cases, the contamination of samples with K^+ and Cl^- ions from the salt bridge may bias the results. Then use of the so-called *double-junction* RE is preferable. A scheme of a double-junction RE is shown in Fig. 9.2. This kind of

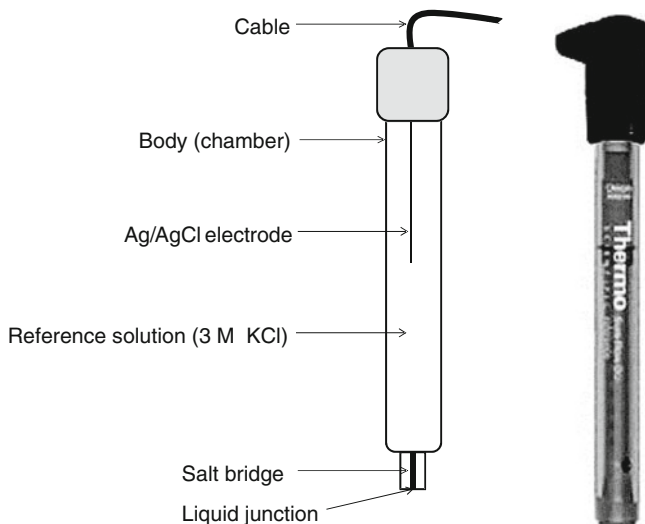


Fig. 9.1 Schematic design of a single-junction reference electrode (*left*) and Thermo-Fisher sure-flow reference electrode (*right*)

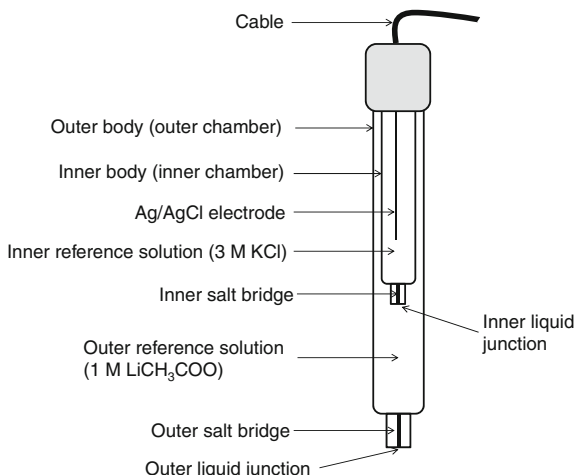
REs consist of two bodies one inside another one, making two chambers. The inner chamber is equipped with an electrode, most commonly—Ag/AgCl and filled with 3 M KCl. The inner reference solution is connected with the outer chamber via inner salt bridge made of a suitable porous material. The outer chamber is filled with electrolyte consisting of ions different from those to be measured. In this way, it is possible to avoid the errors caused by the contamination of sample or calibrator with ions leaking from the reference chamber. The most common choice for the electrolyte in the outer chamber is 1 M LiCH_3COO . Thus, there are two liquid junctions between KCl and LiOAc and between LiOAc and sample solution. Besides silver chloride RE, a large variety of REs are known. Detailed description of various REs is presented in classical book by Ives and Janz [1] and in Cammann's book [2].

There are reports on solid-contact REs without liquid junction, for detailed review see [3]. However, this technology is in early stage of development and will not be discussed here.

9.2 Instrumentation for the Measurements with ISEs

In principal, measurements of EMF require a voltmeter. However, ordinary voltmeters are not suitable for ISEs. This is because ion-selective electrodes, especially those with glass membranes have high electrical resistance, up to 10^8 Ohm. Therefore, measurements with ISEs require pH- or ionometers: high-precision

Fig. 9.2 Schematic design of a double-junction reference electrode



voltmeters with high input impedance. To elucidate the need of high input impedance, let us discuss a fictitious circuit shown in Fig. 9.3. Let us assume that the measuring instrument is an ideal voltmeter, that is, with infinite resistance, while the resistance of the real (non-ideal) instrument equals R_{input} and is connected in parallel to the ideal voltmeter and to the galvanic cell. The signal registered by the instrument equals the potential drop on R_{input} that is, $U_{\text{measured}} = IR_{\text{input}}$. On the other hand, E_{gc} —the EMF of the galvanic cell, is the sole source of I —the current in the circuit. The current flows through R_{input} and R_{gc} , the latter is the own resistance of the cell. These resistances are connected in series, so current is $I = E_{\text{gc}} / (R_{\text{input}} + R_{\text{gc}})$. This means that the measured signal relates to the EMF as follows:

$$U_{\text{measured}} = E_{\text{gc}} R_{\text{input}} / (R_{\text{input}} + R_{\text{gc}}) \quad (9.2)$$

In other words, the signal registered by the instrument approaches the EMF if $R_{\text{input}} \gg R_{\text{gc}}$. In turn, the resistance of the cell is determined by the resistance of the ISE membrane because all other parts of the cell are low-resistant.

Fig. 9.3 Fictitious electrical circuit with a galvanic cell and an ideal voltmeter

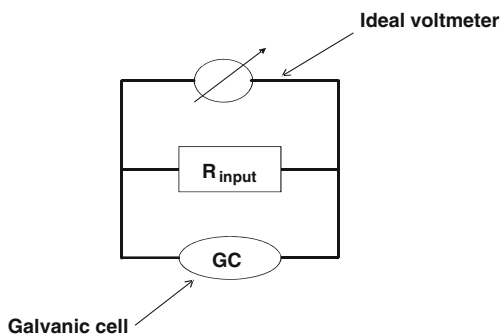




Fig. 9.4 Some examples of modern measuring devices. *Left* ordinary pH meter with a glass pH electrode and a reference electrode; *middle* titrator with electrodes to control the titration process; *right* multichannel EMF measuring station: the potentials of up to 16 ISEs can be measured simultaneously

The deviation of the registered signal from the EMF depends on the $R_{\text{input}}/R_{\text{gc}}$ ratio. If this ratio equals 10^2 , the measured signal is about 1 % less than the EMF; if it is 10^3 , then the loss equals 0.1 %, etc.

Having high input resistance is necessary also for another reason: to maintain low currents during measurements, so that electrodes are not polarized. Modern pH- and ionometers (see Fig. 9.4 for some examples) have input impedances of 10^{14} Ohm and higher, and therefore, the registered signal equals the EMF of the cell, and electrodes are not polarized because of the measurement.

9.3 Direct Potentiometry with ISEs, Calibrators, and Buffer Solutions

The direct potentiometry assumes measurements of the EMF when the ISE and RE are in contact with non-perturbed (native) sample. Respectively, the interpretation of the data relies on the calibration curve plotted against the activity of the analyte ion. The EMF readings therefore deliver information on the activity of the analyte, not on its concentration. Sometimes, this is very advantageous. For instance, calcium ion activity is of higher importance for diagnostic purposes than the total calcium concentration [4]. In most practical applications, however, the users wish to know the free analyte ion concentration or the total content of the analyte rather than the activity. The relation between the concentration and the activity of species is given by the Debye–Hückel theory (see Sect. 2.5). This allows for the calculations of ion activities in calibrators (standard solutions) prepared by the user or supplied by the ISE manufacturer. The critical issue here is the knowledge of the ionic strength of the calibrator. Since the composition of an artificial solution is, obviously, known, the ionic strength is also known and can be calculated with

Table 9.1 Kjelland parameter values (according to [9])

Ion	a_{Kjel}
H ⁺	9
Li ⁺	6
Rb ⁺ , Cs ⁺ , NH ₄ ⁺ , Tl ⁺ , Ag ⁺	2.5
K ⁺ , Cl ⁻ , Br ⁻ , I ⁻ , CN ⁻ , NO ₂ ⁻ , NO ₃ ⁻	3
OH ⁻ , F ⁻ , SCN ⁻ , NCO ⁻ , HS ⁻ , ClO ₃ ⁻ , ClO ₄ ⁻ , BrO ₃ ⁻ , IO ₄ ⁻ , MnO ₄ ⁻	3.5
Na ⁺ , CdCl ⁺ , ClO ₂ ⁻ , IO ₃ ⁻ , HCO ₃ ⁻ , H ₂ PO ₄ ⁻ , HSO ₃ ⁻ , H ₂ AsO ₄ ⁻	4.5
Hg ₂ ²⁺ , SO ₄ ²⁻ , S ₂ O ₃ ²⁻ , SeO ₄ ²⁻ , CrO ₄ ²⁻ , HPO ₄ ²⁻	4
Pb ²⁺ , CO ₃ ²⁻ , SO ₃ ²⁻ , MoO ₄ ²⁻	4.5
Sr ²⁺ , Ba ²⁺ , Cd ²⁺ , Hg ²⁺ , S ²⁻ , WO ₄ ²⁻ , Fe(CN) ₆ ⁴⁻	5
Ca ²⁺ , Cu ²⁺ , Zn ²⁺ , Sn ²⁺ , Mn ²⁺ , Fe ²⁺ , Ni ²⁺ , Co ²⁺	6
Mg ²⁺ , Be ²⁺	8
PO ₄ ³⁻ , Fe(CN) ₆ ³⁻	4
Al ³⁺ , Fe ³⁺ , Cr ³⁺ , La ³⁺ , Ce ³⁺	9
HCOO ⁻ , Citrate ⁻	3.5
Acetate ⁻ , Cl-acetate ⁻ , (CH ₃) ₄ N ⁺ , (C ₂ H ₅) ₂ NH ₂ ⁺ , Citrate ²⁻	4.5
Cl ₃ -acetate ⁻ , (C ₂ H ₅) ₃ NH ⁺ , Citrate ³⁻	5

Eq. (2.42) except of weak electrolytes present in the solution. Thus, the activity of the analyte ion in calibrators is known, and this allows for plotting the calibration curve. The values of a_{Kjel} , the Kjelland parameters needed for these calculations, are summarized in Table 9.1.

The ionic strength of samples is, typically, not known although it sometimes can be estimated by, for example, the conductivity measurements of the samples. This is why the inverse task, the calculation of the concentration on the basis of the activity data obtained from the ISE, is not executable.

The practical approach here is as follows. Since samples to be analyzed, normally, belong to certain type—blood, blood serum, or some industrial solutions, etc., the so-called typical ionic strength of each particular type of samples is approximately known. Calibrators, therefore, must mimic this particular type of samples having the same ionic strength. Then the activity coefficients are the same in all calibrators and in samples of this particular type. The target analyte content in calibrators must cover the whole possible range of the respective concentrations. Since activity coefficients are constant, the calibration curve can be plotted against log of concentration, and the EMF readings in samples directly show the sought free analyte ion content. As most simple example, below are presented calibrators for the measurements of potassium in blood serum with K⁺-ISE. These are three mixed solutions, all having the same ionic strength: $J = 150$ mM. Solution #1 contains 2 mM of KCl and 148 mM NaCl, #2 is 4.5 mM KCl + 145.5 mM NaCl, and #3 is 10 mM KCl + 140 mM NaCl. The K⁺ ion concentrations in these simple calibrators cover the physiologically relevant range, and the span of the values is enough for the calibration of the ISE.

Ion activity coefficients can be calculated using equations below [Eqs. (2.42) and (2.44) are presented here for the reader convenience]:

$$J = \frac{1}{2} \sum_{k=1}^n C_k z_k^2 \quad \log \gamma_I = -\frac{Az_I^2 \sqrt{J}}{1 + a_{\text{Kjel}} B \sqrt{J}} + 0.1z_I J$$

The adjustment of the ionic strength is a common approach in measurements with ISEs. Total ionic strength adjustment buffer (TISAB) was invented first for measurements of F^- [5]. The buffer contains acetic acid, NaCl, sodium citrate, and water. By adding NaOH, the pH is adjusted at 5.5—to prevent interference from hydroxyl ions. The ionic strength of the buffer is high enough, so samples diluted 1:1 with the buffer have a constant ionic strength. Furthermore, fluoride bound with iron and aluminum gets free and forms citric complexes. Therefore, the fraction of the free F^- anions is always the same. In this way, it is possible to calibrate the ISE and then measure total fluoride in samples. Various modifications of TISAB are described in [6].

There is a large number of pH buffers: traditional buffers based on mixtures of weak inorganic or organic acids and NaOH: citrate, acetate, phosphate, borate buffers. The pH of biological samples is normally adjusted at pH 7.4 with phosphate buffer saline, containing 137 mM NaCl, 2.7 mM KCl, 10 mM $Na_2HPO_4 \cdot 2H_2O$, and 2.0 mM KH_2PO_4 . Morpholine acids are also widely used to prepare buffers for clinical and biological studies.

Metal buffers for calibrators of ISEs selective to heavy metals in industrial and environmental applications are typically based on EDTA, NTA, and other similar agents.

Buffers are commercially available and their handling is described in manuals, so we do not go into further details discussing buffers here.

9.4 Standard Addition Methods, Potentiometric Titration with ISEs

Standard addition, standard dilution, and titration methods are thoroughly discussed by Cammann [2] and by Koryta and Stulik [7]. The basics of these methods obviously remain the same in spite of the progress in the ISE technology. Therefore, here, we discuss these issues only briefly.

Addition/dilution and titration methods are advantageous because allow for circumventing the problems of the unknown activity coefficients and even of partial complexation of the analyte. Titration methods, especially the Gran method [8], deliver more accurate results than the direct potentiometry. On the other hand, only the direct potentiometry allows for the continuous monitoring without perturbation of the sample composition.

Let us assume that we have an unknown sample: γ the activity coefficient of the analyte is not known, furthermore, only β fraction of the analyte is present as free ions. Thus, the free target ion activity in the sample is $a = C^{\text{ionized}} \gamma = C^{\text{total}} \gamma \beta$. The respective EMF value is

$$E_1 = E^0 + S \log a^{\text{native}} = E^0 + S \log C^{\text{total}} + S \log \gamma + S \log \beta \quad (9.3)$$

Now, we add ΔC^{total} —a known total quantity of the target ions (as a suitable electrolyte). The EMF value is as follows:

$$E_2 = E^0 + S \log a^{\text{processed}} = E^0 + S \log (C^{\text{total}} + \Delta C^{\text{total}}) + S \log \gamma + S \log \beta \quad (9.4)$$

Now, for the total concentration of the analyte in the native sample, we have

$$C^{\text{total}} = \Delta C^{\text{total}} / \left(10^{\frac{E_2 - E_1}{S}} - 1 \right) \quad (9.5)$$

The critical issue in this procedure is the constancy of γ and β values. Therefore, the added quantity of the analyte must be small. On the other hand, a too small addition causes a too small effect in the EMF, so that the accuracy of the result is low. Normally, it is necessary to make a few trials and find ΔC^{total} value which gives the EMF effect of about 10 mV.

There are situations when we do not know whether the calibration parameters in an unknown sample are the same as in standard solutions. For whatever reason, E^0 may be shifted, and S may be sub- or super-Nernstian. Under these circumstances, the double-addition method helps. This method, however, suggests $C^{\text{ionized}} = C^{\text{total}}$.¹ The EMF when the ISE and the RE are immersed into the native sample is

$$E_1 = E^0 + S \log \gamma + S \log C \quad (9.6)$$

Here, E^0 , S are not necessarily the same as in simple standards and therefore considered unknown. After addition of the ΔC of the analyte, the EMF is

$$E_2 = E^0 + S \log \gamma + S \log (C + \Delta C) \quad (9.7)$$

The second addition of the same ΔC results in:

$$E_3 = E^0 + S \log \gamma + S \log (C + 2\Delta C) \quad (9.8)$$

Now, we have equation which does not contain the unknown E^0 , S values:

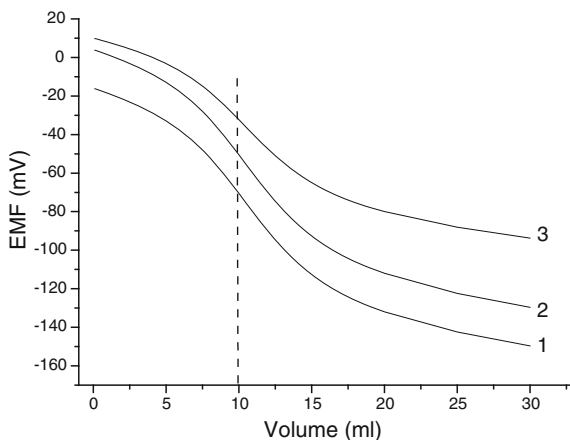
$$\frac{E_3 - E_1}{E_2 - E_1} = \frac{\log \frac{C+2\Delta C}{C}}{\log \frac{C+\Delta C}{C}} \quad (9.9)$$

This equation can be solved by iteration procedure; the most efficient is the bisection method.

The advantage of the potentiometric titration is low sensitivity to the ISE calibration parameters. Example of potentiometric titration curves is shown in Fig. 9.5 The curves refer to titration of analyte A with titrant B, and the AB

¹ Cammann [2] describes the double-addition method for solutions with $C^{\text{ionized}} = \beta C^{\text{total}}$. It is, however, doubtful whether β remains constant when more than one addition is made.

Fig. 9.5 Titration curves calculated for ISEs with different E^0 (mV) and S (mV/ $\log(a)$): 100, 58 (*curve 1*); 120, 58 (*curve 2*); and 100, 45 (*curve 3*)



complex formation constant is 10^4 M^{-1} . The analyte concentration is 0.01 M, and the concentration of the titrant is 0.001 M. Thus, the equivalent volume is 10 ml. The calibration parameters of the ISE used for the titration are shown in the figure capture. One can see that the location of the inflexion point (equivalent point) is the same whatever the standard potential and whatever the ISE slope. However, sub-Nernstian slope results in worsened accuracy.

The Gran titration method [8] is based on the Nernst equation rewritten as

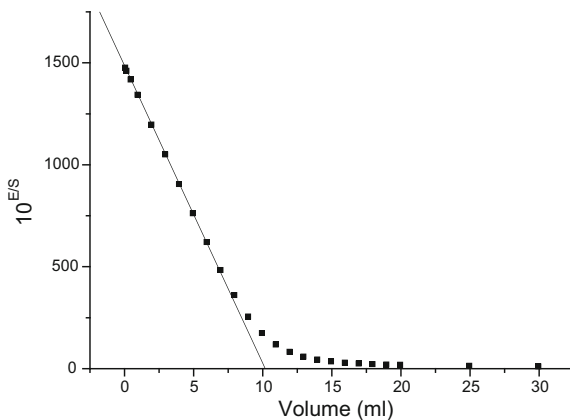
$$E/S = E^0/S + \log a_I \quad (9.10)$$

This immediately results in linear equation:

$$10^{E/S} = 10^{E^0/S} + a_I = \text{Const} + a_I \quad (9.11)$$

Figure 9.6 illustrates the method. The data refer to the titration procedure shown in Fig. 9.5, curve 1. The EMF values are shifted 200 mV up to prevent

Fig. 9.6 Gran plot of the titration procedure shown in Fig. 9.5, curve 1



negative values under logarithm. One can see that the linearity is excellent in the beginning of the titration procedure, and the extrapolation to $10^{E/S} = 0$ does give the equivalence point.

Thus, the Gran method secures better accuracy of the results than the search for the inflection point in the ordinary titration curve. Furthermore, the $10^{E/S}$ data in the linear part of the Gran plot refer to relatively high concentrations of the analyte—far from the detection limit of the ISE. This is in contrast with use of the ordinary titration curve: close and after the equivalence point, the curve can be distorted because the analyte concentration is below the ISE detection limit.

References

1. D.J.G. Ives, G.J. Janz, Reference electrodes, Academic Press, N.Y., 1961.
2. K. Cammann, Das Arbeiten mit Ionenselektiven Elektroden, Springer, Berlin-Heidelberg-New York, 1977.
3. A. Michalska, *Electroanalysis*, 2012, 24, 1253.
4. R. Durst, Ion-selective Electrodes, National Bureau of Standards, Special publication 314, 1969.
5. M.S. Frant, J.W. Ross, *Anal. Chem.*, 1968, 40, 1169.
6. K. Nicholson, E.J. Duff, *Anal. Lett.*, 1981, 14, 887.
7. J. Koryta, K. Stulik, *Iontove-Selektivni Elektrody*, Academia, Praha, 1984.
8. G. Gran, *Analyst*, 1952, 77, 661.
9. J. Dvorak, J. Koryta, V. Bohackova, *Elektrochemie*, 1975, Academia, Praha.

Index

A

Acrylic polymers, 63
Acrylsiloxanes, 63
Activity coefficient, 16
Addition/dilution, 154
Analyte activity, 5
Anion interference with cationic response, 73

B

Bakker protocol, 42
Baucke theory, 106
Bi-ionic potentials method, 38
Bis(butylpentyl)adipate (BBPA), 59
Bis-crown ethers, 55
Bis(2-ethylhexyl)sebacate, 59
Bis[4-(tetramethylbutyl)phenyl]phosphate, 54
Boundary potential, 12

C

Calcium, 6
Calcium didecyl phosphate, 54
Calibration, 3
Calibrators, 152
Calixarenes, 55, 64
Carbon black, 141
CdS, 119
Chalcogenide glasses, 113, 122
 membranes, 7
Charge number, 15
Chemical potential, 15
Clinical analysis, 5
Coated-wire electrodes, 140
Coffee electronic tongue, 132
Combination electrodes, 145
Conducting polymers (CP), 62, 126, 142
Continuous monitoring, 5
Counterions, 52

Cross-sensitivity, 131
Crown ethers, 55, 64
Crystalline electrodes, 7, 113, 119, 138
Crystalline membranes, 113
Cyclohexanone, 61

D

Debye–Hückel theory, 24, 29–31, 152
Detection limit, 33, 42, 44, 59, 116, 122, 126,
 128, 129
Diffusion layer, 25
 Lewenstam/Hulanicki, 121
Diffusion potentials, 17, 19
Dioctylphthalate, 59
Direct potentiometry, 152
Donnan exclusion, 53, 66, 74, 79

E

Eisenman theory, 104
Electrical double layer, 13
Electrical potential, 15
Electrochemical equilibrium, 14
Electrochemical potential, 15
Electrode potential, 17
Electrodes, coated-wire, 140
 crystalline, 7, 113, 119, 138
 fluoride, 8, 113, 115
 indicator, 22
 microelectrodes, 145
 RedOx, 110, 135
 reference (RE), 22, 149
 second-kind, 140
 standard hydrogen, 149
Electromotive force (EMF), 2, 22, 138, 149
Electronic nose, 8, 131
Electronic tongue, 8, 123, 131
Electron–ion-exchanger resins, 141

Equilibrium factor, 68
 Equitransferring electrolytes, 27

F

Field effect transistors, 8
 Fixed interference method, 39
 Flow-through cells, 146
 Fluoride electrodes, 8, 113, 115
 Full electrolyte activity, 29

G

Galvanic cells, liquid junction, 22
 Gibbs free energy, 5, 12, 16, 72, 73
 Gibbs–Duhem equation, 29
 Glass electrodes, 97
 RedOx sensing, 110
 Glass membranes, 6, 100
 pH-selective, 98
 Gouy–Chapman theory, 56, 91
 Gran titration method, 156
 Guanidinium bases, 54
 Guggenheim assumption, 30

H

Heavy metals, 6, 114, 154
 cations, 41, 113, 119
 Heparin, 130
 Hexabutyltriamidophosphate (HBTAP), 81
p-Hexyltrifluoroacetylbenzoate, 56
p-Hexyltrifluoroacetylbenzoate (HFAB), 81
 Hofmeister series, 53, 69
 Hydrated surface layers, 99
 Hydration, 12

I

Impedance, membrane/solution interface, 89
 Impedance method, 89
 Indicator electrode, 22
 Interface, electric potentials, 12
 Interference coefficient, 4
 Ion activity, 24, 29, 42, 99, 109, 136, 152
 coefficients, 30, 154
 Ion bombardment for spectrochemical analysis (IBSCA), 108
 Ion exchange, 7, 43, 126
 Ion exchangers, 43, 51, 56, 65, 130, 141
 Ion propagation, 125
 Ionic additives, 77
 Ionic strength, 30, 116, 129, 152

Ionophores, 7, 34, 51, 128, 140
 neutral, 55, 89
 Ion-selective electrode, response slope, 33
 working range, 33
 Ion-to-ionophore association constants, 54
 Ion-to-ionophore interactions, 81

K

Kjelland parameters, 31, 153

L

Lanthanum fluoride, 115
 Lead, 135
 Lewis acid/base, 12
 Liquid junction, 25
 potential, 26
 Lithium, 6
 Lithium silicate glasses, 99

M

Magnesium, 6
 Matched potential method (MPM), 42
 McInnes assumption, 30
 Membranes, 6, 11
 chalcogenide glass, 122
 cocktails, 61
 crystalline, 113
 glass, 97
 ionophore-based, 51
 ion-site association, 85
 monocrystalline/polycrystalline, 7
 poly(vinylchloride) (PVC), 58
 polycrystalline, 116
 potential, 8, 21
 solution boundary, interfacial kinetics, 89
 Mercurocarborands, 55
 Metal porphyrine complexes, 54
 Methacrylic membranes, 64
 Microelectrodes, 145
 Mixed-alkali effect, 110
 Monensin, 58
 Multisensor arrays, 131
 Multispecies approximation, 78

N

Nernst equation, 2, 12, 17, 28, 33, 74, 156
 Nernst–Planck equation, 20, 66, 125
 Neutral ionophores, complexation of ions, 82
 Nikolsky equation, 4, 35, 103

Nikolsky “simple” theory, 101
Nikolsky–Shultz generalized theory, 105
Nitrate, 135
2-Nitrophenyloctyl ether (oNPOE), 59
Nonionic species, potentiometric sensing, 87
Nonzero current conditions, 129

O

Optical sensors (optodes), 2

P

Partial activity coefficients, 105
pH buffers, 154
pH sensors, 97
Phase-boundary potential, 77
Philips electrode body, 61
Phosphoric glasses, 97
Phosphorous glasses, 6
Physical sensors, 1
Piece-to-piece reproducibility, 48
Plasticizers, 8, 58
Podands, 55
Polyaniline (PANI), 142
Poly-crown ethers, 64
Polyetherketone, 64
Polyethylenedioxythiophene (PEDOT), 142
Polypyrrole (PPy), 142
Polystyrenebutadiene, 64
Polytrioctylthiophene (POT), 142
Polyurethane membranes, 64
Poly[4,5-difluoro-2,2-bis(trifluoromethyl)-1,3-dioxole]-co-poly(tetrafluoroethylene), 65
Poly(trioctylthiophene), 63
Poly(vinylchloride) (PVC), 7, 8, 58
Potassium-selective solid-contact ISE, 143
Potassium tetrakis(*p*-Cl-phenyl)borate, 43, 52
Potentiometric selectivity coefficient, 35
Protamine, 130

Q

Quartz, 97
Quinone/hydroquinone glass, 110

R

Real-time modeling, 125
RedOx electrodes, 110, 135
RedOx sensing, 110

Reference electrodes (RE), 22, 149
 double-junction, 149, 151
 single-junction, 149
Response time, 45
Routine analysis, 149

S

Salofenes, 55
Sandblom–Eisenman–Walker theory, 75
Sandwich membrane, 83
Second-kind electrodes, 140
Selectivity coefficient, 4, 38
Selectivity constant, 7
Selectivity optimization, 77
Selectivity, crystalline membranes, 120
Selectrodes, 140
Semiconductors, 8, 110, 142
Sensor response, 1
Separate solutions method, 38
Silicate glasses, 6, 97, 105, 115
Silicon dioxide, 97
Silicon rubbers, 63
Silver sulfide, crystalline membranes, 113
Single-ion activity, 29
Sodium silicate glasses, 99
Soil acidity/salinity, 6
Solid-contact ISEs, 138
Space modeling, 125
Species interactions, 82
Stability, 46
Stagnant layer, 46
Standard addition, 154
Standard dilution, 154
Standard hydrogen electrode, 149
Steady state, 19

T

Teflon AF2400, 65
Tetraalkylammonium, 51
Tetraalkylarsonium, 51
Tetraalkylphosphonium, 51
Tetradecylammonium bromide (TDABr), 52, 87
Tetrahydrofuran (THF), 61
Tetrakis(*p*-Cl-phenyl)borate, 43, 52, 79, 87
Tetranactin, 56
Thiacalixarene, 65
Titration, 154
Total ionic strength adjustment buffer (TISAB), 154

Trace analysis, 126
Transference number, 26
Tri(2-ethylhexyl) phosphate, 59
Trifluoroacetyl-*p*-heptylbenzene, 55
Tris(2-octyl-oxyethyl)amine, 56
Tuned galvanostatic polarization, 128

U

Unbiased selectivity coefficients, 43
Urethanes, 63

V

Valinomycin, 8, 45, 55, 79, 83
Vinylchloride–vinylacetate, 64
Voltmeters, 150

W

Warburg impedance, 89
Water layer test, 144
Water uptake, stability of solid-contact ISEs,
143